Vaccinia virus-host cell interactions at the metabolic interface

by

Anil Pant

B.S., Tribhuvan University, 2010
M.S., Tribhuvan University, 2014

AN ABSTRACT OF A DISSERTATION

submitted in partial fulfillment of the requirements for the degree

DOCTOR OF PHILOSOPHY

Division of Biology
College of Arts and Sciences

KANSAS STATE UNIVERSITY
Manhattan, Kansas

2021

Abstract

Metabolism is a fundamental cellular process. Because viruses lack their own metabolic capability, they must actively interact with and usurp host metabolic machinery for efficient replication. Vaccinia Virus (VACV) is the prototypic member of *poxviridae* family, and it is widely used as a model system to study pathogen-host interactions. Like all viruses, VACV relies on the host for the supply of nutrients and energy. However, the viral and the host factors that interact at this crucial interface during VACV infection are poorly understood. This dissertation aims to study the alteration of host metabolism during VACV infection and identify the host and viral factors that are important for these changes.

In the first part of the dissertation, we examine why VACV replication heavily relies on glutamine, a non-essential amino acid. In the absence of glutamine, the replication of VACV is severely impaired. We found that the addition of asparagine, an amino acid that exclusively requires glutamine for its biosynthesis, rescues VACV replication from glutamine depletion. Upon VACV infection in the absence of glutamine, asparagine becomes the least abundant amino acid. While the addition of asparagine did not elevate the tricarboxylic acid (TCA) cycle activities or the nucleotide levels, it did reduce the imbalance of amino acid levels resulting from glutamine deprivation. Accordingly, asparagine rescued VACV replication from glutamine depletion by rescuing the post-replicative mRNA translation. Consistent with this, when we disrupted asparagine metabolism using chemical or genetic approaches VACV replication was suppressed. In all, our data show that the asparagine metabolic pathway is important for VACV replication.

The regulation of metabolic pathways is important for virus replication as we found that VACV, upon infection, hijacks cellular machinery to redirect cellular nutrients for efficient viral

replication. We found that VACV infection causes profound changes in several aspects of host metabolism such as the homeostasis of amino acids, central carbon, and numerous lipids. We further demonstrated that VACV infection leads to increased levels of TCA cycle intermediates, such as citrate. The virus growth factor (VGF), the VACV homolog of cellular epidermal growth factor (EGF), was responsible for this increase by activating the host EGF receptor (EGFR) pathway. We showed that VACV infection leads to non-canonical STAT3 phosphorylation at serine 727 in a VGF-dependent manner. Interestingly, both EGFR and downstream STAT3 pathway are key host factors that are induced by VACV to increase host TCA intermediate levels for efficient replication. We also demonstrate that VACV infection reduces the levels of long-chain fatty acids and increases the carnitine-conjugated fatty acids that are critical for beta-oxidation. Furthermore, we show that the VGF-mediated EGFR pathway is crucial for the activation of a host enzyme that sits at the crossroads of key cellular biochemical processes, indicating VACV could launch a multifaceted attack to hijack host nutrient resources through VGF.

Together, our study enhances the understanding of how VACV repurposes host cell metabolism for efficient replication. We elucidated a metabolic vulnerability of VACV infection and identified key host and viral factors that govern the metabolic dynamics during VACV infection. These findings could lead to the development of novel strategies to manage poxvirus infections and facilitate the development of poxviruses-based tools for protein expression, vaccine vectors, and oncolytic treatment. Moreover, these findings can provide knowledge for understanding fundamental mechanisms of cell metabolism.

Vaccinia virus-host cell interactions at the metabolic interface

by

Anil Pant

B.S., Tribhuvan University, 2010
M.S., Tribhuvan University, 2014

A DISSERTATION

submitted in partial fulfillment of the requirements for the degree

DOCTOR OF PHILOSOPHY

Division of Biology
College of Arts and Sciences

KANSAS STATE UNIVERSITY
Manhattan, Kansas

2021

Approved by:

Major Professor
Dr. Zhilong Yang

Copyright

Abstract

Metabolism is a fundamental cellular process. Because viruses lack their own metabolic capability, they must actively interact with and usurp host metabolic machinery for efficient replication. Vaccinia Virus (VACV) is the prototypic member of *poxviridae* family, and it is widely used as a model system to study pathogen-host interactions. Like all viruses, VACV relies on the host for the supply of nutrients and energy. However, the viral and the host factors that interact at this crucial interface during VACV infection are poorly understood. This dissertation aims to study the alteration of host metabolism during VACV infection and identify the host and viral factors that are important for these changes.

In the first part of the dissertation, we examine why VACV replication heavily relies on glutamine, a non-essential amino acid. In the absence of glutamine, the replication of VACV is severely impaired. We found that the addition of asparagine, an amino acid that exclusively requires glutamine for its biosynthesis, rescues VACV replication from glutamine depletion. Upon VACV infection in the absence of glutamine, asparagine becomes the least abundant amino acid. While the addition of asparagine did not elevate the tricarboxylic acid (TCA) cycle activities or the nucleotide levels, it did reduce the imbalance of amino acid levels resulting from glutamine deprivation. Accordingly, asparagine rescued VACV replication from glutamine depletion by rescuing the post-replicative mRNA translation. Consistent with this, when we disrupted asparagine metabolism using chemical or genetic approaches VACV replication was suppressed. In all, our data show that the asparagine metabolic pathway is important for VACV replication.

The regulation of metabolic pathways is important for virus replication as we found that VACV, upon infection, hijacks cellular machinery to redirect cellular nutrients for efficient viral

replication. We found that VACV infection causes profound changes in several aspects of host metabolism such as the homeostasis of amino acids, central carbon, and numerous lipids. We further demonstrated that VACV infection leads to increased levels of TCA cycle intermediates, such as citrate. The virus growth factor (VGF), the VACV homolog of cellular epidermal growth factor (EGF), was responsible for this increase by activating the host EGF receptor (EGFR) pathway. We showed that VACV infection leads to non-canonical STAT3 phosphorylation at serine 727 in a VGF-dependent manner. Interestingly, both EGFR and downstream STAT3 pathway are key host factors that are induced by VACV to increase host TCA intermediate levels for efficient replication. We also demonstrate that VACV infection reduces the levels of long-chain fatty acids and increases the carnitine-conjugated fatty acids that are critical for beta-oxidation. Furthermore, we show that the VGF-mediated EGFR pathway is crucial for the activation of a host enzyme that sits at the crossroads of key cellular biochemical processes, indicating VACV could launch a multifaceted attack to hijack host nutrient resources through VGF.

Together, our study enhances the understanding of how VACV repurposes host cell metabolism for efficient replication. We elucidated a metabolic vulnerability of VACV infection and identified key host and viral factors that govern the metabolic dynamics during VACV infection. These findings could lead to the development of novel strategies to manage poxvirus infections and facilitate the development of poxviruses-based tools for protein expression, vaccine vectors, and oncolytic treatment. Moreover, these findings can provide knowledge for understanding fundamental mechanisms of cell metabolism.

Table of Contents

List of Figures

List of Supplementary Figures

List of Tables

List of Abbreviations

Acetyl-CoA Carboxylase (ACC)

Adenosine Triphosphate (ATP)

Adenovirus 5 (Ad5)

AK Strain Transforming/ protein kinase B (Akt)

Alpha-Ketoglutarate (α-KG)

AMP-Activated Protein Kinase (AMPK)

Analysis of Variance (ANOVA)

Asparagine Synthetase (ASNS)

ATP Citrate Lyase (ACLY)

Basic Leucine Zipper Nuclear Factor 1 (BZLF1)

Calcium-Calmodulin-Dependent Kinase Kinase (CaMKK)

Carbohydrate Response Element-Binding Protein (ChREBP)

Coronavirus Disease 19 (COVID-19)

Dengue Virus (DENV)

Deoxyribonucleic Acid (DNA)

Dimethyl Sulfoxide (DMSO)

Dulbecco's Minimal Essential Medium (DMEM)

Eagle's Minimal Essential Medium (EMEM)

Epidermal Growth Factor (EGF)

Epidermal Growth Factor Receptor (EGFR)

Epstein-Barr Virus (EBV)

Eukaryotic Initiation Factor (eIF)

Factor Inhibiting HIF-1 (FIH-1)

Fatty Acid (FA)

Fibroblast Growth Factor (FGF)

Fibroblast Growth Factor Receptor (FGFR)

Flavin Adenine Dinucleotide ($FADH_)$

G-Protein-Coupled Receptors (GPCRs)

General Control Nonderepressible 2 (GCN2)

Glucose Transporter 4 (GLUT4)

Glucose-6-Phosphate Dehydrogenase (G6PD)

Glutaminase (GLS)

Glyceraldehyde-3-Phosphate Dehydrogenase (GAPDH)

Green Fluorescence Protein (GFP)

Growth Factor Receptor (GFR)

HBV X Protein (HBx)

Hepatitis B Virus (HBV)

Hepatitis C Virus (HCV)

Herpes Simplex Virus Type 1 (HSV-1)

Hexokinase 2 (HK2)

Hours Post Infection (HPI)

Human Cytomegalovirus (HCMV)

Human Foreskin Fibroblasts (HFFs)

Human Immunodeficiency Virus (HIV)

Human Papillomavirus 16 (HPV)

Hypoxia-Inducible Factors (HIF)

Influenza A Virus (IAV)

Kaposi's Sarcoma-Associated Herpesvirus (KSHV)

L-Methionine Sulfoximine (L-MSO)

Lactate Dehydrogenase A (LDHA)

Latency-Associated Nuclear Antigen (LANA)

Latent Membrane Protein 1 (LMP1)

Mammalian Target of Rapamycin (MTOR)

Messenger RNA (mRNA)

Micro RNAs (miRNAs)

Mitogen-Activated Protein Kinase (MAPK)

Murine Norovirus (MNV)

Nicotinamide Adenine Dinucleotide (NADH)

Non-Structural Protein 3 (NS3)

Oxidative Phosphorylation (OXPHOS)

Oxygen Consumption Rate (OCR)

Phosphatase and Tensin Homolog (PTEN)

Phosphoenolpyruvate Carboxykinase 2 (PCK2)

Phosphoinositide 3-Kinase (PI3K)

Prolyl-Hydroxylase Domain-Containing Protein (PHD)

Pyruvate Dehydrogenase Kinase 1 (PDK-1)

Pyruvate Kinase Isozyme M2 (PKM2)

Quantitative Real-Time Polymerase Chain Reaction (qRT-PCR)

Receptor Tyrosine Kinase (RTK)

Respiratory Syncytial Virus (RSV)

Ribonucleic Acid (RNA)

Severe Acute Respiratory Syndrome Coronavirus-2 (SARS-CoV-2)

Signal Transducer and Activator of Transcription 3 (STAT3)

Simian Virus 40 (SV40)

Sirtuin 1 (SIRT1)

Sodium Dodecyl Sulfate–Polyacrylamide Gel Electrophoresis (SDS–PAGE)

Sterol Regulatory Element-Binding Proteins (SREBPs)

Surface Sensing of Translation (SUnSET)

Tricarboxylic Acid (TCA)

Tuberous Sclerosis Protein Complex 2 (TSC2)

Vaccinia Virus (VACV)

Vascular Endothelial Growth Factor (VEGF)

Virus Growth Factor (VGF)

von Hippel-Lindau Tumor Suppressor (VHL)

White Spot Syndrome Virus (WSSV)

Acknowledgements

First and foremost, I would like to thank my mentor Dr. Zhilong Yang for his supervision, continuous support and for helping me grow into the scientist that I am today. You embody what it means to be an amazing a mentor, and I am incredibly fortunate to have had the privilege to learn from you.

I am extremely grateful to my supervisory committee members Dr. Nicholas Wallace, Dr. Raymond (Bob) Rowland, Dr. Jeroen Roelofs, Dr. Ruth Welti for their helpful comments and supervision throughout my graduate studies. I would also like to extend my gratitude to Dr. Shuai Cao (Harry) and Dr. Pragyesh Dhungel for helpful advice and teaching me the tools and techniques in the lab. I would also like to thank the past and present lab members: Dr. Chen Peng, Fred, Candy, Josh, Lara, Mark, Yanan, Marlene, for all the fun and cherished memories that we shared in the lab and social settings. I would like to thank Dr. Bernard Moss (NIH/NIAID) for providing some materials for this study.

I am grateful to all the friends that I have earned during my graduate study at K-State. Special thanks to Alicia, Dalton, Emily, Seton, John, and Bram for teaching me fun American sports and baking yummy cookies. My appreciation also goes out to all the funding sources, and the staffs of the Division of Biology, especially Becki, Melissa, Tari, Sarah, Bob, and Matt.

I would like to thank all the members of the Nepalese Student Association at K-State for organizing various events that made me feel home away from home. Special thanks to Pragyesh Dhungel, Babita Adhikari, Binny Bhandary, Ruben Shrestha, and Sony Shrestha for making my stay in Manhattan, KS wonderful.

I would like to thank my parents and other family members for their unwavering support over the years. Mummy and Daddy, you been my rock throughout this journey and without your

love and support I could not have come this far. Thanks to my mother- and father-in-law for traveling this far to the USA despite the COVID-19 pandemic to help us with our baby. Without their help, I could not have been this productive.

Special thanks to my daughter, Aadhya, who has changed the way I view this world. Thank you for rejuvenating my childhood and making me better at time management.

To Deepa Upreti, my wife and my best friend, thank you for always being there for me. During the last 13 years of our journey together, you have halved my sorrow and doubled my joy. Thank you for critiquing my work, pushing me, and encouraging me in multitude of ways. No words could ever describe my gratitude towards you. You mean everything to me and I love you forever and beyond.

Dedication

This dissertation is dedicated to my mother (Ganga) and my father (Jib Raj). You have supported in each and every step of my life and I am forever in your debt.

Chapter 1 - Hijacked: Virus-Induced Alterations in Cellular Signaling Rewire Host Cell Metabolism

Abstract

Cells are complex machines that are finely tuned to perform specific activities. Cellular functions are regulated by various signaling pathways. Viruses are obligate intracellular parasites, and each step of viral replication is governed by their interactions with the host cell. Viruses must commandeer cellular functions to support productive infection. Due to the high turnover of cellular resources during viral infections, the nutritional demands of virus-infected cells differ from those of uninfected cells. To promote an optimal environment for replication, viruses often rewire the metabolism of infected cells. In this chapter, we will summarize recent findings regarding virus-induced alterations to major cellular metabolic pathways with a focus on how viruses hijack various signaling cascades to induce these changes. We will begin with a general introduction that describes the role played by signaling pathways in cellular metabolism and discuss how different viruses target these pathways to their benefit. We will also highlight gaps in the knowledge base and discuss how the study of virus-induced changes in host metabolism could be used to understand fundamental processes involved in metabolic regulation and how to harness these processes to combat metabolic disorders and cancers.

Introduction

Mammalian cell functions are tightly regulated by various cell signaling pathways. Metabolism is a fundamental process required for cell survival, and signal transduction is essential for the coordination of cell metabolism. Because viruses do not have their own metabolic capabilities, they must actively interact with and usurp key cellular signaling pathways to generate the energy and precursors that are necessary for viral replication. For example, human cytomegalovirus (HCMV) upregulates almost all aspects of cell metabolism to support productive infection [1]. Vaccinia virus (VACV) increases the levels of tricarboxylic acid (TCA) cycle intermediates and glutamine metabolism to support efficient replication [2–4]. Outstanding summaries of virus-induced alterations to the host metabolic process can be found elsewhere [5,6].

Metabolic alterations have emerged as common mechanisms that underlie the progression of both viral infections and cancers. Both viruses and cancers demand increased energy production and macromolecule biosynthesis to propagate. Therefore, the study of virus-host metabolism could potentially contribute to understanding the metabolic mechanisms associated with cancer progression. Furthermore, because viruses are master manipulators of cell functions, studying virus-host interaction at the metabolic interface could reveal fundamental aspects of cellular metabolism. Therefore, a better understanding of the basic mechanism involved in host-pathogen interactions could identify novel targets for the development of therapeutic interventions not only for viral diseases but also other pathologies, including cancer.

Viruses exploit several different strategies to hijack cellular nutrients. Some viruses upregulate core catabolic processes (e.g., glycolysis and the TCA cycle), whereas others target anabolic processes (e.g., nucleotide, fatty acid [FA], and amino acid synthesis) [6]. These

metabolic processes are governed by key cellular signaling cascades, including growth factor signaling and the phosphoinositide 3-kinase (PI3K)-protein kinase B (Akt) and AMP-activated protein kinase (AMPK) pathways [7,8]. Unsurprisingly, viruses have evolved mechanisms that directly or indirectly target these pathways to create an environment that optimally supports virus replication. In this chapter, we summarize the cellular signaling pathways that are known to regulate metabolism and describe our current understanding of how viruses interact with these pathways (**Table 1.1**) to meet the increased demands for metabolites and energy that are necessary for efficient replication.

Growth factor receptor signaling

Among the major factors that govern cellular metabolism and proliferation are the receptor tyrosine kinase (RTK) pathways, particularly **growth factor receptor (GFR) signaling**. The GFR pathway regulates whether a cell remains quiescent (metabolically inactive) or enters a state of active proliferation. Most terminally differentiated mammalian cells exist in a quiescent metabolic state, in which glucose is catabolized via glycolysis to produce pyruvate in the cytoplasm. Pyruvate is then transported to the mitochondria, where it is oxidized to CO_2 via the TCA cycle. The NADH, $NADH_2$, and $FADH_2$ molecules that are produced during glycolysis and the TCA cycle are eventually used to build up a proton gradient. This gradient, then, drives ATP production via oxidative phosphorylation (OXPHOS) [9]. Increased growth factor concentrations activate growth factor signaling pathways that enhance nutrient uptake, primarily glucose and glutamine [10], to support cell proliferation. The onset of cell cycle progression and proliferation increases the cellular demand for carbon, nitrogen, and other nutrients used to generate carbohydrates, proteins, fats, nucleic acids, and energy [8]. The uptake, synthesis, and breakdown of each biomolecule are further regulated by various other signaling cascades, which

will be discussed in more detail later. The constant activation of proliferative signaling and enhanced metabolic activity may result in cancer development [11], which highlights the importance of the tight regulation of cell signaling and metabolism.

Due to its key role in the modulation of cell metabolism, the GFR signaling pathway is targeted by several viruses to repurpose host metabolic pathways for their benefit (**Fig. 1.1, Table 1.1**). Interestingly, several viruses encode growth factors that are homologous to those produced by the cells that they infect, allowing for the modulation of the RTK pathway to support replication (Reviewed in [12,13]). One excellent example is virus growth factor (VGF), the viral homolog of cellular epidermal growth factor (EGF), which is encoded by VACV, a prototypical poxvirus [14,15]. The deletion of VGF decreases VACV replication capacity in resting cells and in mice [16,17], highlighting the importance of this protein for the VACV life cycle. Furthermore, by inducing epidermal growth factor receptor (EGFR) and mitogen-activated protein kinase (MAPK) signaling, VGF can stimulate proliferative responses [18–20], and VGF is important for the motility of infected cells, which facilitates viral spread [21]. VACV infection increases the demand for energy and macromolecules to support replication, and the induction of motility and proliferative responses also require additional energy [22,23]; therefore, VGF could represent a major factor involved in the induction of metabolic changes in VACV-infected cells. Remarkably, our global metabolic profiling of VACV-infected human foreskin fibroblasts (HFFs) showed that VACV infection increases the steady-state levels of several TCA cycle intermediates, including citrate [24]. The deletion of VGF rendered VACV unable to enhance citrate levels, indicating that the stimulation of citrate levels depends on VGF expression. Moreover, VACV infection stimulates the non-canonical phosphorylation of signal transducer and activator of transcription 3 (STAT3) at S727, in a VGF-dependent manner, and citrate

upregulation requires the activities of EGFR, MAPK, and STAT3 signaling [24]. This metabolic reprogramming is important for VACV replication because the inhibition of any of these pathways severely impairs viral replication [24–26].

The upregulation of citrate levels by VGF-induced EGFR, MAPK, and STAT3 signaling [24] provides a mechanistic explanation for the observed alteration in metabolism, centered around the TCA cycle during VACV infection. VACV increases OXPHOS activity, as indicated by increased oxygen consumption rates (OCRs) and ATP levels [3,27,28]. Although VACV induces the inactivation of several host proteins, the translation of OXPHOS-related mRNAs are selectively upregulated by VACV infection [28]. Additionally, VACV upregulates glutamine metabolism [2,3,29], and glutamine represents an important carbon source for the TCA cycle. A study by Greseth and Traktman demonstrated that VACV depends on *de novo* FA synthesis to generate an energy-favorable environment [3], which indicated that VACV might modulate FA metabolism, which represents another major carbon source for the TCA cycle. Although VGF is important for the upregulation of citrate levels, whether VGF expression is sufficient to induce the metabolic changes observed in VACV-infected cells remains unclear. The effects of VGF, which is secreted early during viral infection, on the modulation of other metabolic pathways will be important to examine in the future. Measurements of the metabolic flux that occurs upon VACV infection would provide additional insights into how VGF affects host cell metabolism in real-time. In addition, further studies remain necessary to determine whether the EGF homologs encoded by other poxviruses are similarly involved in rewiring the host metabolism and whether the same cellular signaling cascades are involved in these processes.

The involvement of other forms of RTKs in the rewiring of cellular metabolism following viral infection would also be important to explore. Baculovirus, a type of virus that

infects insects, encodes a fibroblast growth factor (FGF) [30] that is homologous to cellular FGF. The viral FGF, similar to VACV VGF, is essential for the stimulation of energy-consuming processes, such as cell migration [21,31]. Baculovirus infection upregulates several aspects of cell metabolism, including increased glucose and glutamine consumption, increased amino acid metabolism, and increased oxygen consumption [32,33]. These studies provide the basis for studying the role played by baculovirus FGF in the modulation of host metabolism.

Although viruses such as VACV and baculovirus encode and secrete their own growth factors, other viruses appear to stimulate growth factor signaling indirectly. Epstein-Barr virus (EBV), an oncogenic γ-herpesvirus, induces EGFR signaling via the viral latent membrane protein 1 (LMP1) [34]. Remarkably, LMP1-mediated FGF signaling is essential for increasing glucose metabolism in EBV-infected cells [35]. In human nasopharyngeal epithelial cells, LMP1 increases the uptake of glucose and glutamine, enhances the activity of lactate dehydrogenase A (LDHA), increases the production of lactate, reduces the activity of pyruvate kinase, and reduces the pyruvate concentrations [35]. Interestingly, the LMP1 protein of EBV also induces the activation of EGFR, extracellular signal-regulated kinase (ERK)-MAPK, and STAT3 phosphorylation (at both S727 and Y705) [36]. Further tests remain necessary to examine whether the metabolic changes that are induced by the EBV LMP1 protein mediate the activation of the EGFR-MAPK-STAT3 signaling axis and have similar metabolic effects as VACV VGF.

Severe acute respiratory syndrome coronavirus-2 (SARS-CoV-2), the causative agent underlying the current coronavirus disease 19 (COVID-19) pandemic, also induces growth factor signaling. A phosphoproteomics analysis of SARS-CoV-2 revealed the activation of GFR and downstream signaling molecules in infected cells [37]. Remarkably, the SARS-CoV-2 infection also increased the levels of several key enzymes associated with glycolysis, the TCA cycle, and

central carbon metabolism [37,38], which indicates the upregulation of these metabolic pathways at multiple levels. Furthermore, the inhibition of the GFR results in the severe suppression of SARS-CoV-2 replication [37], indicating the crucial role played by this pathway during COVID-19 progression. Further studies examining the correlation between the GFR pathway and the metabolic alterations that have been reported in SARS-CoV-2-infected cells could result in the identification of novel and effective therapeutic strategies against COVID-19.

Although direct effects on metabolic alteration have not yet been established for several other viruses, many viruses are known to co-opt the GFR signaling pathway to promote various stages of viral replication, such as entry, internalization, and the subversion of antiviral responses (reviewed in [12]). The dynamic interactions that occur between the gene products of HCMV, UL135 and UL138 govern the attenuation or sustainment of EGFR signaling [39]. Interestingly, UL138 is important for the induction of latency, and UL135 is essential for the reactivation of HCMV [40]. Because an active infection may be associated with different metabolic requirements than a latent infection, future studies that delineate the functions of these proteins and the EGFR pathway in metabolic changes are warranted, which could be used to identify novel approaches that can be applied to thwart HCMV infections. The influenza A virus (IAV), hepatitis C virus (HCV), and hepatitis B virus (HBV) are examples of the viruses that upregulate the EGFR pathway to increase virus uptake and internalization [41–43]. Furthermore, the IAV and rhinovirus-mediated activation of EGFR can result in the dampening of the interferon-gamma-mediated antiviral responses, which contributes to the establishment of a proviral environment [44]. As discussed later in this chapter, infections with these viruses can lead to profound changes in cellular metabolism. Further studies that elucidate the role played by the EGFR pathway or one of several signaling cascades downstream of EGFR could provide insights

into the complex interactions that occur between virus and host factors during the rewiring of cell metabolism and lead to the development of potent antiviral therapies.

PI3K-Akt-mTOR pathway

Because RTKs, such as GFRs, are activated upon the binding of membrane-localized receptors with extracellular ligands, they have the potential to govern the activation of several other metabolically important signaling cascades within a cell. The ubiquitous **PI3K–Akt pathway** is activated primarily by the binding of growth factors with extracellular receptors. Upon activation, PI3K recruits and activates other kinases, including **Akt,** to perform various functions [8]. The activation of the PI3K-Akt axis results in increased glucose uptake, the stimulation of enzyme activity by several key glycolytic enzymes, and an increase in the overall glycolytic rate of the cell (reviewed in [45]). In addition to enhancing glycolysis, Akt can promote lipid metabolism through several mechanisms. First, Akt serves as an important regulator of the enzyme ATP citrate lyase (ACLY), which converts the citrate transported out of mitochondria into acetyl coenzyme A (Acetyl-CoA), which is necessary for lipid synthesis [46]. Akt activation can lead to the indirect proteolytic release of sterol regulatory element-binding proteins (SREBPs) from the nucleus, leading to the induction of lipogenic genes that are important for lipid metabolism [47]. **Mammalian target of rapamycin (mTOR)** is another key regulator of cellular metabolism (Reviewed in [48]). mTOR is a key component of the multi-subunit mTORC1 and mTORC2 protein complexes, which sense and regulate amino acid metabolism to control protein synthesis, cell growth, and proliferation. The growth factor-induced activation of the PI3K-Akt pathway can activate mTORC1 or relieve it's inhibition [48]. Although mTORC1 acts downstream of Akt, mTORC2 acts upstream of Akt, widening the range of potential Akt substrates [49].

Because the PI3K-Akt-mTOR signaling pathway sits at the crossroads of several important cellular pathways, many viruses have evolved multiple mechanisms to target this pathway (**Fig. 1.1**) (Reviewed in [50]). Although the viral factors that interact with this pathway are known for some viruses, a huge gap exists in the knowledge of how most viruses act to repurpose this cascade for metabolic reprogramming. The VACV-mediated activation of the PI3K-Akt pathway early during infection is important for viral replication and host cell survival [51]. The inhibition of this pathway suppresses VACV replication, indicating the important role of this pathway in VACV replication (unpublished, [51]). Remarkably, we found that VACV infection leads to upregulation of ACLY phosphorylation at S455 (unpublished). The activation of ACLY, which is a key enzyme that governs FA metabolism, is positively regulated by Akt, which raises the interesting question of whether VGF is required to reprogram lipid synthesis and degradation in VACV-infected cells. Lipid metabolism is essential for VACV to create an energy-rich state capable of supporting the increased demands during virus replication [3]. Although, whether VGF or other VACV protein is involved in the upregulation of lipid metabolism remains unclear, we found that VACV infection increases the levels of carnitylated FAs, which are necessary for beta-oxidation [24]. Furthermore, the acylation of several VACV proteins is essential for capsid envelopment and egress from the infected cell [52]. VACV also depends on lipid rafts for entry into the cells [53], and integrin beta-1 (a lipid raft-associated protein) plays a key role in virus endocytosis through the PI3K-Akt pathway [54]. Further tests are required to determine to identities of the viral factors and host cascades involved in the modulation of lipid metabolism during VACV infection.

Several other viruses have also been shown to modulate the PI3K-Akt-mTOR pathway (**Fig 1.1, Table 1.1**); however, whether this modulation has direct impacts on metabolism

remains poorly understood. IAV has been shown to increase glycolysis, glucose uptake, and lactate excretion in a PI3K-Akt pathway-dependent manner [55]. The inhibition of this pathway suppresses glycolysis and, subsequently, reduces IAV replication and increases survival in a mouse model [55]. During which stage of IAV replication this metabolic regulation occurs, and which viral proteins are responsible remain unknown. The E6/E7 proteins expressed by human papillomavirus 16 (HPV16) are important for the activation of the PI3K-Akt pathway [56]. Interestingly, the E7 protein has been shown to be important for inducing glycolysis in HPV16-infected cells through the binding and activation of the glycolytic enzyme pyruvate kinase isozyme M2 (PKM2) [57]. Murine norovirus-infected macrophages have also been shown to upregulate glycolysis in the host cells by activating the Akt pathway, which is important during the early stages of viral replication [58]. Adenovirus E4-ORF1 is important for the activation of the PI3K-Akt pathway [59]. Although this activation is not responsible for inducing glycolysis in adenovirus-infected cells, the effects of this activation on a plethora of other metabolic changes that occur during adenovirus infection remain unknown [60].

Although some viruses activate the PI3K-Akt pathway to enhance glycolysis to support virus replication, others may do the opposite to ensure optimal survival. HCV, most likely through the core protein, suppresses the PI3K-Akt pathway via the binding of tumor necrosis factor-alpha, which inhibits the insulin receptor substrate and disrupts glucose metabolism by inhibiting glucose uptake, via the downregulation of the glucose transporter 4 (GLUT4) and the upregulation of phosphoenolpyruvate carboxykinase 2 (PCK2) [61,62]. In addition to viruses that infect mammalian cells, white spot syndrome virus, an invertebrate virus that infects arthropod cells, also induces glycolysis in a PI3K-Akt-mTOR dependent fashion [63]. The

conservation of metabolic alterations by virus-mediated changes in cell signaling across species indicates the importance of modulating metabolism for diverse viruses.

AMPK pathway

Another important regulator of cellular metabolism is the **AMPK pathway**, which is sometimes referred to as the "metabolic master switch." This pathway is activated in response to an increase in the AMP or ADP to ATP ratio due to a variety of physiological stresses or chemical inducers. Upon activation, this pathway leads to an increase in ATP synthesis via the activation of catabolic processes, such as the beta-oxidation of FAs [64]. Activated AMPK also triggers the destruction of existing defective mitochondria and enhances the synthesis of new mitochondria to support increased energy production during energy-deficient states. Through extensive crosstalk with the growth factor-initiated PI3K-Akt pathway, the AMPK pathway can also regulate the activity of mTORC to reprogram cellular metabolism [65]. Because of the key role played by AMPK in the regulation of cellular metabolism, several viruses have evolved strategies to hijack AMPK signaling (**Fig. 1.2**, **Table 1.1**) and remodel the host metabolome to promote efficient viral replication [66].

HCMV is among the best-studied models of virus-induced alterations to the host cell metabolism. HCMV induces profound changes in cellular metabolic pathways, including increased glycolysis, TCA cycle, glutamine metabolism, glutaminolysis, nucleotide metabolism, FA biosynthesis, and the production of secondary metabolites and signaling molecules such as prostaglandins [1]. HCMV-induced AMPK phosphorylation and activation are central to the induction of these metabolic activation pathways, which result in a conducive environment for viral replication [67]. The HCMV-mediated upregulation of AMPK results in increased glycolysis by enhancing glucose uptake via the upregulation of GLUT4 [67]. The inhibition of

AMPK not only reduces glycolytic flux but also suppresses HCMV replication. Interestingly, the HCMV-induced activation of AMPK results in increased catabolism and reduced anabolism, which limits cell growth [64] while simultaneously stimulating the level of metabolism overall. AMPK activation upon HCMV infection conditions is regulated by a calcium-calmodulin-dependent kinase kinase (CaMKK). One component that could be responsible for the activation of cellular AMPK is the viral immediate-early protein UL38. The expression of this protein is both necessary and sufficient to activate glycolysis by activating glucose consumption and lactate excretion; glutamine consumption and glutamate secretion; and the secretion of proline and alanine [68]. UL38 primarily binds to and inhibits the tuberous sclerosis protein complex 2 (TSC2) to activate the mTOR pathway, which is essential for maintaining a proviral environment [69]. Interestingly, the activation of glycolysis via UL38 is dependent on its ability to inhibit TSC2 [68], suggesting some interplay between the viral protein and the AMPK pathway. Additionally, HCMV proteins such as UL37, US28, US21, and UL146, which regulate calcium signaling, could also play an indirect role in the activation of the AMPK pathway due to major overlaps in the downstream consequences of AMPK and calcium signaling [70].

The dynamic regulation of AMPK was observed during the course of nerve cell infection with herpes simplex virus type 1 (HSV-1) [71]. At an early time point post-infection, HSV-1 downregulates the AMPK pathway to allow for the lipid and protein synthesis that is required for viral replication. This inhibition, however, gradually faded away after 4 h, occurring simultaneously with an increase in sirtuin 1 (SIRT1) expression. The maximum level of AMPK activation was observed later during the viral replication process. This increase in AMPK phosphorylation results in the induction of beta-oxidation and mitochondrial biogenesis, which support viral replication [71].

Simian virus 40 (SV40), an oncogenic polyomavirus, also activates AMPK pathways via its small T-antigen to maintain energy homeostasis during glucose deprivation by inhibiting mTOR and activating apoptosis as an alternate energy source [72]. Although AMPK acts as a proviral pathway, and most viruses tend to increase AMPK pathway activation, AMPK activation results in the suppression of HCV replication [73]. Although the viral proteins that regulate the suppression of AMPK during HCV infection remain to be elucidated, the loss of AMPK function appears to result in lipid accumulation in HCV-infected cells. Because the HCV life cycle heavily depends on cellular lipid levels, the accumulation of lipids could serve as a reservoir of the precursors required for HCV replication [73].

Hypoxia-inducible factor (HIF) pathway

Hypoxia-inducible factors (HIFs) are major regulators of cellular metabolism, especially during conditions of low oxygen availability (hypoxia) [74,75]. Because of the switch to aerobic glycolysis, they promote glucose consumption and lactate excretion [76]. By acting as transcriptional activators of several genes that promote the adaptation to hypoxic conditions, HIFs also modulate key metabolic functions, such as FA, cholesterol, and mitochondrial metabolism [77], which are prime targets of viruses (**Fig. 1.3**, **Table 1.1**).

One very well-studied example of virus-mediated HIF modulation is the VACV C16 protein-mediated stabilization of HIF-1α [4]. VACV C16 binds directly and specifically to the human oxygen-sensing enzyme prolyl-hydroxylase domain-containing protein (PHD)2, inhibiting the PHD2-dependent hydroxylation of HIF-1α. The stabilization of HIF-1α by VACV results in the generation of a hypoxic environment, even under normoxic conditions. The infection of cells with a recombinant virus lacking the C16 protein resulted in the decreased transcription of HIF-1α-responsive genes, such as vascular endothelial growth factor (VEGF),

pyruvate dehydrogenase kinase 1 (PDK-1), and GLUT-1, which are important regulators of cellular metabolism [4]. The C16 protein of VACV, which is essential for HIF-1 activation, was found to be important for the upregulation of glutamine metabolism [29]. VACV-induced HIF-1α stabilization, however, did not result in an increase in lactate or a decrease in TCA cycle intermediates [29], which would be expected during a hypoxic response. In fact, we observed an increase in TCA cycle intermediates in VACV-infected cells [24], which appeared to be mediated, at least in part, by VGF-induced, non-canonical STAT3 phosphorylation. Several studies have shown that glutamine metabolism is important for VACV replication [2,3,29]. We found that asparagine, an amino acid whose biosynthesis exclusively depends on glutamine, was able to rescue VACV replication from glutamine depletion, and asparagine is required for efficient viral protein synthesis, especially at later stages of VACV infection [78,79]. These studies elucidating the role played by C16 in the enhancement of glutamine metabolism, and the role played by VGF in the upregulation of TCA cycle metabolites revealed new avenues for exploration to identify other potential viral and cellular factors that might interact at the metabolic interface during VACV infection. Signaling pathways mediated by EGF, the cellular homolog of VGF, are also important for HIF stabilization via PI3K-Akt pathway activation in cancer cells [80]; therefore, the determination of whether VACV VGF induces metabolic alterations in a HIF-1α-dependent manner would be interesting to explore. How and whether C16 and VGF might act together to rewire host cell metabolism in VACV-infected cells could also be examined by generating a recombinant VACV that lacks both of these proteins.

Although the molecular mechanisms and metabolic consequences of HIF-1α activation are not yet fully understood, this pathway is associated with several other viruses. The E6 and E7 viral proteins of HPV induce HIF-1α activation, which may contribute to the observed induction

of glycolysis following viral infection [81]. The E6 protein attenuates interactions between the von Hippel-Lindau tumor suppressor (VHL) and HIF-1α, which induces the Warburg effect in HPV-infected cells. The HPV E7 protein, which also enhances HIF-1α activity, directly interacts with the PKM2 enzyme, potentially diverting glycolytic intermediates toward anabolic metabolism [57,82]. The E2 protein of human papillomavirus HPV18 also interacts with the mitochondrial membrane to induce the production of reactive oxygen species and induce glycolysis by activating HIF-1α [83].

HBV infection results in profound changes in cellular metabolism, which can affect glycolysis, lipids, amino acids, vitamins, and nucleic acids. The HBV-induced increase in glycolysis has been attributed to at least three proteins; HBV core protein (HBc) [84]; HBV pre-S2 mutant protein, which upregulates the expression and cell membrane localization of the glucose transporter GLUT4 [85]; and the HBV X protein (HBx), which upregulates glucose-6-phosphate dehydrogenase (G6PD) and multiple other enzymes involved in gluconeogenesis [86,87]. HBx is also important for the stabilization of HIF-1α [88]. However, a direct association between the HBx-induced HIF-1α stabilization and alterations in cellular metabolism has not yet been established. Because HBx is necessary for the activation of major metabolic pathways, such as the AMPK and mTORC1 pathways [89], the signaling crosstalk between HIF-1α and other metabolic pathways are likely responsible for the altered metabolism observed in HBV-infected cells.

In addition to activating several key metabolic pathways, such as those associated with the fibroblast growth factor receptor 1 (FGFR)1, PI3K-Akt, and ERK-MAPK, the LMP1 protein of EBV enhances the degradation of PHD1 and PHD3 to activate HIF-1α [90], which upregulates glycolysis through the upregulation of PKM2 and PDH2 [91,92]. Moreover, LMP1

upregulates the key glycolytic enzyme hexokinase 2 (HK2) [93] and the glucose transporter GLUT1 (in an mTORC1-dependent manner) [94], contributing to enhanced glycolysis and indicating the existence of metabolic crosstalk in signaling pathways induced by viral proteins. Another potential mechanism for the induction of glycolysis in EBV-infected cells is the viral protein EBNA3- and EBNA5-mediated stabilization of HIF-1α [95].

Another example of a virus that stabilizes HIF-1α to upregulate glycolysis is Kaposi's sarcoma-associated herpesvirus (KSHV). KSHV infection upregulates HIF-1α and HIF-responsive glycolytic genes, such as PKM2, HK, GLUT1, and PDK1, through viral micro RNAs (miRNAs), and G-protein-coupled receptors (GPCRs) [96–98]. The latency-associated nuclear antigen (LANA), which is necessary for HIF-1α stabilization and nuclear translocation, and the induction of glucose transporter genes, such as GLUT1, is a candidate among several KSHV proteins that might mediate glycolysis in KSHV-transformed cells [99]. Although the viral proteins responsible for the is process have not been identified, HCV stabilizes HIF-1α, upregulating glycolytic enzymes and suppressing OXPHOS activities during HCV infection [100].

Other examples of virus-mediated HIF-1α stabilization and metabolic regulation include the respiratory syncytial virus (RSV) [101] and the H1N1 variant of IAV [102]. A significant shift in metabolism toward glycolysis and the pentose phosphate pathway was observed during RSV infection in human small alveolar epithelial cells [101]. The suppression of HIF-1α also resulted in the reduction of HK2, PDK1, and VEGF levels and reduced viral titers, suggesting the important role of this pathway in the upregulation in RSV replication [101]. The H1N1 IAV variant increases GLUT1 levels by stabilizing HIF-1α via the inhibition of the proteasome and a decrease in factor inhibiting HIF-1 (FIH-1) expression [102]. This mechanism could partially

explain the observed increase in glycolysis, glucose uptake, and lactate excretion during early IAV infection [55,103]. Although the exact metabolic consequence remains unclear, the human immunodeficiency virus type 1 (HIV-1) viral protein Vpr induces the stabilization of HIF-1α [104], resulting in the induction of two key glycolytic enzymes, HK and PKM2 [105].

Oncogenes and tumor suppressors

Several viruses modulate host metabolism by interacting with cellular **oncogenes** (e.g., Myc) **and tumor suppressors** (e.g., p53) or introducing virus-specific oncogenes [7]. Oncogenes and tumor suppressors are important regulators of cellular metabolism [106]. Mutations that result in the activation of KRas or Myc proteins also induce metabolically favorable environments for cell proliferation. The activation of these oncogenes can induce glycolysis, OXPHOS, pentose phosphate pathways, and lactate production. Moreover, KRas and Myc activation result in increased glutamine uptake to feed the TCA cycle for energy production, a process known as glutaminolysis [107]. In addition to activating key lipid metabolism enzymes and nucleotide biosynthesis, Myc is also involved in the biogenesis of organelles, such as mitochondria and ribosomes [107,108]. Tumor suppressors, including but not limited to p53, phosphatase and tensin homolog (PTEN), SIRT3, and SIRT6, also act on several stages of metabolism [7]. The role played by p53 in metabolism has been extensively studied. The wild-type (WT) p53 protein activates mitochondrial metabolism and lipid catabolism, suppressing glycolysis and lipid synthesis, whereas the gain of function mutation in p53 leads to the exact opposite functions [109,110].

An excellent example of the virus-induced activation of the Myc oncogene has been observed in adenovirus-infected cells (**Fig. 1.4**, **Table 1.1**). The infection of a non-tumorigenic breast epithelial cell line with WT adenovirus 5 (Ad5) strain induced glycolytic metabolism,

indicated by increased glucose consumption and lactate production and decreased oxygen consumption [60]. The E4ORF1 protein of Ad5 is sufficient to increase glucose metabolism in infected cells, binding to and activating Myc to increase the transcription of key glycolytic enzymes, including HK2 and PFKM [60]. A point mutation that results in the D68A substitution mutation in E4ORF1 abolishes the ability to activate Myc or activate glycolysis, resulting in replication suppression [60]. The E4ORF1-mediated activation of Myc is not only important for the activation of glycolysis but also for altering glutamine metabolism [111]. Myc activation is necessary for the Ad5-induced increase in glutamine utilization, including the increased expression of glutamine transporters and glutaminolysis enzymes, such as glutaminase (GLS) [111]. The observed decrease in the OCR following AD5 infection, however, is independent of the E4ORF1-induced activation of Myc [60]. Interestingly, the adenovirus E1A protein is also involved in Myc activation [112]. Furthermore, E1A and E1B-55K can induce the suppression of the tumor suppressor p53 [113]. Although the metabolic consequences of these changes remain largely unknown, these findings suggest that the E1A and E1B proteins could also be important for altered cellular metabolism during adenovirus infection [114].

Other viruses that interact with oncogenes or tumor suppressors to increase replication efficiency include KSHV, EBV, HPV, and HCV. The latent KSHV infection of endothelial cells induces the expression and upregulation of Myc, and the targets of Myc including the glutamine transporter SLC1A5, which could explain the upregulation of glutamine uptake and glutamine addiction during KSHV infection [115]. The viral proteins LANA expressed by KSHV, basic leucine zipper nuclear factor 1 (BZLF1) expressed by EBV, E6 expressed by HPV, and NS3 and NS5 expressed by HCV all downregulate the tumor suppressor p53 [116–119]. The impact of this suppression on the observed changes in host metabolism during infections remains unclear.

Other mechanisms

In addition to altering signaling pathways, cellular metabolism could be regulated through **feedback activation/inhibition** mechanisms mediated by various metabolites and byproducts [120]. Several key enzymes and metabolic regulators, such as carbohydrate response element-binding protein (ChREBP) and SREBP, could also exert regulatory functions on the metabolic activities of cells [121]. Viruses seem likely to have evolved mechanisms designed to directly interact with the key metabolic enzymes and regulators found in host cells.

HCMV infection upregulates the levels of Acetyl-CoA carboxylase 1 (ACC1), the rate-limiting enzyme involved in FA biosynthesis [122,123], through two separate mechanisms. First, HCMV infection results in the activation of SREBP-2 [122], the master regulator of sterol biosynthesis [124], which activates ACC1 in an mTORC1 activation-dependent manner [122]. Second, HCMV induces lipogenesis through the proteolytic cleavage and activation of SREBP-1, a major regulator of FA biosynthesis [125] to activate ACC1[123]. The viral protein UL38, which interacts with and inhibits TSC1/2 to activate mTORC1 [69], could also play a key role in the modulation of FA metabolism in HCMV-infected cells.

Another case of interaction between viral and host metabolic factors is the interaction between the dengue virus (DENV) non-structural protein 3 (NS3) and the host cell FA synthase (FASN), a key enzyme necessary for FA biosynthesis [126]. By binding with FASN, NS3 relocates the host enzyme to the virus replication site, increasing the rate of FA biosynthesis [126]. Another great example is the direct interaction between the DENV NS1 and the cellular glycolytic enzyme glyceraldehyde-3-phosphate dehydrogenase (GAPDH) [127]. Interestingly, the DENV infection requires glycolysis for optimal replication [128] and induces glycolytic processes by upregulating the levels of GLUT1 and HK [128]. The binding between DENV NS1

and GAPDH increases GAPDH activity [127] and could represent one example of an interaction between a viral and host factor that elevates glycolysis. Mechanistic studies that identify these interactions can provide a platform for the development of therapeutics against the viral pathogen.

Concluding remarks, limitations of the current studies, and outlook for the future

In summary, virus-induced metabolic alterations generally support viral replication. The central theme of these alterations suggests that interactions between one or more viral factors and various cellular factors can affect metabolic regulation. Although some of the key players involved in the virus-mediated hijacking of cellular metabolism have been identified, several remain unknown. In some cases, a single viral protein can regulate several different host factors, whereas in other cases, similar effects require multiple proteins. Significant crosstalk occurs among the various signaling pathways that govern metabolism, posing the unique challenge of carefully teasing apart the roles played by viral factors in repurposing cellular metabolism.

Although we attempted to review the mechanisms through which viruses hijack cellular signaling to rewire host metabolism, there is a striking lack of mechanistic studies in the field of viral metabolism. Many studies have conferred the functions of viral proteins to key metabolic regulators without describing specific metabolic phenotypes. Conversely, several viruses have been identified to alter key signaling pathways related to metabolism, but the effects of these alterations on host metabolism have not been elucidated. A deeper understanding of metabolic signaling remains crucial for the development of therapeutics that target metabolic pathways in viral infections. Additional studies remain necessary to identify viral and host factors that interact at the metabolic interface.

Although viruses are known to induce metabolic perturbations, and these changes are important for viral replication, the exact stages of viral replication for which these metabolic pathways are important have not been elucidated for several viruses. Alternatively, because the host provides the resources and precursors necessary for viral replication, the effects of the host's metabolic status on viral replication could represent a fertile ground for future research. A better understanding of the dependence of specific viral replication stages on specific metabolic pathways will clarify why viruses target distinct metabolic aspects. Similarly, by understanding the effects of the host metabolic status on virus replication, we could identify mediators of viral tropism by revealing whether some cells are more susceptible to viral infection than others. Susceptibility differences could also explain discrepancies observed in the metabolic reprogramming profiles of different cells following infection with the same virus.

Another major limitation of current studies is that most explorations of virus-host cell metabolism are performed in cultured cells, which have drastically different metabolic profiles from animal models. Most cells in an animal model are quiescent, with reduced metabolic activity, in contrast with the proliferating cells used in most studies. Different tissues and organs might also have different metabolic statuses that might affect tropism and viral infectivity. Furthermore, animal metabolism is governed by the diet and immune system activity of the host, and the effects of these regulations represent understudied areas in the field of virus-host metabolic alterations. Viruses may target metabolism to alter the immune status of a cell or to evade immune clearance. Conversely, viral infection-induced metabolic alterations could trigger immune activation or the activation of antiviral pathways. Some immune cells detect viral metabolites and pathways altered by viruses, adding layers of complexity. Additional *in vivo* studies examining the effects of virus-induced alterations in metabolism are necessary to provide

a better understanding of viral metabolism and the potential development of effective antiviral therapeutics.

Most current studies examining alterations in metabolic processes upon viral infection focus on steady-state metabolite levels. Because metabolism is a dynamic process that can involve rapid changes in the uptake, synthesis, and degradation of biomolecules, observed increases in the levels of certain metabolites could result in multiple interpretations that indicate various, sometimes opposing outcomes. For example, an increase in the steady-state levels of any given metabolite could indicate either increased synthesis or reduced consumption. To overcome these challenges, whenever possible, metabolomics should be coupled with studies that define the ongoing metabolic activities. A better understanding of the interactions between viruses and host metabolism can be achieved through the careful design and rigorous interpretation of metabolic flux profiling. Coupling these studies with studies examining the activation or suppression of enzymatic activities using chemical and genetic approaches could provide detailed pictures of the metabolic landscapes of virus-infected cells.

A great degree of similarity exists between the metabolic alterations that occur following viral infection and those induced by cancer. Studies examining cancer cell metabolism have been instrumental for our understanding of cell metabolism in response to viral infection. Although several viruses have been found to interact with and alter tumor suppressors and oncogenes during the process of rewiring cellular metabolism, whether these metabolic perturbations lead to the transformation of infected cells in a manner that promotes cancer development remains unclear. A better understanding of the virus-induced changes in cell signaling that result in metabolic reprogramming may also identify fundamental mechanisms involved in the regulation of cellular metabolism and the metabolic regulation that occurs during cancer. In addition to

cancers, the study of virus-host interaction at the metabolic interface could also shed light on the progression of various metabolic disorders, such as obesity, dyslipidemia, and increased glucose levels. Metabolic disorders may increase the risk of certain viral diseases, including influenza and coronaviruses [129], whereas other viruses, such as HCV and HIV, might induce metabolic disorders [130]. Additionally, metabolic disorders may impair the immunological response of the host, facilitating viral infections that can worsen the severity of metabolic disorders [129]. The study of virus-induced metabolic alterations might also provide avenues for the development of novel strategies to combat metabolic disorders.

Overall, the study of virus-host metabolism is likely to facilitate the identification of various therapeutic windows associated with the viral dependence on specific enzymes or nutrients, which can be utilized to develop novel therapies against viral diseases and other metabolism-associated pathologies, including cancer.

References

1. Rodríguez-Sánchez I, Munger J. Meal for Two: Human Cytomegalovirus-Induced Activation of Cellular Metabolism. Viruses. 2019;11: 273. doi:10.3390/v11030273

2. Fontaine KA, Camarda R, Lagunoff M. Vaccinia Virus Requires Glutamine but Not Glucose for Efficient Replication. J Virol. 2014;88: 4366–4374. doi:10.1128/JVI.03134-13

3. Greseth MD, Traktman P. De novo Fatty Acid Biosynthesis Contributes Significantly to Establishment of a Bioenergetically Favorable Environment for Vaccinia Virus Infection. PLOS Pathog. 2014;10: e1004021. doi:10.1371/journal.ppat.1004021

4. Mazzon M, Peters NE, Loenarz C, Krysztofinska EM, Ember SWJ, Ferguson BJ, et al. A mechanism for induction of a hypoxic response by vaccinia virus. Proc Natl Acad Sci. 2013;110: 12444–12449. doi:10.1073/pnas.1302140110

5. Sanchez EL, Lagunoff M. Viral activation of cellular metabolism. Virology. 2015;479–480: 609–618. doi:10.1016/j.virol.2015.02.038

6. Thaker SK, Ch'ng J, Christofk HR. Viral hijacking of cellular metabolism. BMC Biol. 2019;17: 59. doi:10.1186/s12915-019-0678-9

7. Eisenreich W, Rudel T, Heesemann J, Goebel W. How Viral and Intracellular Bacterial Pathogens Reprogram the Metabolism of Host Cells to Allow Their Intracellular Replication. Front Cell Infect Microbiol. 2019;9. doi:10.3389/fcimb.2019.00042

8. Ward PS, Thompson CB. Signaling in Control of Cell Growth and Metabolism. Cold Spring Harb Perspect Biol. 2012;4. doi:10.1101/cshperspect.a006783

9. Berg JM, Tymoczko JL, Stryer L. The Citric Acid Cycle. Biochem 5th Ed. 2002 [cited 5 Mar 2020]. Available: https://www.ncbi.nlm.nih.gov/books/NBK21163/

10. Thompson CB, Bielska AA. Growth factors stimulate anabolic metabolism by directing nutrient uptake. J Biol Chem. 2019;294: 17883–17888. doi:10.1074/jbc.AW119.008146

11. Hanahan D, Weinberg RA. Hallmarks of Cancer: The Next Generation. Cell. 2011;144: 646–674. doi:10.1016/j.cell.2011.02.013

12. Hondermarck H, Bartlett NW, Nurcombe V. The role of growth factor receptors in viral infections: An opportunity for drug repurposing against emerging viral diseases such as COVID-19? FASEB BioAdvances. 2020;2: 296–303. doi:10.1096/fba.2020-00015

13. Lateef Z, Wise LM. Exploitation of receptor tyrosine kinases by viral-encoded growth factors. Growth Factors. 2018;36: 118–140. doi:10.1080/08977194.2018.1520229

14. Blomquist MC, Hunt LT, Barker WC. Vaccinia virus 19-kilodalton protein: relationship to several mammalian proteins, including two growth factors. Proc Natl Acad Sci. 1984;81: 7363–7367. doi:10.1073/pnas.81.23.7363

15. Chang W, Lim JG, Hellström I, Gentry LE. Characterization of vaccinia virus growth factor biosynthetic pathway with an antipeptide antiserum. J Virol. 1988;62: 1080–1083.

16. Buller RM, Chakrabarti S, Cooper JA, Twardzik DR, Moss B. Deletion of the vaccinia virus growth factor gene reduces virus virulence. J Virol. 1988;62: 866–874.

17. Lai AC, Pogo BG. Attenuated deletion mutants of vaccinia virus lacking the vaccinia growth factor are defective in replication in vivo. Microb Pathog. 1989;6: 219–226. doi:10.1016/0882-4010(89)90071-5

18. Bonjardim CA. Viral exploitation of the MEK/ERK pathway – A tale of vaccinia virus and other viruses. Virology. 2017;507: 267–275. doi:10.1016/j.virol.2016.12.011

19. Postigo A, Martin MC, Dodding MP, Way M. Vaccinia-induced epidermal growth factor receptor-MEK signalling and the anti-apoptotic protein F1L synergize to suppress cell death during infection. Cell Microbiol. 2009;11: 1208–1218. doi:10.1111/j.1462-5822.2009.01327.x

20. Twardzik DR, Brown JP, Ranchalis JE, Todaro GJ, Moss B. Vaccinia virus-infected cells release a novel polypeptide functionally related to transforming and epidermal growth factors. Proc Natl Acad Sci. 1985;82: 5300–5304. doi:10.1073/pnas.82.16.5300

21. Beerli C, Yakimovich A, Kilcher S, V. Reynoso G, Fläschner G, Müller D, et al. Vaccinia virus hijacks EGFR signalling to enhance virus spread through rapid and directed infected cell motility. Nat Microbiol. 2018;4. doi:10.1038/s41564-018-0288-2

22. Antico Arciuch VG, Elguero ME, Poderoso JJ, Carreras MC. Mitochondrial Regulation of Cell Cycle and Proliferation. Antioxid Redox Signal. 2012;16: 1150–1180. doi:10.1089/ars.2011.4085

23. El-Bacha T, Da Poian AT. Virus-induced changes in mitochondrial bioenergetics as potential targets for therapy. Int J Biochem Cell Biol. 2013;45: 41–46. doi:10.1016/j.biocel.2012.09.021

24. Pant A, Dsouza L, Cao S, Peng C, Yang Z. Viral growth factor- and STAT3 signaling-dependent elevation of the TCA cycle intermediate levels during vaccinia virus infection. PLOS Pathog. 2021;17: e1009303. doi:10.1371/journal.ppat.1009303

25. Andrade AA, Silva PNG, Pereira ACTC, de SOUSA LP, Ferreira PCP, Gazzinelli RT, et al. The vaccinia virus-stimulated mitogen-activated protein kinase (MAPK) pathway is required for virus multiplication. Biochem J. 2004;381: 437–446. doi:10.1042/BJ20031375

26. Langhammer S, Koban R, Yue C, Ellerbrok H. Inhibition of poxvirus spreading by the anti-tumor drug Gefitinib (Iressa™). Antiviral Res. 2011;89: 64–70. doi:10.1016/j.antiviral.2010.11.006

27. Chang C-W, Li H-C, Hsu C-F, Chang C-Y, Lo S-Y. Increased ATP generation in the host cell is required for efficient vaccinia virus production. J Biomed Sci. 2009;16: 80. doi:10.1186/1423-0127-16-80

28. Dai A, Cao S, Dhungel P, Luan Y, Liu Y, Xie Z, et al. Ribosome Profiling Reveals Translational Upregulation of Cellular Oxidative Phosphorylation mRNAs during Vaccinia Virus-Induced Host Shutoff. J Virol. 2017;91. doi:10.1128/JVI.01858-16

29. Mazzon M, Castro C, Roberts LD, Griffin JL, Smith GL. A role for vaccinia virus protein C16 in reprogramming cellular energy metabolism. J Gen Virol. 2015;96: 395–407. doi:10.1099/vir.0.069591-0

30. Ayres MD, Howard SC, Kuzio J, Lopez-Ferber M, Possee RD. The complete DNA sequence of Autographa californica nuclear polyhedrosis virus. Virology. 1994;202: 586–605. doi:10.1006/viro.1994.1380

31. Detvisitsakun C, Berretta MF, Lehiy C, Passarelli AL. Stimulation of cell motility by a viral fibroblast growth factor homolog: Proposal for a role in viral pathogenesis. Virology. 2005;336: 308–317. doi:10.1016/j.virol.2005.03.013

32. Palomares LA, López S, Ramírez OT. Utilization of oxygen uptake rate to assess the role of glucose and glutamine in the metabolism of infected insect cell cultures. Biochem Eng J. 2004;19: 87–93. doi:10.1016/j.bej.2003.12.002

33. Wong TKK, Nielsen LK, Greenfield PF, Reid S. Relationship between oxygen uptake rate and time of infection of Sf9 insect cells infected with a recombinant baculovirus. Cytotechnology. 1994;15: 157–167. doi:10.1007/BF00762390

34. Miller WE, Mosialos G, Kieff E, Raab-Traub N. Epstein-Barr virus LMP1 induction of the epidermal growth factor receptor is mediated through a TRAF signaling pathway distinct from NF-kappaB activation. J Virol. 1997;71: 586–594. doi:10.1128/JVI.71.1.586-594.1997

35. Lo AK-F, Dawson CW, Young LS, Ko C-W, Hau P-M, Lo K-W. Activation of the FGFR1 signalling pathway by the Epstein–Barr virus-encoded LMP1 promotes aerobic glycolysis and transformation of human nasopharyngeal epithelial cells. J Pathol. 2015;237: 238–248. doi:https://doi.org/10.1002/path.4575

36. Kung C-P, Meckes DG, Raab-Traub N. Epstein-Barr Virus LMP1 Activates EGFR, STAT3, and ERK through Effects on PKCδ. J Virol. 2011;85: 4399–4408. doi:10.1128/JVI.01703-10

37. Klann K, Bojkova D, Tascher G, Ciesek S, Münch C, Cinatl J. Growth Factor Receptor Signaling Inhibition Prevents SARS-CoV-2 Replication. Mol Cell. 2020;80: 164-174.e4. doi:10.1016/j.molcel.2020.08.006

38. Bojkova D, Klann K, Koch B, Widera M, Krause D, Ciesek S, et al. Proteomics of SARS-CoV-2-infected host cells reveals therapy targets. Nature. 2020;583: 469–472. doi:10.1038/s41586-020-2332-7

39. Buehler J, Zeltzer S, Reitsma J, Petrucelli A, Umashankar M, Rak M, et al. Opposing Regulation of the EGF Receptor: A Molecular Switch Controlling Cytomegalovirus Latency and Replication. PLOS Pathog. 2016;12: e1005655. doi:10.1371/journal.ppat.1005655

40. Umashankar M, Rak M, Bughio F, Zagallo P, Caviness K, Goodrum F. Antagonistic Determinants Controlling Replicative and Latent States of Human Cytomegalovirus Infection. J Virol. 2014 [cited 20 Jan 2021]. doi:10.1128/JVI.03506-13

41. Eierhoff T, Hrincius ER, Rescher U, Ludwig S, Ehrhardt C. The Epidermal Growth Factor Receptor (EGFR) Promotes Uptake of Influenza A Viruses (IAV) into Host Cells. PLOS Pathog. 2010;6: e1001099. doi:10.1371/journal.ppat.1001099

42. Iwamoto M, Saso W, Sugiyama R, Ishii K, Ohki M, Nagamori S, et al. Epidermal growth factor receptor is a host-entry cofactor triggering hepatitis B virus internalization. Proc Natl Acad Sci. 2019;116: 8487–8492. doi:10.1073/pnas.1811064116

43. Lupberger J, Zeisel MB, Xiao F, Thumann C, Fofana I, Zona L, et al. EGFR and EphA2 are host factors for hepatitis C virus entry and possible targets for antiviral therapy. Nat Med. 2011;17: 589–595. doi:10.1038/nm.2341

44. Ueki IF, Min-Oo G, Kalinowski A, Ballon-Landa E, Lanier LL, Nadel JA, et al. Respiratory virus–induced EGFR activation suppresses IRF1-dependent interferon λ and antiviral defense in airway epithelium. J Exp Med. 2013;210: 1929–1936. doi:10.1084/jem.20121401

45. Robey RB, Hay N. Is Akt the "Warburg kinase"?—Akt-energy metabolism interactions and oncogenesis. Semin Cancer Biol. 2009;19: 25–31. doi:10.1016/j.semcancer.2008.11.010

46. Berwick DC, Hers I, Heesom KJ, Moule SK, Tavare JM. The identification of ATP-citrate lyase as a protein kinase B (Akt) substrate in primary adipocytes. J Biol Chem. 2002;277: 33895–33900. doi:10.1074/jbc.M204681200

47. Porstmann T, Griffiths B, Chung Y-L, Delpuech O, Griffiths JR, Downward J, et al. PKB/Akt induces transcription of enzymes involved in cholesterol and fatty acid biosynthesis via activation of SREBP. Oncogene. 2005;24: 6465–6481. doi:10.1038/sj.onc.1208802

48. Laplante M, Sabatini DM. mTOR Signaling. Cold Spring Harb Perspect Biol. 2012;4. doi:10.1101/cshperspect.a011593

49. Oh WJ, Wu C, Kim SJ, Facchinetti V, Julien L-A, Finlan M, et al. mTORC2 can associate with ribosomes to promote cotranslational phosphorylation and stability of nascent Akt polypeptide. EMBO J. 2010;29: 3939–3951. doi:10.1038/emboj.2010.271

50. Dunn EF, Connor JH. Chapter 9 - HijAkt: The PI3K/Akt Pathway in Virus Replication and Pathogenesis. In: Shenolikar S, editor. Progress in Molecular Biology and Translational Science. Academic Press; 2012. pp. 223–250. doi:10.1016/B978-0-12-396456-4.00002-X

51. Soares JAP, Leite FGG, Andrade LG, Torres AA, Sousa LPD, Barcelos LS, et al. Activation of the PI3K/Akt Pathway Early during Vaccinia and Cowpox Virus Infections Is Required for both Host Survival and Viral Replication. J Virol. 2009;83: 6883–6899. doi:10.1128/JVI.00245-09

52. Grosenbach DW, Hruby DE. Biology of vaccinia virus acylproteins. Front Biosci J Virtual Libr. 1998;3: d354-364. doi:10.2741/a280

53. Chung C-S, Huang C-Y, Chang W. Vaccinia Virus Penetration Requires Cholesterol and Results in Specific Viral Envelope Proteins Associated with Lipid Rafts. J Virol. 2005;79: 1623–1634. doi:10.1128/JVI.79.3.1623-1634.2005

54. Izmailyan R, Hsao J-C, Chung C-S, Chen C-H, Hsu PW-C, Liao C-L, et al. Integrin β1 Mediates Vaccinia Virus Entry through Activation of PI3K/Akt Signaling. J Virol. 2012;86: 6677–6687. doi:10.1128/JVI.06860-11

55. Smallwood HS, Duan S, Morfouace M, Rezinciuc S, Shulkin BL, Shelat A, et al. Targeting Metabolic Reprogramming by Influenza Infection for Therapeutic Intervention. Cell Rep. 2017;19: 1640–1653. doi:10.1016/j.celrep.2017.04.039

56. Zhang L, Wu J, Ling MT, Zhao L, Zhao K-N. The role of the PI3K/Akt/mTOR signalling pathway in human cancers induced by infection with human papillomaviruses. Mol Cancer. 2015;14: 87. doi:10.1186/s12943-015-0361-x

57. Zwerschke W, Mazurek S, Massimi P, Banks L, Eigenbrodt E, Jansen-Dürr P. Modulation of type M2 pyruvate kinase activity by the human papillomavirus type 16 E7 oncoprotein. Proc Natl Acad Sci. 1999;96: 1291–1296. doi:10.1073/pnas.96.4.1291

58. Passalacqua KD, Lu J, Goodfellow I, Kolawole AO, Arche JR, Maddox RJ, et al. Glycolysis Is an Intrinsic Factor for Optimal Replication of a Norovirus. mBio. 2019;10. doi:10.1128/mBio.02175-18

59. Frese KK, Lee SS, Thomas DL, Latorre IJ, Weiss RS, Glaunsinger BA, et al. Selective PDZ protein-dependent stimulation of phosphatidylinositol 3-kinase by the adenovirus E4-ORF1 oncoprotein. Oncogene. 2003;22: 710–721. doi:10.1038/sj.onc.1206151

60. Thai M, Graham NA, Braas D, Nehil M, Komisopoulou E, Kurdistani SK, et al. Adenovirus E4ORF1-induced MYC activation promotes host cell anabolic glucose metabolism and virus replication. Cell Metab. 2014;19: 694–701. doi:10.1016/j.cmet.2014.03.009

61. Banerjee S, Saito K, Ait-Goughoulte M, Meyer K, Ray RB, Ray R. Hepatitis C Virus Core Protein Upregulates Serine Phosphorylation of Insulin Receptor Substrate-1 and Impairs the Downstream Akt/Protein Kinase B Signaling Pathway for Insulin Resistance. J Virol. 2008;82: 2606–2612. doi:10.1128/JVI.01672-07

62. Kawaguchi T, Yoshida T, Harada M, Hisamoto T, Nagao Y, Ide T, et al. Hepatitis C Virus Down-Regulates Insulin Receptor Substrates 1 and 2 through Up-Regulation of Suppressor of Cytokine Signaling 3. Am J Pathol. 2004;165: 1499–1508.

63. Su M-A, Huang Y-T, Chen I-T, Lee D-Y, Hsieh Y-C, Li C-Y, et al. An Invertebrate Warburg Effect: A Shrimp Virus Achieves Successful Replication by Altering the Host Metabolome via the PI3K-Akt-mTOR Pathway. PLOS Pathog. 2014;10: e1004196. doi:10.1371/journal.ppat.1004196

64. Herzig S, Shaw RJ. AMPK: guardian of metabolism and mitochondrial homeostasis. Nat Rev Mol Cell Biol. 2018;19: 121–135. doi:10.1038/nrm.2017.95

65. Mihaylova MM, Shaw RJ. The AMPK signalling pathway coordinates cell growth, autophagy and metabolism. Nat Cell Biol. 2011;13: 1016–1023. doi:10.1038/ncb2329

66. Moreira D, Silvestre R, Cordeiro-Da-Silva A, Estaquier J, Foretz M, Viollet B. AMP-activated protein kinase as a target for pathogens: friends or foes? Curr Drug Targets. 2016;17: 942–953.

67. McArdle J, Moorman NJ, Munger J. HCMV Targets the Metabolic Stress Response through Activation of AMPK Whose Activity Is Important for Viral Replication. PLOS Pathog. 2012;8: e1002502. doi:10.1371/journal.ppat.1002502

68. Rodríguez-Sánchez I, Schafer XL, Monaghan M, Munger J. The Human Cytomegalovirus UL38 protein drives mTOR-independent metabolic flux reprogramming by inhibiting TSC2. PLOS Pathog. 2019;15: e1007569. doi:10.1371/journal.ppat.1007569

69. Moorman NJ, Cristea IM, Terhune SS, Rout MP, Chait BT, Shenk T. Human Cytomegalovirus Protein UL38 Inhibits Host Cell Stress Responses by Antagonizing the Tuberous Sclerosis Protein Complex. Cell Host Microbe. 2008;3: 253–262. doi:10.1016/j.chom.2008.03.002

70. Dunn DM, Munger J. Interplay Between Calcium and AMPK Signaling in Human Cytomegalovirus Infection. Front Cell Infect Microbiol. 2020;10. doi:10.3389/fcimb.2020.00384

71. Martin C, Leyton L, Arancibia Y, Cuevas A, Zambrano A, Concha MI, et al. Modulation of the AMPK/Sirt1 axis during neuronal infection by herpes simplex virus type 1. J Alzheimers Dis JAD. 2014;42: 301–312. doi:10.3233/JAD-140237

72. Kumar SH, Rangarajan A. Simian Virus 40 Small T Antigen Activates AMPK and Triggers Autophagy to Protect Cancer Cells from Nutrient Deprivation. J Virol. 2009;83: 8565–8574. doi:10.1128/JVI.00603-09

73. Mankouri J, Tedbury PR, Gretton S, Hughes ME, Griffin SDC, Dallas ML, et al. Enhanced hepatitis C virus genome replication and lipid accumulation mediated by inhibition of AMP-activated protein kinase. Proc Natl Acad Sci. 2010;107: 11549–11554. doi:10.1073/pnas.0912426107

74. Semenza GL. Hypoxia-Inducible Factor 1 (HIF-1) Pathway. Sci STKE. 2007;2007: cm8–cm8. doi:10.1126/stke.4072007cm8

75. Semenza GL, Roth PH, Fang HM, Wang GL. Transcriptional regulation of genes encoding glycolytic enzymes by hypoxia-inducible factor 1. J Biol Chem. 1994;269: 23757–23763.

76. Semenza GL. Regulation of cancer cell metabolism by hypoxia-inducible factor 1. Semin Cancer Biol. 2009;19: 12–16. doi:10.1016/j.semcancer.2008.11.009

77. Mylonis I, Simos G, Paraskeva E. Hypoxia-Inducible Factors and the Regulation of Lipid Metabolism. Cells. 2019;8: 214. doi:10.3390/cells8030214

78. Pant A, Yang Z. Asparagine: An Achilles Heel of Virus Replication? ACS Infect Dis. 2020 [cited 18 Aug 2020]. doi:10.1021/acsinfecdis.0c00504

79. Pant A, Cao S, Yang Z. Asparagine Is a Critical Limiting Metabolite for Vaccinia Virus Protein Synthesis during Glutamine Deprivation. J Virol. 2019;93. doi:10.1128/JVI.01834-18

80. Peng X-H, Karna P, Cao Z, Jiang B-H, Zhou M, Yang L. Cross-talk between epidermal growth factor receptor and hypoxia-inducible factor-1alpha signal pathways increases resistance to apoptosis by up-regulating survivin gene expression. J Biol Chem. 2006;281: 25903–25914. doi:10.1074/jbc.M603414200

81. Guo Y, Meng X, Ma J, Zheng Y, Wang Q, Wang Y, et al. Human Papillomavirus 16 E6 Contributes HIF-1α Induced Warburg Effect by Attenuating the VHL-HIF-1α Interaction. Int J Mol Sci. 2014;15: 7974–7986. doi:10.3390/ijms15057974

82. Mazurek S, Zwerschke W, Jansen-Dürr P, Eigenbrodt E. Effects of the human papilloma virus HPV-16 E7 oncoprotein on glycolysis and glutaminolysis: role of pyruvate kinase type M2 and the glycolytic-enzyme complex. Biochem J. 2001;356: 247–256. doi:10.1042/0264-6021:3560247

83. Lai D, Tan CL, Gunaratne J, Quek LS, Nei W, Thierry F, et al. Localization of HPV-18 E2 at Mitochondrial Membranes Induces ROS Release and Modulates Host Cell Metabolism. PLOS ONE. 2013;8: e75625. doi:10.1371/journal.pone.0075625

84. Xie Q, Fan F, Wei W, Liu Y, Xu Z, Zhai L, et al. Multi-omics analyses reveal metabolic alterations regulated by hepatitis B virus core protein in hepatocellular carcinoma cells. Sci Rep. 2017;7: 41089. doi:10.1038/srep41089

85. Teng C-F, Hsieh W-C, Wu H-C, Lin Y-J, Tsai H-W, Huang W, et al. Hepatitis B Virus Pre-S2 Mutant Induces Aerobic Glycolysis through Mammalian Target of Rapamycin Signal Cascade. PLOS ONE. 2015;10: e0122373. doi:10.1371/journal.pone.0122373

86. Liu B, Fang M, He Z, Cui D, Jia S, Lin X, et al. Hepatitis B virus stimulates G6PD expression through HBx-mediated Nrf2 activation. Cell Death Dis. 2015;6: e1980–e1980. doi:10.1038/cddis.2015.322

87. Shin H-J, Park Y-H, Kim S-U, Moon H-B, Park DS, Han Y-H, et al. Hepatitis B virus X protein regulates hepatic glucose homeostasis via activation of inducible nitric oxide synthase. J Biol Chem. 2011;286: 29872–29881. doi:10.1074/jbc.M111.259978

88. Yoo Y-G, Na T-Y, Seo H-W, Seong JK, Park CK, Shin YK, et al. Hepatitis B virus X protein induces the expression of MTA1 and HDAC1, which enhances hypoxia signaling in hepatocellular carcinoma cells. Oncogene. 2008;27: 3405–3413. doi:10.1038/sj.onc.1211000

89. Bagga S, Rawat S, Ajenjo M, Bouchard MJ. Hepatitis B virus (HBV) X protein-mediated regulation of hepatocyte metabolic pathways affects viral replication. Virology. 2016;498: 9–22. doi:10.1016/j.virol.2016.08.006

90. Kondo S, Seo SY, Yoshizaki T, Wakisaka N, Furukawa M, Joab I, et al. EBV latent membrane protein 1 up-regulates hypoxia-inducible factor 1alpha through Siah1-mediated down-regulation of prolyl hydroxylases 1 and 3 in nasopharyngeal epithelial cells. Cancer Res. 2006;66: 9870–9877. doi:10.1158/0008-5472.CAN-06-1679

91. Sung W-W, Chu Y-C, Chen P-R, Liao M-H, Lee J-W. Positive regulation of HIF-1A expression by EBV oncoprotein LMP1 in nasopharyngeal carcinoma cells. Cancer Lett. 2016;382: 21–31. doi:10.1016/j.canlet.2016.08.021

92. Sung W-W, Chen P-R, Liao M-H, Lee J-W. Enhanced aerobic glycolysis of nasopharyngeal carcinoma cells by Epstein-Barr virus latent membrane protein 1. Exp Cell Res. 2017;359: 94–100. doi:10.1016/j.yexcr.2017.08.005

93. Xiao L, Hu Z-Y, Dong X, Tan Z, Li W, Tang M, et al. Targeting Epstein-Barr virus oncoprotein LMP1-mediated glycolysis sensitizes nasopharyngeal carcinoma to radiation therapy. Oncogene. 2014;33: 4568–4578. doi:10.1038/onc.2014.32

94. Zhang J, Jia L, Lin W, Yip YL, Lo KW, Lau VMY, et al. Epstein-Barr Virus-Encoded Latent Membrane Protein 1 Upregulates Glucose Transporter 1 Transcription via the mTORC1/NF-κB Signaling Pathways. J Virol. 2017;91. doi:10.1128/JVI.02168-16

95. Darekar S, Georgiou K, Yurchenko M, Yenamandra SP, Chachami G, Simos G, et al. Epstein-Barr Virus Immortalization of Human B-Cells Leads to Stabilization of Hypoxia-Induced Factor 1 Alpha, Congruent with the Warburg Effect. PLOS ONE. 2012;7: e42072. doi:10.1371/journal.pone.0042072

96. Carroll PA, Kenerson HL, Yeung RS, Lagunoff M. Latent Kaposi's sarcoma-associated herpesvirus infection of endothelial cells activates hypoxia-induced factors. J Virol. 2006;80: 10802–10812. doi:10.1128/JVI.00673-06

97. Ma T, Patel H, Babapoor-Farrokhran S, Franklin R, Semenza GL, Sodhi A, et al. KSHV induces aerobic glycolysis and angiogenesis through HIF-1-dependent upregulation of pyruvate kinase 2 in Kaposi's sarcoma. Angiogenesis. 2015;18: 477–488. doi:10.1007/s10456-015-9475-4

98. Yogev O, Lagos D, Enver T, Boshoff C. Kaposi's Sarcoma Herpesvirus MicroRNAs Induce Metabolic Transformation of Infected Cells. PLOS Pathog. 2014;10: e1004400. doi:10.1371/journal.ppat.1004400

99. Cai Q, Murakami M, Si H, Robertson ES. A Potential α-Helix Motif in the Amino Terminus of LANA Encoded by Kaposi's Sarcoma-Associated Herpesvirus Is Critical for Nuclear Accumulation of HIF-1α in Normoxia. J Virol. 2007;81: 10413–10423. doi:10.1128/JVI.00611-07

100. Ripoli M, D'Aprile A, Quarato G, Sarasin-Filipowicz M, Gouttenoire J, Scrima R, et al. Hepatitis C Virus-Linked Mitochondrial Dysfunction Promotes Hypoxia-Inducible Factor 1α-Mediated Glycolytic Adaptation. J Virol. 2010;84: 647–660. doi:10.1128/JVI.00769-09

101. Morris DR, Qu Y, Agrawal A, Garofalo RP, Casola A. HIF-1α Modulates Core Metabolism and Virus Replication in Primary Airway Epithelial Cells Infected with Respiratory Syncytial Virus. Viruses. 2020;12: 1088. doi:10.3390/v12101088

102. Ren L, Zhang W, Han P, Zhang J, Zhu Y, Meng X, et al. Influenza A virus (H1N1) triggers a hypoxic response by stabilizing hypoxia-inducible factor-1α via inhibition of proteasome. Virology. 2019;530: 51–58. doi:10.1016/j.virol.2019.02.010

103. Ritter JB, Wahl AS, Freund S, Genzel Y, Reichl U. Metabolic effects of influenza virus infection in cultured animal cells: Intra- and extracellular metabolite profiling. BMC Syst Biol. 2010;4: 61. doi:10.1186/1752-0509-4-61

104. Deshmane SL, Mukerjee R, Fan S, Del Valle L, Michiels C, Sweet T, et al. Activation of the oxidative stress pathway by HIV-1 Vpr leads to induction of hypoxia-inducible factor 1alpha expression. J Biol Chem. 2009;284: 11364–11373. doi:10.1074/jbc.M809266200

105. Barrero CA, Datta PK, Sen S, Deshmane S, Amini S, Khalili K, et al. HIV-1 Vpr Modulates Macrophage Metabolic Pathways: A SILAC-Based Quantitative Analysis. PLOS ONE. 2013;8: e68376. doi:10.1371/journal.pone.0068376

106. Levine AJ, Puzio-Kuter AM. The Control of the Metabolic Switch in Cancers by Oncogenes and Tumor Suppressor Genes. Science. 2010;330: 1340–1344. doi:10.1126/science.1193494

107. Stine ZE, Walton ZE, Altman BJ, Hsieh AL, Dang CV. MYC, Metabolism, and Cancer. Cancer Discov. 2015;5: 1024–1039. doi:10.1158/2159-8290.CD-15-0507

108. Dang CV. MYC, Metabolism, Cell Growth, and Tumorigenesis. Cold Spring Harb Perspect Med. 2013;3. doi:10.1101/cshperspect.a014217

109. Liu J, Zhang C, Hu W, Feng Z. Tumor suppressor p53 and metabolism. J Mol Cell Biol. 2019;11: 284–292. doi:10.1093/jmcb/mjy070

110. Zhang X, Qin Z, Wang J. The role of p53 in cell metabolism. Acta Pharmacol Sin. 2010;31: 1208–1212. doi:10.1038/aps.2010.151

111. Thai M, Thaker SK, Feng J, Du Y, Hu H, Ting Wu T, et al. MYC-induced reprogramming of glutamine catabolism supports optimal virus replication. Nat Commun. 2015;6: 1–9. doi:10.1038/ncomms9873

112. Chakraborty AA, Tansey WP. Adenoviral E1A function through Myc. Cancer Res. 2009;69: 6–9. doi:10.1158/0008-5472.CAN-08-3026

113. Martin MED, Berk AJ. Adenovirus E1B 55K Represses p53 Activation In Vitro. J Virol. 1998;72: 3146–3154. doi:10.1128/JVI.72.4.3146-3154.1998

114. Prusinkiewicz MA, Mymryk JS. Metabolic Reprogramming of the Host Cell by Human Adenovirus Infection. Viruses. 2019;11: 141. doi:10.3390/v11020141

115. Sanchez EL, Carroll PA, Thalhofer AB, Lagunoff M. Latent KSHV Infected Endothelial Cells Are Glutamine Addicted and Require Glutaminolysis for Survival. PLOS Pathog. 2015;11: e1005052. doi:10.1371/journal.ppat.1005052

116. Cai Q-L, Knight JS, Verma SC, Zald P, Robertson ES. EC5S Ubiquitin Complex Is Recruited by KSHV Latent Antigen LANA for Degradation of the VHL and p53 Tumor Suppressors. PLOS Pathog. 2006;2: e116. doi:10.1371/journal.ppat.0020116

117. McGivern DR, Lemon SM. Virus-specific mechanisms of carcinogenesis in hepatitis C virus associated liver cancer. Oncogene. 2011;30: 1969–1983. doi:10.1038/onc.2010.594

118. Sato Y, Kamura T, Shirata N, Murata T, Kudoh A, Iwahori S, et al. Degradation of Phosphorylated p53 by Viral Protein-ECS E3 Ligase Complex. PLOS Pathog. 2009;5: e1000530. doi:10.1371/journal.ppat.1000530

119. Tommasino M, Accardi R, Caldeira S, Dong W, Malanchi I, Smet A, et al. The role of TP53 in Cervical carcinogenesis. Hum Mutat. 2003;21: 307–312. doi:https://doi.org/10.1002/humu.10178

120. Locasale JW. New concepts in feedback regulation of glucose metabolism. Curr Opin Syst Biol. 2018;8: 32–38. doi:10.1016/j.coisb.2017.11.005

121. Jeon T-I, Osborne TF. SREBPs: metabolic integrators in physiology and metabolism. Trends Endocrinol Metab. 2012;23: 65–72. doi:10.1016/j.tem.2011.10.004

122. Spencer CM, Schafer XL, Moorman NJ, Munger J. Human Cytomegalovirus Induces the Activity and Expression of Acetyl-Coenzyme A Carboxylase, a Fatty Acid Biosynthetic Enzyme Whose Inhibition Attenuates Viral Replication. J Virol. 2011;85: 5814–5824. doi:10.1128/JVI.02630-10

123. Yu Y, Maguire TG, Alwine JC. Human Cytomegalovirus Infection Induces Adipocyte-Like Lipogenesis through Activation of Sterol Regulatory Element Binding Protein 1. J Virol. 2012;86: 2942–2949. doi:10.1128/JVI.06467-11

124. Madison BB. Srebp2: A master regulator of sterol and fatty acid synthesis. J Lipid Res. 2016;57: 333–335. doi:10.1194/jlr.C066712

125. Horton JD, Goldstein JL, Brown MS. SREBPs: activators of the complete program of cholesterol and fatty acid synthesis in the liver. J Clin Invest. 2002;109: 1125–1131. doi:10.1172/JCI15593

126. Heaton NS, Perera R, Berger KL, Khadka S, LaCount DJ, Kuhn RJ, et al. Dengue virus nonstructural protein 3 redistributes fatty acid synthase to sites of viral replication and increases cellular fatty acid synthesis. Proc Natl Acad Sci. 2010;107: 17345–17350. doi:10.1073/pnas.1010811107

127. Allonso D, Andrade IS, Conde JN, Coelho DR, Rocha DCP, Silva ML da, et al. Dengue Virus NS1 Protein Modulates Cellular Energy Metabolism by Increasing Glyceraldehyde-3-Phosphate Dehydrogenase Activity. J Virol. 2015;89: 11871–11883. doi:10.1128/JVI.01342-15

128. Fontaine KA, Sanchez EL, Camarda R, Lagunoff M. Dengue Virus Induces and Requires Glycolysis for Optimal Replication. J Virol. 2015;89: 2358–2366. doi:10.1128/JVI.02309-14

129. Smith M, Honce R, Schultz-Cherry S. Metabolic Syndrome and Viral Pathogenesis: Lessons from Influenza and Coronaviruses. J Virol. 2020;94. doi:10.1128/JVI.00665-20

130. Sommer P, Sweeney G. Functional and Mechanistic Integration of Infection and the Metabolic Syndrome. Korean Diabetes J. 2010;34: 71–76. doi:10.4093/kdj.2010.34.2.71

Figures and table- Chapter 1

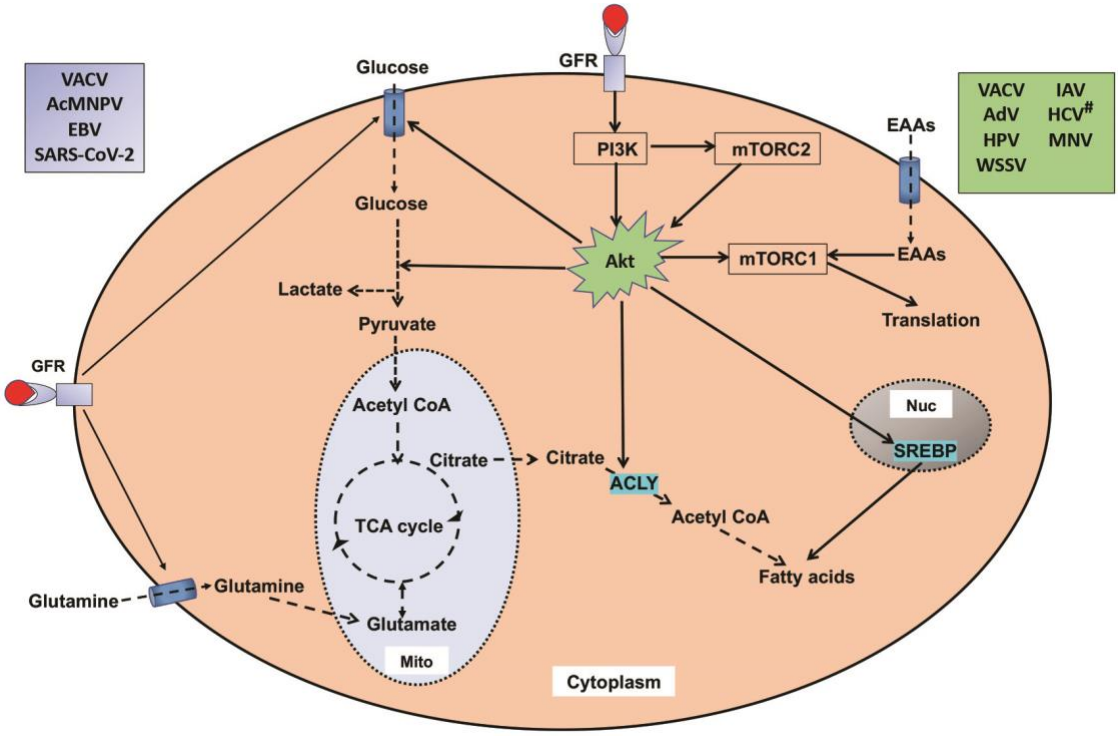

Figure 1.1. Growth factor signaling and Akt pathway are targeted by viruses to alter host metabolism.

Viruses (listed in the blue-shaded box), either directly or indirectly, activate the GFR signaling. GFR signaling governs the uptake of glucose and glutamine, and metabolic pathways such as glycolysis. Viruses (listed in the green-shaded box), activate the Akt signaling to regulate metabolic pathways, regulators, and enzymes. Dashed arrows indicate the flow of metabolites. Solid arrows indicate the target of GFR or Akt signaling. # indicates that HCV downregulates Akt signaling.

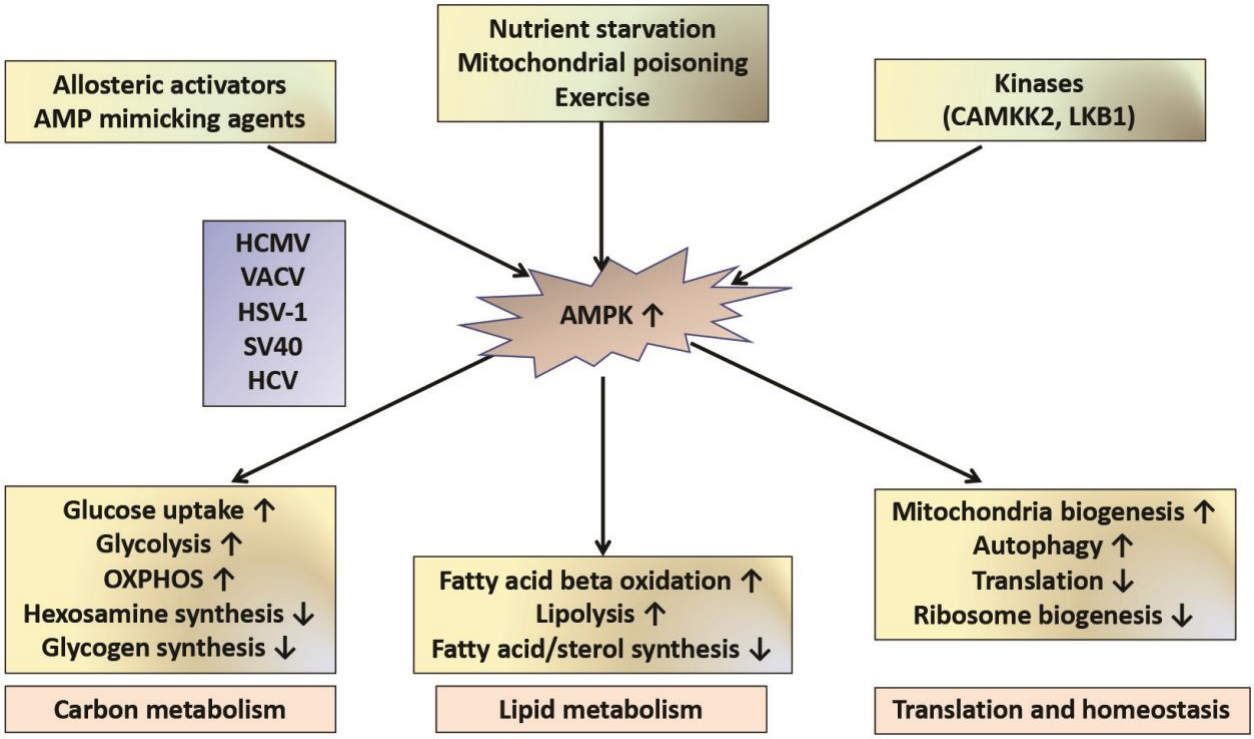

Figure 1.2. Viruses regulate AMPK pathway for their benefit.

Viruses (listed in the blue-shaded box) stimulate the AMPK pathway to induce changes in the metabolism of carbon, lipids, and pathways related to translation and homeostasis. The upwards and downwards arrows indicate upregulation or downregulation in the indicated pathways.

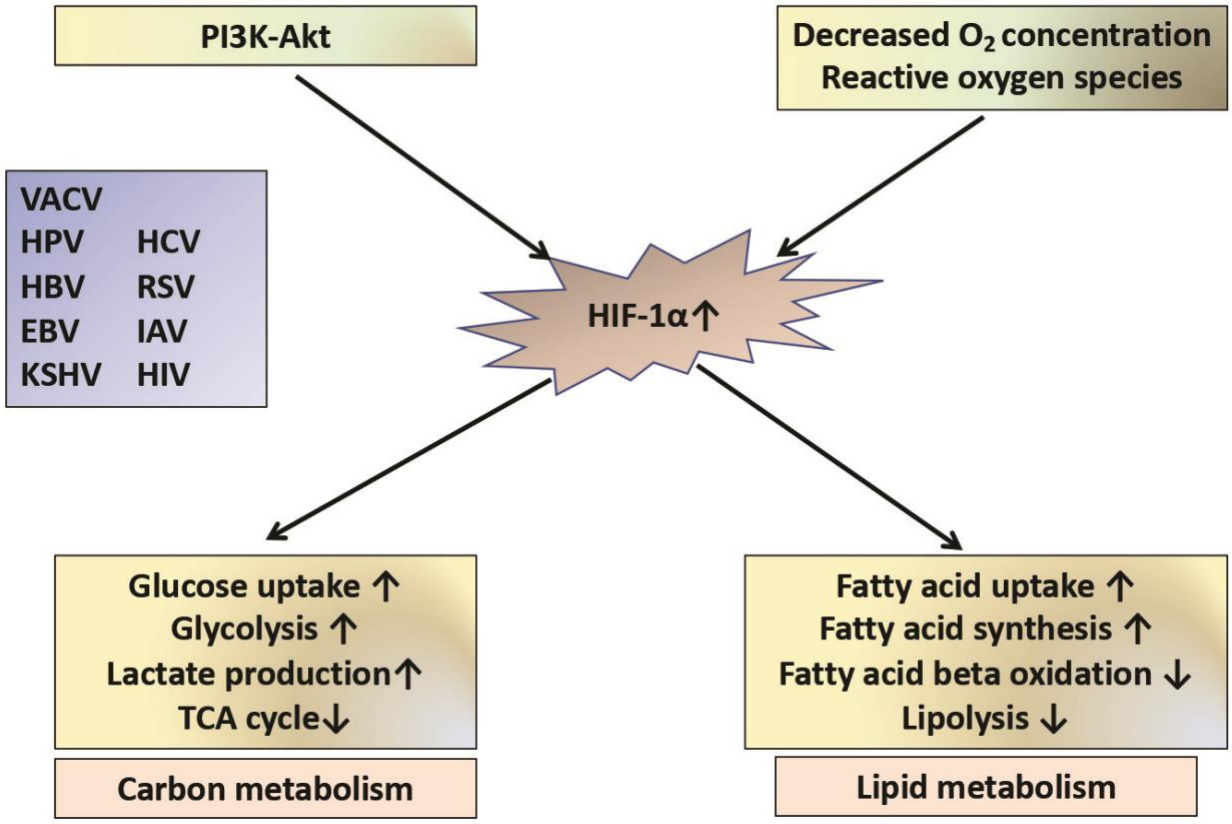

Figure 1.3. Viruses target the HIF pathway to create a metabolically favorable environment.

Viruses (listed in the blue-shaded box) stimulate the HIF pathway to induce changes in the metabolism of carbon and lipids. The upwards and downwards arrows indicate upregulation or downregulation in the indicated pathways.

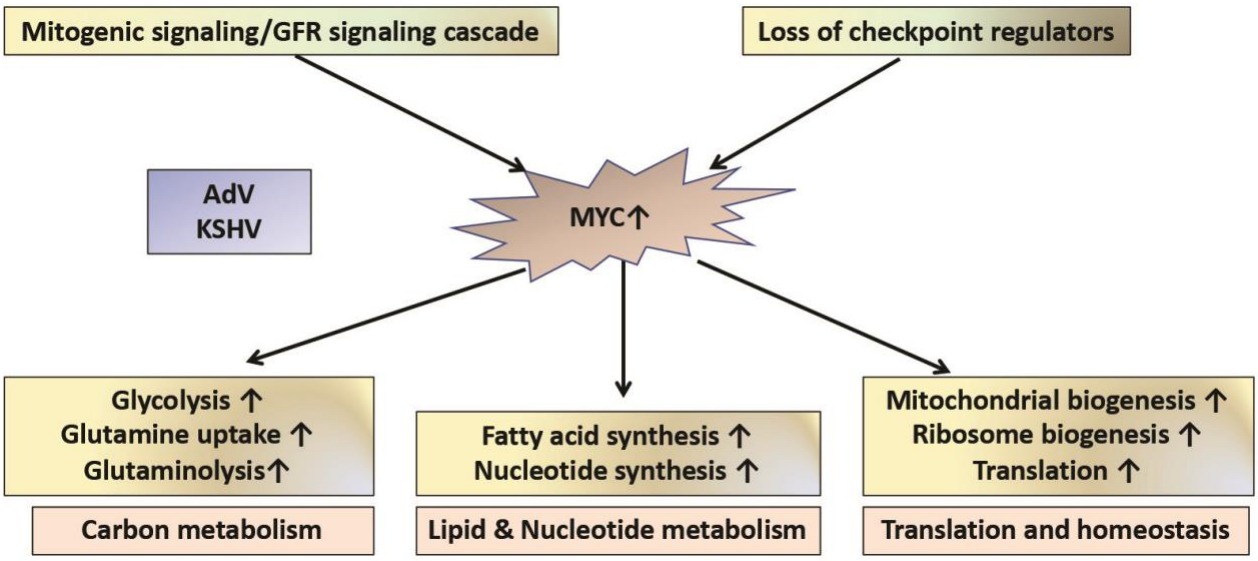

Figure 1.4. Regulation of the Myc oncogene by viruses to rewire host metabolism.
Viruses (listed in the blue-shaded box) stimulate the Myc oncogene to induce changes in the metabolism of carbon, lipids, nucleotides, and pathways related to translation and homeostasis. The upwards and downwards arrows indicate upregulation or downregulation in the indicated pathways.

Table 1.1. Viruses target several cellular signaling pathways to rewire host cell metabolism.

A list of the signaling pathways that are important for regulating cellular metabolism that are targeted by different viruses. (+) indicates upregulation; (-) indicates downregulation; and (?) indicates unknown.

Signaling pathway	Virus	Virus protein	Cellular target	Metabolic effect	References
Growth Factor Signaling	VACV	VGF	EGFR (+), MAPK (+), pSTAT3 S727 (+)	TCA cycle (+)	24
	Baculovirus	FGF	?	Glucose, Glutamine uptake (+)	30
	EBV	LMP1	FGF1 (+)	Glycolysis (+)	35
PI3K-AKT-mTOR Pathway	VACV	VGF	AKT (+)	Lipid metabolism (?)	Unpublished
	HPV 16	E6/E7	PI3K-AKT pathway (+)	Glycolysis (+)	56, 57
	WSSV	?	PI3K-AKT pathway (+)	Glycolysis (+)	63
	ADV	E4-ORF1	PI3K-AKT pathway (+)	?	59
	MNV	?	PI3K-AKT pathway (+)	Glycolysis (+)	58
	HCV	Core protein (?)	PI3K-AKT pathway (-)	Glycolysis (-)	61, 62
	IAV	?	PI3K-AKT pathway (+)	Glycolysis (+)	55
	EBV	LMP1	mTOR (+)	Glycolysis (+)	94
AMPK Pathway	HCMV	UL38?	CaMKK-AMPK (+)	Glycolysis (+)	67, 68
	SV40	Small T antigen	AMPK (+)	Energy homeostasis	72
	HCV	?	AMPK (-)	Lipid accumulation (+)	73
	HSV-1	?	AMPK [Early (-), Late (+)]	Lipid/Protein synthesis (+) Early, Beta oxidation (+) Late	71
Hypoxia-inducible factors	VACV	C16	HIF-1α (+)	Glutamine metabolism (+) (?)	4, 29
	HPV-16, 18	E6, E7, E2	HIF-1α (+)	Glycolysis (+)	57, 81, 83
	HBV	HBx	HIF-1α (+)	Glycolysis (+) (?)	86, 87, 88

	EBV	LMP1, EBNA3, EBNA5	HIF-1α (+)	Glycolysis (+)	90, 91, 92, 95
	KSHV	miRNA, GPCR, LANA (?)	HIF-1α (+)	Glycolysis (+)	97, 98, 99
	HCV	?	HIF-1α (+)	Glycolysis (+), OXPHOS (-)	100
	RSV	?	HIF-1α (+)	Glycolysis (+), PPP (+)	101
	IAV	?	HIF-1α (+)	Glycolysis (+) (?)	102
	HIV	Vpr	HIF-1α (+)	Glycolysis (+)	104, 105
Oncogenes and tumor suppressors	ADV	E4ORF1	Myc (+)	Glycolysis (+), Glutaminolysis (+)	60, 111
	ADV	E1A, E1B	Myc (+), p53 (-)	?	112, 113
	KSHV	?	Myc (+)	Glutaminolysis (+)	115
	KSHV	LANA	p53 (-)	?	116
	EBV	BZLF1	p53 (-)	?	118
	HCV	NS3, NS5	p53 (-)	?	117
	HPV	E6	p53 (-)	?	119

Chapter 2 - Asparagine is a Critical Limiting Metabolite for Vaccinia Virus Protein Synthesis during Glutamine Deprivation

Running Title: Role of asparagine availability in VACV replication

Authors: Anil Pant, Shuai Cao, Zhilong Yang*

Author affiliation: Division of Biology, Kansas State University, Manhattan, Kansas 66506, USA

*Correspondence: Zhilong Yang, E-mail: zyang@ksu.edu

Published as: **Pant, A**., Cao, S., & Yang, Z. (2019). Asparagine is a Critical Limiting Metabolite for Vaccinia Virus Protein Synthesis during Glutamine Deprivation. *Journal of Virology*, 93(13).

Abstract

Viruses actively interact with host metabolism because viral replication relies on host cells to provide nutrients and energy. Vaccinia virus (VACV; the prototype poxvirus) prefers glutamine to glucose for efficient replication to the extent that VACV replication is hindered in glutamine-free medium. Remarkably, our data show that VACV replication can be fully rescued from glutamine depletion by asparagine supplementation. By global metabolic profiling, as well as genetic and chemical manipulation of the asparagine supply we provide evidence demonstrating that the production of asparagine, which exclusively requires glutamine for biosynthesis, accounts for VACV's preference of glutamine to glucose rather than glutamine's superiority over glucose in feeding the tricarboxylic acid (TCA) cycle. Further, we show that sufficient asparagine supply is required for efficient VACV protein synthesis. Our study highlights that the asparagine supply, the regulation of which has been evolutionarily tailored in mammalian cells, presents a critical barrier to VACV replication due to a high asparagine content of viral proteins and a rapid demand of viral protein synthesis. The identification of asparagine availability as a critical limiting factor for efficient VACV replication suggests a new direction of anti-viral strategy development.

Importance

Viruses rely on their infected host cells to provide nutrients and energy for replication. Vaccinia virus, the prototypic member of poxviruses that comprise many significant human and animal pathogens, prefers glutamine to glucose for efficient replication. Here we show that the preference is not because glutamine is superior to glucose as the carbon source to fuel the tricarboxylic acid cycle for vaccinia virus replication. Rather interestingly, the preference is because the asparagine supply for efficient viral protein synthesis becomes limited in the absence

of glutamine that is necessary for asparagine biosynthesis. We provide further genetic and chemical evidence to demonstrate that asparagine availability plays a critical role in efficient vaccinia virus replication. This discovery identifies a weakness of vaccinia virus and suggests a possible direction to intervene poxvirus infection.

Keywords: Poxvirus, Vaccinia virus, Asparagine, Glutamine, Metabolism, Metabolic profiling, Protein synthesis

Introduction

Viruses do not have metabolic machinery; so viral replication relies on the host for supply of nutrients and energy. Unsurprisingly, metabolism is a crucial interface of virus-host interactions. Many viral infections are characterized as being heavily dependent on particular metabolites (e.g., glutamine, glucose or fatty acids) for optimal replication. Many viruses induce alterations in metabolic pathways such as glycolysis, synthesis of fatty acids, nucleotides, and energy metabolism. The abilities of viruses to make these alterations often shape the outcome of viral infections (1-4).

Vaccinia virus (VACV) is the prototype poxvirus, with a large double-stranded DNA genome that encodes more than 200 annotated genes (5, 6). Many poxviruses cause fatal diseases such as variola virus-induced smallpox, which is one of the most devastating infectious diseases in human history. Although eradicated in nature, smallpox is still a valid national security concern due to potential unregistered stocks or *de novo* synthesis of live variola virus (7-9). Moreover, other poxviruses cause human and animal diseases. On the other hand, poxviruses are practically useful as oncolytic agents for cancer treatments, as well as vectors for vaccine development and recombinant protein production (10-13). For efficient VACV replication in cell culture, VACV prefers glutamine to glucose; the depletion of glutamine, but not glucose, from culture medium significantly decreases VACV production (14, 15). In line with this finding, VACV infection upregulates glutamine metabolism (16). Nevertheless, why VACV prefers glutamine to glucose for replication remains elusive.

Glutamine is a non-essential amino acid that is abundantly utilized by mammalian cells beyond its role as a protein building block (17). Glutamine feeds the tricarboxylic acid cycle (TCA cycle; **Fig. 2.1A**) through glutamate and alpha-ketoglutarate (α-KG) in a process known as

anaplerosis (18-20). Glutamine also acts as a biosynthetic precursor for many molecules including amino acids, nucleotides, and fatty acids (21, 22). Although several non-essential amino acids require intermediates of glutamine metabolism for *de novo* biosynthesis, only asparagine biosynthesis exclusively depends on glutamine because the amination of the synthesis reaction requires glutamine (23, 24). The biosynthesis of asparagine using glutamine is catalyzed by the enzyme asparagine synthetase (ASNS) (25, 26).

A new and growing body of work suggests that asparagine is more than just a polypeptide subunit. It is essential in coordinating overall protein synthesis, cellular responses to amino acid homeostasis, and metabolic availability during biological processes and disease development. For example, asparagine acts as a metabolic regulator of TCA cycle intermediates and the cellular supply of nitrogen (which supports the synthesis of non-essential amino acids); and for cancer cells, asparagine bioavailability is essential for survival, proliferation and tumor development (23, 24, 27, 28). Asparagine is also important for supporting Kaposi's sarcoma-associated herpesvirus (KSHV) transformed cancer cell proliferation due to its critical role in nucleotide biosynthesis during glutamine depletion (29). However, the role of asparagine availability in virus replication has not been explored.

In the current study, we show that asparagine is a limiting metabolite for VACV replication through its critical role in VACV protein synthesis. In contrast to the generic paradigm that glutamine is superior to glucose in fueling the TCA cycle, we show that the preference for glutamine reflects the requirement of sufficient asparagine supply during replication. Indeed, interfering with asparagine metabolism severely impairs VACV replication, highlighting the importance of asparagine availability during VACV lifecycle. Our findings demonstrate an essential role of asparagine availability for efficient VACV replication.

Understanding this critical host-dependent barrier to VACV replication might not only spur the development of new, host-oriented antiviral therapies but also improve the development of poxviruses as therapeutic tools.

Results

Asparagine fully rescues VACV replication from glutamine depletion

To test why VACV prefers glutamine to glucose for efficient replication, we examined whether α-KG and glutamate—the products of glutaminolysis that feed the TCA cycle (**Fig. 2.1A**)—could rescue VACV replication from glutamine depletion. Measuring virus titers showed that α-KG and glutamate supplementation only partially rescued VACV replication in the absence of glutamine (**Fig. 2.1B**), in agreement with earlier studies (14, 15). This indicates that while anaplerosis of the TCA cycle is important, this function of glutamine is not responsible for its superiority to glucose in promoting VACV replication.

Notably, VACV replication was fully rescued from glutamine depletion when asparagine was added to the medium (**Fig. 2.1B**). In contrast, when the medium contained glutamine, adding asparagine did not boost viral titers, suggesting growth could be equally rescued by either glutamine or asparagine. Moreover, asparagine rescued GFP expression from a recombinant VACV expressing GFP in the absence of glutamine (**Fig. 2.1C**).

VACV replication kinetics over a 72-h period using an initial VACV multiplicity of infection (MOI) of 0.001 in the glutamine-free medium was also consistently rescued by asparagine (**Fig. 2.1D**). The 72-h proliferation rate of HFFs differed little from cells grown in medium containing glucose only or glucose plus asparagine (**Fig. 2.1E**), suggesting that the difference in VACV titers is not due to altered HFF proliferation. Other non-essential amino acids that can be synthesized from glutamine but were not present in the cell culture medium

(e.g., proline, alanine, and serine), did not rescue VACV replication from glutamine-deficiency (**Fig. 2.1F**). We also tested the effect of asparagine in supporting VACV replication upon glutamine depletion in BS-C-1 that is a monkey kidney epithelial cell line. Similar to the results in HFFs, asparagine fully rescued VACV titers from glutamine depletion in BS-C-1 cells (**Fig. 2.1G, H**). Together these results demonstrate that asparagine can rescue VACV replication from glutamine depletion.

Asparagine does not enhance TCA cycle activities during VACV infection

Under the glutamine-free condition, asparagine might rescue VACV replication by improving anaplerosis of the TCA cycle. To test this idea, VACV-infected HFFs were profiled for metabolic activities in three different conditions: glucose, glucose plus glutamine, and glucose plus asparagine (**Table 2.1**). Glucose plus glutamine significantly enhanced the concentrations of several TCA cycle intermediates (α-KG, succinate, fumarate, and malate) compared to glucose only condition, while the addition of asparagine did not (**Fig. 2.2A**). Even in the absence of glutamine, glucose was sufficient to maintain the levels of oxidative phosphorylation intermediates required for ATP production (**Fig. 2.2B**). These results show that rescue of VACV replication by asparagine in the glutamine-deficient medium is not driven by enhancement of the TCA cycle and that glucose can support enough TCA cycle activities for VACV infection. Additionally, when glutaminase activity is inhibited with the BPTES, VACV titers decreased by only 2-fold in the presence of glucose but decreased by 12-fold in the absence of glucose (glutamine was present in both conditions; **Fig. 2.2C**). Together, these results indicate that asparagine-mediated rescue of VACV replication is not due to enhanced TCA cycle activities in glutamine-depleted condition.

Our interpretation is also supported by the fact that the TCA cycle is not directly fed by asparagine converting to aspartate in VACV-infected cells. Adding aspartate to glutamine-deficient medium rescued only low levels of VACV replication (**Fig. 2.2D**) and adding asparagine did not elevate aspartate concentration (**Fig. 2.3A).** This is consistent with the fact that in mammalian cells asparaginase does not actively convert asparagine to aspartate (28). Notably, glutamine itself could support VACV replication even in the absence of glucose, while the asparagine-mediated rescue of VACV replication from glutamine-depleted condition required glucose in the medium (**Fig. 2.2E**). Moreover, VACV titer was significantly lower when glucose was not added to the glutamine-depleted medium (**Fig. 2.2F**). These results suggest that glutamine can provide functions of both glucose and asparagine during VACV infection.

For VACV-infected HFFs cultured in glutamine-deficient medium, adding asparagine did not increase the glutamine and glutamate concentration either (**Fig. 2.3A**). Moreover, using L-MSO to inhibit *de novo* glutamine synthesis only minimally reduced VACV replication (1.4-fold) when the glutamine-deficient medium was supplemented with asparagine (**Fig. 2.2G**), showing that VACV replication is not rescued because asparagine supplementation increases glutamine or glutamate to feed the TCA cycle. L-MSO treatment decreased VACV titer for 3.2-fold in glucose only medium (**Fig. 2.2H**), indicating a stronger inhibitory effect of L-MSO on VACV replication when *de novo* glutamine synthesis is suppressed in the absence of exogenous glutamine.

Asparagine rescues VACV protein synthesis from glutamine depletion

Notably, our global metabolic profiling data showed that most amino acids (14 out of 20) accumulated in cultures with glucose only, which led to an amino acid imbalance compared to

cultures containing glutamine and glucose (**Fig. 2.3A**). Within infected-cells cultured in glucose only medium, amino acids whose biosynthesis is closely tied to glutamine concentration (i.e., alanine, proline, aspartate, glutamate, and asparagine) (30, 31) had a lower or similar concentration (**Fig. 2.3A**). Among the five amino acids, asparagine is the only amino acid that exclusively requires glutamine for its biosynthesis and is also the only amino acid that fully rescues VACV replication from glutamine depletion. Remarkably, adding asparagine significantly decreased the accumulation of most amino acids in glutamine-depleted condition (**Fig. 2.3A**). Moreover, asparagine concentration was significantly lower than other amino acids except for glutamine in glucose only condition, while its level was significantly higher than or similar to most other amino acids when glutamine is present (**Fig. 2.3B**).

These results prompted us to hypothesize that asparagine availability is a critical limiting factor in maintaining amino acid balance for efficient protein synthesis in VACV-infected cells. This implies that, without glutamine, the rate of protein synthesis is suppressed by a low asparagine supply that cannot support the acute demand for nascent protein synthesis during the brief time window of VACV replication; exogenous asparagine can correct this amino acid imbalance. Higher demand for asparagine in VACV-infected cells can also be attributed to a 93% higher asparagine content in VACV-encoded proteins than that in human genome-encoded proteins (**Fig. 2.3C**). Asparagine content in VACV late proteins, which are expressed at very high levels for viral particles (32, 33), is 101% higher than human proteins (**Fig. 2.3C**). The hypothesis is supported by the result that VACV protein levels were much lower in cells cultured with glucose only compared to in cells cultured with glutamine or asparagine (**Fig. 2.3D**). Nascent cellular protein synthesis was also less in uninfected HFFs grown in glucose only medium (**Fig. 2.3E**). However, because there are pre-existing cellular proteins, glutamine

depletion in the absence of asparagine did not affect uninfected HFF proliferation (**Fig. 2.1E**). VACV infection directs cellular machinery to synthesize viral proteins, as can be seen in the different patterns of newly synthesized proteins with or without VACV infection (**Fig. 2.3E**). The level of nascent viral protein synthesis was lower in VACV-infected HFFs in medium containing glucose only (**Fig. 2.3E**). Because all viral proteins need to be newly synthesized after infection, the negative effect on protein synthesis in glucose only medium presents a severe impact on VACV replication.

GCN2 is a metabolic-stress-sensing protein kinase that senses amino acid availability and phosphorylates eIF2α to suppress protein synthesis during amino acid deficiency (34, 35). In addition to the effect of a limited supply of asparagine on protein synthesis, there is a possibility that the amino acid imbalance stimulates GCN2/eIF2α phosphorylation to decrease protein synthesis. GCN2 phosphorylation increased in cells grown in glucose only medium over the course of viral infection and in mock-infected cells, although the phosphorylation levels were significantly lower than calyculin A treatment that served as the positive control of GCN2 phosphorylation (**Fig. 2.4A**). Interestingly, eIF2α phosphorylation was not affected in uninfected HFFs in different culture media, while eIF2α phosphorylation increased in cells grown in glucose only medium during VACV infection (**Fig. 2.4B).** Although the changes in eIF2α phosphorylation were not high in different media during VACV replication, its impact should not be neglected as a small increase in eIF2α phosphorylation may cause significant suppression in mRNA translation (36).

Asparagine rescues VACV post-replicative mRNA translation from glutamine-deficiency

VACV genes are expressed in a cascade fashion. Upon entry, VACV early genes are immediately expressed, then DNA is replicated, and intermediate genes are expressed followed by late genes (5). To find which stage of viral replication was affected, HFFs were infected with one of three reporter VACVs that encode a secreted Gaussia luciferase gene under viral early (vEGluc), intermediate (vIGluc), and late (vLGluc) promoters. Viral gene expression was measured by Gaussia luciferase activities in cell culture medium. In all three conditions, early gene expression was similar but VACV intermediate and late gene expression was significantly higher in medium containing asparagine or glutamine (**Fig. 2.5A-C**). The promoters of each class of VACV genes share the same transcription mechanism and use the same transcription factors (5). Therefore, the C11, G8, and F17 mRNA levels can reflect the mRNA levels of VACV early, intermediate and late mRNAs. qRT-PCR profiled VACV early (C11R, 4 hpi), intermediate (G8R, 6 hpi) and late (F17R, 12 hpi) gene mRNA levels under different nutrient conditions (**Fig. 2.5D-F**) (5). Unsurprisingly, the levels of early viral mRNAs were not affected by nutrient conditions (**Fig. 2.5D**). VACV intermediate mRNA levels did not differ either, and asparagine or glutamine only mildly increased viral late mRNA levels by less than 1.5-fold (**Fig. 2.5EF**). Because VACV intermediate and late mRNA synthesis rely on viral DNA replication and viral DNA replication factors are mostly encoded by viral early genes (6, 37), the glucose only medium in the absence of glutamine and asparagine is not expected to have a significant effect on VACV DNA replication. These results indicate that asparagine rescues VACV protein synthesis from glutamine-deficiency mainly at the post-replicative (both intermediate and late) mRNA translation stage.

There was a significant increase in adenosine levels in the presence of glutamine, likely because glutaminolysis can contribute to nucleotide synthesis (**Fig. 2.5G**) (21, 22). However, our metabolic profiling of VACV-infected cells grown with glucose or asparagine supplementation showed that they had similar nucleoside concentrations (**Fig. 2.5G**). Accordingly, adding nucleosides to glutamine-depleted medium did not rescue VACV replication (**Fig. 2.5H**). These results support the observations that asparagine has no or only small effects on VACV RNA synthesis.

ASNS knockdown impairs VACV replication

Standard cell culture medium lacks asparagine, but cells synthesize it *de novo* by ASNS using glutamine as the amino group donor (**Fig. 2.6A**). To test whether asparagine biosynthesis affects VACV replication, ASNS protein expression was reduced with two different siRNAs (**Fig. 2.6B**). ASNS knockdown significantly impaired VACV replication (**Fig. 2.6C, D**), but did not suppress HFF proliferation (**Fig. 2.6E**). In ASNS siRNA-treated cells, VACV protein synthesis was down-regulated (**Fig. 2.6F**). This agrees with the result that siRNA-mediated interference of ASNS also decreased nascent viral protein synthesis in VACV-infected cells (**Fig. 2.6G**). Since these experiments were performed in the presence of glutamine, the results indicate a critical role of asparagine biosynthesis in VACV replication.

Chemically suppressing asparagine metabolism decreases VACV replication

Conversion of asparagine to aspartate is catalyzed by asparaginase (38). To test how depleting asparagine affects VACV replication, asparaginase from *E. coli* was added to culture medium containing glutamine. This led to a significant decrease in VACV replication that could be partially rescued by supplementing with asparagine (**Fig. 2.7A**). Asparaginase treatment also decreased Gaussia luciferase activity in vLGluc-infected cells, which again could be partially

rescued with supplemental asparagine (**Fig. 2.7B**). Although asparaginase treatment decreased VACV titers in medium containing asparagine, it did not affect viral replication in medium containing glucose only without asparagine and glutamine (**Fig. 2.7C**). Importantly, asparaginase treatment did not decrease HFF cell viability (**Fig. 2.7D**).

To test whether chemical interference of ASNS impedes VACV replication, albizziine, a competitive inhibitor of ASNS (39), was added to the culture medium. Albizziine reduced VACV replication by 41-fold in medium with glutamine but had no apparent effect on VACV replication in cells grown with glucose only (**Fig. 2.8A**). In cells grown with asparagine plus glucose, albizziine reduced VACV titers by only two-fold (**Fig. 2.8A**). Furthermore, albizziine treatment decreased Gaussia luciferase activity in vLGluc-infected HFFs grown with medium containing glutamine and glucose, but not glucose only (**Fig. 2.8B**). Albizziine did not affect HFF cell viability (**Fig. 2.8C**). Overall, these findings again demonstrate interfering with asparagine metabolism suppresses VACV replication.

Discussion

This study used a combination of nutrient manipulation, genetic and chemical interference to establish that asparagine is a critical limiting amino acid for VACV protein synthesis that accounts for glutamine dependency of VACV replication. During VACV infection in glutamine-containing medium, glutamine not only feeds the TCA cycle but also acts as a substrate for asparagine biosynthesis to support VACV replication (**Fig. 2.9A**). Since the *de novo* synthesis of asparagine uses glutamine as the amino-group donor, asparagine cannot be sufficiently synthesized in the absence of exogenous glutamine—this renders asparagine a limiting metabolite that can be exogenously supplied (**Fig. 2.9B**). In the absence of glutamine, a carbon source like glucose is required to feed the TCA cycle (**Fig. 2.9B;** in mammalian cells,

asparagine is unable to feed the TCA cycle by converting to aspartate). When asparagine supply is blocked by chemical or genetic interference, VACV replication is suppressed, supporting our idea that asparagine is a limiting factor of VACV replication (**Fig. 2.9B**). Although glutamine can contribute to the biosynthesis of several non-essential amino acids via glutamate, asparagine biosynthesis exclusively requires glutamine (23, 24), which is consistent with the result that rescue of VACV replication from glutamine depletion is specific to asparagine.

Glucose and glutamine are two common carbon sources for mammalian cells (40, 41). Previous studies have established that VACV prefers glutamine to glucose for efficient replication (14, 15). Yet, supplementation of α-KG or glutamate only partially rescued VACV replication from glutamine depletion (14, 15) (**Fig. 2.1B**), and glutaminase inhibition had a more severe effect on VACV replication in the absence of glucose (**Fig. 2.2C**). These results indicate that the utilization of glutamine to feed the TCA cycle only partially accounts for its role during VACV replication and is not the cause of the glutamine preference during VACV replication. Our results identified asparagine biosynthesis as a critical function glutamine provides for efficient VACV replication. Thus, glutamine provides both the functions of glucose and asparagine required during VACV infection. Interestingly, Greseth et al. showed that *de novo* fatty acid biosynthesis is important for efficient VACV replication (14). It would be interesting to examine whether asparagine is required for efficient fatty acid synthesis during VACV replication in the future.

Asparagine mainly functions through its availability as a limiting nutrient for VACV post-replicative protein synthesis. This is supported by the evidence showing an overall accumulation of most of the amino acids in glutamine depletion condition during VACV infection, suggesting they can be supplied by glucose metabolism. In contrast, asparagine does

not accumulate, and supplemental asparagine reduced the accumulation of amino acids in glutamine-depleted condition. Interestingly, knockdown of ASNS or glutamine depletion has little effect on cell proliferation in uninfected HFFs, although the nascent cellular protein synthesis decreases, which is likely because the demand of nascent protein synthesis in uninfected HFFs is lower due to pre-existing proteins in cells. While the limited availability of asparagine in glutamine depletion has no effect on uninfected cell proliferation, the suppression is magnified during the post-replicative stage of VACV protein synthesis. Three mechanisms can contribute to the suppression of viral post-replicative, but not early protein synthesis due to the shortage of asparagine supply. First, there is an increased demand of nascent protein synthesis during the late time of VACV infection to produce a large amount of viral particles. Second, VACV proteins have an almost 100% higher asparagine content than human proteins. Although asparagine contents are higher in all VACV early and post-replicative (intermediate and late) proteins comparing to human proteins, the post-replicative proteins are expressed at much higher levels to build the viral particles (32, 33), which explains the suppression of viral protein synthesis is at the post-replicative stage of VACV infection. The two reasons as discussed above can lead to an exhaustion of asparagine supply in VACV-infected cells late during infection. Finally, the shortage of asparagine supply in glucose only medium creates an amino acid imbalance that causes an upregulation eIF2α phosphorylation in VACV-infected cells. We are aware that the eIF2α phosphorylation changes are not high. However, it has been suggested that small changes in eIF2α phosphorylation may cause a significant effect on overall mRNA translation rates due to the limited supply of eIF2B (36). Therefore, it is likely that the eIF2α phosphorylation upregulation can reinforce the suppression of VACV post-replicative protein synthesis in glucose only medium. It is likely that these three mechanisms synergize to exert the

outcome of viral post-replicative protein synthesis suppression. Since many viral infections demand rapid and robust nascent protein synthesis to build up viral particles, asparagine might also be a limiting metabolite in the replication of other viruses.

Emerging evidence demonstrates that asparagine plays a unique and specialized role in regulating various biological processes and disease development in mammalian cells in addition to being a simple protein building block (30, 42-44). Asparagine biosynthesis and metabolism are evolutionarily tailored in mammalian cells so that its supply is limited and highly regulated. ASNS is the only enzyme to catalyze asparagine *de novo* synthesis. In glucose metabolism, asparagine is a non-essential amino acid to be synthesized at the very end of the TCA cycle, and the synthesis is exclusively glutamine dependent (**Fig. 2.1A**). Unlike in flies and worms, asparagine is not used to feed the TCA cycle by converting to aspartate in mammalian cells (mammalian cell asparaginase is inactive) for reasons not completely understood (45, 46). These unusual features render it an attractive target in studying disease development and treatment. To this end, asparagine has received increasing attention recently, especially for its essential role in cancer development. A recent study indicates that asparagine controls breast cancer metastasis in an animal model (27). Asparagine is also important for cancer cell proliferation in multiple cancer cells, especially in the absence of glutamine, due to the requirement for various functions of asparagine (23, 24, 28, 29, 47). The crucial role of asparagine bioavailability in cancer development might, at least partly, account for its limited supply in mammalian cells. Asparagine metabolism is also critical in vessel formation (47). This, together with its importance for VACV replication, suggests that asparagine metabolism is a critical limiting factor in multiple biological processes and diseases, which highlights the importance of studying metabolic regulation of asparagine to understand its roles in various life processes.

Asparagine metabolism can serve as an attractive target for novel anti-poxvirus strategy development. In fact, L-asparaginase has been used to treat various cancers, including acute lymphoblastic leukemia (ALL), acute myeloid leukemia (AML), and non-Hodgkin's lymphoma for decades (48-51). In the future, it would be interesting to investigate how modulation of asparagine metabolism affects poxvirus infection in an animal model. Furthermore, its role in cancer cell proliferation and cancer development implicates asparagine metabolism as a target for designing improved poxvirus-based cancer therapies.

Materials and methods

Cells and viruses

Primary Human Foreskin Fibroblasts (HFFs; kindly provided by Dr. Nicholas Wallace, Kansas State University) were cultured in DMEM (Fisher Scientific) supplemented with 10% Fetal Bovine Serum (FBS, Peak Serum), 2 mM Glutamine (VWR), and 100 U/ml of Penicillin, 100 µg/ml Streptomycin (VWR). BS-C-1 cells (ATCC CCL-26) were grown in EMEM (Fisher Scientific) supplemented with 10% FBS, 2 mM Glutamine, and 100 U/ml of Penicillin, 100 µg/ml Streptomycin. All cells were incubated at 37°C in an incubator with 5% CO_2. VACV Western Reserve (WR) strain (ATCC VR-1354) was used in this study. Amplification, purification, infection, and titration of VACV were carried out using methods described elsewhere (52). Recombinant VACVs encoding a Gaussia luciferase gene under an early (C11R, vEGluc), intermediate (G8R, vIGluc), or late promoter (F17R, vLGluc) were constructed by Dr. Jason Laliberte at the National Institute of Allergy and Infectious Diseases (NIAID) and generously provided by Dr. Bernard Moss (NIAID). Recombinant VACV encoding a Green Fluorescence Protein (GFP) was described elsewhere (53).

Antibodies and chemicals

L-Glutamate, L-aspartate, L-Serine, L-Proline, and L-Alanine were purchased from VWR. L-Asparagine, Dimethyl 2-Oxoglutarate (Dimethyl α-ketoglutarate), L-Methionine Sulfoximine (L-MSO), Asparaginase and puromycin were purchased from Sigma-Aldrich. Dimethyl Sulfoxide (DMSO) and L-albizziine were purchased from Thermo Fisher Scientific. The EmbryoMax Nucleosides (100x) solution was purchased from EMD Millipore. Calyculin A was purchased from Santa Cruz Biotechnology.

Anti-GCN2 (Phos T899) and Anti-GAPDH antibodies were purchased from Abcam. Antibodies against GCN2, Phospho-eIF2α (Ser51), total eIF2α were purchased from Cell Signaling Technology. ASNS antibody was purchased from Proteintech. Anti-puromycin antibody was purchased from Sigma-Aldrich. Antibodies against the whole VACV viral particle were kindly provided by Dr. Bernard Moss.

Glutamine depletion and rescue

For glutamine depletion, DMEM without glucose, L-glutamine, sodium pyruvate, and phenol red (Fisher Scientific) was used. This medium also lacks L-asparagine. The medium was supplemented with 2% dialyzed FBS (Fisher Scientific), to thoroughly deplete small molecules and amino acids while still providing other essential factors for cell growth. For glutamine depletion and rescue experiments, 1 g/L glucose (Fisher Scientific), 2 mM glutamine, and 2 mM L-asparagine or other metabolites were added to the medium when necessary. The cells were washed with 1x PBS (VWR) prior to VACV infection.

Global metabolic profiling

HFFs were grown in T-175 flasks. At about 95-100% confluency, they were washed with 1xPBS twice and then infected with VACV at the MOI of 3 in different media. After 8 hours

post infection (hpi) the cells were harvested by scraping, and the pellet was washed twice with ice-cold PBS. The pellet was then dissolved in the extraction solvent (methanol) and stored at -80°C until shipment to Metabolon Inc. (Durham, North Carolina) for metabolic profiling. All of the metabolic profiling experiments were performed with four biological replicates.

Proprietary analytical procedures were carried out to ensure high quality data after minimizing the system artifacts, misassignments, and background noise among the samples. The raw reads were first normalized in terms of raw area counts, and then each biochemical was rescaled to set the median equal to one. Then, missing values were imputed with the minimum. Values for each sample were normalized by Bradford protein concentration in each sample. Each biochemical was then rescaled to set the median equal to one, and again missing values were imputed with the minimum. Three-way analysis of variation (ANOVA) with contrast tests was performed to calculate the fold change of metabolites.

Cell viability assays

For the trypan-blue exclusion assay, cell viability was measured as described elsewhere (54). Briefly, after treatment, cells of each well (12-well plate) were treated with 300 µl of trypsin and resuspended with 500 µl of DMEM by pipetting. Twenty µl of cell suspension was gently mixed with 20 µl of 4% trypan blue (VWR). The numbers of living and dead cells were counted using a hemocytometer. MTT Cell Proliferation Assay (Cayman Chemicals) was performed according to the manufacturer's instructions. Briefly, equal numbers of cells were seeded in a 96-well plate, allowing to grow overnight in a 37°C incubator, followed by necessary treatments and the absorbance measurement at 570 nm using a microplate reader.

Gaussia luciferase assay

Cells were infected with recombinant VACV encoding a *Gaussia* luciferase gene for indicated time periods. The activities of *Gaussia* luciferase in culture medium were measured at indicated hpi using a Pierce Gaussia Luciferase Flash Assay Kit (Thermo Scientific) and a luminometer.

Western blotting analysis

The procedure was described elsewhere with minor modifications (55). For Western blotting analysis, cells were collected and lysed using RIPA lysis buffer (150 mM NaCl, 1% NP-40, 50 mM Tris-Cl, pH 8.0). Cell lysates were reduced by 100 mM DTT and denatured by sodium dodecyl sulfate–polyacrylamide gel electrophoresis (SDS–PAGE) loading buffer and boiling for 5 min before SDS–PAGE. After electrophoresis, the proteins were transferred to a polyvinylidene difluoride membrane (Fisher Scientific). The membrane was then blocked in TBS-Tween (TBST) [50 mM Tris-HCl (pH 7.5), 200 mM NaCl, 0.05% Tween 20] containing 5% bovine serum albumin (BSA; VWR) for 1 h, incubated with primary antibody in the same TBST/BSA buffer for 1 h, washed with TBST three times for 10 min/each time, incubated with horseradish peroxidase-conjugated secondary antibody for 1 h, washed three times with TBST, and developed with chemiluminescent substrate (National Diagnostics). The whole procedure was carried out at room temperature. Antibodies were stripped from the membrane by Restore buffer (Thermo Fisher Scientific) for Western blotting analysis using another antibody.

Nascent protein synthesis analysis

To label the newly synthesized proteins, the puromycin labeling-based SUrface SEnsing of Translation (SUnSET) method was used. This method allows for the detection in protein synthesis in whole cell lysates using Western blotting analysis and can be used as a newly

developed valid alternative to using traditional radioactive isotopes to label nascent protein synthesis (56, 57). Briefly, 10 μg/mL of puromycin (Sigma Aldrich) was added to the cells 10 min prior to sample collection. The cells were then harvested for immunoblotting using anti-puromycin antibody.

Real-time PCR (RT-PCR)

Total RNA was extracted using TRIzol reagent (Ambion) followed by purification using Invitrogen PureLink RNA Mini Kit (Thermo Fisher Scientific). The RNA was used to synthesize cDNA using SuperScript III First-strand synthesis kit (Invitrogen) according to the manufacturer's instructions using random hexamer primers. Relative mRNA levels were quantified by the CFX96 Real-time PCR Instrument (Bio-Rad) with All-in-One 2x qPCR Mix (GeneCopoeia) and primers specific for indicated genes. The qPCR program was started with an initial denaturation step at 95°C for 3 min, followed by 40 cycles of denaturation at 95°C for 10 s, annealing and reading fluorescence at 52°C for 30 s, and extension at 72°C for 30 s. 18S rRNA was used as a normalization factor for different samples.

RNA interference

Specific and negative control siRNAs (siNC) were purchased from Integrated DNA Technologies (IDT). HFFs were transfected at a concentration of 5 nm using Lipofectamine RNAiMAX (Fisher Scientific), according to manufacturer's instructions. Knockdown efficiency was measured by Western blotting analysis of protein levels.

Amino acid content calculation

The amino acid sequence of proteins encoded by Western Reserve VACV (NC_006998.1) was downloaded from NCBI database. The proteins were classified as early, intermediate or late based on previous publications (58, 59). The amino acid sequences of 20,404

human proteins that were reviewed and manually annotated from literature and curator-evaluated computational analysis were downloaded from UniProt. The asparagine content of the proteins was calculated using ExPASy ProtParam tool (60).

Statistical analysis

Unless otherwise stated, the data represented are the mean of at least three biological replicates. For the analyses of global metabolic profiling, four biological replicates were used for each treatment, and the data were analyzed in an R Studio (version 1.1.442). A two-tailed paired *t-test* was used to evaluate significance in the difference between two means. Error bars represent the standard deviation of the experimental replicates. The following convention for symbols is used to indicate the statistical significance ns=$p > 0.05$, *= $p \leq 0.05$, **= $p \leq 0.01$, ***= $p \leq 0.001$ and ****= $p \leq 0.0001$.

Acknowledgments

We thank Dr. Nicholas Wallace (Kansas State University) for providing HFFs. We thank Dr. Bernard Moss for providing many materials and reagents. We also thank Fernando Cantu in our laboratory for help. The work was supported by grants from the National Institutes of Health to ZY (R21AI128406 and a subproject of P20GM113117). AP is also supported, in part, by Johnson Cancer Research Center of Kansas State University.

References

1. Goodwin CM, Xu S, Munger J. Stealing the Keys to the Kitchen: Viral Manipulation of the Host Cell Metabolic Network. Trends Microbiol. 2015;23(12):789-98. doi: 10.1016/j.tim.2015.08.007.

2. Sanchez EL, Lagunoff M. Viral activation of cellular metabolism. Virology. 2015;479-480:609-18. doi: 10.1016/j.virol.2015.02.038.

3. Shenk T, Alwine JC. Human Cytomegalovirus: Coordinating Cellular Stress, Signaling, and Metabolic Pathways. Annu Rev Virol. 2014;1(1):355-74. doi: 10.1146/annurev-virology-031413-085425. PubMed PMID: 26958726.

4. Yu Y, Clippinger AJ, Alwine JC. Viral effects on metabolism: changes in glucose and glutamine utilization during human cytomegalovirus infection. Trends Microbiol. 2011;19(7):360-7. doi: 10.1016/j.tim.2011.04.002. PubMed PMID: 21570293; PubMed Central PMCID: PMCPMC3130066.

5. Moss B. Poxviridae: The viruses and their replication. Fields Virology, eds, Knipe DM, Howley PM. 2013;2:2129-59.

6. Moss B. Poxvirus DNA replication. Cold Spring Harbor perspectives in biology. 2013;5(9). doi: 10.1101/cshperspect.a010199. PubMed PMID: 23838441; PubMed Central PMCID: PMCPMC3753712.

7. Impelluso G, Lentzos F. The Threat of Synthetic Smallpox: European Perspectives. Health Security. 2017;15(6):582-6. doi: 10.1089/hs.2017.0045.

8. Noyce RS, Lederman S, Evans DH. Construction of an infectious horsepox virus vaccine from chemically synthesized DNA fragments. PLoS One. 2018;13(1):e0188453. doi: 10.1371/journal.pone.0188453. PubMed PMID: 29351298.

9. Editorial. The spectre of smallpox lingers. Nature. 2018;560(7718):281. doi: 10.1038/d41586-018-05936-x. PubMed PMID: 30104592.

10. Moss B. Genetically engineered poxviruses for recombinant gene expression, vaccination, and safety. PNAS. 1996;93(21):11341-8. doi: 10.1073/pnas.93.21.11341.

11. Park B-H, Hwang T, Liu T-C, Sze DY, Kim J-S, Kwon H-C, et al. Use of a targeted oncolytic poxvirus, JX-594, in patients with refractory primary or metastatic liver cancer: a phase I trial. The Lancet Oncology. 2008;9(6):533-42. doi: 10.1016/S1470-2045(08)70107-4.

12. Chan WM, McFadden G. Oncolytic Poxviruses. Ann Rev Virol. 2014;1:191-214. doi: 10.1146/annurev-virology-031413-085442. PubMed PMID: WOS:000350745100011.

13. Moss B. Reflections on the early development of poxvirus vectors. Vaccine. 2013;31(39):4220-2. doi: 10.1016/j.vaccine.2013.03.042. PubMed PMID: 23583893; PubMed Central PMCID: PMC3755097.

14. Greseth MD, Traktman P. De novo fatty acid biosynthesis contributes significantly to establishment of a bioenergetically favorable environment for vaccinia virus infection. PLoS pathogens. 2014;10(3):e1004021. doi: 10.1371/journal.ppat.1004021. PubMed PMID: 24651651; PubMed Central PMCID: PMC3961357.

15. Fontaine KA, Camarda R, Lagunoff M. Vaccinia virus requires glutamine but not glucose for efficient replication. J Virol. 2014;88(8):4366-74. doi: 10.1128/JVI.03134-13. PubMed PMID: 24501408; PubMed Central PMCID: PMCPMC3993723.

16. Mazzon M, Castro C, Roberts LD, Griffin JL, Smith GL. A role for vaccinia virus protein C16 in reprogramming cellular energy metabolism. J Gen Virol. 2015;96(Pt 2):395-407. doi: 10.1099/vir.0.069591-0.

17. Curi R, Lagranha CJ, Doi SQ, Sellitti DF, Procopio J, Pithon-Curi TC, et al. Molecular mechanisms of glutamine action. Journal of Cellular Physiology. 2005;204(2):392-401. doi: 10.1002/jcp.20339.

18. Bodner GM. Metabolism Part II: The tricarboxylic acid (TCA), citric acid, or Krebs cycle. J Chem Educ. 1986;63(8):673. doi: 10.1021/ed063p673.

19. Owen OE, Kalhan SC, Hanson RW. The Key Role of Anaplerosis and Cataplerosis for Citric Acid Cycle Function. J Biol Chem. 2002;277(34):30409-12. doi: 10.1074/jbc.R200006200.

20. Xiao D, Zeng L, Yao K, Kong X, Wu G, Yin Y. The glutamine-alpha-ketoglutarate (AKG) metabolism and its nutritional implications. Amino Acids. 2016;48(9):2067-80. doi: 10.1007/s00726-016-2254-8.

21. DeBerardinis RJ, Cheng T. Q's next: the diverse functions of glutamine in metabolism, cell biology and cancer. Oncogene. 2010;29(3):313-24. doi: 10.1038/onc.2009.358. PubMed PMID: 19881548; PubMed Central PMCID: PMCPMC2809806.

22. Smith RJ. Glutamine metabolism and its physiologic importance. JPEN J Parenter Enteral Nutr. 1990;14(4 Suppl):40S-4S. doi: 10.1177/014860719001400402. PubMed PMID: 2205730.

23. Krall AS, Xu S, Graeber TG, Braas D, Christofk HR. Asparagine promotes cancer cell proliferation through use as an amino acid exchange factor. Nat Commun. 2016;7:11457. doi: 10.1038/ncomms11457. PubMed PMID: 27126896; PubMed Central PMCID: PMCPMC4855534.

24. Zhang J, Fan J, Venneti S, Cross JR, Takagi T, Bhinder B, et al. Asparagine plays a critical role in regulating cellular adaptation to glutamine depletion. Mol Cell.

2014;56(2):205-18. doi: 10.1016/j.molcel.2014.08.018. PubMed PMID: 25242145; PubMed Central PMCID: PMCPMC4224619.

25. Lomelino CL, Andring JT, McKenna R, Kilberg MS. Asparagine synthetase: Function, structure, and role in disease. J Biol Chem. 2017;292(49):19952-8. doi: 10.1074/jbc.R117.819060.

26. Patterson MK, Orr GR. Asparagine Biosynthesis by the Novikoff Hepatoma ISOLATION, PURIFICATION, PROPERTY, AND MECHANISM STUDIES OF THE ENZYME SYSTEM. J Biol Chem. 1968;243(2):376-80.

27. Knott SRV, Wagenblast E, Khan S, Kim SY, Soto M, Wagner M, et al. Asparagine bioavailability governs metastasis in a model of breast cancer. Nature. 2018;554(7692):378-81. doi: 10.1038/nature25465.

28. Pavlova NN, Hui S, Ghergurovich JM, Fan J, Intlekofer AM, White RM, et al. As Extracellular Glutamine Levels Decline, Asparagine Becomes an Essential Amino Acid. Cell metabolism. 2018;27(2):428-38 e5. doi: 10.1016/j.cmet.2017.12.006. PubMed PMID: 29337136.

29. Zhu Y, Li T, Ramos da Silva S, Lee JJ, Lu C, Eoh H, et al. A Critical Role of Glutamine and Asparagine gamma-Nitrogen in Nucleotide Biosynthesis in Cancer Cells Hijacked by an Oncogenic Virus. mBio. 2017;8(4). doi: 10.1128/mBio.01179-17. PubMed PMID: 28811348; PubMed Central PMCID: PMCPMC5559638.

30. Wu G. Amino acids: metabolism, functions, and nutrition. Amino Acids. 2009;37(1):1-17. Epub 2009/03/21. doi: 10.1007/s00726-009-0269-0. PubMed PMID: 19301095.

31. Sookoian S, Pirola CJ. Alanine and aspartate aminotransferase and glutamine-cycling pathway: their roles in pathogenesis of metabolic syndrome. World J Gastroenterol. 2012;18(29):3775-81. Epub 2012/08/10. doi: 10.3748/wjg.v18.i29.3775. PubMed PMID: 22876026; PubMed Central PMCID: PMCPMC3413046.

32. Resch W, Hixson KK, Moore RJ, Lipton MS, Moss B. Protein composition of the vaccinia virus mature virion. Virology. 2007;358(1):233-47. doi: 10.1016/j.virol.2006.08.025. PubMed PMID: 17005230.

33. Chung CS, Chen CH, Ho MY, Huang CY, Liao CL, Chang W. Vaccinia virus proteome: identification of proteins in vaccinia virus intracellular mature virion particles. J Virol. 2006;80(5):2127-40. doi: 10.1128/JVI.80.5.2127-2140.2006. PubMed PMID: 16474121; PubMed Central PMCID: PMCPMC1395410.

34. Castilho BA, Shanmugam R, Silva RC, Ramesh R, Himme BM, Sattlegger E. Keeping the eIF2 alpha kinase Gcn2 in check. Biochim Biophys Acta. 2014;1843(9):1948-68. Epub 2014/04/16. doi: 10.1016/j.bbamcr.2014.04.006. PubMed PMID: 24732012.

35. Sood R, Porter AC, Olsen DA, Cavener DR, Wek RC. A mammalian homologue of GCN2 protein kinase important for translational control by phosphorylation of eukaryotic

initiation factor-2alpha. Genetics. 2000;154(2):787-801. PubMed PMID: 10655230; PubMed Central PMCID: PMCPMC1460965.

36. Walsh D, Mathews MB, Mohr I. Tinkering with translation: protein synthesis in virus-infected cells. Cold Spring Harbor perspectives in biology. 2013;5(1):a012351. doi: 10.1101/cshperspect.a012351. PubMed PMID: 23209131; PubMed Central PMCID: PMC3579402.

37. Czarnecki MW, Traktman P. The vaccinia virus DNA polymerase and its processivity factor. Virus research. 2017;234:193-206. doi: 10.1016/j.virusres.2017.01.027. PubMed PMID: 28159613; PubMed Central PMCID: PMCPMC5476500.

38. Shrivastava A, Khan AA, Khurshid M, Kalam MA, Jain SK, Singhal PK. Recent developments in l-asparaginase discovery and its potential as anticancer agent. Critical Reviews in Oncology/Hematology. 2016;100:1-10. doi: 10.1016/j.critrevonc.2015.01.002.

39. Andrulis IL, Evans-Blackler S, Siminovitch L. Characterization of single step albizziin-resistant Chinese hamster ovary cell lines with elevated levels of asparagine synthetase activity. J Biol Chem. 1985;260(12):7523-7.

40. Neermann J, Wagner R. Comparative analysis of glucose and glutamine metabolism in transformed mammalian cell lines, insect and primary liver cells. Journal of Cellular Physiology. 1998;166(1):152-69. doi: 10.1002/(SICI)1097-4652(199601)166:1<152::AID-JCP18>3.0.CO;2-H.

41. Vander Heiden MG, Cantley LC, Thompson CB. Understanding the Warburg Effect: The Metabolic Requirements of Cell Proliferation. Science. 2009;324(5930):1029-33. doi: 10.1126/science.1160809.

42. Meijer AJ. Amino acids as regulators and components of nonproteinogenic pathways. J Nutr. 2003;133(6 Suppl 1):2057S-62S. doi: 10.1093/jn/133.6.2057S. PubMed PMID: 12771365.

43. Yang Q, Vijayakumar A, Kahn BB. Metabolites as regulators of insulin sensitivity and metabolism. Nature reviews Molecular cell biology. 2018. doi: 10.1038/s41580-018-0044-8. PubMed PMID: 30104701.

44. Jefferson LS, Kimball SR. Amino acids as regulators of gene expression at the level of mRNA translation. J Nutr. 2003;133(6 Suppl 1):2046S-51S. doi: 10.1093/jn/133.6.2046S. PubMed PMID: 12771363.

45. Jiang J, Pavlova NN, Zhang J. Asparagine, a critical limiting metabolite during glutamine starvation. Molecular & Cellular Oncology. 2018;0(0):e1441633. doi: 10.1080/23723556.2018.1441633.

46. Balasubramanian MN, Butterworth EA, Kilberg MS. Asparagine synthetase: regulation by cell stress and involvement in tumor biology. American Journal of Physiology-

Endocrinology and Metabolism. 2013;304(8):E789-E99. doi: 10.1152/ajpendo.00015.2013.

47. Huang H, Vandekeere S, Kalucka J, Bierhansl L, Zecchin A, Bruning U, et al. Role of glutamine and interlinked asparagine metabolism in vessel formation. EMBO J. 2017;36(16):2334-52. doi: 10.15252/embj.201695518. PubMed PMID: 28659375; PubMed Central PMCID: PMCPMC5556263.

48. Egler RA, Ahuja SP, Matloub Y. L-asparaginase in the treatment of patients with acute lymphoblastic leukemia. J Pharmacol Pharmacother. 2016;7(2):62-71. doi: 10.4103/0976-500X.184769.

49. Broome JD. Evidence that the L-Asparaginase Activity of Guinea Pig Serum is responsible for its Antilymphoma Effects. Nature. 1961;191(4793):1114-5. doi: 10.1038/1911114a0.

50. Adamson RH, Fabro S. Antitumor activity and other biologic properties of L-asparaginase (NSC-109229)-a review. Cancer Chemother Rep. 1968;52(6):617-26. PubMed PMID: 4895425.

51. Mauer AM. Therapy of acute lymphoblastic leukemia in childhood. Blood. 1980;56(1):1-10. PubMed PMID: 6992886.

52. Cotter CA, Earl PL, Wyatt LS, Moss B. Preparation of Cell Cultures and Vaccinia Virus Stocks. Curr Protoc Protein Sci. 2017;89:5 12 1-5 8. doi: 10.1002/cpps.34. PubMed PMID: 28762495.

53. Yang Z, Moss B. Interaction of the vaccinia virus RNA polymerase-associated 94-kilodalton protein with the early transcription factor. J Virol. 2009;83(23):12018-26. doi: 10.1128/JVI.01653-09. PubMed PMID: 19759131; PubMed Central PMCID: PMCPMC2786748.

54. Strober W. Trypan Blue Exclusion Test of Cell Viability. Current Protocols in Immunology. 2015;111(1):A3.B.1-A3.B. doi: 10.1002/0471142735.ima03bs111.

55. Dhungel P, Cao S, Yang Z. The 5'-poly(A) leader of poxvirus mRNA confers a translational advantage that can be achieved in cells with impaired cap-dependent translation. PLoS pathogens. 2017;13(8):e1006602. doi: 10.1371/journal.ppat.1006602. PubMed PMID: 28854224.

56. Goodman CA, Hornberger TA. Measuring protein synthesis with SUnSET: a valid alternative to traditional techniques? Exerc Sport Sci Rev. 2013;41(2):107-15. doi: 10.1097/JES.0b013e3182798a95. PubMed PMID: 23089927; PubMed Central PMCID: PMCPMC3951011.

57. Schmidt EK, Clavarino G, Ceppi M, Pierre P. SUnSET, a nonradioactive method to monitor protein synthesis. Nat Methods. 2009;6(4):275-7. doi: 10.1038/nmeth.1314. PubMed PMID: 19305406.

58. Yang Z, Bruno DP, Martens CA, Porcella SF, Moss B. Simultaneous high-resolution analysis of vaccinia virus and host cell transcriptomes by deep RNA sequencing. Proc Natl Acad Sci U S A. 2010;107(25):11513-8. doi: 10.1073/pnas.1006594107. PubMed PMID: 20534518; PubMed Central PMCID: PMCPMC2895082.

59. Yang Z, Reynolds SE, Martens CA, Bruno DP, Porcella SF, Moss B. Expression profiling of the intermediate and late stages of poxvirus replication. J Virol. 2011;85(19):9899-908. doi: 10.1128/JVI.05446-11. PubMed PMID: 21795349; PubMed Central PMCID: PMCPMC3196450.

60. Gasteiger E. HC, Gattiker A., Duvaud S., Wilkins M.R., Appel R.D., Bairoch A. Protein Identification and Analysis Tools on the ExPASy Server. In: Walker JM, editor. The Proteomics Protocols Handbook: Humana Press; 2005. p. 571-607.

Figures and tables- Chapter 2

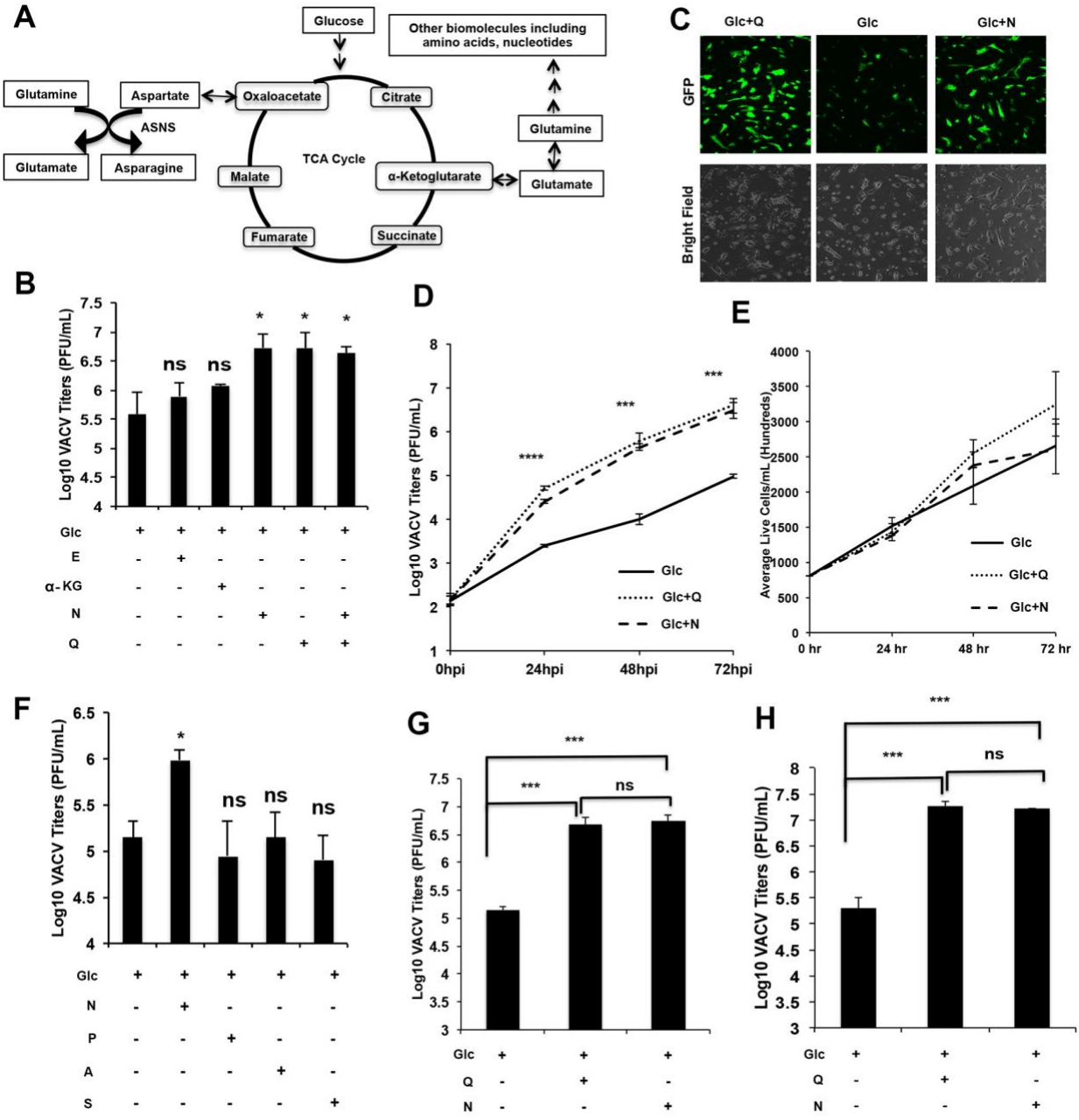

Figure 2.1. Asparagine fully rescues VACV replication from glutamine depletion.
(A) Schematic of the role of glutamine in the TCA cycle and biomolecule synthesis. Note that asparagine exclusively requires glutamine for its biosynthesis. **(B)** Asparagine fully rescues VACV replication from glutamine depletion, while α- KG and glutamate do not. HFFs were infected with VACV at an MOI of 2 in media containing 1 g/L glucose (Glc), 2 mM glutamine

(Q), 2 mM asparagine (N), 7 mM α-KG, or 5 mM glutamate (E) as indicated. VACV titers were measured by a plaque assay at 24 hpi. **(C)** Asparagine rescues GFP expression from recombinant VACV in the absence of glutamine. HFFs were infected with a recombinant VACV encoding a GFP gene at an MOI of 2 in the indicated medium. GFP expression was observed under a microscope at 24 hpi. **(D)** Asparagine rescues VACV growth kinetics from glutamine depletion. HFFs were infected with VACV at an MOI of 0.001 in medium containing the indicated nutrients. VACV titers were measured by a plaque assay at the indicated times post infection. **(E)** HFF proliferation is not affected in different growth media. Equal numbers of HFFs were seeded in the indicated media. The cell numbers were counted over a 72-h period of using a hemocytometer. **(F)** Proline (P), alanine (A) and serine (S) cannot rescue VACV replication from glutamine depletion. Experiments were carried out similar to (B) with 5 mM proline, 1 mM alanine or 1 mM serine used. **(G)** Asparagine rescues VACV replication from glutamine depletion in BS-C-1 cells. BS-C-1 cells were infected with VACV at an MOI of 2 in indicated media and virus titers were measured at 24 hpi. **(H)** BS-C-1 cells were infected with VACV at an MOI of 0.01 in indicated media, and the virus titers were measured at 48 hpi by a plaque assay. Error bars represent the standard deviation of at least three biological replicates. ns=$p > 0.05$, *= $p \leq 0.05$, ***= $p \leq 0.001$ and ****= $p \leq 0.0001$.

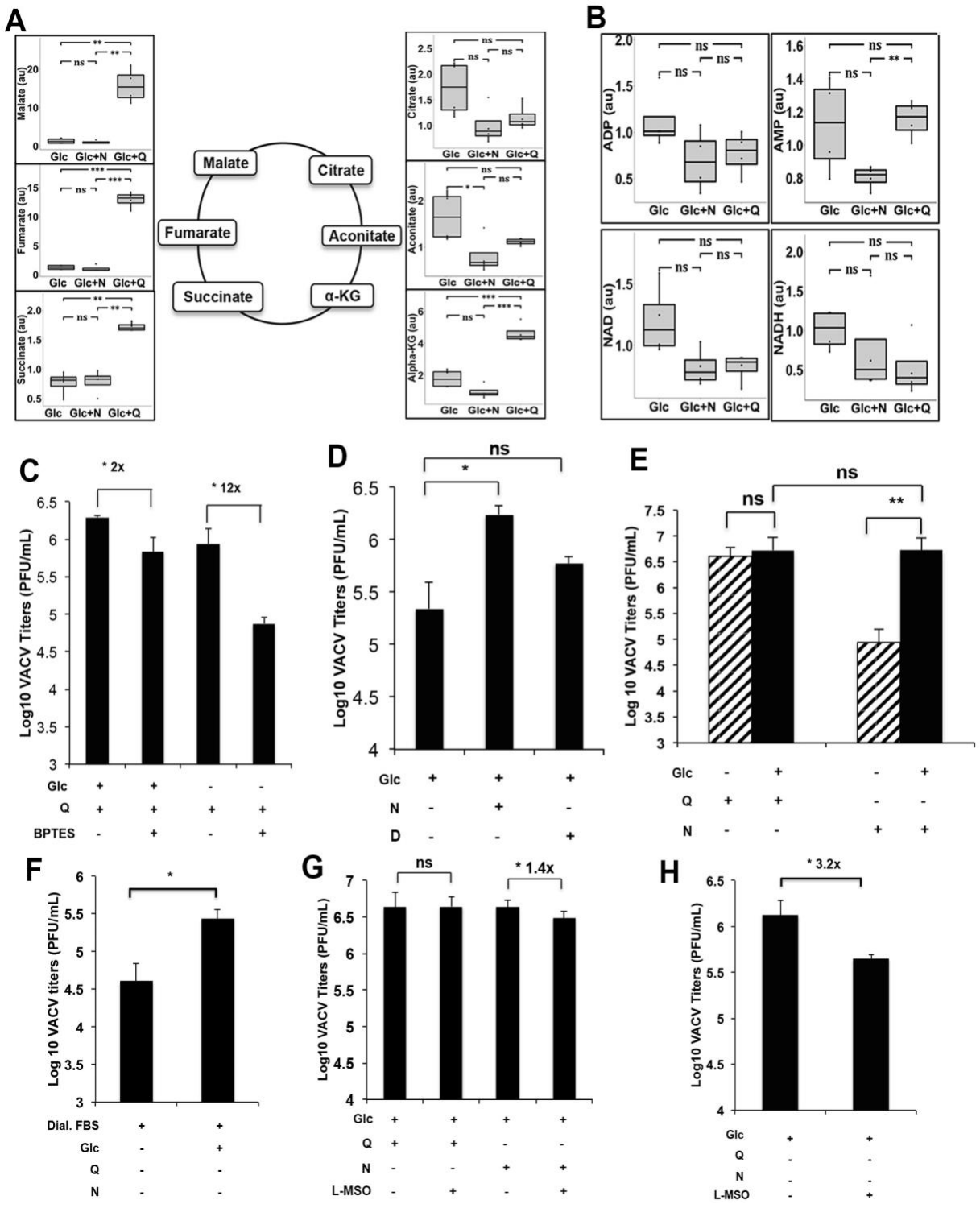

Figure 2.2. Asparagine supplementation does not enhance TCA cycle activities under glutamine-depleted condition during VACV infection.

(A) Asparagine addition does not recapitulate glutamine's effect on TCA cycle activities. Levels of TCA cycle intermediates in HFFs infected with VACV (MOI of 3) for 8 h, in media

containing glucose (Glc), glucose plus asparagine (Glc+N), or glucose plus glutamine (Glc+Q), were determined by global metabolic profiling. **(B)** Levels of oxidative phosphorylation intermediates in VACV-infected HFFs are not significantly different (from the same metabolic profiling as described in A). **(C)** Inhibiting glutaminase activity more severely affected VACV replication in the absence of glucose. HFFs were infected with VACV, at an MOI of 2 for 24 h, in medium containing 10 □M BPTES or DMSO (control). The numbers indicate the fold change in VACV titer compared to DMSO treatment. **(D)** Aspartate is not as efficient as asparagine in supporting VACV replication. VACV titers in HFFs infected with VACV, at an MOI of 2 for 24 h, in media with glucose (Glc), asparagine (N) or aspartate (D) were measured by a plaque assay. **(E)** Rescue of VACV replication from glutamine depletion requires the presence of glucose. HFFs were infected with VACV, at an MOI of 2 for 24 h, in different media in the presence or absence of glucose as indicated. VACV titer was measured by a plaque assay. **(F)** VACV replication decreases when glucose is not added to the culture medium in the absence of glutamine. HFFs were infected with VACV, at an MOI of 2 for 24 h, in media with 2% dialyzed FBS in the presence or absence of glucose (Glc). VACV titer was measured by a plaque assay. **(G)** Inhibition of glutamine synthetase only slightly affected VACV replication in the presence of glutamine or asparagine. HFFs were infected with VACV, at an MOI of 2 for 24 h, in indicated medium containing 2 mM L-Methionine Sulfoximine (L-MSO) or DMSO. VACV titers were determined by a plaque assay. **(H)** L-MSO has a more significant effect in VACV replication in the absence of glutamine or asparagine. Experiments performed as described in (G) in media containing glucose only. Error bars represent the standard deviation of at least three replicates. ns=$p > 0.05$, *= $p \leq 0.05$, **= $p \leq 0.01$, ***= $p \leq 0.001$. The numbers above the bars represent fold change.

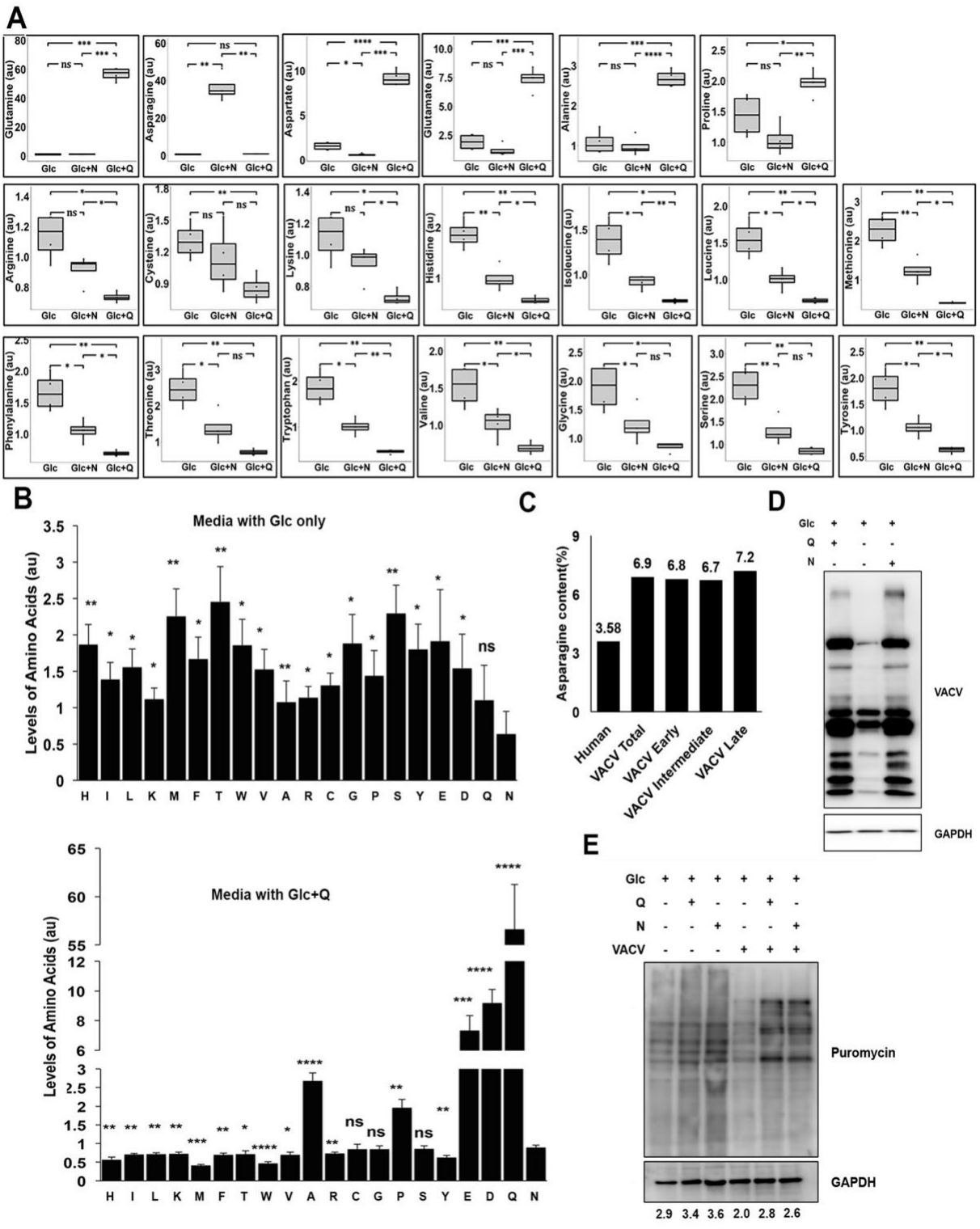

Figure 2.3. Asparagine rescues VACV protein synthesis from glutamine depletion.

(A) Addition of asparagine decreases accumulation of most amino acids in glutamine-depleted condition. Relative Levels of amino acids in HFFs infected with VACV at an MOI of 3 for 8 h in

media as described in Fig 2A, were determined by global metabolic profiling. **(B)** Upon glutamine depletion, asparagine is the least abundant amino acid in VACV infected cells. Upon glutamine repletion, asparagine is one of the most abundant amino acids. The levels of amino acids in HFFs infected with VACV at an MOI of 3 for 8 h in media with glucose (top) and glucose plus glutamine (bottom) were determined by global metabolic profiling. Statistical significance is shown by comparing to asparagine level. **(C)** Asparagine contents of VACV and human genome-encoded proteins calculated by ExPASy ProtParam tool. The numbers above the bar indicate the percentage of asparagine content. **(D)** Asparagine rescues VACV protein synthesis from glutamine depletion. Western blotting analysis was carried out in HFFs infected with VACV at an MOI of 2 for 24 h in the indicated medium. GAPDH was used as a loading control. **(E)** Rescue of nascent protein synthesis by asparagine under glutamine-depleted condition. HFFs were infected with VACV at an MOI of 2 or mock-infected for 16 h in the indicated medium. Cells were treated with 10 μg/mL puromycin for 10 min before collection followed by Western blotting analysis using anti-puromycin and anti-GAPDH antibodies (the latter as a loading control). The numbers indicate GAPDH normalized puromycin intensities. Error bars represent the standard deviation of four biological replicates. ns=$p > 0.05$, *= $p \leq 0.05$, **= $p \leq 0.01$, ***= $p \leq 0.001$ and ****= $p \leq 0.0001$.

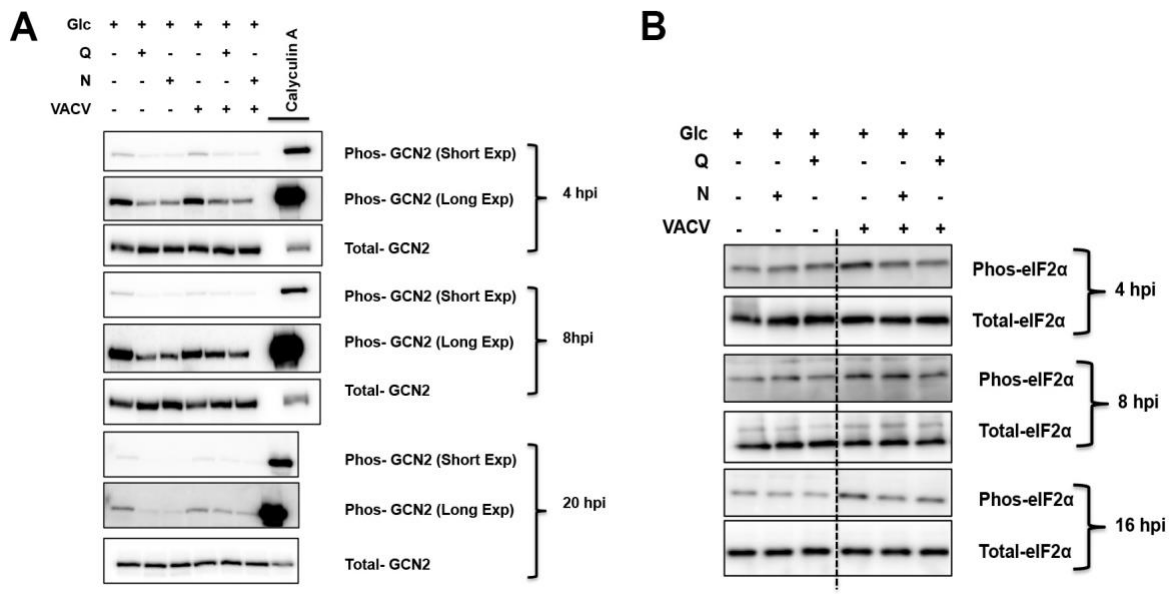

Figure 2.4. GCN2 and eIF2α phosphorylation are affected by different growth conditions in VACV-infected cells.

(A) GCN2 phosphorylation in HFFs infected with VACV or mock-infected in different media. HFFs were infected with VACV for 4 h, 8 h, and 20 h in the indicated media. The levels of proteins were determined by Western blotting analysis using indicated antibodies. HFFs were treated with 100 nM Calyculin A for 30 minutes as a positive control for GCN2 phosphorylation. **(B)** eIF2α phosphorylation in HFFs infected with VACV or mock-infected in different media. HFFs were infected with VACV for 4 h, 8 h, and 16 h in the indicated media. The levels of proteins were determined by Western blotting analysis using indicated antibodies. The blots of uninfected and VACV-infected cell lysates were from lanes on the same gel separated by a vertical dashed line.

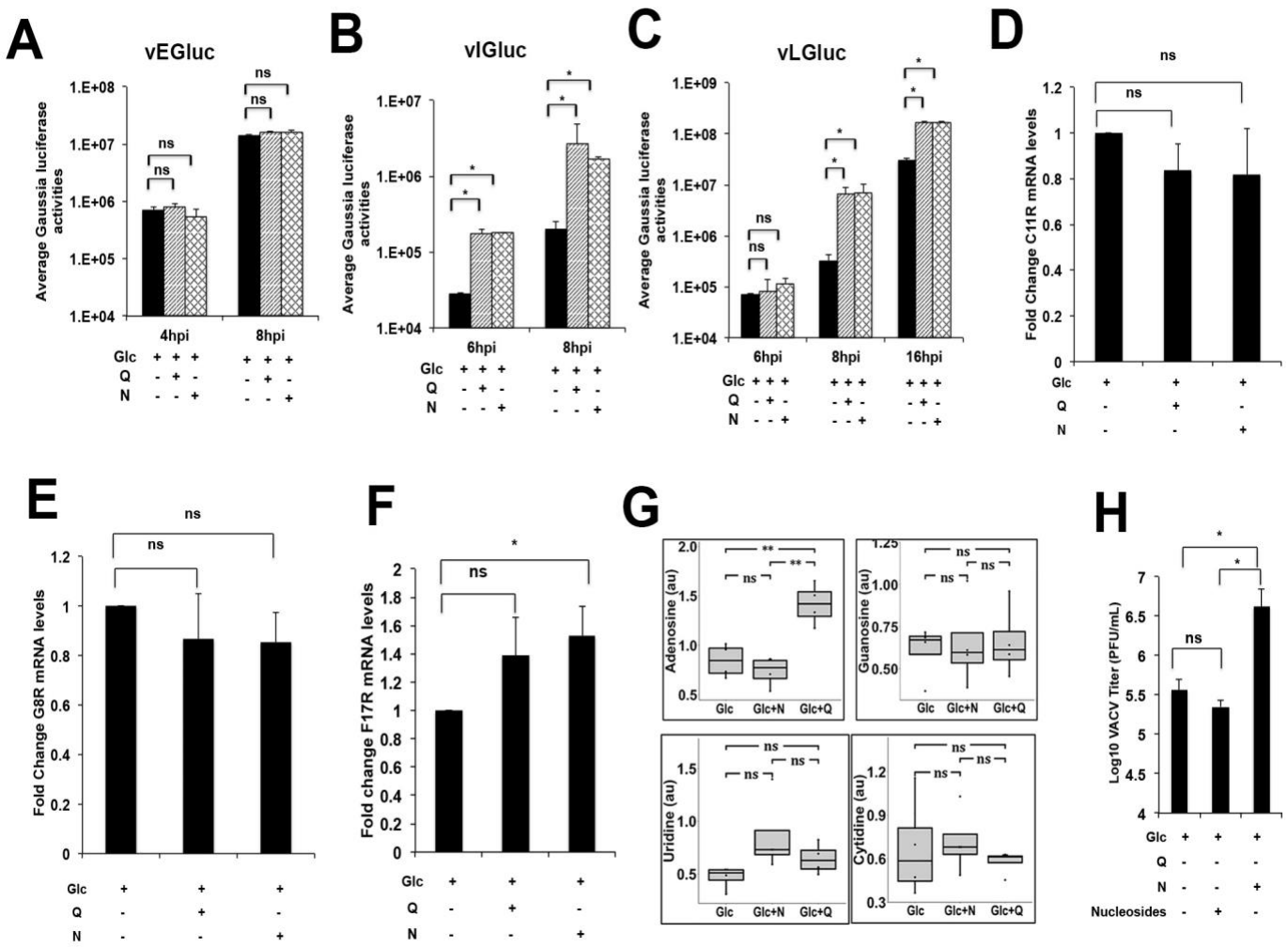

Figure 2.5. Asparagine rescues VACV post-replicative mRNA translation from glutamine depletion.

(A-C) Efficient VACV intermediate and late gene expression, but not early gene expression, requires the presence of asparagine in the glutamine-depleted medium. HFFs infected with VACV that expressed Gaussia luciferase under early (vEGLuc, A), intermediate

(vIGLuc, B), and late promoters (vLGLuc, C), respectively, in indicated medium followed by Gaussia luciferase activity measurement at indicated times. **(D-F)** Effects of asparagine or glutamine in glucose only medium on VACV early (C11R, D), intermediate (G8R, E) and late (F17R, F) mRNA levels. RNA was extracted from HFFs infected with VACV at an MOI of 2 and qRT-PCR was performed. (**G)** Asparagine addition does not increase levels of nucleosides in the glutamine-depleted medium. Relative levels of nucleosides in HFFs infected with VACV at an MOI of 3 for 8 h in medium containing glucose (Glc), glucose plus asparagine (Glc+N) or glucose plus glutamine (Glc+Q), were determined by global metabolic profiling. **(H)** Addition of exogenous nucleosides in the glutamine-depleted medium does not rescue VACV replication. HFFs were infected with VACV at an MOI of 2 in the indicated medium in the presence or absence of 1x nucleosides for 24 h, followed by VACV titer measurement using a plaque assay. Error bars represent the standard deviation of at least three biological replicates. ns=$p > 0.05$, *= $p \leq 0.05$, **= $p \leq 0.01$.

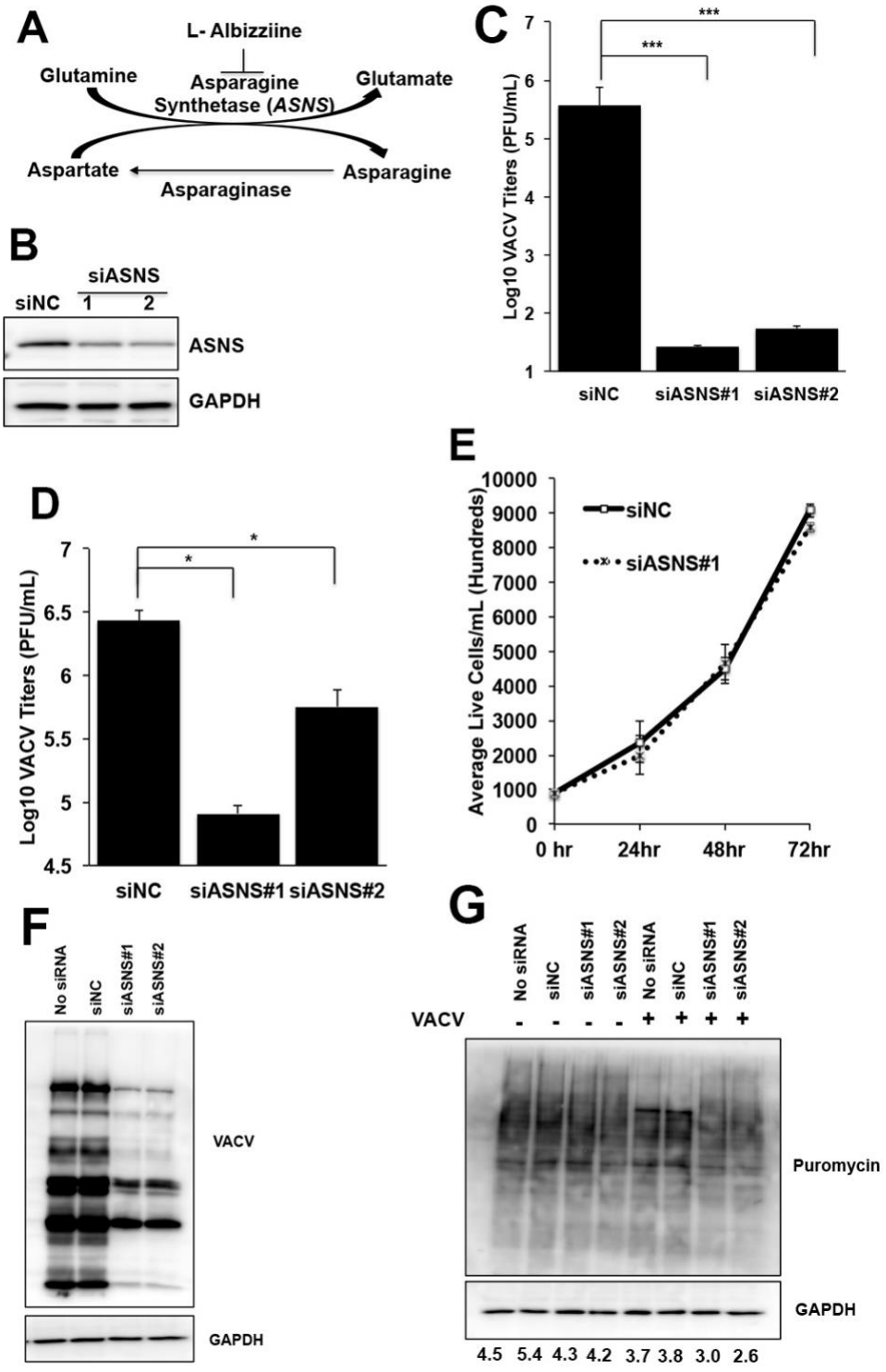

Figure 2.6. ASNS knockdown impairs VACV replication.

(A) Schematic of asparagine metabolism. ASNS catalyzes the *de novo* biosynthesis of asparagine. Asparaginase catalyzes the conversion of asparagine to aspartate (inactive in

mammalian cells). L-albizziine is a competitive inhibitor of ASNS. **(B)** ASNS siRNAs efficiently knock down ASNS protein level. HFFs were transfected with indicated siRNA for 72 h, and the indicated proteins were detected using specific antibodies. **(C, D)** ASNS knockdown severely impairs VACV replication. HFFs were transfected with indicated siRNAs for 72 h and then infected with VACV at an MOI of 0.001 (C) or 2 (D). VACV titers were measured at 72 and 24 hpi, respectively, using a plaque assay. **(E)** ASNS knockdown does not affect the proliferation of HFFs. HFFs treated with indicated siRNAs and numbers of live cells were counted using a hemocytometer for the indicated time period. **(F)** ASNS knockdown impairs VACV protein synthesis. HFFs transfected with the indicated siRNAs were infected with VACV at an MOI of 2 for 24 h, and the proteins were analyzed by Western blotting analysis using VACV antibody. (**G**) ASNS knockdown inhibits nascent protein synthesis in VACV-infected cells. HFFs transfected with indicated siRNAs were infected with VACV at an MOI of 2 or mock-infected for 24 h. Cells were treated with 10 μg/mL puromycin for 10 min before harvesting for Western blotting analysis using indicated antibodies. The numbers indicated GAPDH normalized puromycin intensities. Error bars represent the standard deviation of at least three biological replicates. *= $p \leq 0.05$, ***= $p \leq 0.001$.

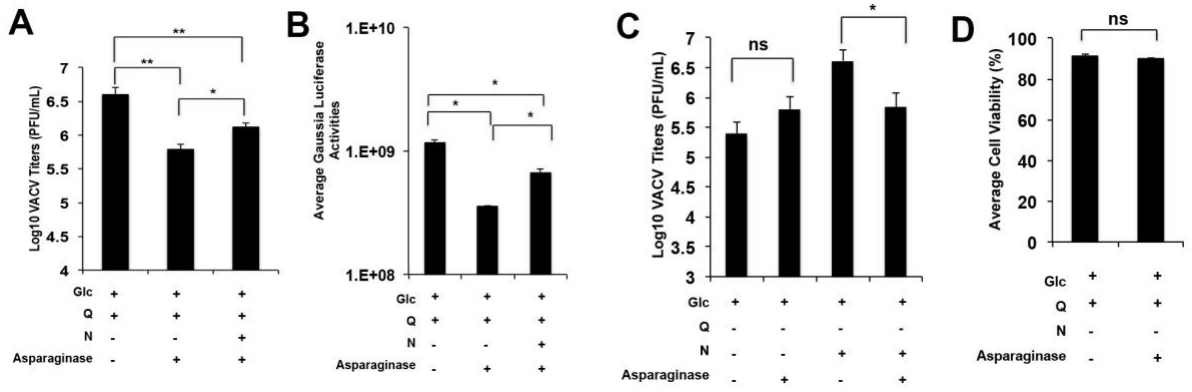

Figure 2.7. Asparaginase treatment impairs VACV replication.

(A) Asparaginase treatment reduces VACV replication. HFFs were pretreated with 10 U of asparaginase for 24 h and infected with VACV at an MOI of 2 for 24 h in indicated medium. Plaque assays measured VACV titers. **(B)** Asparaginase treatment reduces VACV gene expression. HFFs were pretreated with 10 U of asparaginase for 24 h and infected with vLGLuc at an MOI of 2 for 16 h. Gaussia luciferase activities were measured. **(C)** Asparaginase reduces VACV replication in medium containing asparagine but has no effect on medium containing glucose only without asparagine and glutamine. HFFs were treated with asparaginase and infected with VACV at an MOI of 2 for 24 h in the indicated medium. Plaque assays measured VACV titers. **(D)** Asparaginase treatment does not reduce HFF cell viability. HFFs were treated with 10 U of asparaginase for 48 h before the cell viability was measured by Trypan blue exclusion assay. Error bars represent the standard deviation of at least three biological replicates. ns=$p > 0.05$, *= $p \leq 0.05$, and **= $p \leq 0.01$.

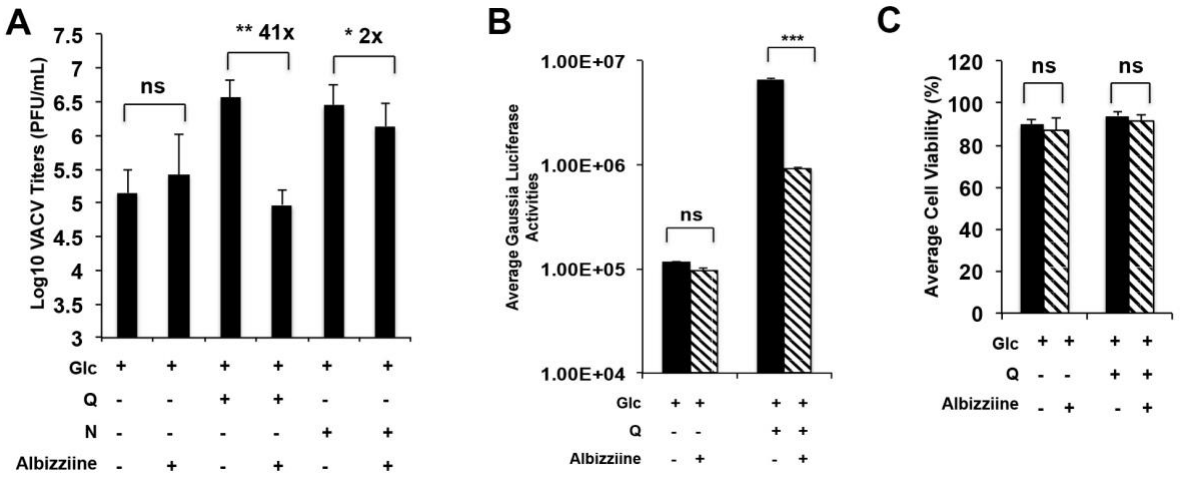

Figure 2.8. L-albizziine treatment impairs VACV replication.

(A) Inhibition of ASNS by L-albizziine reduces VACV replication in glutamine containing medium. HFFs were infected with VACV, at an MOI of 2 in the indicated medium in the presence or absence of 5 mM L-albizziine. VACV titers were measured at 24 hpi by a plaque assay. **(B)** Albizziine reduces gaussia luciferase activity of recombinant VACV in glutamine-containing media. HFFs were infected with vLGLuc at an MOI of 2 in indicated media in the presence or absence of 5 mM L-albizziine. Gaussia luciferase activity was measured at 8 hpi. **(C)** Albizziine treatment does not reduce HFF cell viability. HFFs were cultured in indicated medium in the presence or absence of 10 mM L-albizziine for 24 h. Cell viability was measured by Trypan blue-exclusion assay. Error bars represent the standard deviation of at least three biological replicates. ns=$p > 0.05$, *= $p \leq 0.05$, **= $p \leq 0.01$, and ***= $p \leq 0.001$. The numbers above the bars represent fold change.

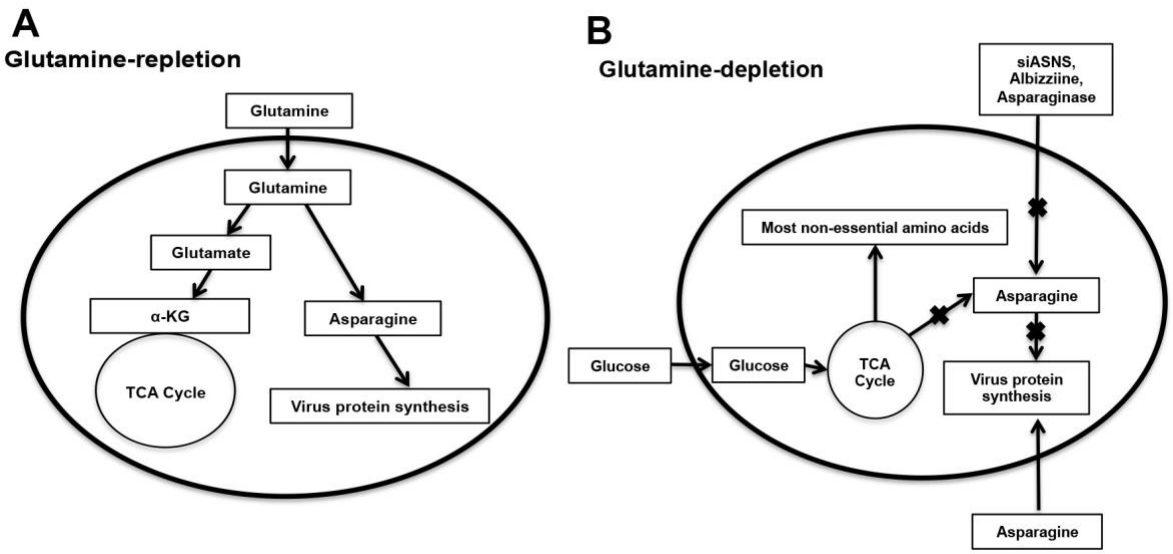

Figure 2.9. Proposed model for the role of asparagine in VACV replication.
(A) In VACV infected cells under glutamine-replete condition, glutamine supports the TCA cycle activities (glucose is dispensable) and also allows asparagine *de novo* biosynthesis that promotes viral protein synthesis. **(B)** Under glutamine-depleted condition or other ways in which the asparagine supply is affected, VACV post-replicative protein synthesis is inhibited although glucose is able to sustain the TCA cycle activities and biosynthesis of most other non-essential amino acids.

Table 2.1. Levels of various metabolites upon infection of HFFs with VACV.

Samples were prepared as described in materials and methods. Global metabolic profiling was done by Metabolon Inc. (Durham, NC) using proprietary techniques. The mean values of the metabolites of four biological replicates detected by global metabolic profiling after normalizing the data with BCA protein assay is shown.

Super	Sub Pathway	Biochemical Name	Glc	Glc + N	Glc + Q
Amino Acid	Glycine, Serine and Threonine Metabolism	glycine	1.8818	1.2362	0.8507
		N-acetylglycine	1.5295	1.0690	0.8637
		betaine	1.5974	1.1713	0.8993
		serine	2.2930	1.2953	0.8544
		N-acetylserine	2.0188	0.9825	0.5863
		threonine	2.4555	1.3971	0.7191
		N-acetylthreonine	1.9251	1.0229	0.7870
		homoserine lactone	1.8493	1.5705	0.6175
	Alanine and Aspartate Metabolism	alanine	1.0758	0.9882	2.6772
		N-acetylalanine	2.0497	1.1565	0.9972
		aspartate	1.5420	0.5916	9.1995
		N-acetylaspartate (NAA)	1.6326	0.9966	0.9081
		asparagine	0.6367	36.2614	0.8955
		N-acetylasparagine	1.4213	1.0842	0.4343
		glutamate	1.9136	1.1897	7.3297

	Glutamate Metabolism	glutamine	1.1028	1.1637	56.6077
		alpha-ketoglutaramate*	0.4252	0.7239	9.1441
		N-acetylglutamate	1.7724	1.1766	0.8636
		N-acetylglutamine	1.6627	0.9289	2.1403
		gamma-carboxyglutamate	1.6299	0.9594	0.9563
		glutamate, gamma-methyl ester	1.5325	1.2830	6.3971
		pyroglutamine*	1.6711	1.5886	2.9939
		N-acetyl-aspartyl-glutamate (NAAG)	1.3366	0.9357	0.6884
		beta-citrylglutamate	1.2068	0.8205	0.7509
		carboxyethyl-GABA	0.9279	0.4257	0.3889
		N-methyl-GABA	1.5991	0.8610	0.8796
		S-1-pyrroline-5-carboxylate	1.1309	0.8027	4.6471
	Histidine Metabolism	histidine	1.8656	0.9971	0.5691
		N-acetylhistidine	1.4502	0.4984	0.3503
		imidazole propionate	0.4556	1.6186	2.1862
		imidazole lactate	2.8831	1.2115	0.3007
		carnosine	1.6698	1.0648	0.8985
		4-imidazoleacetate	1.7973	1.2298	0.7754
	Lysine Metabolism	lysine	1.1148	0.9473	0.7268
		N6,N6,N6-trimethyllysine	2.3720	0.9445	0.5136
		5-(galactosylhydroxy) L- lysine	0.8254	0.6146	1.0282

		saccharopine	2.3161	0.9209	0.9011
		2-aminoadipate	2.5072	0.9590	0.2661
		pipecolate	3.5884	1.7770	0.1115
		6-oxopiperidine-2- carboxylate	1.6278	0.7307	0.6811
		5-aminovalerate	3.0547	1.5832	1.1345
		N,N,N-trimethyl-5- aminovalerate	1.6073	1.0161	0.7976
	Phenylalanine Metabolism	phenylalanine	1.6667	1.0552	0.6943
		N-acetylphenylalanine	1.2333	0.7376	0.6207
		1-carboxyethylphenylalanine	1.7908	1.1093	0.5119
		phenyllactate (PLA)	1.8874	0.8388	0.3236
	Tyrosine Metabolism	tyrosine	1.7995	1.0601	0.6242
		4-hydroxyphenylpyruvate	0.9099	0.7065	0.4521
		3-(4-hydroxyphenyl)lactate	3.2315	1.1975	0.0721
		O-methyltyrosine	0.9164	0.6126	0.7328
		N-formylphenylalanine	0.9526	0.7122	0.9469
	Tryptophan Metabolism	tryptophan	1.8578	1.0098	0.4685
		C-glycosyltryptophan	1.0127	0.6727	1.0000
		kynurenine	1.1125	0.9273	5.3861
		indolelactate	3.0800	1.0263	0.0451
		leucine	1.5522	1.0022	0.7143
		4-methyl-2-oxopentanoate	0.7605	1.0796	0.8464

	Leucine, Isoleucine and Valine Metabolism	isovalerylcarnitine (C5)	1.7726	0.8765	0.6589
		beta-hydroxyisovalerate	0.6704	0.5377	0.6956
		isoleucine	1.3854	0.9191	0.7074
		N-acetylisoleucine	0.9390	0.6026	0.6093
		3-methyl-2-oxovalerate	0.6616	0.9783	0.7976
		2-methylbutyrylcarnitine (C5)	1.3643	1.0999	0.5150
		methylsuccinate	0.6389	0.7469	0.7395
		valine	1.5244	1.0235	0.6950
		1-carboxyethylvaline	2.3207	1.2689	0.7732
		3-methyl-2-oxobutyrate	0.7430	1.0382	0.8203
		isobutyrylcarnitine (C4)	1.3287	1.1507	0.6647
	Methionine, Cysteine, SAM and Taurine Metabolism	methionine	2.2557	1.2380	0.4114
		N-acetylmethionine	2.6450	1.8309	1.0624
		N-formylmethionine	2.1157	1.4269	0.8719
		methionine sulfone	0.1859	0.1883	0.5679
		methionine sulfoxide	1.1441	1.0273	4.3073
		N-acetylmethionine	0.9249	0.8458	1.1967
		S-adenosylmethionine	2.0409	1.7928	0.8916
		S-adenosylhomocysteine	2.1413	1.2588	1.0603
		homocysteine	1.6955	0.9524	0.9041
		cystathionine	2.5584	1.6184	1.4234

		cysteine	1.3037	1.1321	0.8495
		N-acetylcysteine	0.9444	0.7393	1.2352
		cystine	0.1195	0.5642	0.0499
		lanthionine	1.3975	0.9397	0.9502
		hypotaurine	4.1631	1.9340	1.5121
		taurine	3.8526	1.3187	1.2370
		N-acetyltaurine	2.2228	1.0813	0.9021
		3-sulfo-L-alanine	0.3154	0.2519	1.0256
	Urea cycle; Arginine and Proline Metabolism	arginine	1.1367	0.9166	0.7339
		argininosuccinate	1.2748	0.4604	6.9681
		ornithine	0.8470	0.9759	2.2514
		2-oxoarginine*	0.5359	0.5637	0.5354
		citrulline	1.1130	1.4448	0.6518
		proline	1.4366	1.0433	1.9626
		dimethylarginine (SDMA + ADMA)	1.6497	0.9374	0.7336
		trans-4-hydroxyproline	1.0180	1.0941	0.9987
		pro-hydroxy-pro	1.4301	0.9723	1.7912
	Creatine Metabolism	creatine	1.4440	1.0483	0.9076
		creatinine	1.8121	1.0884	0.9503
		creatine phosphate	2.3719	1.0486	0.9731
		putrescine	0.4104	1.3321	1.2023

	Polyamine Metabolism	spermidine	1.3006	1.3371	0.7414
		5-methylthioadenosine (MTA)	2.3509	1.6771	0.9509
		N-acetylputrescine	0.7944	2.5626	2.0039
		(N(1)+N(8))-acetylsperimdine	1.8852	1.9526	1.1059
	Glutathione	glutathione, reduced (GSH)	4.1123	2.0947	4.7345
		glutathione, oxidized (GSSG)	1.6414	1.0133	1.7158
		cysteine-glutathione disulfide	0.4830	0.8494	0.1935
		S-methylglutathione	5.9649	1.8556	1.9624
		S-lactoylglutathione	2.1245	3.3003	4.6601
		cysteinylglycine	3.6614	1.9740	3.1225
		5-oxoproline	0.5617	0.9949	5.3714
Peptide	Gamma-glutamyl Amino Acid	gamma-glutamylalanine	1.5640	1.0507	1.1563
		gamma-glutamylcysteine	1.0114	0.4806	4.2390
		gamma-glutamylglutamate	2.7709	1.1745	5.5500
		gamma-glutamylglutamine	0.0411	0.0411	1.1389
		gamma-glutamylisoleucine*	2.1627	0.9513	1.0152
		gamma-glutamyl-epsilon- lysine	0.6843	0.5420	0.9686
		gamma-glutamylthreonine	1.6045	1.1047	1.7267
		gamma-glutamylvaline	1.4313	0.8510	1.3570
		gamma-glutamyl-2- aminobutyrate	1.6053	0.7296	0.4786
		leucylglycine	0.5033	0.8135	1.0203

	Dipeptide	phenylalanylglycine	0.6284	0.6430	0.8585
	Acetylated	phenylacetylglycine	1.3107	1.1526	0.5943
Carbohydrate	Glycolysis, Gluconeogenesis, and Pyruvate Metabolism	glucose	0.7137	1.1001	0.9387
		glucose 6-phosphate	0.8806	0.5645	0.6546
		fructose 1,6-bishphsphate	0.7828	0.8326	1.2205
		dihydroxyacetone phosphate (DHAP)	0.8555	0.6433	0.9006
		2-phosphoglycerate	1.3084	0.3762	0.6612
		3-phosphoglycerate	0.3825	0.4804	0.9529
		phosphoenolpyruvate (PEP)	0.3916	0.3904	1.0609
		pyruvate	0.6244	0.6954	1.3269
		lactate	0.5178	0.8311	0.6825
		glycerate	0.7853	0.6166	1.1012
	Pentose Phosphate Pathway	6-phosphogluconate	0.6747	0.8684	1.0248
		sedoheptulose-7-phosphate	1.4886	0.4947	0.2602
	Pentose Metabolism	ribitol	2.7864	1.3731	0.6256
		ribonate	2.7754	0.9796	0.6638
		arabitol/xylitol	2.2754	1.1125	0.6655
		arabonate/xylonate	1.4631	0.6750	0.4987
		ribulonate/xylulonate*	0.6831	1.2017	1.0189
	Glycogen	maltotetraose	0.2941	0.2941	0.7799
	Disaccharides and	sucrose	1.1254	1.1372	0.9855

	Fructose, Mannose and Galactose Metabolism	fructose	0.6304	1.5168	3.0039
		mannitol/sorbitol	1.5420	1.6320	0.9433
		mannose	0.7000	0.8728	1.3429
		galactonate	2.7641	1.2744	0.7581
	Nucleotide Sugar	UDP-glucose	1.4234	0.8289	0.6762
		UDP-galactose	1.4279	0.7916	0.7191
		UDP-glucuronate	1.4430	0.4788	0.2795
		guanosine 5'-diphospho-fucose	1.1094	0.5542	0.6528
		UDP-N-galactosamine	1.3927	0.8679	0.8061
		cytidine 5'-monophospho-N-acetylneuraminic acid	1.5704	0.6240	0.9416
	Aminosugar Metabolism	glucuronate	1.5262	1.1837	1.1946
		N-acetylneuraminate	0.9946	0.6826	0.9556
		N-acetylglucosaminylasparagine	2.0310	1.0993	0.8912
		erythronate*	1.8187	1.0250	0.8481
		N-acetylglucosamine/N- acetylgalactosamine	0.5775	0.6205	1.0179
Energy	TCA Cycle	citrate	1.7202	1.0020	1.1582
		aconitate [cis or trans]	1.6671	0.8184	1.1169
		alpha-ketoglutarate	1.7781	0.9625	4.6373
		succinate	0.7641	0.7835	1.7204
		fumarate	1.2650	1.0564	12.9296
		malate	1.3126	0.9793	15.7390

		2-methylcitrate/homocitrate	0.6596	0.5954	0.4071
	OXPHOS	phosphate	0.8344	0.8118	0.7642

Chapter 3 - Viral Growth Factor and STAT3 Signaling-Dependent Elevation of the TCA Cycle Intermediate levels During Vaccinia Virus Infection

Anil Pant, Lara Dsouza, Shuai Cao, Chen Peng, and Zhilong Yang*

Division of Biology, Kansas State University, Manhattan, Kansas 66506, USA

*Correspondence: zyang@ksu.edu

Published as: **Pant, A.,** Dsouza, L., Peng, C., Cao, S., & Yang, Z. Viral Growth Factor and STAT3 Signaling-Dependent Elevation of the TCA Cycle Intermediates During Vaccinia Virus Infection (2021). *PLOS Pathogens*. 17(2): e1009303.

Abstract

Metabolism is a crucial frontier of host-virus interaction as viruses rely on their host cells to provide nutrients and energy for propagation. Vaccinia virus (VACV) is the prototype poxvirus. It makes intensive demands for energy and macromolecules in order to build hundreds and thousands of viral particles in a single cell within hours of infection. Our comprehensive metabolic profiling reveals profound reprogramming of cellular metabolism by VACV infection, including increased levels of the intermediates of the tri-carboxylic acid (TCA) cycle independent of glutaminolysis. By investigating the level of citrate, the first metabolite of the TCA cycle, we demonstrate that the elevation of citrate depends on VACV-encoded viral growth factor (VGF), a viral homolog of cellular epidermal growth factor. Further, the upregulation of citrate is dependent on STAT3 signaling, which is activated non-canonically at the serine727 upon VACV infection. The STAT3 activation is dependent on VGF, and VGF-dependent EGFR and MAPK signaling. Together our study reveals a novel mechanism by which VACV manipulates cellular metabolism through a specific viral factor and by selectively activating a series of cellular signaling pathways.

Keywords: Growth factor, TCA cycle, Citrate, Metabolism, EGFR, MAPK, STAT3, Non-canonical STAT3 signaling, Poxvirus, Vaccinia virus

Author summary

Vaccinia virus (VACV) is a large DNA virus with an acute and increasing demand for energy and macromolecules to build hundreds and thousands of viral particles in a single cell within hours of infection. The demand postulates reprogramming of the TCA cycle, as it is the central metabolic hub of a cell that generates metabolites for energy production and macromolecule synthesis. We show that VACV infection reprograms cellular metabolism

globally, elevating the TCA cycle intermediate levels and modulating related cell metabolism. The elevation of the TCA cycle intermediates depends on the virus-encoded growth factor that stimulates non-canonical STAT3 signaling during VACV infection. We provide the metabolic foundation of viral growth factor to boost VACV infection.

Introduction

Viruses do not have metabolism and rely on their host cells for energy and molecular precursors to replicate. Different viral infections often have different metabolic needs from their host cells. Hence, many viruses have developed strategies to rewire cellular metabolism, and often this ability shapes the outcome of virus replication (1–3). While metabolism is arguably a hot frontier of virus-host interaction, the molecular mechanisms underlying virus-induced metabolic reprogramming are mostly unknown. Identifying the mechanisms by which a virus usurps host cell metabolism will facilitate understanding viral infection and uncover fundamental mechanisms of metabolic regulation.

Vaccinia virus (VACV), the prototypic member of the *poxviridae* family, is a large, enveloped virus with a double-stranded DNA genome that encodes over 200 genes (4). It had been used as the vaccine to eradicate smallpox, one of the deadliest diseases in human history (5). Poxviruses continue to cause significant morbidity and mortality in humans and animals. There are also concerns about unregistered smallpox virus stocks that could be used for bioterrorism (6–8). In addition, the study of VACV is of great importance because of promising development in its use to treat cancers (9), to produce recombinant proteins (10), and to develop vaccines against other infectious diseases (11). Recent evidence suggests that VACV is an outstanding model to study how a virus reprograms cellular metabolism. VACV rewires host metabolism such that it upregulates glutamine metabolism (12, 13). It also depends on *de novo* fatty acid synthesis to generate an energy-favorable environment (14), suggesting the virus may need to modulate fatty acid synthesis. We have shown that VACV selectively upregulates the translation efficiency of oxidative phosphorylation (OXPHOS) mRNAs, indicating the requirement of increased and continuous supply of energy during virus replication (15).

Interestingly, while these metabolic alterations by VACV could converge to the tricarboxylic acid cycle (TCA cycle), little is known about how VACV infection impacts the TCA cycle. Citrate, the first intermediate of the TCA cycle and the primary source of cytosolic fatty acid synthesis, stands at the crossroads of these two critical processes in cellular metabolism (**Fig 3.2A**) (16). Not surprisingly, citrate metabolism contributes to the growth and proliferation of organisms ranging from algae, fungi, bacteria, plants and worms to mammalian cells (17–22). Given the vital role of this metabolite, it is conceivable that its biosynthesis and breakdown would be affected by many viruses. However, very little is known about how a viral infection may affect this key metabolite of cell metabolism.

VACV encodes two copies of viral growth factor (VGF) gene, C11R, in the inverted terminal repetition (ITR) of its genome. VGF is a viral polypeptide with homology to cellular epidermal growth factor (EGF) and transforming growth factor (23–26). It is the most highly expressed gene among the 118 early genes during VACV infection (27, 28). This secreted protein induces proliferative effects on VACV-infected cells (29–31), and facilitates cell motility and virus spread (32). VGF brings about these effects by binding to the EGF receptor (EGFR) to stimulate the mitogen associated protein kinase (MAPK) signaling (33). Majority of cells in an animal are in resting status and it was shown that VACV with the VGF gene deleted has a reduced replication in resting cells (34). VGF gene deleted VACV is significantly less virulent in mice (34, 35). The proliferative response generation needs heightened energy and macromolecule metabolism, which depends on the TCA cycle (36, 37). These arguments suggest that VACV VGF could be a key regulator to reprogram host metabolism during VACV infection.

In this study, we report that VACV infection elevates the levels of citrate and other intermediates of the TCA cycle and modulates the metabolites closely related to the TCA cycle. We demonstrate that the increased citrate level upon VACV infection depends on VGF expression and cellular EGFR and MAPK signaling. We show that VACV infection induces selective upregulation of non-canonical signal transducer and activator of transcription 3 (STAT3) phosphorylation at the serine727 (S727) via VGF, EGFR, and MAPK signaling. Remarkably, the STAT3 signaling is also required for citrate level elevation during VACV infection. We further demonstrate that the elevation of TCA cycle intermediate levels and VGF-mediated upregulation of non-canonical STAT3 phosphorylation could be independent of glutamine metabolism. These findings identify a novel function of VGF that is needed to reprogram cellular metabolism through a molecular mechanism involving non-canonical STAT3 activation. VGF could be of great utility in understanding how growth factors modulate cellular metabolism and cellular metabolic engineering.

Materials and methods

Cells and viruses

Human Foreskin Fibroblasts (HFFs) were a kind gift from Dr. Nicholas Wallace at Kansas State University and were maintained in Dulbecco's minimal essential medium (DMEM; Fisher Scientific) supplemented with 10% fetal bovine serum (FBS; Peak Serum), 2 mM glutamine (VWR), 100 U/ml of penicillin, and 100 μg/ml streptomycin (VWR). BS-C-1 cells (ATCC CCL-26) were cultured in Eagle's minimal essential medium (EMEM; Fisher Scientific) with supplements as described above for other cells. All cells were grown in a humidified incubator at 37°C with 5% CO_2. VACV Western Reserve (WR) strain (ATCC VR-1354) was used in this study. Amplification, purification, and titration of VACV were performed using

methods described previously (87). Unless otherwise stated, infection of cells was performed with the indicated multiplicity of infection (MOI) of indicated viruses in special DMEM (Fisher Scientific) without glucose, L-glutamine, sodium pyruvate, and phenol red. This medium was supplemented with 2% dialyzed FBS, 1 g/L glucose (Fisher Scientific), and 2 mM glutamine. Where indicated, only glucose or glucose plus 2 mM L-asparagine was used instead of glucose plus glutamine.

Generation of VGF (C11R) deletion and revertant VACV

VGF-deleted VACV was generated by homologous recombination by replacing the VGF-encoding C11R gene with a green fluorescent protein (GFP) gene. The GFP coding sequence following a P11 promoter flanked by 500-bp homologous sequences upstream and downstream of the C11R gene was generated by overlapping PCR and transfected into VACV-infected HeLa cells. Recombinant viruses expressing GFP were harvested from HeLa cells (ATCC CCL-2) and plaque purified in BS-C-1 cells. Recombinant VACV vΔVGF with the deletion of two copies of C11R at both ends of the virus genome was verified by PCR. The C11R revertant recombinant VACV vΔVGF_Rev was generated with a similar method by inserting a DNA fragment containing one copy of the C11R gene under the C11 promoter followed by the dsRED coding sequence under a P11 promoter into the space between the VACWR146 and VACWR147 loci in the central region of the VACV genome.

Chemicals and antibodies

The chemical inhibitors stattic, afatinib, and PD0325901, 3-Bromopyruvate, PFK-15, and Etomoxir were purchased from Selleck chemicals and used at indicated concentrations. Cytosine-1-β-D-arabinofuranoside (AraC) and cycloheximide were purchased from Sigma-Aldrich. Ruxolitinib was purchased from VWR. CPI-613 was purchased from Biovision Inc.

Antibodies against phospho-STAT3 (S727), phospho-STAT3 (Y705), and total STAT3 were purchased from Cell Signaling Technology. Anti-glyceraldehyde-3-phosphate dehydrogenase (anti-GAPDH) antibody was purchased from Santa Cruz Biotechnology. Antibodies raised against VACV E3 protein were kind gift from Dr. Yan Xiang (UTHSA) (88). Antibodies against VACV L2 protein were kindly provided by Dr. Bernard Moss (NIAID). A commercially synthesized recombinant VGF peptide corresponding to the cleaved fragment of VACV VGF (25) was purchased from GenScript.

Cell viability assays

Cell viability assay was performed using the trypan blue exclusion assay as described elsewhere (89). The cells were grown in a 12-well plate for indicated treatments were harvested with 300 µl of trypsin and resuspended with 500 µl of DMEM by pipetting. An equal volume (20 µl) of the cell suspension was gently mixed with 4% trypan blue (VWR). The number of live and dead cells in each condition was counted using a hemocytometer.

Measurement of citrate, oxaloacetate (OAA), Acetyl-CoA, and ATP

The citrate measurement was carried out using EnzyChrom Citrate Assay Kit (BioAssay Systems) according to the manufacturer's instructions. $4x10^6$ HFFs were collected in 100 µl of ice-cold PBS. The cells were homogenized by sonication, and the cell lysis was verified by observation under a microscope. The lysed cell suspension was centrifuged at 19,000 xg at 4°C for 5 min. Twenty µl of the clear supernatant was mixed with 80 µl of fresh working reagent and in a 96-well black clear bottom plate (Corning) and incubated protected from light at room temperature for 15 minutes. Fluorescence reading at λex/em = 535/595 nm was measured, and the level of citrate in the sample was calculated using a standard curve generated alongside each experiment.

For the measurement of OAA, we followed the protocols outlined in the Oxaloacetate Assay Kit (Sigma-Aldrich). Briefly, $4x10^6$ HFFs were collected and homogenized in the assay buffer. The sample was centrifuged at 15,000 x g for 10 min at 4°C. After mixing 50 µl of the fresh working reagent with 50 µl of the deproteinized sample, the mixture was incubated at room temperature for 30 min. Finally, Fluorescence reading of samples, standards, and controls was measured at λex/em = 535/595 nm, and the level of OAA in the sample was calculated.

The level of Acetyl-CoA was measured using the PicoProbe Acetyl CoA Assay Kit (Abcam) according to the manufacturer's instructions. Briefly, $4x10^6$ HFFs were collected and homogenized in the assay buffer in ice. The cells were lysed by sonication, and the sample was centrifuged at 10,000 xg for 10 min at 4°C. The supernatant was collected and then deproteinized with a perchloric acid method. Then, ten µl of the deproteinized sample was added to each well, and the final volume was brought up to 50 µl with assay buffer. The coenzyme A present was quenched by adding a quencher for 5 minutes, and eventually, it was removed with quencher remover. Finally, 50 µl of fresh reaction mixture was added to the above samples, and the mixture was incubated at 37°C for half an hour. Fluorescence reading of samples, standards, and controls was measured at λex/em = 535/595 nm to calculate the level of Acetyl-CoA in the sample.

The levels of ATP were measured using an ATP Detection Assay Kit – Luminescence (Cayman Chemical Company). Briefly, after desired treatment, $4x10^5$ HFFs were washed with ice-cold 1x PBS and homogenized in 500 µL prechilled 1x ATP detection sample buffer. After mixing 100 µl of the fresh reaction mixture (containing D-Luciferin and ATP detection luciferase) with 10 µl of the sample, standards, or blank, the mixture was incubated at room temperature for 15 min protected from light. Finally, the luminescence was measured using a

luminometer and the ATP levels in the sample was calculated using a standard curve generated alongside each experiment.

Global metabolic profiling

Metabolic profiling was carried out with Metabolon, as described previously (38). Briefly, four biological replicates of each treatment were used for each treatment. HFFs were grown in T-175 flasks. Once the cells reached about 95% confluence, they were washed twice with 1x PBS at 37°C and infected with VACV at an MOI of 3 and cultured in different media. At 8 and 16 hpi, the cells were harvested by scraping, and the pellets were washed twice in ice-cold 1x PBS. The pellet was then dissolved in the extraction solvent (methanol) and was stored at −80°C until shipment to Metabolon (Durham, North Carolina). Proprietary analytical procedures were carried to ensure high-quality data after minimizing the system artifacts, misassignments, and background noise among the samples. Following normalization to the protein concentration, log transformation, and imputation of missing values, with the minimum observed value for each compound, ANOVA contrasts were used to identify biochemicals that differed significantly between experimental groups.

Western blotting analysis

Western blot was performed as described previously (90). Briefly, the cells were lysed in NP-40 cell lysis buffer after the required treatment, reduced with 100 mM dithiothreitol (DTT), and denatured by sodium dodecyl sulfate-polyacrylamide gel electrophoresis (SDS–PAGE) loading buffer. After boiling at 99°C for 5 min, the samples were loaded on the SDS–PAGE, followed by transferring to a polyvinylidene difluoride membrane. The membrane was blocked in 5% bovine serum albumin (BSA; VWR) blocking buffer in TBST buffer for 1 h at room temperature and incubated with the primary antibody in the same BSA blocking buffer for

overnight at 4°C. After 3x washes of 10 minutes each with TBST, the membrane was incubated with horseradish peroxidase-conjugated secondary antibody for 1 h at room temperature. The membranes were developed with Thermo Scientific SuperSignal West Femto Maximum Sensitivity Substrate. Antibodies were stripped from the membrane by Restore (Thermo Fisher Scientific, Waltham, MA, United States) for Western blotting analysis using another antibody.

Gaussia luciferase assay

The *Gaussia* luciferase activity assay was performed as previously described (38). Briefly, cells were infected with a recombinant VACV encoding *Gaussia* luciferase under the VGF (C11R) viral early promoter (vEGluc) for indicated time. The cell culture media was used to measure the *Gaussia* luciferase activities assay using Pierce Gaussia luciferase flash assay kit (Thermo Scientific) and a luminometer.

Plaque assay and plaque size determination

BS-C-1 cell monolayers were infected with indicated viruses. One-hour post infection, the media was changed to EMEM containing supplements as described above plus 0.5% methylcellulose (Fisher Scientific). The viruses were allowed to grow and form plaque for 48 hrs. The growth medium was discarded, and the cells were treated with 0.1% (w/v) crystal violet (Fisher Scientific) in 20% ethanol for 10 minutes. The image of plate containing plaques was taken and the plaque diameters were measured using the ImageJ software (version 1.51w) (91). The diameter of 50 plaques were measured per condition and the data was analyzed in RStudio (version 1.2.5033) (92).

Quantitative reverse transcription PCR (qRT-PCR)

Total RNA was extracted from cells using TRIzol reagent (Ambion), and then it was using the Invitrogen PureLink RNA mini kit (Thermo Fisher Scientific). 500 ng RNA was used

as a template to reverse transcribe into cDNA using random hexamer primers and SuperScript III first-strand synthesis kit (Invitrogen). CFX96 Real-Time PCR Detection System (Bio-Rad) with All-in-One 2X quantitative PCR (qPCR) mix (GeneCopoeia) and primers specific for indicated genes was used to detect the relative levels of indicated mRNAs in the sample using following settings: Initial denaturation at 95°C for 3 min, followed by 39 cycles of denaturation at 95°C for 10 s, annealing and reading fluorescence at 52°C for 30 s, and extension at 72°C for 30 s. 18sRNA was used as an internal control for normalization.

RNA interference

The indicated specific siRNAs and negative control siRNAs were purchased from Qiagen. The siRNAs were transfected at a concentration of 5 nM in Lipofectamine RNAiMAX transfection reagent (Fisher Scientific) following the manufacturer's instructions. The efficiency of knockdown was measured by Western blotting analysis.

Statistical analyses

Data presented indicate a mean of at least three biological replicates, unless otherwise stated. For the global metabolic profiling, four biological repeats were used for each condition, and the data was analyzed and visualized in RStudio (version 1.2.5033) (92) and MetaboAnalyst software (93). Error bars indicate the standard deviation of the experimental replicates. A two-tailed paired *t*-test was performed to evaluate any significant difference between the two means. We used the following convention for symbols to indicate statistical significance: ns, $P > 0.05$; *, $P \leq 0.05$; **, $P \leq 0.01$; ***, $P \leq 0.001$; ****, $P \leq 0.0001$.

Results

VACV infection induces profound reprogramming of cellular metabolism globally under glutamine depleted conditions

VACV replication is substantially reduced in cells cultured in glucose-containing, but glutamine-depleted medium (12, 14). We have previously shown that VACV replication is not affected in medium containing glucose and asparagine under glutamine-depleted condition (38). As previous studies have shown, VACV upregulates glutaminolysis (12, 13), our finding that asparagine can fully rescue VACV replication from glutamine-depletion provides a valuable system to study how VACV modulates cellular metabolism in a glutamine-independent manner. A metabolic profiling during VACV infection in the presence of both glucose and glutamine had been carried out by Fontaine et al. previously (12). To obtain a global view of the host cell metabolic changes upon VACV infection under the glutamine-depletion condition, we performed a metabolic profiling to compare the levels of metabolites in VACV-infected and mock-infected human foreskin fibroblasts (HFFs) cultured in medium containing glucose plus asparagine at 8 and 16 hours post-infection (hpi) (**Fig 3.1A**). At 8 hpi, the virus is actively replicating, while the virus has completed most of the replication cycle at 16 hpi. We chose the HFFs because they are primary cells, and the metabolism in these cells is not already dysregulated as it is in transformed cancer cells.

In media with glucose plus asparagine, our metabolic profiling detected 173 and 190 metabolites significantly altered by VACV infection, with a general increase at 8 hpi (109 up, 64 down) and decrease at 16 hpi (51 up, 139 down), respectively (**Table 3.1**). Significant changes in metabolites were prominent in the categories of TCA cycle, amino acids, and carnitylated fatty acids that are used for β-oxidation (**Fig S3.1, Table 3.2**). The substantial changes in cellular

metabolism upon VACV infection were clearly revealed by a Principal Component Analysis (PCA), a statistical procedure to summarize the information content in large datasets. (**Fig 3.1B**).

VACV replication is classified into three stages; early, intermediate, and late, as a cascade based on the timing of its gene expression (4). Our previous study indicated that VACV replication was not affected at the early gene expression stage but was blocked at intermediate and late replication stages in the absence of glutamine and asparagine in the glucose-containing medium (38). We also carried out metabolic profiling of VACV-infected and mock-infected HFFs cultured in medium containing glucose without glutamine and asparagine (**Fig 3.1A**). In glucose only medium, we found 220 and 145 metabolites significantly altered by VACV infection at 8 hpi (156 up, 64 down) and 16 hpi (95 up, 50 down), respectively (**S1 File**). Interestingly, while we observed a similar global metabolic reprogramming pattern as in the glucose plus asparagine medium at 8 hpi, more metabolites were still up in glucose only medium compared to glucose plus asparagine medium at 16 hpi (**Fig 3.1C, Fig S3.1, Table 3.2**), likely because more nutrients are used in the asparagine containing medium at the later stage of replication, in which VACV replication rate is much higher (38). These results suggest that the metabolic reprogramming by VACV starts at the early stages of replication. At the later stage, the metabolites are likely consumed to support virus replication.

VACV infection elevates TCA cycle intermediate levels, including citrate

Next, we closely investigated the levels of the TCA cycle intermediates as it is the central hub of cellular metabolism (**Fig 3.2A)**, and a global metabolic reprogramming likely involved the alteration of the TCA cycle intermediates. Notably, at 8 hpi, most of the TCA cycle intermediates are significantly higher in VACV-infected cells than in mock-infected cells, in both glucose plus asparagine and glucose only conditions (the succinate levels were similar in

mock- and VACV-infected cells) (**Fig 3.2B**). At 16 hpi, although we still observed the general trend that the TCA intermediate levels increased in VACV-infected cells, the elevation levels decreased (**Fig S3.2**), again suggesting that the elevation of the metabolites occurred at an earlier time and the metabolites were consumed at the later time of infection. Interestingly, the level of glutamate, whose biosynthesis can be fed by the TCA cycle intermediate, α-ketoglutarate (39), increased significantly in VACV infected cells in the absence of glutamine (**Fig 3.2C)**. Together, these results reveal the enhanced levels of the TCA cycle-related metabolites during VACV replication.

To further validate the findings of metabolic profiling, we measured the citrate level as it is the first molecule of the TCA cycle. Using a citrate assay kit, we confirmed that the citrate level significantly increased by approximately 3.3- and 3.2-fold in VACV-infected HFFs cultured in media containing either glucose only or glucose plus asparagine, respectively (**Fig 3.2D**). Remarkably, we also observed a similar increase of the citrate level in VACV-infected HFFs cultured in medium containing glutamine and glucose **(Fig 3.2E**), indicating the elevation of citrate in the presence of exogenous glutamine. The upregulation of citrate could be observed at 2 hpi (**Fig 3.2E**). The level of oxaloacetate (OAA), another critical metabolite of the TCA cycle and citrate metabolism (**Fig 3.2A**) increased by two-fold at 8 hpi (**Fig 3.2F**). Interestingly, in the metabolic profiling in the presence of glucose and glutamine, Fontaine et al. found a 1.49 and 1.37-fold increase of citrate levels upon VACV infection at 4 and 8 hpi, respectively, although it is not statistically significant (12). Most of the other detected TCA cycle intermediates were also moderately (although not significantly) upregulated by up to 1.37-fold at 8 hpi (12). Taken together, our findings corroborate that VACV infection elevates the steady-

state levels of TCA cycle intermediates, which can provide metabolic foundations to modulate TCA cycle-related activities and biomolecule synthesis.

Previous work from multiple groups had demonstrated that VACV promotes oxygen consumption and ATP production in different cell types (14, 15, 40), indicating an enhanced TCA cycle activity. We examined if VACV infection increases ATP production in HFFs and observed a significant, although not as high as in HeLa cells (15, 40), increase in ATP production after VACV infection (**Fig 3.2G**). These findings indicate a biologically relevant activity of the elevated TCA cycle intermediate levels. To further examine if TCA cycle activity is important for VACV replication, we treated HFFs with Enasidenib (targeting the enzyme isocitrate dehydrogenase 2 of the TCA cycle). We observed a significant decrease of VACV replication (39- and 83-fold decrease at the MOI of 2 and 0.1 respectively) (**Fig 3.2H**) upon Enasidenib treatment at a concentration that did not alter cell viability (**Fig 3.2I**). These results indicate an essential role of high TCA cycle activity in VACV replication.

VACV infection reprograms TCA cycle-related metabolism

Acetyl-CoA is an indispensable player in citrate biosynthesis and breakdown (**Fig 3.2A**). At 8 hpi we observed a significant 81% and 74% decrease of the Acetyl-CoA levels upon VACV infection through metabolic profiling in medium with glucose or glucose plus asparagine, respectively (**Fig 3.3A**). The level of Acetyl-CoA was still significantly reduced at 16 hpi (**Fig S3.3**). Notably, there was a similar significant reduction in the Acetyl-CoA level in culture medium containing glutamine (**Fig 3.3B**). In the absence of glutamine, glucose and fatty acids are two other major carbon sources of the TCA cycle (**Fig 3.2A**) (41). These findings suggest that Acetyl-CoA is heavily consumed, or its synthesis is suppressed during VACV infection. Although the lipid species are both up and down-regulated (**Fig S3.1 AB**), the fatty acyl-

carnitines, which are used up in β-oxidation to be converted to acetyl-CoA after being transported to the mitochondria (42), significantly increased in the metabolic profiling **(Fig 3.3 CD).** Interestingly, those non-carnitine-conjugated long-chain fatty acid levels decreased significantly at 8 hpi (**Fig 3.3E**). Although not statistically significant, the metabolic profiling in the presence of glutamine by Fontaine et al. showed a moderate increase in all the detected carnitine-conjugated fatty acids at 8 hpi (12). These results suggest the metabolism of fatty acids is significantly reprogramed towards an enhanced levels of carnitine conjugation during VACV infection. Analysis of the glycolysis products by metabolic profiling in glutamine-depletion conditions indicated that several essential glycolysis products decreased in VACV-infected HFFs (**Fig 3.3G, S4 Fig**). The levels of lactate were also similar in both growth conditions upon VACV infection (**Fig 3.3F, Fig S3.5**), suggesting that VACV infection did not utilize glucose to undergo anaerobic respiration. In the presence of glutamine, the levels of most of the glycolysis intermediates were not significantly altered in the metabolic profiling of VACV-infected HFFs carried out by Fontaine et al (12). Because VACV infection did not increase the level of glucose, the lowered glycolysis could suggest two possibilities. First, glycolysis products were heavily consumed to feed the TCA cycle in VACV-infected cells under glutamine-depletion conditions. Second, glycolysis was down-regulated during VACV infection, which would suggest a more important role of fatty acids to feed the TCA cycle. Overall, these results reveal a systematic reprogramming of TCA cycle-related metabolism during VACV infection.

Inhibition of glycolysis or fatty acid β-oxidation abolishes citrate level increase during VACV infection

Our metabolic profiling data could not answer the question if glycolysis or β-oxidation individually contributes to the increase of citrate levels during VACV infection. We used several

inhibitors targeting glycolysis and β-oxidation to assess their effects on citrate levels during VACV infection. As can be seen in **Fig 3.4A**, bromopyruvate (targeting the first enzyme, hexokinase, of glycolysis (43)), PFK15 (targeting the rate-limiting enzyme, 6-phosphofructo-2-kinase, of glycolysis (44)), CPI-613 (targeting pyruvate dehydrogenase and α-ketoglutarate dehydrogenase (45)), and etomoxir (targeting carnitine palmitoyltransferase-1 of β-oxidation (46)) all decreased the citrate levels in VACV-infected HFFs, at the concentrations that did not affect HFF viability in the absence of infection (**Fig 3.4B**). In uninfected cells, PFK-15 and etomoxir, but not bromopyruvate and CPI-613, also decreased the citrate levels (**Fig 3.4A**). It has been reported that etomoxir treatment significantly suppresses VACV replication (14). Here we observed significant reduction of VACV replication by bromopyruvate, CPI-613 and PFK-15 treatment, respectively (**Fig 3.4CD**). These findings indicate that both the glycolysis and β-oxidation contribute significantly to the increased citrate levels during VACV infection.

VGF gene deletion abolishes the elevation of citrate level during VACV infection

Our previous study indicated that VACV replication was suppressed at a late replication stage in medium containing glucose only, without glutamine/asparagine (38). The upregulation of citrate and other metabolites in HFFs cultured in glucose only medium suggests an early event of VACV replication is responsible. We further tested if viral DNA replication inhibition affected the upregulation of citrate level in VACV-infected cells using AraC, a well-established inhibitor of DNA replication but not viral early protein synthesis (47). AraC treatment did not inhibit the increase in citrate level upon VACV infection (**Fig 3.5A**), indicating an event prior to viral DNA replication could stimulate the citrate level. However, treatment with cycloheximide (CHX), a well-known inhibitor of mRNA translation (48), abolished the citrate level's increase upon VACV infection. In contrast, cycloheximide treatment did not affect the citrate level in

uninfected HFFs (**Fig 3.5B**). These results suggest that early VACV protein expression is required to enhance the citrate level upon VACV infection.

We tested several viral early genes and found that VGF is needed for VACV to increase the citrate level. We generated a recombinant VACV with both copies of the VGF gene deleted (vΔVGF). We also made a VGF revertant VACV (vΔVGF_Rev), with one copy of the VGF gene under its natural promoter inserted at a different locus of the original VGF gene in the central region of the viral genome. VGF was known to be critical for VACV replication and virulence in infected mice (34, 35). While the role of VGF in cultured cells was less prominent, we observed a significant 4.2-fold yield reduction of vΔVGF in HFFs (**Fig S3.6A**), similar to what had been observed in BSC40 cells (32). While VACV infection of HFFs could not form clear and measurable plaques, we observed significantly smaller plaques of vΔVGF in BS-C-1 cells (**Fig S3.6B**), similar to what had been observed previously in BSC40 cells (32). Remarkably, while WT-VACV infection resulted in a significant increase in citrate level, the deletion of VGF rendered VACV unable to enhance the level of citrate upon infection, regardless of the culture medium contents (**Fig 3.5C-E**). Interestingly, vΔVGF_Rev partially recused the citrate level enhancement, consistent with that the VGF mRNA level in the vΔVGF_Rev was approximately 50% of that in WT-VACV infected cells (**Fig 3.5F**). Moreover, VACV early gene expression was not affected by the deletion of VGF, evidenced by similar levels of two viral early proteins, E3 and L2, in WT, vΔVGF, and vΔVGF_Rev infected HFFs (**Fig 3.5G**), further corroborating that the reduced level of citrate in vΔVGF-infected cells was due to a lack of VGF expression. Interestingly, we also observed a reduction of ATP level in vΔVGF-infected than in WT VACV-infected HFFs (**Fig. 3.2G**). Overall, our results demonstrate VACV elevation of the citrate level depends on VGF expression.

To investigate if VGF is sufficient for the increased level of citrate, we used a synthetic peptide of processed VGF to treat HFFs. However, we could not observe a rescue of citrate level (**Fig S3.7**). The finding is not conclusive as it is not clear the failure to elevate the citrate level by this peptide was due to VGF alone is not sufficient or the synthetic peptide is not fully and biologically active. Further studies using different approaches are needed.

EGFR, MAPK, and STAT3 signaling pathways are needed for citrate level increase in VACV-infected cells

VGF is homologous to cellular EGF that activates the EGFR and MAPK pathways (32, 49). We hypothesized that VGF-mediated cell signaling is required for the increasing citrate level upon VACV infection. We first tested the effect of afatinib, an irreversible inhibitor of the EGFR pathway on citrate metabolism (50). We found that VACV infection resulted in an increase in citrate levels, while EGFR inhibition with afatinib at a concentration that did not affect cell viability reduced the increase in the citrate level upon VACV infection **(Fig 3.6A, Fig S3.8A).** Although it also decreased the citrate level in uninfected controls, the reduction was only about 18%. Afatinib treatment significantly reduced VACV titer by 43-fold at the same concentration (**Fig S3.8B**), agreeing with a previous study on the effect of EGFR inhibitors on VACV replication (51). We then tested the effect of inhibiting the MAPK pathway on citrate level using PD0325901, a selective inhibitor of MAPK/ERK pathway (52). While VACV infection resulted in an increase in citrate level in vehicle-treated cells, PD0325901 treatment significantly reduced the citrate level in VACV infected cells to the level comparable to uninfected cells (**Fig 3.6B**). Furthermore, MAPK pathway inhibition resulted in a 67-fold reduction of VACV titer (**Fig S3.9A**), at a concentration that did not affect the viability of HFFs (**Fig S3.9B**), consistent with an earlier study (49). It is worth noting that both EGFR and MAPK

pathways are activated by VGF during VACV infection (32, 49, 53). Therefore, our results indicate that the EGFR and MAPK signaling pathways are required for the upregulation of the citrate level during VACV infection.

One downstream signaling molecules of the EGFR-MAPK axis is the STAT3, as EGFR induced MAPK pathway is a major upstream activator of non-canonical STAT3 phosphorylation at serine 727 (S727) (54, 55). Notably, stattic, an inhibitor of STAT3 activation (56), significantly reduced the increase in citrate level in VACV-infected cells but not in uninfected cells (**Fig 3.6C**). Chemical inhibition of the STAT3 pathway by stattic resulted in a 177-fold reduction in VACV titers in HFFs (**Fig S3.10A**), consistent with our results in other cell types and an unbiased screening of compounds of VACV inhibitors (57). Stattic treatment did not affect HFF viability at the same concentration (**Fig S3.10B**), suggesting that STAT3 signaling is also required for VACV-induced citrate level increase. Further supporting the critical role of STAT3 signaling in citrate level upregulation during VACV infection, specific siRNA treatment significantly decreased the citrate level during VACV infection (**Figs 3.6FG**) without affecting the HFF viability (**Fig S3.10C**).

VACV infection stimulates non-canonical STAT3 activation in a VGF-dependent manner

STAT3 can be phosphorylated at tyrosine 705 position (Y705) (induced mainly by JAK1/ 2 pathway) and at serine 727 (S727) (induced mainly by MAPK pathway); known as the canonical and non-canonical phosphorylation, respectively (55, 58). We analyzed STAT3 phosphorylation in HFFs infected with WT or vΔVGF or vΔVGF_Rev VACV at 2 and 4 hpi, using medium containing glucose and glutamine. VACV infection selectively upregulated the non-canonical STAT3 phosphorylation at the S727 (**Fig 3.7A**). Notably, the deletion of VGF

abolished STAT3 S727 phosphorylation, which could be rescued by the VGF revertant mutant (**Fig 3.7A**). In contrast, the canonical Y705 phosphorylation of STAT3 did not increase upon VACV infection (**Fig 3.7A**). The VGF dependent upregulation of the non-canonical STAT3 pathway was seen as early as 10-minute post-infection and could still be observed at 8 hpi (**Fig 3.7B**). The early stimulation of STAT3 S727 phosphorylation is consistent with the fact that VGF is an early gene and it starts to be expressed immediately after VACV enters the cells (4). Similar results were found when using medium containing no glutamine (**Fig 3.7C**), indicating the VGF dependent phosphorylation of STAT3 at S727 can be achieved in a glutamine-independent manner.

Next, we determined if the EGFR and MAPK signaling is needed for STAT3 phosphorylation at S727 during VACV infection. Afatinib treatment noticeably decreased the S727 phosphorylation in VACV infected cells. However, it did not affect Y705 phosphorylation (**Fig 3.7D**), indicating a pivotal role of the EGFR pathway in non-canonical STAT3 activation during VACV infection. MAPK inhibitor, PD0325901, inhibited S727, and Y705 STAT3 phosphorylation, the former was more evident in VACV-infected cells (**Fig 3.7E**). The results suggest that the PD0325901 also inhibited STAT3 Y705 phosphorylation, likely via signaling crosstalk. There is no S727 specific STAT3 inhibitor available. The STAT3 inhibitor, stattic, partially inhibited the VACV infection-mediated increase of S727 phosphorylation, but with no noticeable effect on Y705 phosphorylation (**Fig 3.7F**). The latter was not changed much upon VACV infection. These results demonstrate the requirements of VGF, EGFR, and MAPK in non-canonical activation of STAT3 at S727. Together with the results in **Fig 3.6**, the results also indicate the indispensable roles of VGF, EGFR, MAPK, and STAT3 in citrate level elevation

during VACV infection. While the non-canonical STAT3 signaling is activated to elevate the citrate level, the canonical pathway is not stimulated by VACV infection.

We examined if the JAK-STAT3 axis that phosphorylates Y705 is required for citrate induction during VACV infection, although it is not further activated by VACV infection. Ruxolitinib, an inhibitor of JAK1/2 that is the primary upstream activator of STAT3 Y705 phosphorylation (59), did not affect S727 phosphorylation but inhibited the Y705 phosphorylation in both uninfected and VACV infected cells (**Fig 3.7G**). Ruxolitinib deceased citrate level in the uninfected cells by 23% while it significantly reduced the induction by 55% in VACV infection (**Fig 3.7H**) without affecting HFF viability (**Fig S3.11**). This result suggests that the canonical STAT3 activity is also required for VACV elevation of the citrate level. Furthermore, viral early proteins were still expressed with the treatments with EGFR, MAPK, STAT3, or JAK1/2 inhibitors. EGFR, MAPK, and JAK1/2 inhibitors had little effects on viral early protein levels, evidenced by the expression of a viral early protein E3 and a reporter VACV with *Gaussia* luciferase expression under the control of the VACV early VGF gene promoter (38) (**Fig 3.7IJ**). While the STAT3 inhibitor (stattic) treatment decreased VACV early protein levels, considerable amounts of viral early proteins were still expressed (**Fig 3.7IJ**). The result suggests that stattic also suppresses VACV replication at or prior to viral gene expression steps.

Discussion

In this study, we discovered a novel VACV metabolic reprogramming strategy that elevates the intermediates of the TCA cycle, the cellular metabolic hub. We determined the viral factor and cellular signaling pathways driving this metabolic alteration for an elevated citrate level, the first molecule of the TCA cycle. The findings lead to a model by which VACV elevates the TCA cycle intermediate levels (**Fig 3.8**): VACV produces VGF at an early time of

infection. The VGF then stimulates the EGFR/MAPK/non-canonical STAT3 signaling axis in the infected and perhaps also in the uninfected neighboring cells to reprogram the TCA cycle and its related cellular metabolism. While the canonical STAT3 signaling is not stimulated by VACV infection, its basal activity is still required. At this point, we cannot conclude if VGF alone is sufficient to exert this effect as our data using a synthetic VGF peptide failed to elevate the citrate level in the absence of VACV infection (**Fig S3.7**). Further investigations using a system more closely mimicking the natural route of VGF expression and processing in the absence of VACV infection is needed to answer this question. Moreover, the mechanistic details of the TCA cycle reprogramming and the broad impacts of the elevated TCA cycle intermediate levels are yet to be fully determined.

The steady-state levels of metabolites in cells are a net outcome of dynamic metabolism, including uptake from and secretion to extracellular space, synthesis and consumption. While our data in this study and studies from multiple groups suggest that VACV infection promotes the TCA cycle and related metabolism including oxygen consumption, ATP production, glutaminolysis (13–15), our results that VACV infection elevates the levels of citrate and other TCA cycle intermediates, and alters other related metabolites, does not give a quantitative and definitive answer on how the synthesis or consumption contributes to the final outcomes.

We have previously shown that VACV replication is fully rescued in medium containing glucose and asparagine in glutamine-depleted conditions (38, 60). This culture medium provides a unique VACV infection system to study VACV-induced manipulation of cellular metabolism in the absence of the complications caused by VACV's upregulation of glutaminolysis (12, 13). Glucose, glutamine, and fatty acids are the three major carbon sources to feed the TCA cycle. while it was known that VACV stimulates glutaminolysis, our results using chemical inhibitors

indicate that both glycolysis and β-oxidation of fatty acids are needed to increase the TCA cycle intermediates (**Fig 3.4**). Because of the upregulation of the carnitine-conjugated lipids, VACV may promote β-oxidation of fatty acids to elevate the TCA cycle. The metabolic profiling data support a possibility that fatty acyl-carnitines, which enter mitochondria to feed the TCA cycle, are selectively upregulated in the absence of glutamine. More mechanistic and comprehensive investigations of various branches of glycolysis and fatty acid metabolism are needed, including the modulation of the activities of key enzymes involved and the metabolic flux of the carbon by VACV infection.

The TCA cycle is at the heart of major cellular pathways for carbohydrate, lipid, and amino acid metabolism. TCA cycle intermediates and other metabolic products are the sources for the production of cellular energy and many biosynthetic precursors. The TCA cycle is also named the citric acid cycle due to its first molecule, citrate. Citrate is essential not only to drive the TCA cycle forward in the mitochondria but is also transported to the cytosol to be used for fatty acid biosynthesis (16). Our finding that VACV infection elevates the citrate level and many other TCA cycle intermediates, but simultaneously decreases the Acetyl-CoA level, suggests that the virus has evolved to reprogram the hub of cellular metabolism to create a favorable environment for its replication. Our results can explain the chemical foundations for the oxidative phosphorylation pathway (OXPHOS) upregulation by VACV infection. The OXPHOS is the major source of cellular energy in ATP (61). During VACV infection, there is an increase in the oxygen consumption rate (OCR), an indicator of energy metabolism (14), as well as ATP production (15, 40). Increased citrate and TCA cycle intermediates upon VACV infection also provide the substrates to upregulate the biosynthesis of other biomolecules, evidenced by the metabolic profiling indicating higher glutamate production, and carnitylated lipids during VACV

infection in the absence of glutamine. Greseth et al. demonstrated that VACV replication requires *de novo* fatty acids biosynthesis (14), which requires citrate as a source of precursor.

VGF induces cell proliferative responses (29, 31). The identification of VGF as the required VACV protein to stimulate the citrate level provides the metabolic foundation of VGF's functions in many aspects of VACV infection. Although it does not affect VACV replication in some proliferating cells, the deletion of VGF from VACV reduces VACV replication in resting cells and proliferating HFFs (**Fig S3.6**). Because the metabolic level is higher in proliferating cells than in resting cells (62), the different replication phenotypes are at least partially due to different metabolic statuses in these cells. As most of the cells are in resting state in an animal, the VGF's function to stimulate the TCA cycle intermediates could also explain the reduced replication and virulence in mice (34, 35). Since cell mobility consumes energy (63), it explains that VGF is crucial for facilitating cell motility for virus spread (32). In addition to enhancing the motility, the secreted VGF induces EGFR in a paracrine fashion (64), which may instruct the neighboring uninfected cells to be metabolically prepared for infection.

STAT3 is a transcription factor activated by growth factors, oncogenes, and cytokines that leads to cell proliferation, migration, and differentiation, etc. (65). While the canonical pathway of STAT3 activation with Y705 phosphorylation has been well-understood to stimulate gene transcription in cell proliferation, cell cycle, and cell survival, the mechanism, and function of the non-canonical activation of STAT3 by S727 phosphorylation in these processes are less well understood (66). In agreement with the notion that the STAT3-mediated biological processes require energy, STAT3 has been shown to stimulate mitochondrial OXPHOS and the activities of electron transport chain (ETC) complex (67–70). However, the mechanism by which STAT3 stimulates the energy production mechanism is still not clear. While some studies

suggest that a small portion of STAT3 localizes to the mitochondria and promotes the ETC complex activity directly (67, 69), others suggest that STAT3 does not go into the mitochondria but only closely associates with mitochondria (71). Interestingly, here we found that STAT3 signaling is required to stimulate citrate level upon VACV infection, suggesting STAT3 signaling may indirectly promote OXPHOS and ETC through elevating the TCA cycle. Interestingly, a recent study suggests that STAT3 transcriptionally induces the citrate synthase and, hence, citrate level to regulate lymphocyte growth (18). However, we could not observe the citrate synthase and its activity upregulation during VACV infection (not shown). More mechanistic studies are required to understand the link between STAT3 signaling and the TCA cycle activation. It is of particular interest that VACV infection selectively stimulates non-canonical STAT3 phosphorylation at the S727, but not the canonical site at Y705, although both are required for citrate level elevation. As VGF is a homolog of cellular growth factor, our result that VGF selectively stimulates EGFR-MAPK-STAT3 (S727) provides new molecular tools to understand the functions of different growth factors with diverse roles in many physiologically relevant conditions, notably, a valuable model to understand different functions and activating mechanisms of the canonical and non-canonical STAT3 signaling. Note that our results do not exclude the EGFR-MAPK-STAT3 signaling affects VACV replication other than reprogramming the TCA cycle and related metabolism. Also, STAT3 pathway is upregulated in several viral infections (72, 73, 73–80). It would be interesting to elucidate how different viruses exploit different axis of the STAT3 signaling to affect viral infections.

VGF-deleted VACV preferentially replicate in cancer cells in mice (81). Cancer cells usually have higher and dysregulated metabolism to support cell proliferation and growth (82). It has been noted by other studies that non-canonical activation of STAT3 at S727 is related to

certain types of cancers (70, 83–85). Because most cells in animals are in resting state, in which the replication of VACV with VGF deletion is lower than in proliferating cells (34), our finding provides a metabolic mechanism of VGF-deleted VACV's cancer cell tropism in animals.

Our results that STAT3 inhibition reduces VACV replication is somehow discrepant to a previous report that inhibition of STAT3 enhanced the replication of ACAM2000, a VACV strain currently used as a vaccine in mice, and keratinocytes (86). We have independently confirmed the suppression effects on VACV replication using multiple inhibitors and multiple cell types (57). We do not fully understand the discrepancy, although it could possibly be explained by different cell types or virus strains used in these studies.

Overall, we found that VACV infection elevates host cell metabolic activities, including the TCA cycle that could be achieved in a glutamine-independent manner. We identified VACV VGF as an essential viral factor that elevates the level of a central molecule of metabolism, citrate. Non-canonical STAT3 signaling is activated upon VACV infection through the VGF-EGFR-MAPK signaling axis to stimulate citrate upregulation. Our study revealed a global metabolic reprogramming effect on host cells by VACV infection and identified the cellular and viral mechanisms underlying it. The results have a broad impact on understanding poxvirus replication and prevention and understanding growth factors-induced metabolism.

Acknowledgments

We thank Drs. Nicholas Wallace (Kansas State University), Bernard Moss and Yan Xiang for providing reagents. We thank members of the Yang Lab for helpful comments and discussion, especially Mr. Mark Gray for proofreading.

Z.Y. is supported by grants from the National Institutes of Health (R01AI143709 from NIAID, P20GM103418 Bridging Award from NIGMS). The content is solely the responsibility

of the authors and does not necessarily represent the official views of the National Institutes of Health. A.P. is also supported, in part, by the Johnson Cancer Research Center of Kansas State University.

References

1. Goodwin CM, Xu S, Munger J. Stealing the Keys to the Kitchen: Viral Manipulation of the Host Cell Metabolic Network. Trends Microbiol. 2015;23: 789–798. doi:10.1016/j.tim.2015.08.007

2. Sanchez EL, Lagunoff M. Viral activation of cellular metabolism. Virology. 2015;479–480: 609–618. doi:10.1016/j.virol.2015.02.038

3. Thaker SK, Ch'ng J, Christofk HR. Viral hijacking of cellular metabolism. BMC Biol. 2019;17: 59. doi:10.1186/s12915-019-0678-9

4. Moss B. Poxviridae: the viruses and their replication. 5th ed. In: Knipe DM, Howley PM, editors. Fields virology. 5th ed. Philadelphia, PA: Lippincott Williams & Wilkins; 2013. pp. 2129–2159.

5. Rotz L, Doston D, Damon I, Becher J. Vaccinia (Smallpox) Vaccine: Recommendations of the Advisory Committee on Immunization Practices (ACIP), 2001. In: MMWR. Recommendations and reports : Morbidity and mortality weekly report. Recommendations and reports [Internet]. MMWR Recomm Rep; 22 Jun 2001 [cited 27 May 2020]. Available: https://pubmed.ncbi.nlm.nih.gov/15580803/

6. Impelluso G, Lentzos F. The Threat of Synthetic Smallpox: European Perspectives. Health Secur. 2017;15: 582–586. doi:10.1089/hs.2017.0045

7. Noyce RS, Lederman S, Evans DH. Construction of an infectious horsepox virus vaccine from chemically synthesized DNA fragments. PLOS ONE. 2018;13: e0188453. doi:10.1371/journal.pone.0188453

8. Nature. The spectre of smallpox lingers. Nature. 2018;560: 281–281. doi:10.1038/d41586-018-05936-x

9. Chan WM, McFadden G. Oncolytic Poxviruses. Annu Rev Virol. 2014;1: 191–214. doi:10.1146/annurev-virology-031413-085442

10. Moss B. Genetically engineered poxviruses for recombinant gene expression, vaccination, and safety. Proc Natl Acad Sci. 1996;93: 11341–11348. doi:10.1073/pnas.93.21.11341

11. Moss B. Reflections on the early development of poxvirus vectors. Vaccine. 2013;31: 4220–4222. doi:10.1016/j.vaccine.2013.03.042

12. Fontaine KA, Camarda R, Lagunoff M. Vaccinia Virus Requires Glutamine but Not Glucose for Efficient Replication. J Virol. 2014;88: 4366–4374. doi:10.1128/JVI.03134-13

13. Mazzon M, Castro C, Roberts LD, Griffin JL, Smith GL. A role for vaccinia virus protein C16 in reprogramming cellular energy metabolism. J Gen Virol. 2015;96: 395–407. doi:10.1099/vir.0.069591-0

14. Greseth MD, Traktman P. De novo Fatty Acid Biosynthesis Contributes Significantly to Establishment of a Bioenergetically Favorable Environment for Vaccinia Virus Infection. PLOS Pathog. 2014;10: e1004021. doi:10.1371/journal.ppat.1004021

15. Dai A, Cao S, Dhungel P, Luan Y, Liu Y, Xie Z, et al. Ribosome Profiling Reveals Translational Upregulation of Cellular Oxidative Phosphorylation mRNAs during Vaccinia Virus-Induced Host Shutoff. J Virol. 2017;91. doi:10.1128/JVI.01858-16

16. Owen OE, Kalhan SC, Hanson RW. The Key Role of Anaplerosis and Cataplerosis for Citric Acid Cycle Function. J Biol Chem. 2002;277: 30409–30412. doi:10.1074/jbc.R200006200

17. Costello LC, Franklin RB. A review of the important central role of altered citrate metabolism during the process of stem cell differentiation. J Regen Med Tissue Eng. 2013;2. doi:10.7243/2050-1218-2-1

18. MacPherson S, Horkoff M, Gravel C, Hoffmann T, Zuber J, Lum JJ. STAT3 Regulation of Citrate Synthase Is Essential during the Initiation of Lymphocyte Cell Growth. Cell Rep. 2017;19: 910–918. doi:10.1016/j.celrep.2017.04.012

19. Murray SL, Hynes MJ. Metabolic and Developmental Effects Resulting from Deletion of the citA Gene Encoding Citrate Synthase in Aspergillus nidulans. Eukaryot Cell. 2010;9: 656–666. doi:10.1128/EC.00373-09

20. Rahman MM, Rosu S, Joseph-Strauss D, Cohen-Fix O. Down-regulation of tricarboxylic acid (TCA) cycle genes blocks progression through the first mitotic division in Caenorhabditis elegans embryos. Proc Natl Acad Sci. 2014;111: 2602–2607. doi:10.1073/pnas.1311635111

21. Ruprich-Robert G, Zickler D, Berteaux-Lecellier V, Vélot C, Picard M. Lack of mitochondrial citrate synthase discloses a new meiotic checkpoint in a strict aerobe. EMBO J. 2002;21: 6440–6451. doi:10.1093/emboj/cdf632

22. Song P, Li L, Liu J. Proteomic Analysis in Nitrogen-Deprived Isochrysis galbana during Lipid Accumulation. PLoS ONE. 2013;8. doi:10.1371/journal.pone.0082188

23. Blomquist MC, Hunt LT, Barker WC. Vaccinia virus 19-kilodalton protein: relationship to several mammalian proteins, including two growth factors. Proc Natl Acad Sci. 1984;81: 7363–7367. doi:10.1073/pnas.81.23.7363

24. Brown JP, Twardzik DR, Marquardt H, Todaro GJ. Vaccinia virus encodes a polypeptide homologous to epidermal growth factor and transforming growth factor. Nature. 1985;313: 491–492. doi:10.1038/313491a0

25. Chang W, Lim JG, Hellström I, Gentry LE. Characterization of vaccinia virus growth factor biosynthetic pathway with an antipeptide antiserum. J Virol. 1988;62: 1080–1083.

26. Stroobant P, Rice AP, Gullick WJ, Cheng DJ, Kerr IM, Waterfield MD. Purification and characterization of vaccinia virus growth factor. Cell. 1985;42: 383–393. doi:10.1016/s0092-8674(85)80133-1

27. Yang Z, Bruno DP, Martens CA, Porcella SF, Moss B. Simultaneous high-resolution analysis of vaccinia virus and host cell transcriptomes by deep RNA sequencing. Proc Natl Acad Sci. 2010;107: 11513–11518. doi:10.1073/pnas.1006594107

28. Yang Z, Cao S, Martens CA, Porcella SF, Xie Z, Ma M, et al. Deciphering Poxvirus Gene Expression by RNA Sequencing and Ribosome Profiling. J Virol. 2015;89: 6874–6886. doi:10.1128/JVI.00528-15

29. Buller RM, Chakrabarti S, Moss B, Fredrickson T. Cell proliferative response to vaccinia virus is mediated by VGF. Virology. 1988;164: 182–192. doi:10.1016/0042-6822(88)90635-6

30. Postigo A, Martin MC, Dodding MP, Way M. Vaccinia-induced epidermal growth factor receptor-MEK signalling and the anti-apoptotic protein F1L synergize to suppress cell death during infection. Cell Microbiol. 2009;11: 1208–1218. doi:10.1111/j.1462-5822.2009.01327.x

31. Twardzik DR, Brown JP, Ranchalis JE, Todaro GJ, Moss B. Vaccinia virus-infected cells release a novel polypeptide functionally related to transforming and epidermal growth factors. Proc Natl Acad Sci. 1985;82: 5300–5304. doi:10.1073/pnas.82.16.5300

32. Beerli C, Yakimovich A, Kilcher S, V. Reynoso G, Fläschner G, Müller D, et al. Vaccinia virus hijacks EGFR signalling to enhance virus spread through rapid and directed infected cell motility. Nat Microbiol. 2018;4. doi:10.1038/s41564-018-0288-2

33. Bonjardim CA. Viral exploitation of the MEK/ERK pathway – A tale of vaccinia virus and other viruses. Virology. 2017;507: 267–275. doi:10.1016/j.virol.2016.12.011

34. Buller RM, Chakrabarti S, Cooper JA, Twardzik DR, Moss B. Deletion of the vaccinia virus growth factor gene reduces virus virulence. J Virol. 1988;62: 866–874.

35. Lai AC, Pogo BG. Attenuated deletion mutants of vaccinia virus lacking the vaccinia growth factor are defective in replication in vivo. Microb Pathog. 1989;6: 219–226. doi:10.1016/0882-4010(89)90071-5

36. Antico Arciuch VG, Elguero ME, Poderoso JJ, Carreras MC. Mitochondrial Regulation of Cell Cycle and Proliferation. Antioxid Redox Signal. 2012;16: 1150–1180. doi:10.1089/ars.2011.4085

37. El-Bacha T, Da Poian AT. Virus-induced changes in mitochondrial bioenergetics as potential targets for therapy. Int J Biochem Cell Biol. 2013;45: 41–46. doi:10.1016/j.biocel.2012.09.021

38. Cotter CA, Earl PL, Wyatt LS, Moss B. Preparation of Cell Cultures and Vaccinia Virus Stocks. Curr Protoc Microbiol. 2015;39: 14A.3.1-14A.318. doi:10.1002/9780471729259.mc14a03s39

39. Meng X, Zhong Y, Embry A, Yan B, Lu S, Zhong G, et al. Generation and characterization of a large panel of murine monoclonal antibodies against vaccinia virus. Virology. 2011;409: 271–279. doi:10.1016/j.virol.2010.10.019

40. Strober W. Trypan Blue Exclusion Test of Cell Viability. Curr Protoc Immunol. 2015;111: A3.B.1-A3.B.3. doi:10.1002/0471142735.ima03bs111

41. Pant A, Cao S, Yang Z. Asparagine Is a Critical Limiting Metabolite for Vaccinia Virus Protein Synthesis during Glutamine Deprivation. J Virol. 2019;93. doi:10.1128/JVI.01834-18

42. Cao S, Realegeno S, Pant A, Satheshkumar PS, Yang Z. Suppression of Poxvirus Replication by Resveratrol. Front Microbiol. 2017;8. doi:10.3389/fmicb.2017.02196

43. Schneider CA, Rasband WS, Eliceiri KW. NIH Image to ImageJ: 25 years of image analysis. Nat Methods. 2012;9: 671–675. doi:10.1038/nmeth.2089

44. R Core Team. R: A Language and Environment for Statistical Computing. Vienna, Austria: R Foundation for Statistical Computing; 2020. Available: https://www.R-project.org/

45. Pang Z, Chong J, Li S, Xia J. MetaboAnalystR 3.0: Toward an Optimized Workflow for Global Metabolomics. Metabolites. 2020;10: 186. doi:10.3390/metabo10050186

46. Berg JM, Tymoczko JL, Stryer L. Amino Acids Are Made from Intermediates of the Citric Acid Cycle and Other Major Pathways. Biochem 5th Ed. 2002 [cited 28 May 2020]. Available: https://www.ncbi.nlm.nih.gov/books/NBK22459/

47. Chang C-W, Li H-C, Hsu C-F, Chang C-Y, Lo S-Y. Increased ATP generation in the host cell is required for efficient vaccinia virus production. J Biomed Sci. 2009;16: 80. doi:10.1186/1423-0127-16-80

48. Anderson NM, Mucka P, Kern JG, Feng H. The emerging role and targetability of the TCA cycle in cancer metabolism. Protein Cell. 2018;9: 216–237. doi:10.1007/s13238-017-0451-1

49. Houten SM, Wanders RJA. A general introduction to the biochemistry of mitochondrial fatty acid β-oxidation. J Inherit Metab Dis. 2010;33: 469–477. doi:10.1007/s10545-010-9061-2

50. Ko YH, Pedersen PL, Geschwind JF. Glucose catabolism in the rabbit VX2 tumor model for liver cancer: characterization and targeting hexokinase. Cancer Lett. 2001;173: 83–91. doi:10.1016/S0304-3835(01)00667-X

51. Clem BF, O'Neal J, Tapolsky G, Clem AL, Imbert-Fernandez Y, Kerr DA, et al. Targeting 6-phosphofructo-2-kinase (PFKFB3) as a therapeutic strategy against cancer. Mol Cancer Ther. 2013;12: 1461–1470. doi:10.1158/1535-7163.MCT-13-0097

52. Zachar Z, Marecek J, Maturo C, Gupta S, Stuart SD, Howell K, et al. Non-redox-active lipoate derivates disrupt cancer cell mitochondrial metabolism and are potent anticancer agents in vivo. J Mol Med Berl Ger. 2011;89: 1137–1148. doi:10.1007/s00109-011-0785-8

53. Rupp H, Zarain-Herzberg A, Maisch B. The Use of Partial Fatty Acid Oxidation Inhibitors for Metabolic Therapy of Angina Pectoris and Heart Failure. Herz. 2002;27: 621–636. doi:10.1007/s00059-002-2428-x

54. Renis HE, Johnson HG. Inhibition of plaque formation of vaccinia virus by cytosine arabinoside hydrochloride. Bacteriol Proc. 1962; 140.

55. Young CW, Robinson PF, Sacktor B. Inhibition of the synthesis of protein in intact animals by acetoxycycloheximide and a metabolic derangement concomitant with this blockade. Biochem Pharmacol. 1963;12: 855–865. doi:10.1016/0006-2952(63)90116-3

56. Andrade AA, Silva PNG, Pereira ACTC, de SOUSA LP, Ferreira PCP, Gazzinelli RT, et al. The vaccinia virus-stimulated mitogen-activated protein kinase (MAPK) pathway is required for virus multiplication. Biochem J. 2004;381: 437–446. doi:10.1042/BJ20031375

57. Li D, Ambrogio L, Shimamura T, Kubo S, Takahashi M, Chirieac L, et al. BIBW2992, an irreversible EGFR/HER2 inhibitor highly effective in preclinical lung cancer models. Oncogene. 2008;27: 4702–4711. doi:10.1038/onc.2008.109

58. Langhammer S, Koban R, Yue C, Ellerbrok H. Inhibition of poxvirus spreading by the anti-tumor drug Gefitinib (Iressa^{TM}). Antiviral Res. 2011;89: 64–70. doi:10.1016/j.antiviral.2010.11.006

59. Barrett SD, Bridges AJ, Dudley DT, Saltiel AR, Fergus JH, Flamme CM, et al. The discovery of the benzhydroxamate MEK inhibitors CI-1040 and PD 0325901. Bioorg Med Chem Lett. 2008;18: 6501–6504. doi:10.1016/j.bmcl.2008.10.054

60. Magalhães JC de, Andrade AA, Silva PNG, Sousa LP, Ropert C, Ferreira PCP, et al. A Mitogenic Signal Triggered at an Early Stage of Vaccinia Virus Infection IMPLICATION OF MEK/ERK AND PROTEIN KINASE A IN VIRUS MULTIPLICATION. J Biol Chem. 2001;276: 38353–38360. doi:10.1074/jbc.M100183200

61. Gough DJ, Koetz L, Levy DE. The MEK-ERK Pathway Is Necessary for Serine Phosphorylation of Mitochondrial STAT3 and Ras-Mediated Transformation. PLoS ONE. 2013;8. doi:10.1371/journal.pone.0083395

62. Rawlings JS, Rosler KM, Harrison DA. The JAK/STAT signaling pathway. J Cell Sci. 2004;117: 1281–1283. doi:10.1242/jcs.00963

63. Schust J, Sperl B, Hollis A, Mayer TU, Berg T. Stattic: A Small-Molecule Inhibitor of STAT3 Activation and Dimerization. Chem Biol. 2006;13: 1235–1242. doi:10.1016/j.chembiol.2006.09.018

64. Peng C, Zhou Y, Cao S, Pant A, Campos Guerrero ML, McDonald P, et al. Identification of Vaccinia Virus Inhibitors and Cellular Functions Necessary for Efficient Viral Replication by Screening Bioactives and FDA-Approved Drugs. Vaccines. 2020;8: 401. doi:10.3390/vaccines8030401

65. Poli V, Camporeale A. STAT3-Mediated Metabolic Reprograming in Cellular Transformation and Implications for Drug Resistance. Front Oncol. 2015;5. doi:10.3389/fonc.2015.00121

66. Mascarenhas J, Hoffman R. Ruxolitinib: The First FDA Approved Therapy for the Treatment of Myelofibrosis. Clin Cancer Res. 2012;18: 3008–3014. doi:10.1158/1078-0432.CCR-11-3145

67. Pant A, Yang Z. Asparagine: An Achilles Heel of Virus Replication? ACS Infect Dis. 2020 [cited 18 Aug 2020]. doi:10.1021/acsinfecdis.0c00504

68. Mitchell P, Moyle J. Chemiosmotic hypothesis of oxidative phosphorylation. Nature. 1967;213: 137–139. doi:10.1038/213137a0

69. DeBerardinis RJ, Lum JJ, Hatzivassiliou G, Thompson CB. The Biology of Cancer: Metabolic Reprogramming Fuels Cell Growth and Proliferation. Cell Metab. 2008;7: 11–20. doi:10.1016/j.cmet.2007.10.002

70. Baron S, Fons M, Albrecht T. Viral Pathogenesis. 4th ed. In: Baron S, editor. Medical Microbiology. 4th ed. Galveston (TX): University of Texas Medical Branch at Galveston; 1996. Available: http://www.ncbi.nlm.nih.gov/books/NBK8149/

71. King CS, Cooper JA, Moss B, Twardzik DR. Vaccinia virus growth factor stimulates tyrosine protein kinase activity of A431 cell epidermal growth factor receptors. Mol Cell Biol. 1986;6: 332–336.

72. Levy DE, Lee C. What does Stat3 do? J Clin Invest. 2002;109: 1143–1148. doi:10.1172/JCI15650

73. Avalle L, Poli V. Nucleus, Mitochondrion, or Reticulum? STAT3 à La Carte. Int J Mol Sci. 2018;19. doi:10.3390/ijms19092820

74. Gough DJ, Corlett A, Schlessinger K, Wegrzyn J, Larner AC, Levy DE. Mitochondrial STAT3 supports Ras-dependent oncogenic transformation. Science. 2009;324: 1713–1716. doi:10.1126/science.1171721

75. Tammineni P, Anugula C, Mohammed F, Anjaneyulu M, Larner AC, Sepuri NBV. The Import of the Transcription Factor STAT3 into Mitochondria Depends on GRIM-19, a Component of the Electron Transport Chain. J Biol Chem. 2013;288: 4723–4732. doi:10.1074/jbc.M112.378984

76. Wegrzyn J, Potla R, Chwae Y-J, Sepuri NBV, Zhang Q, Koeck T, et al. Function of Mitochondrial Stat3 in Cellular Respiration. Science. 2009;323: 793–797. doi:10.1126/science.1164551

77. Zhang Q, Raje V, Yakovlev VA, Yacoub A, Szczepanek K, Meier J, et al. Mitochondrial Localized Stat3 Promotes Breast Cancer Growth via Phosphorylation of Serine 727. J Biol Chem. 2013;288: 31280–31288. doi:10.1074/jbc.M113.505057

78. Avalle L, Camporeale A, Morciano G, Caroccia N, Ghetti E, Orecchia V, et al. STAT3 localizes to the ER, acting as a gatekeeper for ER-mitochondrion Ca 2+ fluxes and apoptotic responses. Cell Death Differ. 2019;26: 932–942. doi:10.1038/s41418-018-0171-y

79. Suarez AAR, Renne NV, Baumert TF, Lupberger J. Viral manipulation of STAT3: Evade, exploit, and injure. PLOS Pathog. 2018;14: e1006839. doi:10.1371/journal.ppat.1006839

80. Pinkham C, An S, Lundberg L, Bansal N, Benedict A, Narayanan A, et al. The role of signal transducer and activator of transcription 3 in Rift Valley fever virus infection. Virology. 2016;496: 175–185. doi:10.1016/j.virol.2016.06.004

81. McCartney EM, Helbig KJ, Narayana SK, Eyre NS, Aloia AL, Beard MR. Signal transducer and activator of transcription 3 is a proviral host factor for hepatitis C virus. Hepatol Baltim Md. 2013;58: 1558–1568. doi:10.1002/hep.26496

82. Yoshida T, Hanada T, Tokuhisa T, Kosai K, Sata M, Kohara M, et al. Activation of STAT3 by the Hepatitis C Virus Core Protein Leads to Cellular Transformation. J Exp Med. 2002;196: 641–653. doi:10.1084/jem.20012127

83. Zhu S, Luo H, Liu H, Ha Y, Mays ER, Lawrence RE, et al. p38MAPK plays a critical role in induction of a pro-inflammatory phenotype of retinal Müller cells following Zika virus infection. Antiviral Res. 2017;145: 70–81. doi:10.1016/j.antiviral.2017.07.012

84. Morgan EL, Wasson CW, Hanson L, Kealy D, Pentland I, McGuire V, et al. STAT3 activation by E6 is essential for the differentiation-dependent HPV18 life cycle. PLOS Pathog. 2018;14: e1006975. doi:10.1371/journal.ppat.1006975

85. King CA. Kaposi's Sarcoma-Associated Herpesvirus Kaposin B Induces Unique Monophosphorylation of STAT3 at Serine 727 and MK2-Mediated Inactivation of the

STAT3 Transcriptional Repressor TRIM28. J Virol. 2013;87: 8779–8791. doi:10.1128/JVI.02976-12

86. Lepiller Q, Abbas W, Kumar A, Tripathy MK, Herbein G. HCMV Activates the IL-6-JAK-STAT3 Axis in HepG2 Cells and Primary Human Hepatocytes. PLOS ONE. 2013;8: e59591. doi:10.1371/journal.pone.0059591

87. Santarelli R, Gonnella R, Di Giovenale G, Cuomo L, Capobianchi A, Granato M, et al. STAT3 activation by KSHV correlates with IL-10, IL-6 and IL-23 release and an autophagic block in dendritic cells. Sci Rep. 2014;4: 1–7. doi:10.1038/srep04241

88. McCart JA, Ward JM, Lee J, Hu Y, Alexander HR, Libutti SK, et al. Systemic Cancer Therapy with a Tumor-selective Vaccinia Virus Mutant Lacking Thymidine Kinase and Vaccinia Growth Factor Genes. Cancer Res. 2001;61: 8751–8757.

89. Hanahan D, Weinberg RA. Hallmarks of Cancer: The Next Generation. Cell. 2011;144: 646–674. doi:10.1016/j.cell.2011.02.013

90. Frank DA, Mahajan S, Ritz J. B lymphocytes from patients with chronic lymphocytic leukemia contain signal transducer and activator of transcription (STAT) 1 and STAT3 constitutively phosphorylated on serine residues. J Clin Invest. 1997;100: 3140–3148. doi:10.1172/JCI119869

91. Qin HR, Kim H-J, Kim J-Y, Hurt EM, Klarmann GJ, Kawasaki BT, et al. Activation of Stat3 through a Phosphomimetic Serine727 Promotes Prostate Tumorigenesis Independent of Tyrosine705 phosphorylation. Cancer Res. 2008;68: 7736–7741. doi:10.1158/0008-5472.CAN-08-1125

92. Yeh Y-T, Ou-Yang F, Chen I-F, Yang S-F, Wang Y-Y, Chuang H-Y, et al. STAT3 ser727 phosphorylation and its association with negative estrogen receptor status in breast infiltrating ductal carcinoma. Int J Cancer. 2006;118: 2943–2947. doi:10.1002/ijc.21771

93. He Y, Fisher R, Chowdhury S, Sultana I, Pereira CP, Bray M, et al. Vaccinia Virus Induces Rapid Necrosis in Keratinocytes by a STAT3-Dependent Mechanism. PLoS ONE. 2014;9. doi:10.1371/journal.pone.0113690

Figures and tables- Chapter 3

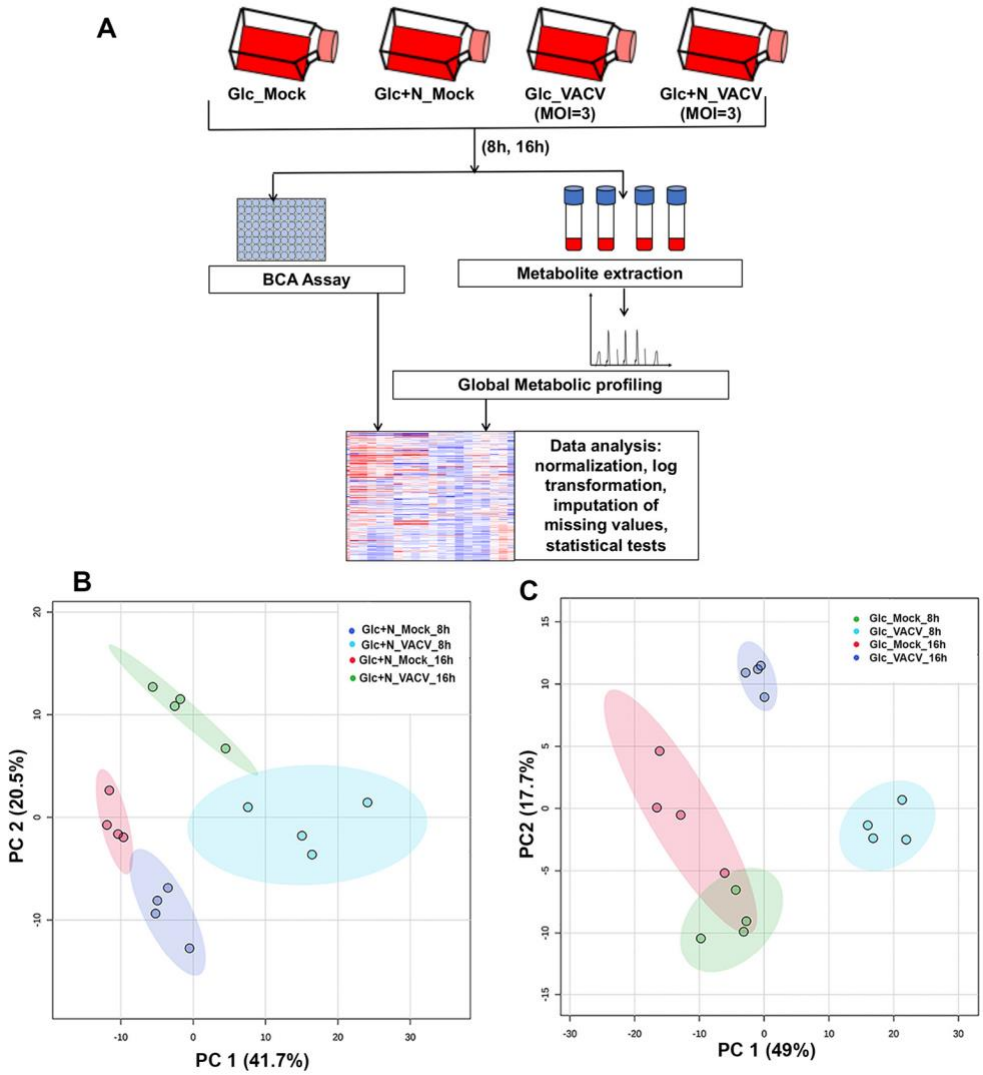

Figure 3.1. VACV infection reprograms cellular metabolism profoundly and globally under the glutamine-depletion conditions.

(A) Experimental design of global metabolic profiling. Four biological replicates of HFFs per treatment were either mock-infected or infected with VACV at an MOI of 3 for either 8 or 16 hours in medium with glucose (Glc) or glucose plus asparagine (Glc+N). Metabolites were extracted, and their levels were measured. **(B & C)** Principal component analysis (PCA) showing a clear separation between VACV-infected and uninfected HFFs in glucose plus asparagine medium **(B)** and in HFFs in glucose only medium **(C).** Each small circle indicates one sample. The shaded region indicates the 95% confidence interval PC1 represents the effect of VACV infection and PC2 represents the effect of time.

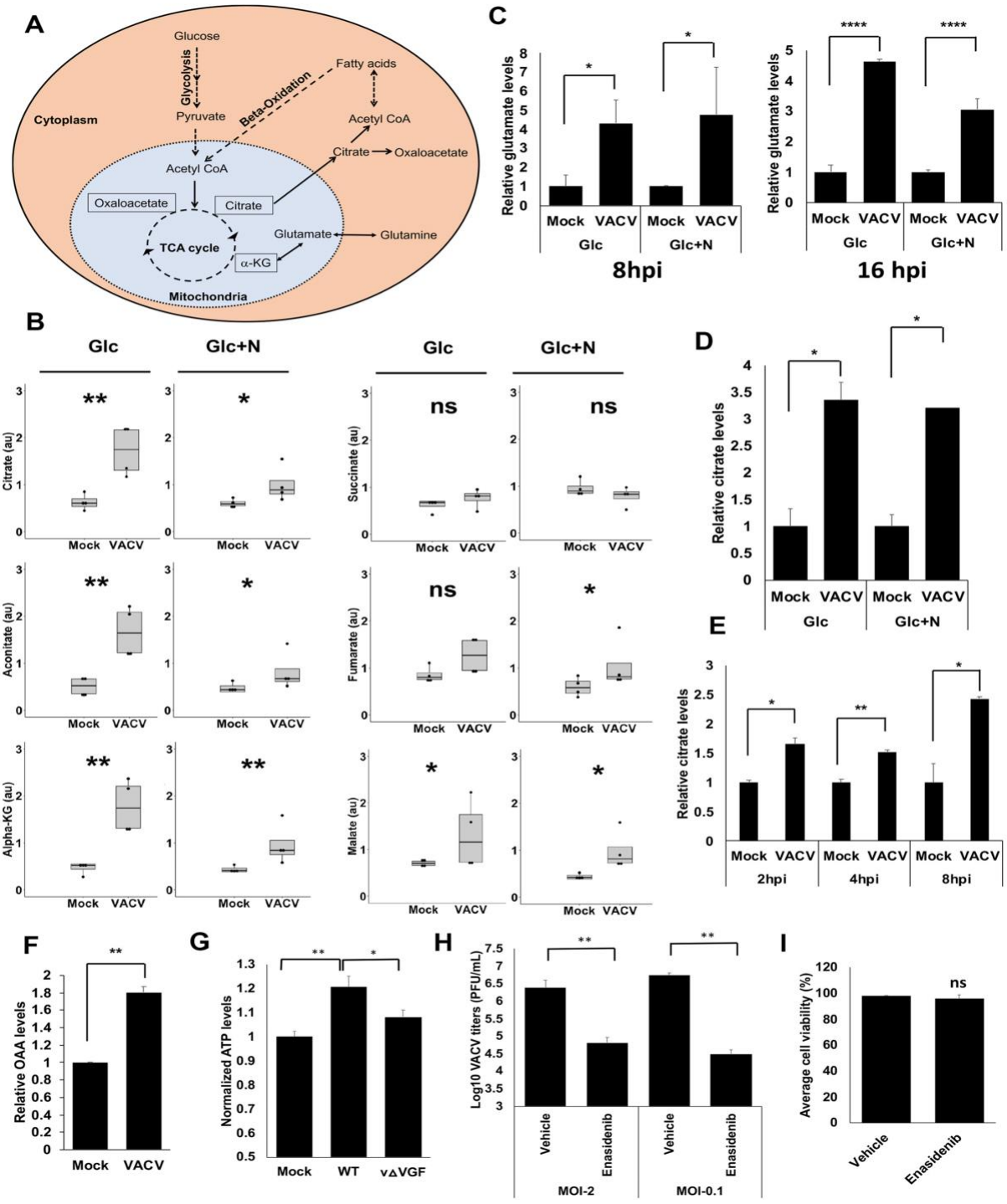

Figure 3.2. VACV infection elevates the levels of TCA cycle intermediates, including citrate.

(A) Simplified overview of the TCA cycle and citrate metabolism. The pyruvate generated from glycolysis can be converted into Acetyl-CoA that reacts with OAA to form citrate in the mitochondria of a cell. The citrate can then be transported out of the mitochondria where it gets

converted to Acetyl-CoA and OAA. The cytosolic Acetyl-CoA can act as a precursor for fatty acid biosynthesis. The fatty acids undergo β-oxidation in the mitochondria to convert into Acetyl-CoA to feed the TCA cycle. Glutamine can also feed in the TCA cycle to increase the citrate level by converting it to α -KG. **(B)** VACV infection increases the levels of most of the TCA cycle intermediates in the absence of exogenous glutamine. The levels of TCA cycle intermediates at 8 hpi in the metabolic profiling of Fig. 3.1A were shown. **(C)** VACV infection increases the level of glutamate. The level of glutamate in HFFs in the global metabolic profiling of Fig. 3.1A were shown. **(D)** VACV infection increases the citrate level in HFFs cultured in medium without exogenous glutamine. HFFs infected with indicated viruses at MOI of 5 in media with glucose only (Glc) or glucose plus asparagine (Glc+N). Citrate level was measured at 8 hpi using a citrate assay kit. **(E)** VACV infection increases the citrate level in HFFs cultured in medium with glutamine. HFFs infected with WT VACV at an MOI of 5 in medium with glucose plus glutamine and the citrate level was measured at indicated time points using a citrate assay kit. **(F)** VACV infection increases the levels of OAA. HFFs infected with WT VACV at MOI of 5 in HFFs cultured in medium with glucose plus glutamine and the OAA level was measured at 8 hpi. **(G)** VACV infection increases the ATP levels in HFFs. HFFs were infected with MOI of 2 of WT-VACV or vΔVGF (VACV with VGF gene deleted) in medium containing glucose and glutamine. The ATP levels were measured at 8 hpi by using an ATP assay kit. **(H)** TCA Cycle activity is important for VACV replication. HFFs infected with WT VACV at MOI of 2 or 0.1 in media with glucose plus glutamine in the presence or absence of 50 μM Enasidenib. VACV titers measured at 24 and 48 hpi for MOI 2 and 0.1 respectively using a plaque assay. **(I)** Enasidenib treatment has minimal effect on HFF viability. HFFs were treated with 50 μM Enasidenib in medium with glucose plus glutamine. Cell viability measured by a trypan blue assay at 48 h post treatment. Error bars represent the standard deviation of at least three biological replicates. ns, $P > 0.05$; *, $P \leq 0.05$; **, $P \leq 0.01$; ****, $P \leq 0.0001$.

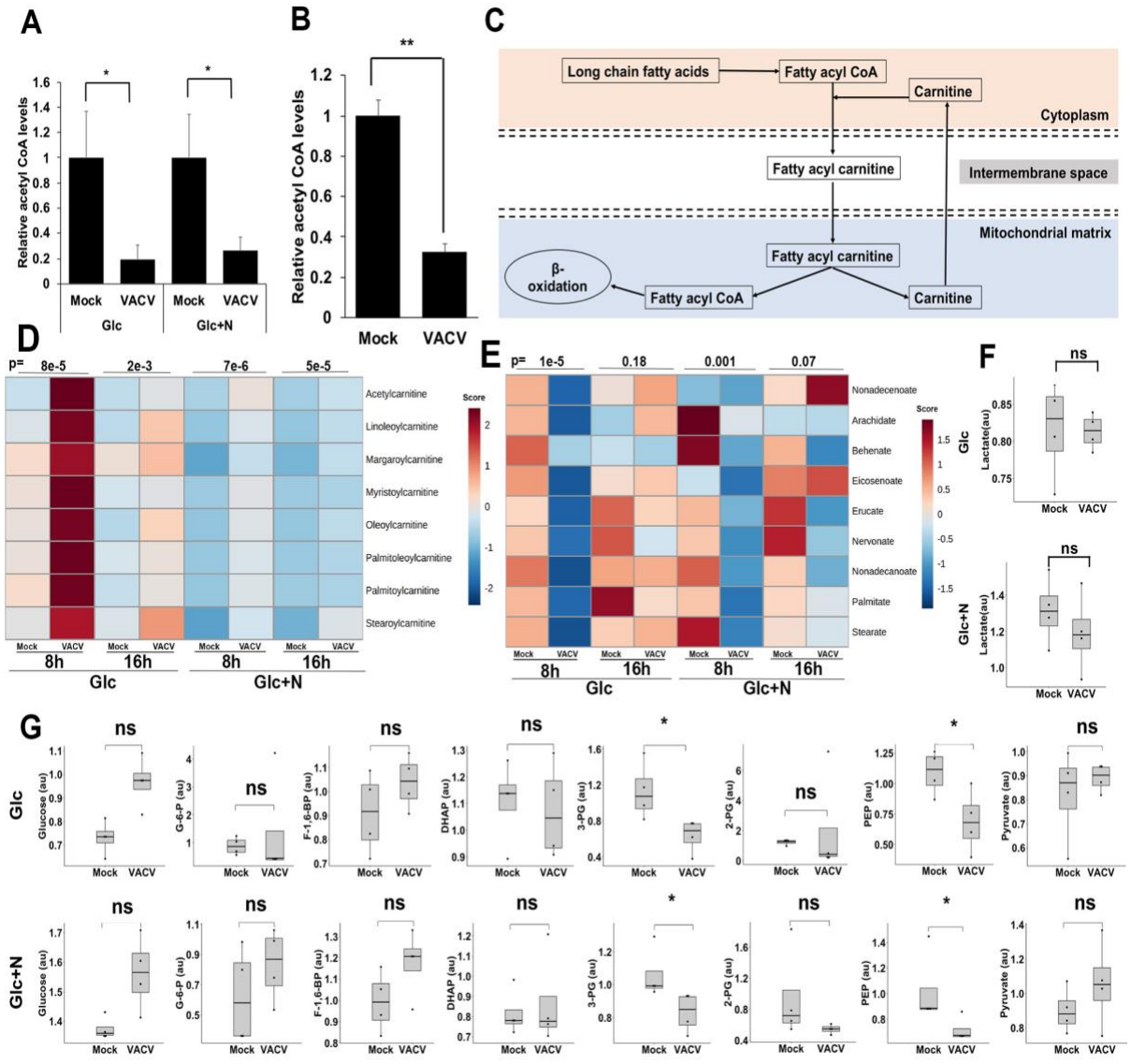

Figure 3.3. VACV infection alters the TCA cycle-related metabolism.

(A) A decrease in Acetyl-CoA upon VACV infection in HFFs cultured in media without glutamine. The level of Acetyl-CoA at 8 hpi in the metabolic profiling of Fig. 3.1A was shown. **(B)** VACV infection decreases the level of acetyl CoA in HFFs cultured in medium containing glutamine. HFFs infected with WT VACV at an MOI of 2 in media with glucose plus glutamine and the Acetyl-CoA level was measured at 8 hpi using an Acetyl-CoA assay kit. **(C)** Simplified overview of carnitine metabolism in oxidation. The long-chain fatty acids are acylated and then carnitylated by carnitine palmitoyltransferase system, which is then transported into the mitochondrial matrix for β-oxidation to fuel the TCA cycle. **(D)** VACV infection increases the levels of carnitine-conjugated fatty acids. The metabolic profiling data of fatty acyl carnitines in

VACV-infected HFFs (Table 3.2) was uploaded to the MetaboAnalyst tool and then a hierarchically clustered heatmap was generated using Ward's minimum variance and Euclidean distance measure. Color keys indicate the levels of different metabolites; blue: lowest, red: highest. The number on top of the plots represent the p-values comparing the average levels of indicated metabolites levels in mock- and VACV-infected HFFs **(E)** The levels of long-chain fatty acids are reduced in VACV-infected HFFs. The metabolic profiling data of long-chain fatty acids in VACV-infected HFFs (Table 3.2) was processed as in Fig 3.3D. **(F)** The glycolysis intermediates are either unaffected or reduced by VACV. The levels of glycolysis intermediates in HFFs infected with MOI-3 of WT-VACV in medium with glucose (Glc) or glucose plus asparagine (Glc+N) at 8 hpi as determined by global metabolic profiling in Fig. 3.1a. **(G)** VACV infection does not affect the level of lactate. The level of lactate in HFFs infected with MOI-3 of WT-VACV in media with glucose (Glc) or glucose plus asparagine (Glc+N) at 8 hpi was determined by global metabolic profiling in Fig. 3.1A. Error bars represent the standard deviation of at least three biological replicates. ns, $P > 0.05$; *, $P \leq 0.05$; **, $P \leq 0.01$; ***, $P \leq 0.001$; ****, $P \leq 0.0001$.

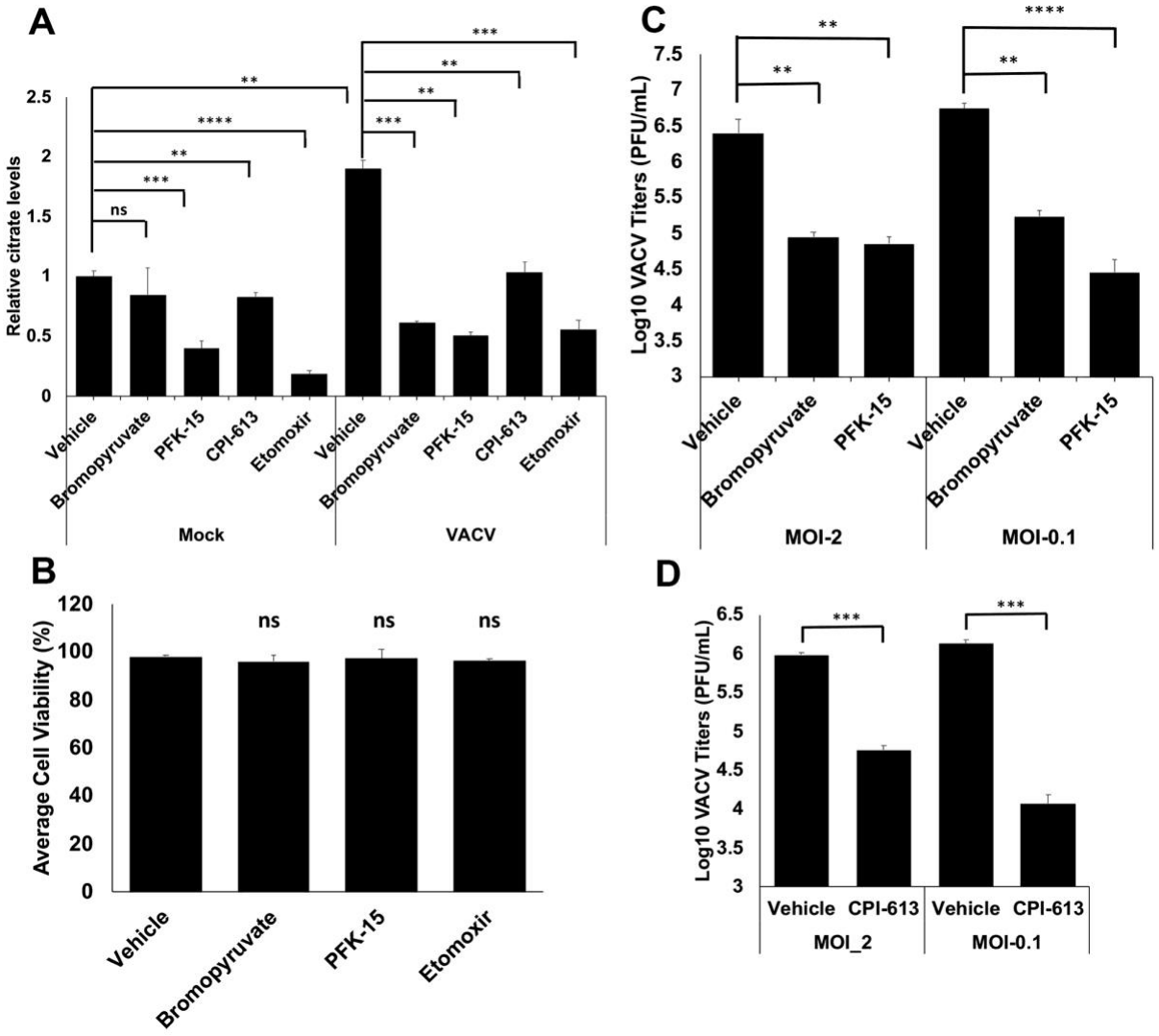

Figure 3.4. Both Glycolysis and β-oxidation contribute towards the citrate level enhancement during VACV infection.

(A) Inhibition of glycolysis and fatty acid oxidation reduces the increase of citrate levels during VACV infection. HFFs were mock-infected or infected with WT-VACV at an MOI of 5 in medium with glucose plus glutamine in the presence or absence of 50 μM bromopyruvate, 50 μM PFK-15, 100 μM of CPI-613, and 50 μM etomoxir. Citrate levels measured at 4 hpi using a citrate assay kit. **(B)** HFFs treated with indicated chemicals at a concentration as listed in Fig 3.4A in medium with glucose plus glutamine. Cell viability measured by a trypan blue assay at 48 h post treatment. **(C)** Glycolysis inhibition suppresses VACV replication. HFFs infected with WT VACV at an MOI of 2 (for 24 h) or MOI of 0.1 (for 48 h) in medium with glucose plus glutamine with or without 50 μM bromopyruvate, 50 μM PFK-15. Virus titers measured by a

plaque assay. **(D)** Inhibition of pyruvate dehydrogenase and α-ketoglutarate dehydrogenase reduces VACV titers. HFFs infected with WT VACV at an MOI of 2 (for 24 h) or MOI of 0.1 (for 48 h) in medium with glucose plus glutamine in the presence or absence of 100 μM CPI-613. Virus titers were measured by a plaque assay. Error bars represent the standard deviation of at least three biological replicates. ns, $P > 0.05$; **, $P \leq 0.01$; ***, $P \leq 0.001$; ****, $P \leq 0.0001$.

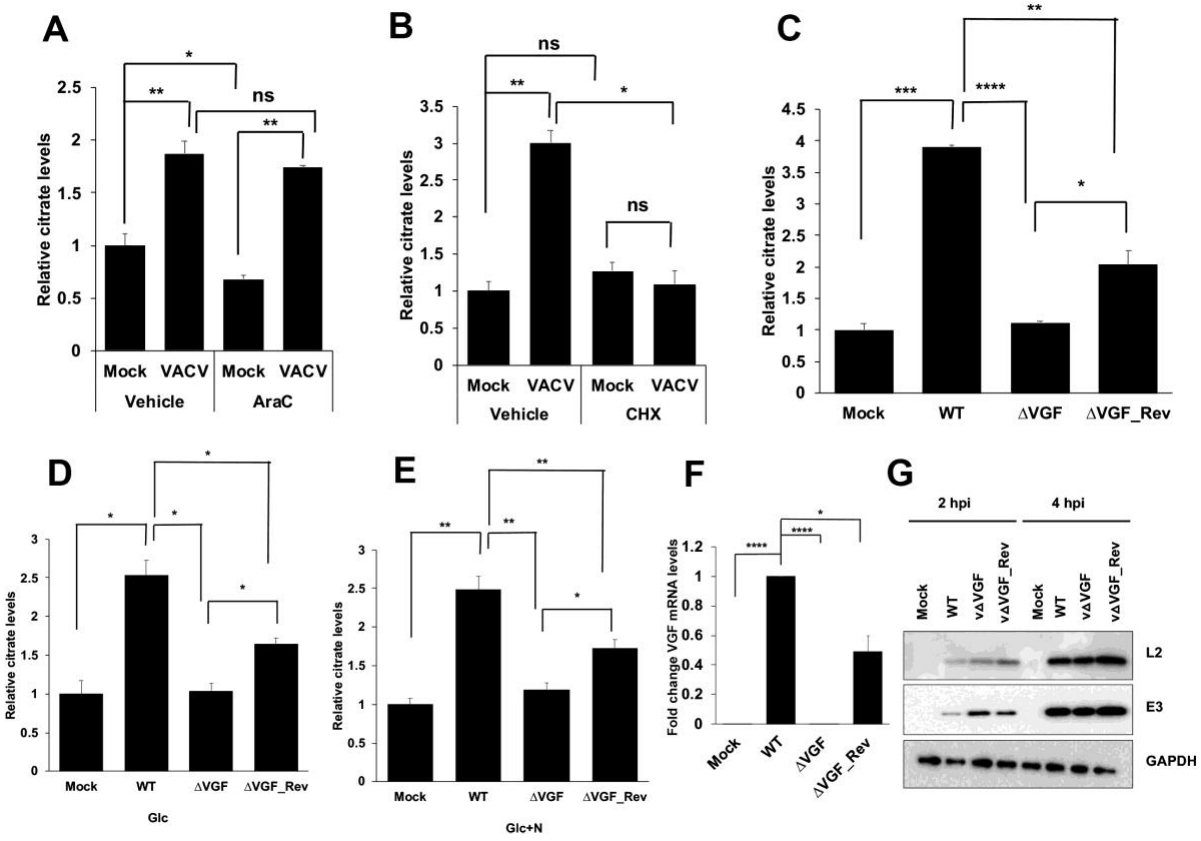

Figure 3.5. VACV growth factor (VGF) deletion abolishes the elevation of citrate level during viral infection.

(A) Inhibition of DNA synthesis does not inhibit the increased citrate level upon VACV infection. HFFs were infected with VACV at an MOI of 5 in medium with glucose plus glutamine in the presence or absence of 40 µg/mL AraC. Citrate level was measured at 8 hpi. **(B)** Inhibition of protein synthesis reduces citrate level in VACV-infected HFFs. HFFs were infected with VACV at an MOI of 5 in medium with glucose plus glutamine in the presence or absence of 100 µg/mL Cycloheximide. Citrate level was measured at 2 hpi. **(C-E)** VGF is required for the elevation of citrate level during VACV infection. **(C)** HFFs were infected with either WT-VACV or vΔVGF or a VGF revertant vΔVGF_Rev at an MOI of 5 in medium with glucose plus glutamine. Citrate level was measured at 4 hpi. **(D)** HFFs were infected with indicated viruses at an MOI of 5 in medium with glucose only (Glc). Citrate level was measured at 4 hpi. **(E)** HFFs were infected with indicated viruses at an MOI of 5 in with glucose + asparagine (Glc+N), and citrate level was measured at 4 hpi. **(F)** VGF mRNA expression in WT-VACV, vΔVGF, and

vΔVGF_Rev. RNA was extracted from HFFs infected with indicated viruses at an MOI of 5 for 1 h in medium with glucose plus glutamine, and reverse transcription-quantitative PCR (qRT-PCR) analysis was performed. **(G)** VGF deletion does not affect the levels of other VACV early proteins. HFFs infected with indicated viruses at an MOI of 5. Western blotting analysis was performed at indicated time post infection to measure the levels of VACV E3 and L2 proteins. Error bars represent the standard deviation of at least three biological replicates. ns, $P > 0.05$; *, $P \leq 0.05$; **, $P \leq 0.01$; ***, $P \leq 0.001$; ****, $P \leq 0.0001$.

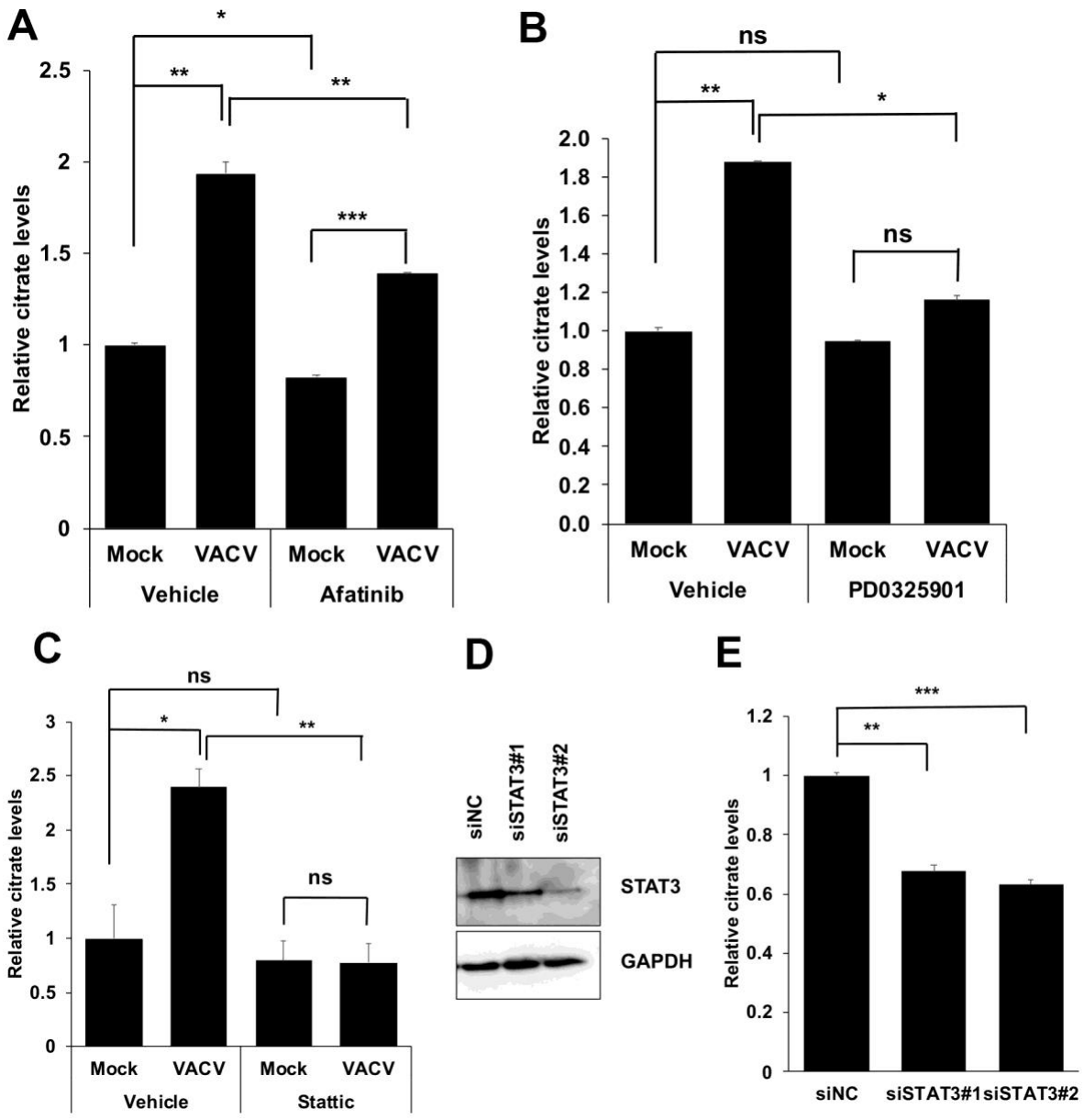

Figure 3.6. Inhibition of the STAT3 pathway and its upstream signaling decreases citrate levels during VACV infection.

(A) Inhibition of the EGFR pathway decreases the citrate level in VACV-infected HFFs. HFFs were infected with WT VACV at an MOI of 5 in the presence or absence of 3 μM afatinib. The citrate level was measured at 4 hpi. **(B)** Inhibition of the MAPK pathway decreases the citrate level during VACV infection. HFFs were infected with WT VACV at an MOI of 5 in the presence or absence of 20 μM PD0325901. The citrate level was measured at 2 hpi. **(C)** Inhibition of the STAT3 pathway decreases the citrate level in VACV-infected cells. HFFs were

infected with VACV at an MOI of 5 in the presence or absence of 3 μM stattic. The citrate level was measured at 4 hpi. **(F)** siRNA mediated knockdown of STAT3. HFFs were transfected with a negative control siRNA or two specific siRNA targeting STAT3 for 48 h. Western blotting analysis was performed to measure the level of STAT3. **(G)** siRNA-mediated knockdown of STAT3 decreases citrate level during VACV infection. HFFs were transfected with indicated siRNAs for 48 h and then infected with an MOI of 5 of VACV for 4 h, and the citrate level was measured. All the infections were performed in media with glucose plus glutamine. Error bars represent the standard deviation of at least three biological replicates. ns, $P > 0.05$; *, $P \leq 0.05$; **, $P \leq 0.01$; ***, $P \leq 0.001$.

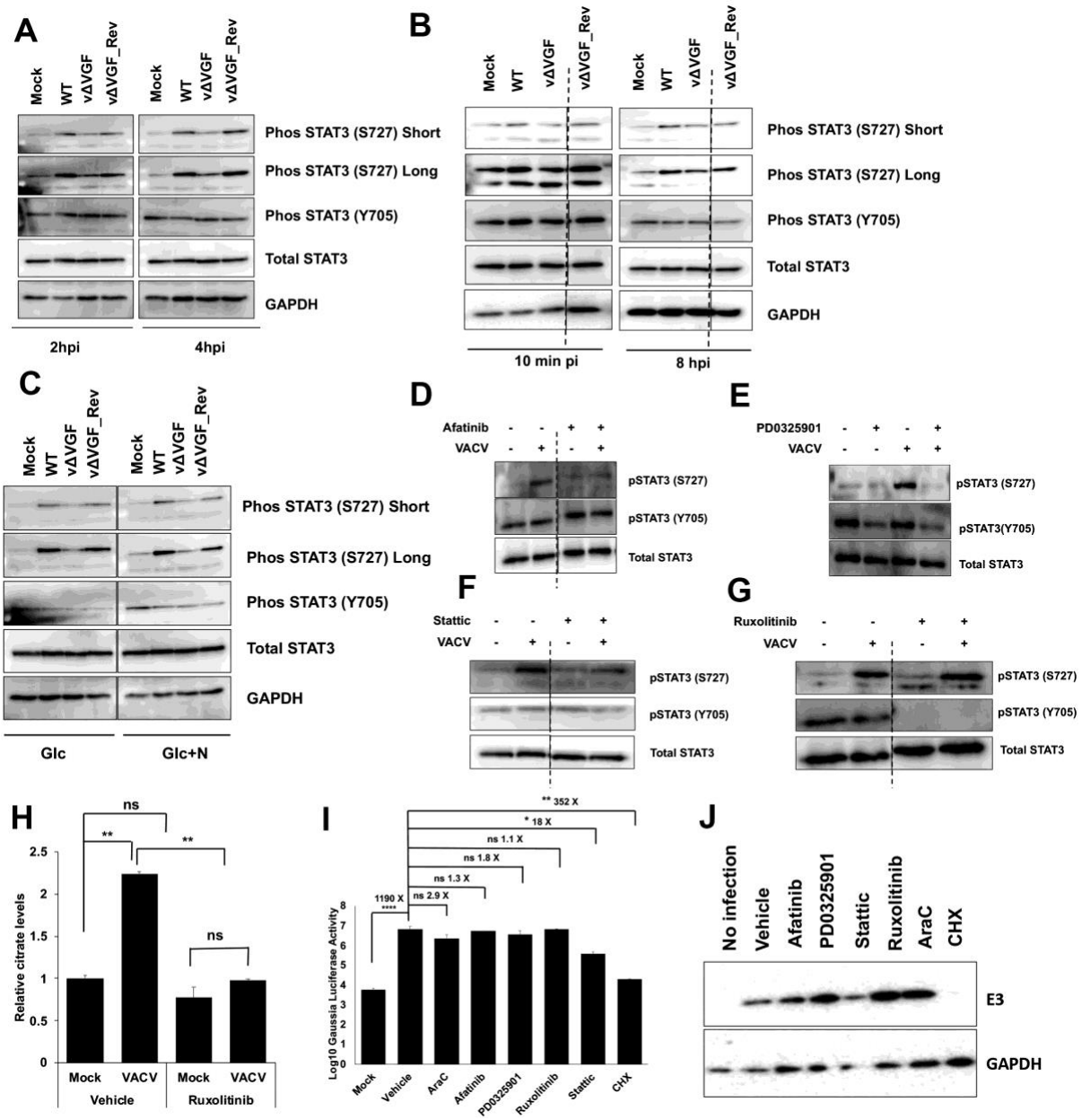

Figure 3.7. VACV infection induces non-canonical STAT3 phosphorylation at S727 in a VGF-dependent manner.

(A) VACV VGF is indispensable to activate STAT3 (S727) phosphorylation. HFFs infected with indicated viruses at an MOI of 5 for the indicated time. Western blotting analysis was performed to measure the levels of various forms of STAT3. (**B)** Upregulation of STAT3 S727 phosphorylation starts early during VACV infection. HFFs infected with indicated viruses at an MOI of 5. The samples were collected at 10 min post-infection and 8 hpi, respectively, followed by Western blotting analysis. **(C)** VACV activates STAT3 (S727) phosphorylation in the absence of glutamine in the medium. HFFs were infected with indicated viruses at an MOI of 5

in medium with glucose only (Glc) or with glucose+asparagine (Glc+N). Protein levels were detected by performing a Western blotting analysis at 4 hpi. **(D)** Inhibition of the EGFR pathway decreases STAT3 S727 phosphorylation in VACV infected cells. HFFs were infected with MOI of 5 of WT-VACV with or without 3 μM afatinib treatment. Western blotting analysis was performed at 4 hpi to test the levels of different forms of STAT3 protein. **(E)** Inhibition of the MAPK pathway decreases both Y705 and S727 phosphorylation. HFFs were infected with MOI of 5 of VACV in medium with or without 20 μM PD0325901 treatment. Western blotting analysis was performed at 2 hpi to detect the levels of different forms of STAT3 protein. **(F)** Stattic treatment inhibits S727 phosphorylation. HFFs were infected with MOI of 5 of WT VACV with or without 3 μM stattic. At 4 hpi, Western blotting analysis was performed to detect the levels of different forms of STAT3 protein. **(G)** STAT3 S727 phosphorylation is independent of the JAK1/2 pathway. HFFs were infected with an MOI of 5 of VACV in medium with or without 5 μM ruxolitinib treatment. Western blotting analysis was performed at 4 hpi to measure different protein levels. **(H)** Ruxolitinib treatment decreases the induction of citrate level upon VACV infection. HFFs were infected with WT VACV at an MOI of 5 in the presence or absence of ruxolitinib treatment. The citrate level was measured at 4 hpi. **(I)** Effects of inhibition of STAT3 and its upstream signaling pathways on VACV early protein expression. HFFs infected with WT VACV at an MOI of 2 in the presence or absence of 3 μM afatinib, 20 μM PD0325901, 3 μM stattic, 5 μM ruxolitinib, 40 μg/mL AraC, or 100 μg/mL cycloheximide. The levels of VACV E3 protein was measured at 2 hpi by a Western blotting analysis. **(J)** Effects of inhibition of STAT3 and its upstream signaling pathways on VACV early protein levels. HFFs infected at an MOI of 2 with a recombinant VACV expressing *Gaussia* luciferase under virus early VGF promoter in the presence or absence of 3 μM afatinib, 20 μM PD0325901, 3 μM stattic, 5 μM ruxolitinib, 40 μg/mL AraC, or 100 μg/mL cycloheximide. Early gene expression was measured by a *Gaussia* luciferase activity assay kit at 2 hpi. All experiments were performed in media with glucose plus glutamine unless otherwise stated. Error bars represent the standard deviation of at least three biological replicates. ns, $P > 0.05$; *, $P \leq 0.05$; **, $P \leq 0.01$; ****, $P \leq 0.0001$. The blots were from different lanes on the same gel and the dashed lines indicate that some non-relevant lanes were removed.

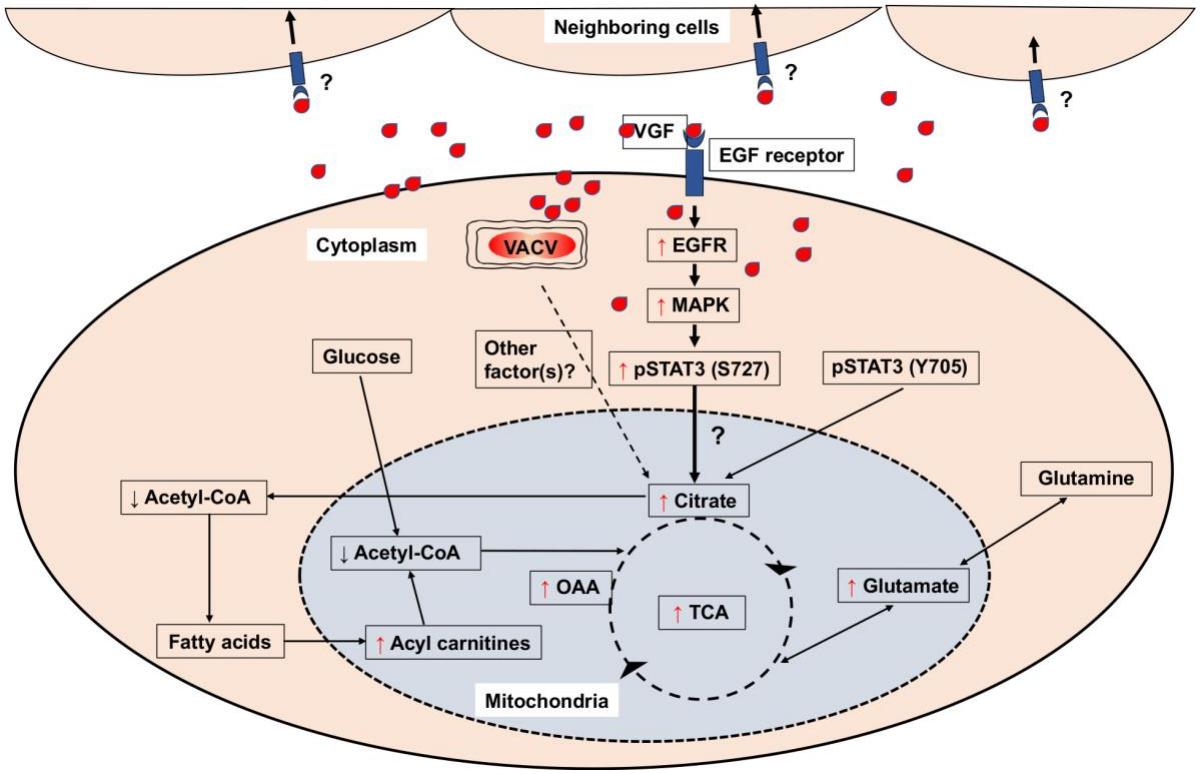

Figure 3.8. Proposed model by which VACV infection promotes the TCA cycle.

VACV infection enhances the levels of TCA cycle intermediates and related products. Upon VACV infection, the levels of Acetyl-CoA decrease, while the levels of fatty acyl carnitines (key metabolites for β-oxidation of fatty acids) increase. The increase in the level of citrate can be attributed to the VACV VGF mediated upregulation of non-canonical STAT3 phosphorylation at S727 via EGFR and MAPK pathways. Although not upregulated by VACV, the Y705 phosphorylation of STAT3 is also important for enhancing citrate level. It is unclear if additional viral factors are also required to elevate the TCA cycle and if VGF alone can exert the function in uninfected cells. Red upward arrows indicate increase and black downward arrows indicate decrease of indicated intermediates.

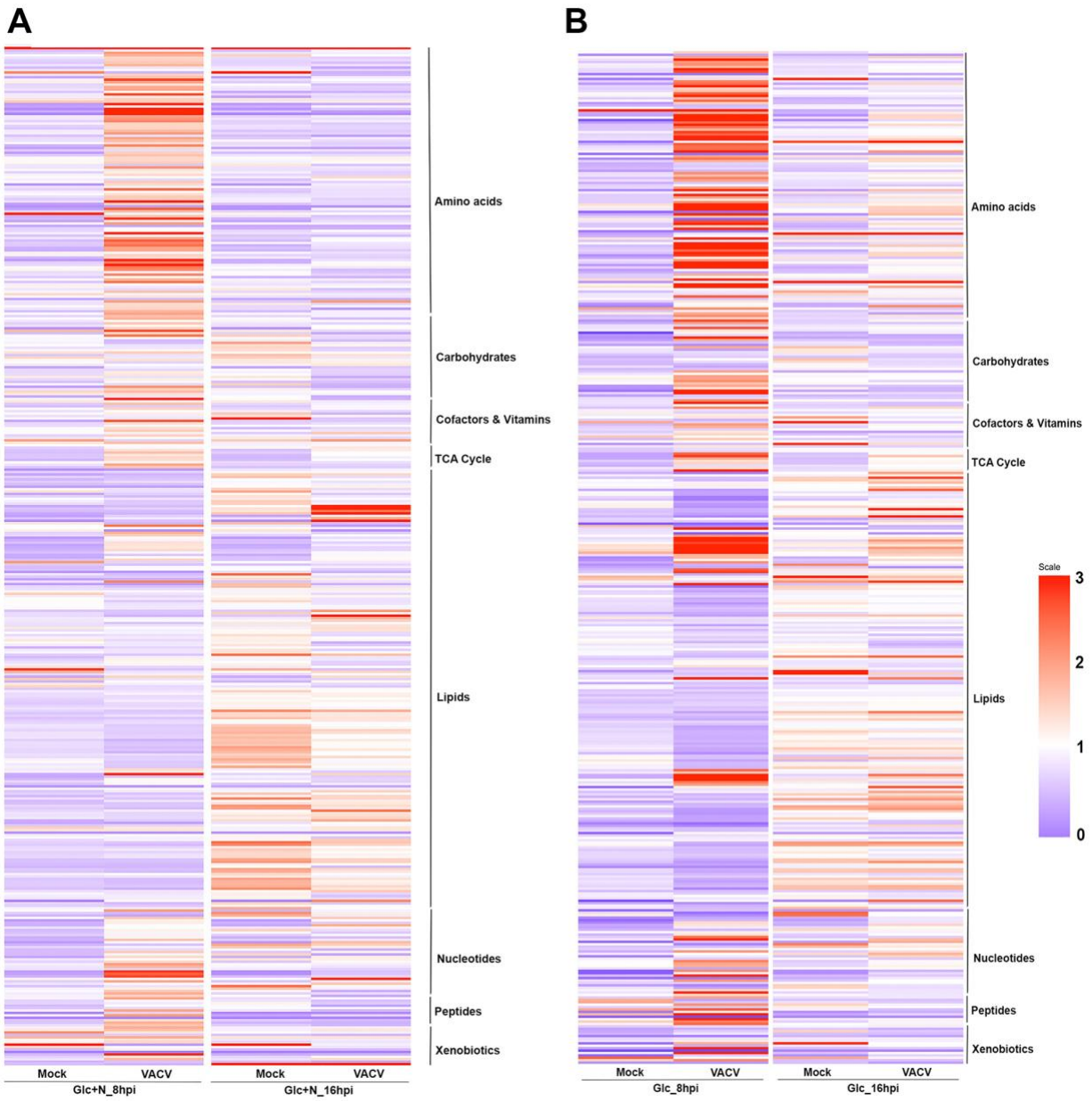

Figure S 3.1. Heatmap of changes in metabolite levels during VACV infection

(A) Heatmap of VACV-induced alteration of metabolism in HFFs in medium with glucose plus asparagine. (B) Heatmap of VACV-induced alteration of metabolism in medium with glucose only. Color keys indicate the levels of different metabolites; blue: lowest, red: highest.

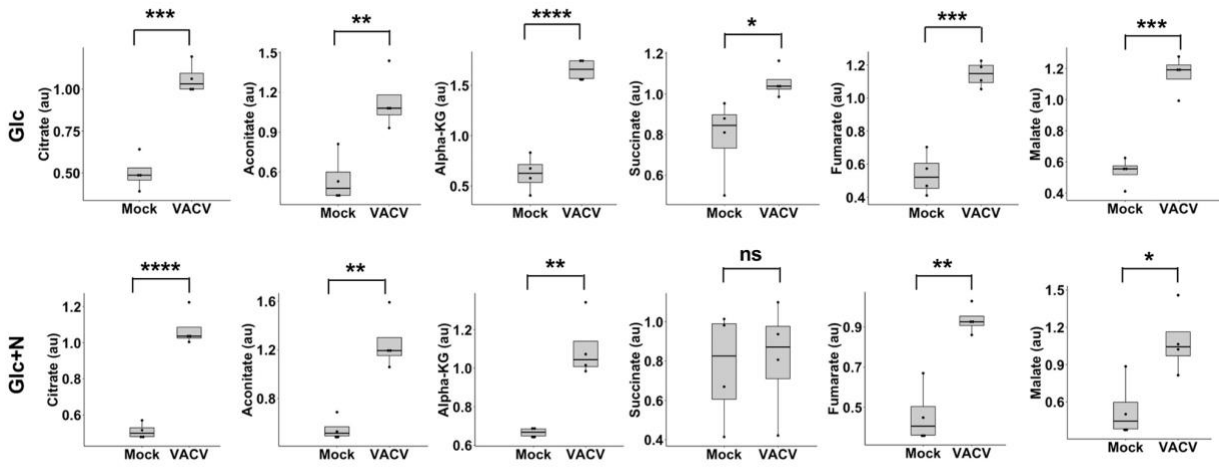

Figure S 3.2. Levels of the TCA cycle intermediates at 16 hpi.

VACV infection increases the levels of most of the TCA cycle intermediates in the absence of glutamine in the medium. HFFs infected with VACV at an MOI of 3 of in medium with glucose only (Glc) or glucose+asparagine (Glc+N). The levels of TCA cycle intermediates at 16 hpi were measured by performing metabolic profiling. ns, $P > 0.05$; *, $P \leq 0.05$; **, $P \leq 0.01$; ***, $P \leq 0.001$; ****, $P \leq 0.0001$.

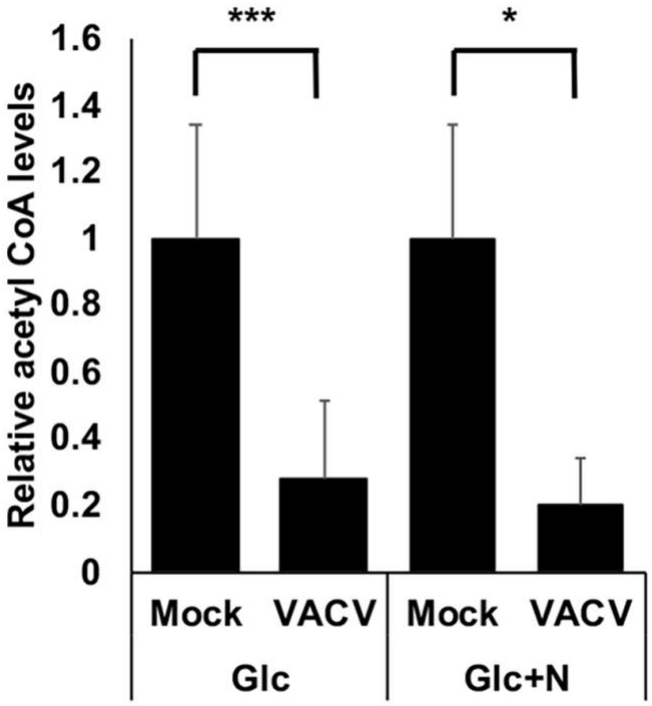

Figure S 3.3. Levels of acetyl-CoA at 16 hpi.

VACV infection decreases the level of acetyl-CoA. HFFs infected with VACV at an MOI of 3 in medium with glucose only (Glc) or glucose + asparagine (Glc+N). The level of acetyl CoA at 16 hpi was measured by performing metabolic profiling. Error bars represent the standard deviation of four biological replicates. *, $P \leq 0.05$; ***, $P \leq 0.001$.

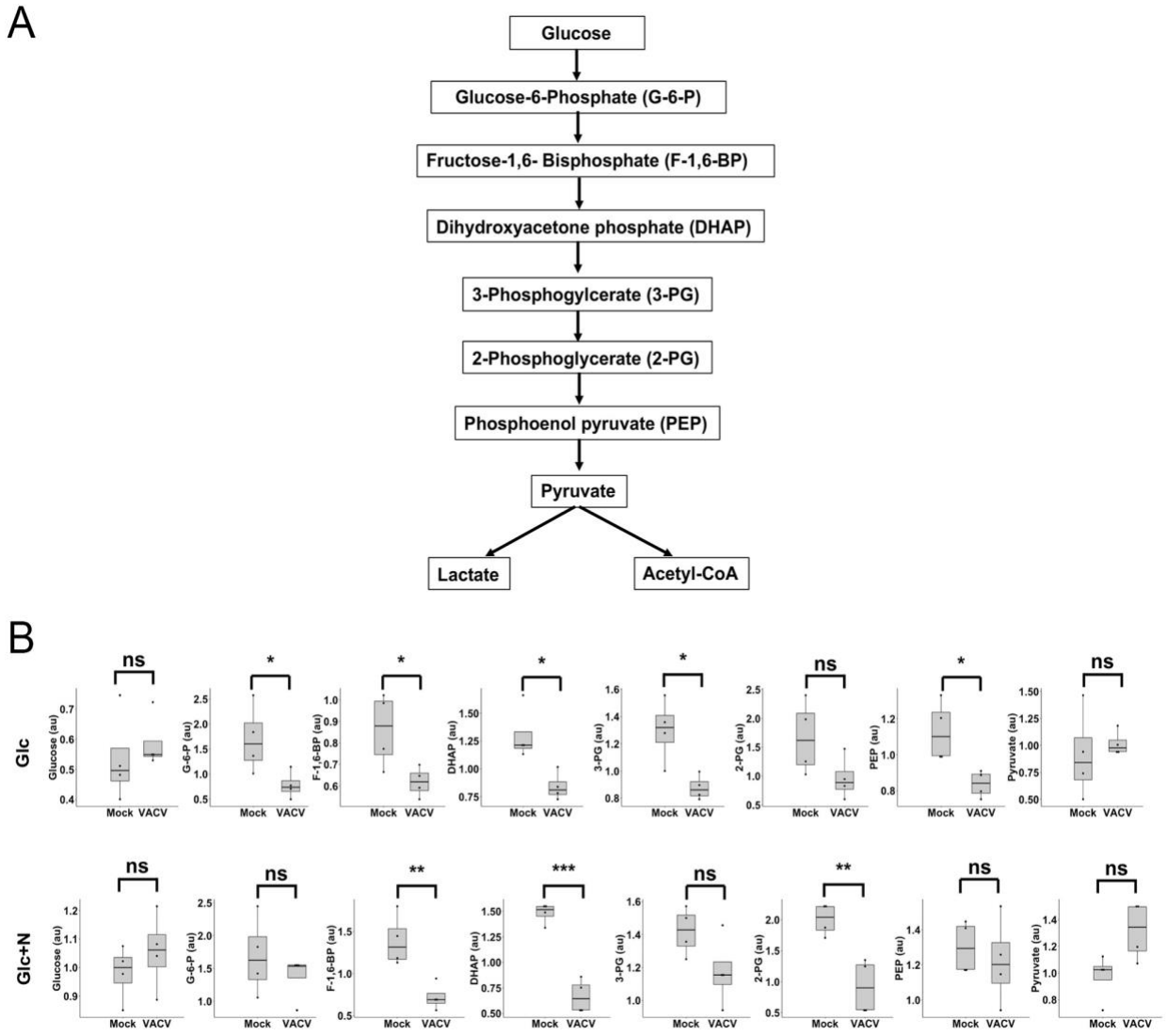

Figure S 3.4. Effect of VACV infection on glycolytic intermediate levels at 16 hpi.

(A) Outline of glycolysis pathway. Glucose after a series of reactions is converted into pyruvate, which can then either be converted to lactate under anaerobic conditions or to acetyl coenzyme A under aerobic conditions. (B) The glycolysis intermediates are either unaffected or reduced during VACV infection. The levels of glycolysis intermediates in HFFs infected with MOI-3 of WT-VACV in media with glucose (Glc) or glucose plus asparagine (Glc+N) at 16 hpi as determined by global metabolic profiling in Fig. 3.1A. ns, $P > 0.05$; *, $P \leq 0.05$; **, $P \leq 0.01$; ***, $P \leq 0.001$.

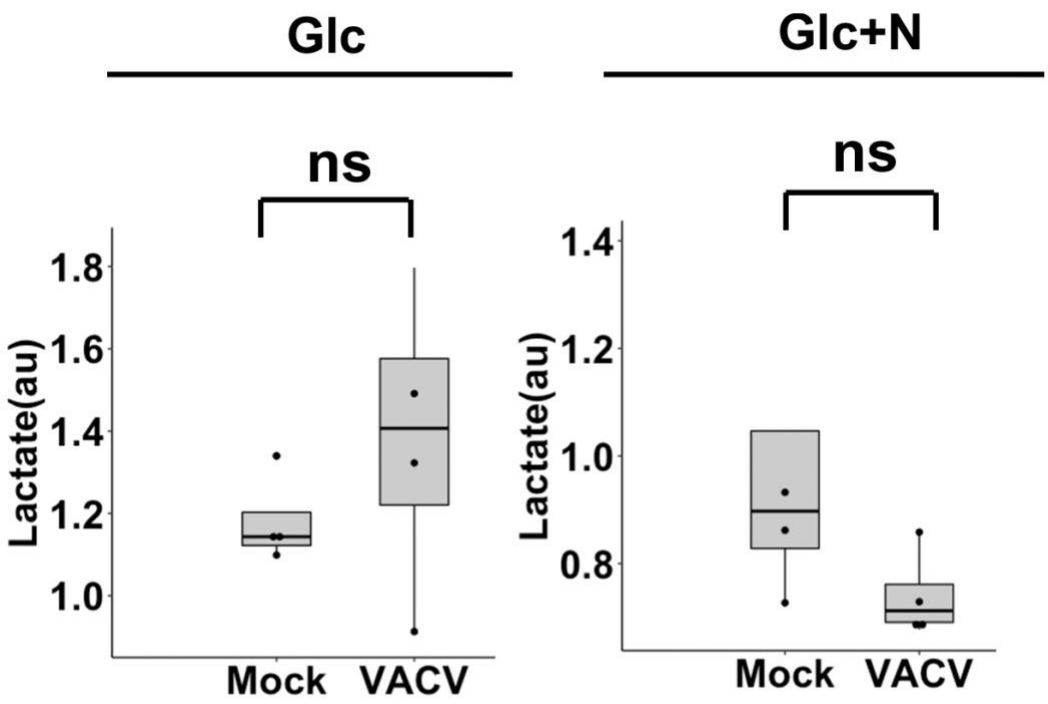

Figure S 3.5. Levels of lactate upon VACV infection at 16 hpi.

VACV infection does not significantly affect the level of lactate. The level of lactate in HFFs infected with MOI=3 of WT-VACV in media with glucose (Glc) or glucose plus asparagine (Glc+N) at 8 hpi was determined by global metabolic profiling in Fig. 3.1A. Error bars represent the standard deviation of four biological replicates. ns, $P > 0.05$.

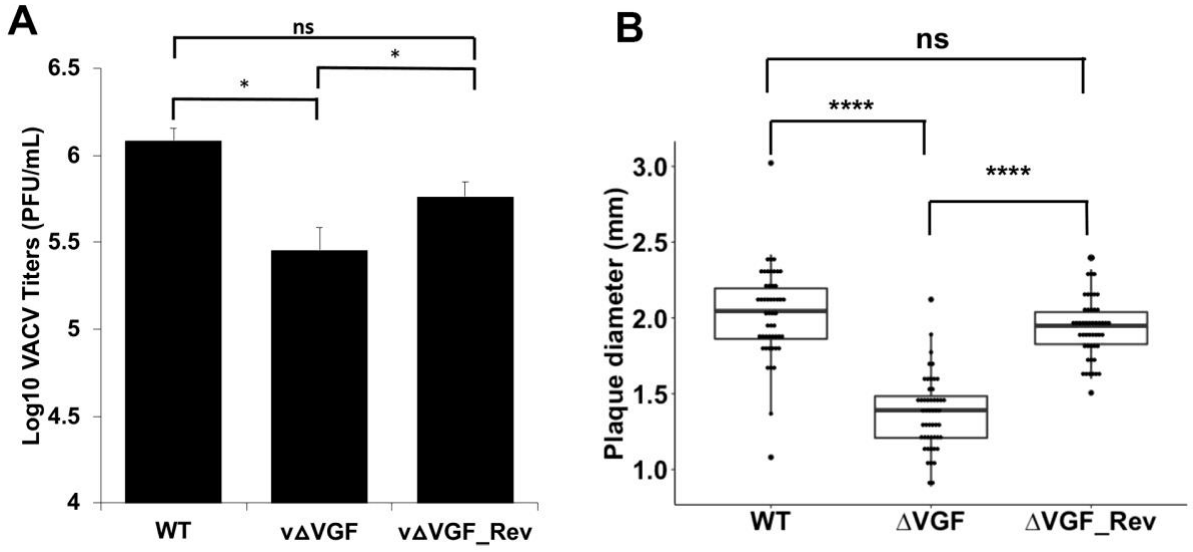

Figure S 3.6. Effect of deletion of VGF on VACV titers and plaque size.

(A) VGF deletion reduces VACV replication in HFFs. HFFs infected with indicated viruses at MOI of 0.001 in medium with glucose plus glutamine with 0.001% dialyzed FBS. Virus titers measured at 72 hpi using a plaque assay. (B) VGF deletion decreases plaque size. The virus samples acquired from S6 Fig (A) were used to infect a confluent monolayer of BS-C-1 cells for 48 h. The diameters of 50 plaques from each treatment were measured and analyzed as described in the methods section. Error bars represent the standard deviation of at least three biological replicates in (A) and 50 plaques in (B). ns, $P > 0.05$; *, $P \leq 0.05$; ****, $P \leq 0.0001$.

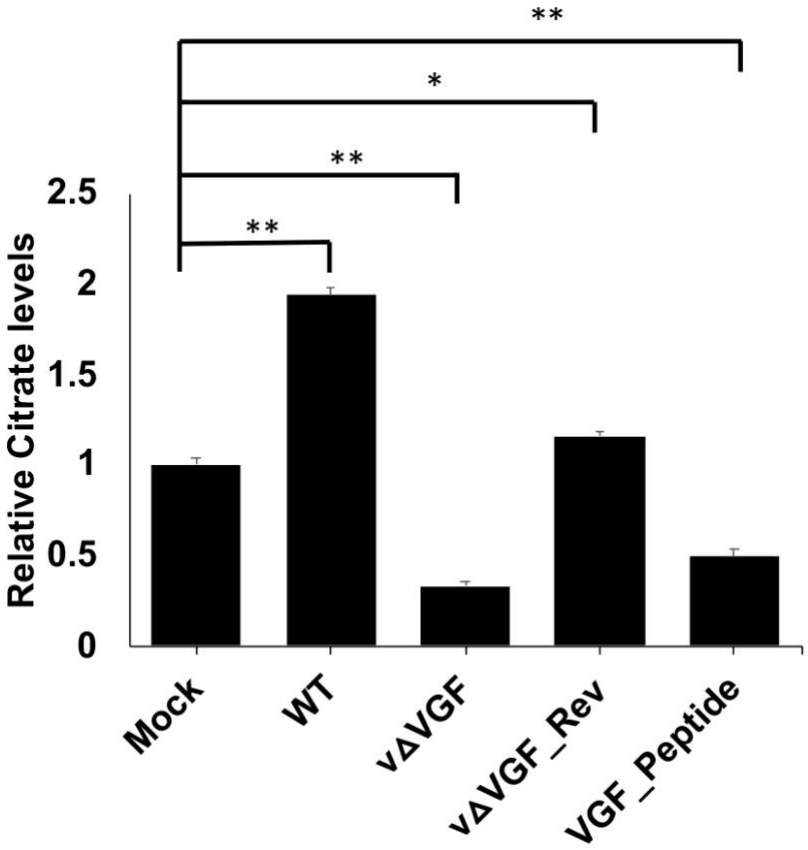

Figure S 3.7. Effect of treatment of synthetic VGF peptide on citrate levels.

A synthetic VGF peptide alone did not enhance the levels of citrate in HFFs. HFFs were either mock-infected, infected with indicated viruses at an MOI of 5 or treated with 2500 ng/mL of a synthetic VGF peptide. After 4 h of treatment, citrate levels in the samples were measured by a citrate assay kit. Error bars represent the standard deviation of at least three biological replicates. *, $P \leq 0.05$; **, $P \leq 0.01$.

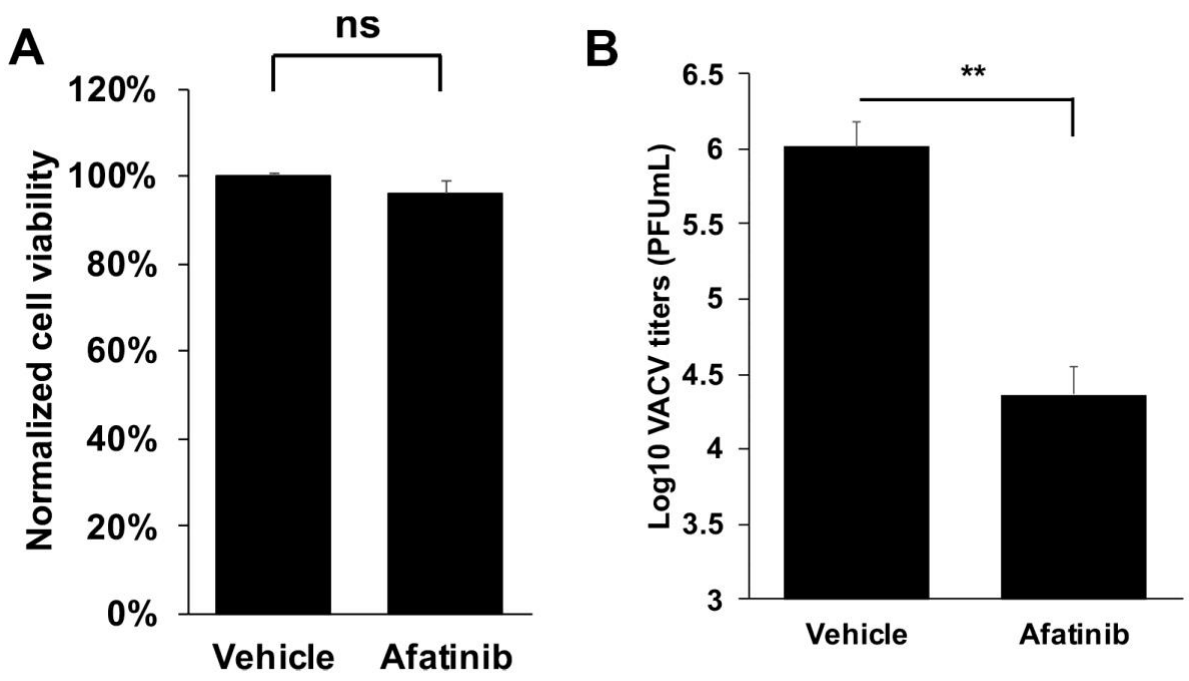

Figure S 3.8. EGFR inhibitor suppresses VACV replication.

(A) HFFs were grown in the presence or absence of 3 µM afatinib for 24 h. Cell viability was measured using a trypan blue exclusion assay. (B) Inhibition of the EGFR pathway reduces VACV titers. HFFs were infected with VACV at an MOI of 2 in the presence or absence of 3 µM afatinib for 24 h. Virus titers were measured using a plaque assay. Error bars represent the standard deviation of at least three biological replicates. ns, $P > 0.05$; **, $P \leq 0.01$.

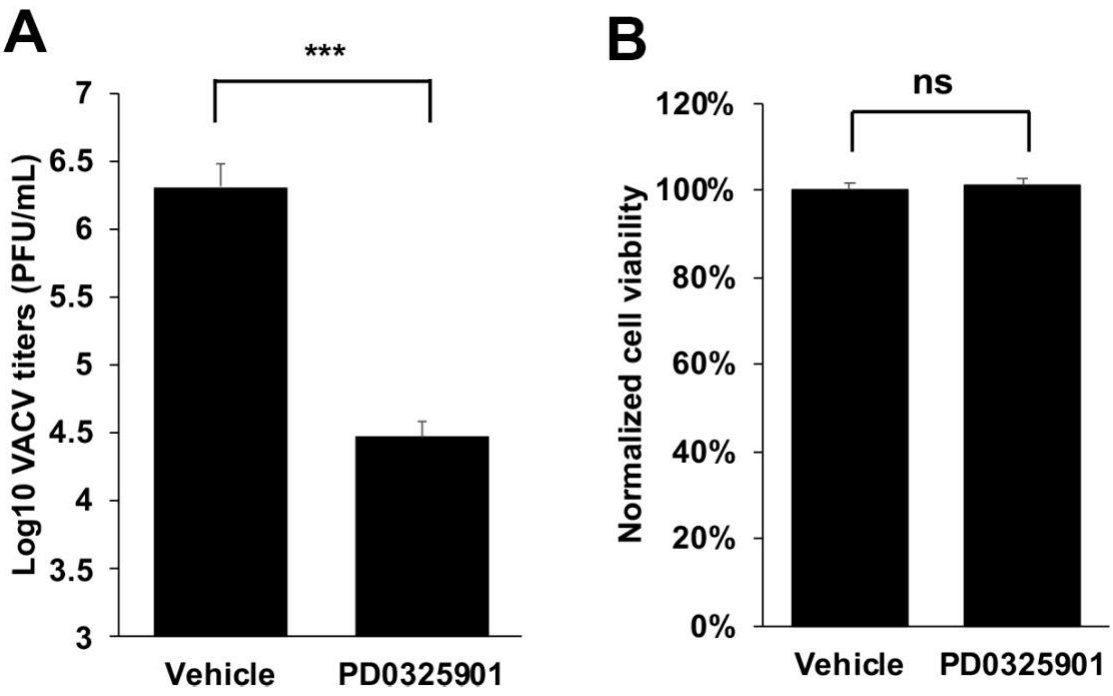

Figure S 3.9. MAPK pathway inhibitor suppresses VACV replication.

(A) Inhibition of the MAPK pathway suppresses VACV replication. HFFs were infected with VACV at an MOI of 2 in the presence or absence of 50 µM PD0325901 for 24 h. A plaque assay was performed to measure virus titers. (B) Inhibition of the MAPK pathway does not decrease HFF viability. HFFs were grown in for 24 h in the presence or absence of 50 µM PD0325901. Cell viability was determined using a trypan blue exclusion assay. Error bars represent the standard deviation of at least three biological replicates. ns, $P > 0.05$; ***, $P \leq 0.001$.

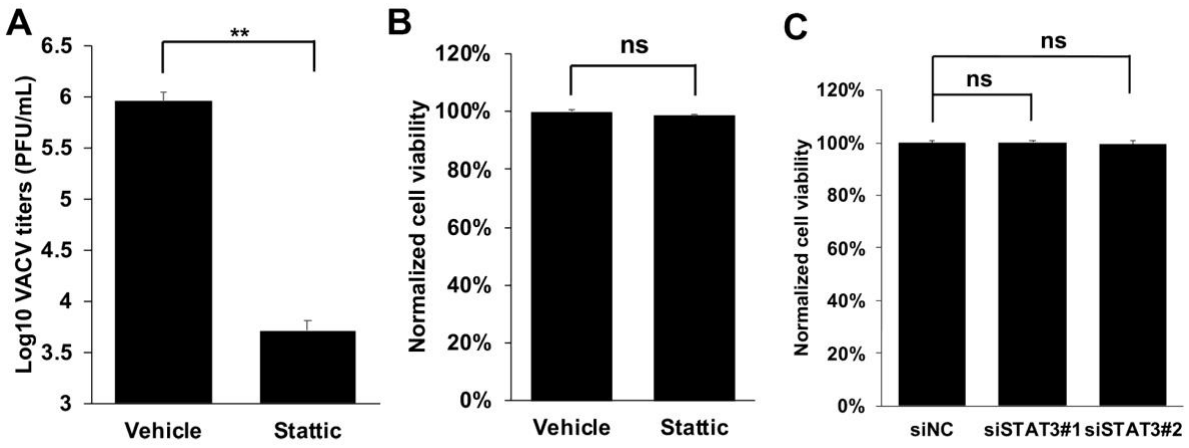

Figure S 3.10. STAT3 inhibitor suppresses VACV replication.

(A) Inhibition of the STAT3 pathway suppresses VACV replication. HFFs were infected with WT VACV at an MOI of 2 in the presence or absence of 3 µM stattic for 24 h. VACV titers were measured using a plaque assay. (B) HFFs were grown in the presence or absence of 3 µM stattic for 24 h. Cell viability was determined using a trypan blue exclusion assay. (C) STAT3 knockdown does not affect HFF viability. HFFs were transfected with indicated siRNAs for 72h, and a trypan blue exclusion assay was performed to determine the cell viability. Error bars represent the standard deviation of at least three biological replicates. ns, $P > 0.05$; **, $P \leq 0.01$.

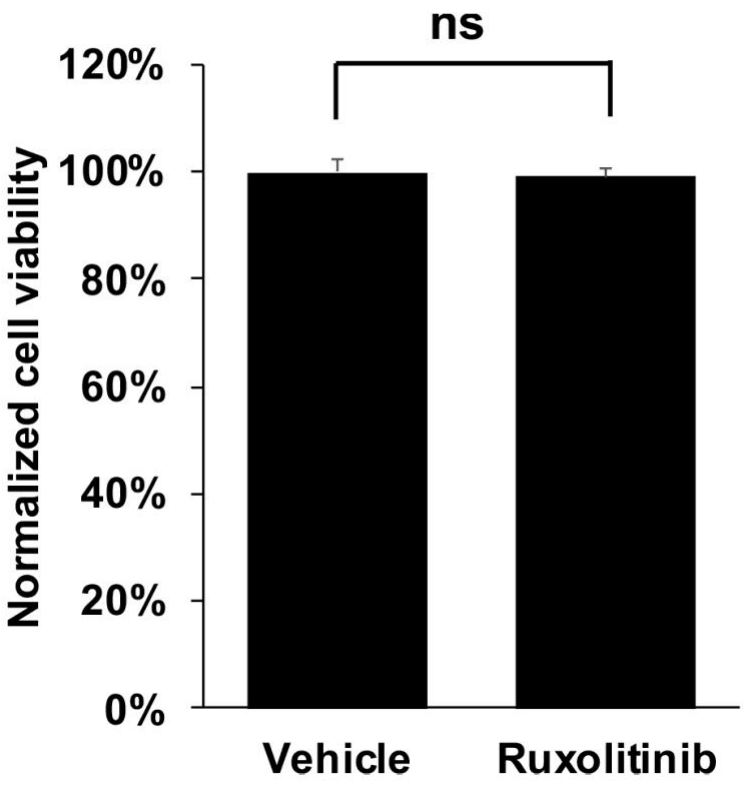

Figure S 3.11. Inhibition of JAK 1/2 pathway has minimal effect on HFF viability. Inhibition of the JAK1/2 pathway does not alter HFF viability. HFFs were grown in the presence or absence of 50 µM ruxolitinib for 24 h. Cell viability was determined by a trypan blue exclusion assay using a hemocytometer. All experiments were performed in media with glucose plus glutamine. Error bars represent the standard deviation of at least three biological replicates. ns, $P > 0.05$.

Table 3.1. The number of metabolites significantly different upon VACV infection in medium with glucose or glucose plus asparagine.

The numbers approaching a significant difference are also shown in the lower two rows. The red upward arrows indicate increase and the green downwards arrows indicate decrease in indicated conditions.

	Infected/Uninfected			
	8h		**16h**	
	Glc	**Glc+N**	**Glc**	**Glc+N**
Total Biochemicals $p \leq 0.05$	220	173	145	190
Biochemicals ↑ ↓	156 | 64	109 | 64	95 | 50	51 | 139
Total Biochemicals $0.05 < p < 0.10$	43	37	44	56
Biochemicals ↑ ↓	14 | 29	19 | 18	26 |18	11 | 45

Table 3.2. The number of metabolites significantly different upon VACV infection in medium with glucose or glucose plus asparagine.

Numbers in boldface indicate p≤0.05 (boldface number greater than one indicates that the mean values are significantly higher for that comparison; boldface number lower than one significantly lower).

Super Pathway	Sub Pathway	Biochemical Name	Glc 8h	Glc+N 8h	Glc 16h	Glc+N 16h
Amino Acid	Glycine, Serine and Threonine Metabolism	glycine	**2.82**	**1.79**	**1.57**	0.79
		N-acetylglycine	**1.86**	1.17	1.04	**0.67**
		betaine	**3.49**	**1.59**	1.26	1.06
		serine	**2.41**	**1.48**	**1.61**	0.94
		N-acetylserine	**2.04**	**1.61**	1.07	**0.69**
		threonine	**2.66**	**1.64**	**1.63**	0.80
		N-acetylthreonine	**2.25**	**1.78**	1.09	**0.75**
		homoserine lactone	**2.35**	**2.39**	**3.16**	**1.46**
	Alanine and Aspartate Metabolism	alanine	1.05	1.33	1.29	1.08
		N-acetylalanine	**2.63**	**2.13**	1.24	0.92
		aspartate	**1.31**	1.23	**2.30**	**1.55**
		N-acetylaspartate (NAA)	**1.64**	**1.34**	1.10	**0.75**
		asparagine	1.15	1.36	**0.53**	0.80
		N-acetylasparagine	**2.18**	**1.31**	0.80	**0.57**
	Glutamate Metabolism	glutamate	**3.65**	**3.50**	**4.45**	**2.49**
		glutamine	**1.49**	1.21	**1.68**	1.13
		alpha-ketoglutaramate*	1.00	1.23	**0.28**	**0.29**
		N-acetylglutamate	**1.79**	**1.88**	1.02	**0.63**
		N-acetylglutamine	**1.90**	**1.68**	1.06	**0.65**
		gamma-carboxyglutamate	**2.18**	**1.43**	0.87	**0.44**

		glutamate, gamma-methyl ester	**2.44**	**2.07**	0.99	1.10
		pyroglutamine*	**1.76**	**2.18**	**1.84**	0.91
		N-acetyl-aspartyl-glutamate (NAAG)	**1.52**	1.40	0.77	**0.42**
		beta-citrylglutamate	1.21	1.04	0.90	**0.58**
		carboxyethyl-GABA	**2.70**	**0.18**	**0.05**	**0.05**
		N-methyl-GABA	**1.68**	1.32	**2.35**	1.24
		S-1-pyrroline-5-carboxylate	**2.61**	1.10	**2.11**	**2.42**
	Histidine Metabolism	histidine	**1.92**	1.06	**1.45**	**0.72**
		N-acetylhistidine	1.45	1.00	0.88	0.76
		imidazole propionate	1.00	**3.55**	1.00	0.85
		imidazole lactate	**3.55**	**3.65**	**2.08**	**0.70**
		carnosine	**2.05**	**1.57**	1.21	**0.62**
		4-imidazoleacetate	**2.90**	**1.85**	**1.26**	1.15
	Lysine Metabolism	lysine	**1.33**	0.99	1.11	0.85
		N6,N6,N6-trimethyllysine	**2.03**	**1.81**	0.86	**0.60**
		5-(galactosylhydroxy)-L-lysine	0.86	0.86	**0.50**	0.75
		saccharopine	**2.76**	**4.15**	1.48	1.03
		2-aminoadipate	**6.56**	**5.04**	**12.2**	**5.31**
		pipecolate	**3.86**	**3.19**	**1.75**	**0.69**
		6-oxopiperidine-2-carboxylate	**1.87**	0.82	**1.90**	1.19
		5-aminovalerate	**3.97**	**2.53**	**2.10**	1.04
		N,N,N-trimethyl-5-aminovalerate	**2.08**	**1.48**	**1.59**	0.78
	Phenylalanine Metabolism	phenylalanine	**1.78**	1.17	**1.33**	0.80
		N-acetylphenylalanine	**1.97**	0.59	**0.33**	0.62
		1-carboxyethylphenylalanine	**5.92**	**4.17**	**1.86**	1.49
		phenyllactate (PLA)	**2.66**	**2.27**	1.00	**0.63**
	Tyrosine Metabolism	tyrosine	**2.00**	1.26	**1.46**	**0.78**
		4-hydroxyphenylpyruvate	0.85	0.85	1.00	0.91

		3-(4-hydroxyphenyl)lactate	**3.40**	**2.84**	**1.77**	**0.65**
		O-methyltyrosine	0.75	0.63	**0.63**	**0.33**
		N-formylphenylalanine	1.14	**0.57**	**0.49**	0.88
	Tryptophan Metabolism	tryptophan	**1.86**	1.20	**1.36**	**0.78**
		C-glycosyltryptophan	1.12	0.84	**0.66**	**0.42**
		kynurenine	**1.78**	1.20	1.21	**0.78**
		indolelactate	**3.41**	**1.99**	**1.69**	**0.54**
	Leucine, Isoleucine and Valine Metabolism	leucine	**1.67**	1.10	**1.25**	**0.79**
		4-methyl-2-oxopentanoate	1.08	1.02	**1.64**	0.95
		isovalerylcarnitine (C5)	**2.27**	1.34	**1.36**	**0.60**
		beta-hydroxyisovalerate	1.11	0.61	0.87	**0.31**
		isoleucine	**1.48**	1.00	1.16	**0.79**
		N-acetylisoleucine	1.10	0.67	0.60	**2.16**
		3-methyl-2-oxovalerate	1.03	0.95	1.32	0.98
		2-methylbutyrylcarnitine (C5)	**1.68**	**1.90**	1.19	**0.75**
		methylsuccinate	1.24	0.79	0.79	**1.70**
		valine	**1.85**	1.15	1.16	0.82
		1-carboxyethylvaline	**5.01**	**3.92**	**2.51**	0.96
		3-methyl-2-oxobutyrate	1.16	0.98	1.40	0.89
		isobutyrylcarnitine (C4)	**1.81**	**1.82**	1.26	0.88
	Methionine, Cysteine, SAM and Taurine Metabolism	methionine	**2.29**	1.27	**1.24**	0.81
		N-acetylmethionine	**2.50**	**2.64**	1.19	0.81
		N-formylmethionine	**3.72**	**3.59**	**2.51**	**1.69**
		methionine sulfone	1.00	1.01	**1.29**	1.00
		methionine sulfoxide	**1.43**	1.14	**1.35**	0.87
		N-acetylmethionine sulfoxide	1.12	**1.41**	0.95	0.71
		S-adenosylmethionine (SAM)	**2.22**	**2.91**	**3.29**	**1.64**
		S-adenosylhomocysteine (SAH)	**3.21**	**2.45**	0.90	0.73

		homocysteine	**2.03**	**2.84**	1.67	0.52
		cystathionine	**4.57**	**5.93**	**12.3**	**4.55**
		cysteine	**1.61**	**1.81**	1.37	0.87
		N-acetylcysteine	**1.53**	1.14	**0.49**	1.13
		cystine	**0.11**	**0.21**	**0.36**	0.74
		lanthionine	1.65	**3.00**	**3.37**	**2.18**
		hypotaurine	**5.39**	**4.10**	**3.16**	1.20
		taurine	**5.28**	**3.47**	**2.44**	1.10
		N-acetyltaurine	**2.29**	**1.61**	**1.49**	1.20
		3-sulfo-L-alanine	1.29	1.31	1.37	1.00
	Urea cycle; Arginine and Proline Metabolism	arginine	**1.35**	0.95	1.12	0.82
		argininosuccinate	**2.10**	1.39	**4.24**	1.67
		ornithine	1.14	1.08	**1.34**	1.12
		2-oxoarginine*	**0.54**	**0.51**	**0.56**	**0.61**
		citrulline	**2.94**	**1.75**	**5.69**	**2.64**
		proline	**2.38**	**2.46**	**1.91**	**1.51**
		dimethylarginine (SDMA + ADMA)	0.92	1.15	**0.58**	**0.44**
		trans-4-hydroxyproline	**1.63**	**1.40**	1.06	0.79
		pro-hydroxy-pro	1.18	1.31	**0.35**	**0.25**
	Creatine Metabolism	creatine	**1.42**	**1.62**	**1.38**	0.86
		creatinine	**2.31**	**1.61**	1.27	0.83
		creatine phosphate	**2.80**	**1.87**	1.31	**0.66**
	Polyamine Metabolism	putrescine	0.80	1.56	**1.99**	0.68
		spermidine	**1.76**	1.38	0.80	**0.48**
		5-methylthioadenosine (MTA)	**2.65**	**2.50**	**2.85**	**1.97**
		N-acetylputrescine	**1.91**	**4.42**	**2.04**	1.01
		(N(1) + N(8))-acetylspermidine	**4.78**	**11.18**	1.57	**1.85**

	Guanidino and Acetamido Metabolism	4-guanidinobutanoate	**3.08**	1.01	1.17	**0.43**
	Glutathione Metabolism	glutathione, reduced (GSH)	**7.56**	**19.27**	**12.3**	**2.33**
		glutathione, oxidized (GSSG)	**2.66**	**3.38**	**2.93**	**1.91**
		cysteine-glutathione disulfide	**0.61**	**0.76**	0.97	1.20
		S-methylglutathione	**103.5**	**37.56**	**20.5**	**2.48**
		S-lactoylglutathione	2.49	12.49	1.88	0.40
		cysteinylglycine	**1.23**	**8.55**	2.03	1.86
		5-oxoproline	0.91	0.84	**0.52**	**0.52**
Peptide	Gamma-glutamyl Amino Acid	gamma-glutamylalanine	1.11	**1.54**	**0.49**	**0.48**
		gamma-glutamylcysteine	**3.00**	5.77	**5.32**	1.07
		gamma-glutamylglutamate	**1.97**	**1.70**	**2.05**	**1.72**
		gamma-glutamylglutamine	**0.19**	1.00	1.00	1.00
		gamma-glutamylisoleucine*	**2.00**	**1.82**	1.07	**0.66**
		gamma-glutamyl-epsilon-lysine	0.78	0.97	0.83	0.77
		gamma-glutamylthreonine	1.21	**2.33**	**1.65**	0.76
		gamma-glutamylvaline	**1.58**	**1.54**	0.88	**0.60**
		gamma-glutamyl-2-aminobutyrate	**1.51**	**1.55**	**0.60**	**0.27**
	Dipeptide	leucylglycine	**0.23**	1.27	0.65	**0.29**
		phenylalanylglycine	0.33	0.98	**0.43**	**0.33**
	Acetylated Peptides	phenylacetylglycine	**1.84**	**1.51**	1.04	1.11
Carbohydrate	Glycolysis, Gluconeogenesis, and Pyruvate Metabolism	glucose	1.11	0.85	1.06	0.88
		glucose 6-phosphate	1.18	0.96	**0.44**	0.64
		fructose 1,6-diphosphate/glucose 1,6-diphosphate/myo-inositol diphosphates	0.98	0.89	**0.69**	**0.41**
		dihydroxyacetone phosphate (DHAP)	0.84	0.79	**0.63**	**0.36**
		2-phosphoglycerate	**1.25**	0.42	0.56	**0.35**
		3-phosphoglycerate	**0.47**	**0.58**	**0.65**	**0.66**

		phosphoenolpyruvate (PEP)	**0.53**	**0.51**	**0.71**	0.75
		pyruvate	0.92	0.87	1.07	1.09
		lactate	0.85	0.87	**0.73**	**0.74**
		glycerate	1.09	**0.43**	**0.48**	**0.45**
	Pentose Phosphate Pathway	6-phosphogluconate	0.81	0.79	0.97	0.83
		sedoheptulose-7-phosphate	**1.92**	1.75	0.80	**0.25**
	Pentose Metabolism	ribitol	**10.54**	**5.51**	**2.68**	**0.51**
		ribonate	**3.50**	1.32	0.81	**0.47**
		arabitol/xylitol	**3.90**	**1.90**	1.00	1.00
		arabonate/xylonate	2.63	0.61	**0.18**	**0.19**
		ribulonate/xylulonate*	1.24	0.89	1.18	0.88
	Glycogen Metabolism	maltotetraose	0.66	**0.34**	**0.24**	**0.27**
	Disaccharides and Oligosaccharides	sucrose	**255.7**	**6.24**	**2.52**	**5.41**
	Fructose, Mannose and Galactose Metabolism	fructose	**1.64**	1.14	**0.63**	**0.47**
		mannitol/sorbitol	**2.99**	**1.65**	0.85	**0.40**
		mannose	0.83	0.85	**0.42**	**0.53**
		galactonate	**5.53**	**1.98**	1.62	**0.37**
	Nucleotide Sugar	UDP-glucose	1.24	1.23	0.97	**0.52**
		UDP-galactose	1.33	1.21	1.03	**0.59**
		UDP-glucuronate	**1.59**	**0.48**	0.61	**0.22**
		guanosine 5'-diphospho-fucose	1.04	0.72	0.96	**0.53**
		UDP-N-acetylglucosamine/galactosamine	1.19	1.22	1.04	**0.53**
		cytidine 5'-monophospho-N-acetylneuraminic acid	**1.98**	**2.63**	1.89	**3.02**
	Aminosugar Metabolism	glucuronate	**2.52**	1.22	0.71	**0.39**
		N-acetylneuraminate	1.16	1.08	1.15	1.08
		N-acetylglucosaminylasparagine	**2.17**	**1.71**	1.15	**0.66**

		erythronate*	**4.45**	**1.68**	**1.72**	1.00
		N-acetylglucosamine/N-acetylgalactosamine	0.75	0.95	1.08	0.88
Energy	TCA Cycle	citrate	**2.74**	**1.67**	**2.03**	**1.71**
		aconitate [cis or trans]	**3.35**	**1.74**	**1.97**	**1.83**
		alpha-ketoglutarate	**3.80**	**2.23**	**2.54**	1.35
		succinate	1.24	0.82	1.29	0.86
		fumarate	**1.48**	**1.77**	**2.04**	**1.65**
		malate	**1.85**	**2.26**	**2.08**	**1.63**
		2-methylcitrate/homocitrate	0.96	1.11	0.99	0.94
	Oxidative Phosphorylation	phosphate	0.99	**0.79**	0.94	0.86
Lipid	Fatty Acid Metabolism	acetyl CoA	**0.19**	**0.26**	**0.28**	**0.20**
	Medium Chain Fatty Acid	caprylate (8:0)	1.63	**0.16**	**0.12**	**0.21**
		pelargonate (9:0)	0.77	1.04	0.77	1.27
		caprate (10:0)	0.71	**0.41**	**0.63**	1.00
		laurate (12:0)	0.82	**0.35**	**0.40**	1.01
	Long Chain Fatty Acid	palmitate (16:0)	**0.72**	**0.64**	0.85	0.78
		stearate (18:0)	**0.68**	**0.56**	0.99	0.78
		nonadecanoate (19:0)	**0.60**	**0.55**	0.96	**0.68**
		10-nonadecenoate (19:1n9)	**0.56**	0.70	1.08	1.01
		arachidate (20:0)	**0.68**	**0.60**	1.08	0.80
		eicosenoate (20:1)	**0.55**	**0.59**	1.01	0.82
		behenate (22:0)*	**0.60**	**0.41**	0.92	**0.51**
		erucate (22:1n9)	**0.60**	**0.58**	0.86	**0.53**
		nervonate (24:1n9)*	**0.43**	**0.43**	0.68	**0.44**
	Polyunsaturated Fatty Acid (n3 and n6)	docosapentaenoate (n3 DPA; 22:5n3)	0.83	1.45	**0.40**	1.02
		docosahexaenoate (DHA; 22:6n3)	0.65	0.62	0.72	0.94
		arachidonate (20:4n6)	0.64	0.90	**1.49**	**1.72**

		docosadienoate (22:2n6)	**0.45**	0.64	0.87	0.79
		dihomo-linoleate (20:2n6)	**0.50**	**0.63**	1.13	0.91
		mead acid (20:3n9)	0.59	0.85	1.62	0.88
		docosatrienoate (22:3n6)*	0.86	0.93	0.75	0.91
	Fatty Acid, Dicarboxylate	glutarate (C5-DC)	**2.81**	**2.00**	**2.12**	**1.47**
		2-hydroxyglutarate	**2.50**	**2.22**	**2.32**	**1.57**
		2-hydroxyadipate	**4.08**	**1.64**	**6.96**	**4.29**
		maleate	1.26	**0.29**	**0.35**	0.67
	Fatty Acid Metabolism (also BCAA Metabolism)	butyrylcarnitine (C4)	**2.60**	1.60	1.38	**0.27**
		propionyl CoA	**0.11**	**0.10**	**0.06**	**0.07**
		propionylcarnitine (C3)	**1.45**	**1.89**	1.02	**0.59**
		methylmalonate (MMA)	0.89	0.75	0.81	0.65
	Fatty Acid Metabolism(Acyl Carnitine)	acetylcarnitine (C2)	**3.80**	**1.53**	1.36	1.27
		myristoylcarnitine (C14)	**2.65**	**1.95**	1.09	1.09
		palmitoylcarnitine (C16)	**2.45**	**2.51**	**1.52**	1.10
		palmitoleoylcarnitine (C16:1)*	**2.96**	**2.62**	1.29	**1.43**
		stearoylcarnitine (C18)	**1.61**	**1.30**	**1.42**	**1.31**
		linoleoylcarnitine (C18:2)*	**3.61**	**4.07**	**2.86**	**4.87**
		oleoylcarnitine (C18:1)	**2.85**	**3.29**	**2.59**	**1.98**
		margaroylcarnitine (C17)*	**1.77**	**1.90**	1.22	**1.63**
	Carnitine Metabolism	deoxycarnitine	**2.84**	**1.98**	**1.57**	0.92
		carnitine	1.24	**1.67**	**1.33**	0.83
	Endocannabinoid	N-oleoyltaurine	1.11	1.78	**3.25**	**3.45**
		N-stearoyltaurine	0.83	1.24	**2.20**	**2.12**
		palmitoleoyl ethanolamide*	1.20	**2.49**	**9.59**	**28.64**
	Inositol Metabolism	myo-inositol	**2.95**	**2.11**	**2.36**	1.14
	Phospholipid Metabolism	choline	**2.20**	1.23	1.20	0.85
		choline phosphate	**1.39**	1.06	0.83	**0.49**

		cytidine 5'-diphosphocholine	**6.22**	**5.94**	**3.35**	1.66
		glycerophosphorylcholine (GPC)	**1.53**	**1.55**	1.10	1.16
		phosphoethanolamine	**7.04**	1.00	**2.31**	0.91
		cytidine-5'-diphosphoethanolamine	**4.20**	1.67	**1.85**	0.56
		glycerophosphoethanolamine	**2.19**	**1.75**	0.85	**0.69**
		glycerophosphoinositol*	**1.94**	1.12	0.74	**0.51**
		trimethylamine N-oxide	**0.81**	**0.74**	0.96	0.84
	Phosphatidylcholine (PC)	1-myristoyl-2-palmitoyl-GPC (14:0/16:0)	**0.72**	**0.70**	0.98	**0.58**
		1-myristoyl-2-arachidonoyl-GPC (14:0/20:4)*	0.97	0.93	0.93	0.77
		1,2-dipalmitoyl-GPC (16:0/16:0)	**0.56**	**0.54**	1.00	**0.53**
		1-palmitoyl-2-palmitoleoyl-GPC (16:0/16:1)*	0.79	**0.75**	0.98	**0.64**
		1-palmitoyl-2-stearoyl-GPC (16:0/18:0)	**0.52**	**0.60**	1.39	0.67
		1-palmitoyl-2-oleoyl-GPC (16:0/18:1)	0.78	0.79	1.05	**0.74**
		1-palmitoyl-2-gamma-linolenoyl-GPC (16:0/18:3n6)*	0.89	0.91	0.88	**0.73**
		1-palmitoyl-2-arachidonoyl-GPC (16:0/20:4n6)	0.85	0.84	0.95	**0.71**
		1-palmitoyl-2-docosahexaenoyl-GPC (16:0/22:6)	1.01	1.01	1.22	0.85
		1-stearoyl-2-oleoyl-GPC (18:0/18:1)	0.70	0.76	1.12	0.66
		1-stearoyl-2-arachidonoyl-GPC (18:0/20:4)	0.89	0.81	1.07	0.72
		1-stearoyl-2-docosahexaenoyl-GPC (18:0/22:6)	0.89	0.86	1.17	0.71
		1,2-dioleoyl-GPC (18:1/18:1)	0.79	0.80	1.01	**0.74**
		1-oleoyl-2-linoleoyl-GPC (18:1/18:2)*	0.83	**0.72**	0.98	0.90
		1-oleoyl-2-docosahexaenoyl-GPC (18:1/22:6)*	0.95	0.92	0.98	0.81

		1,2-dilinoleoyl-GPC (18:2/18:2)	0.82	0.84	0.99	0.97
	Phosphatidylethanolamine (PE)	1,2-dipalmitoyl-GPE (16:0/16:0)*	**0.48**	**0.44**	**1.54**	**0.46**
		1-palmitoyl-2-oleoyl-GPE (16:0/18:1)	**0.53**	**0.54**	1.03	**0.52**
		1-palmitoyl-2-arachidonoyl-GPE (16:0/20:4)*	**0.58**	**0.60**	**0.67**	**0.51**
		1-palmitoyl-2-docosahexaenoyl-GPE (16:0/22:6)*	**0.67**	**0.48**	0.94	**0.62**
		1-palmitoleoyl-2-oleoyl-GPE (16:1/18:1)*	**0.57**	**0.62**	0.88	**0.53**
		1-stearoyl-2-oleoyl-GPE (18:0/18:1)	**0.48**	**0.49**	0.93	**0.45**
		1-stearoyl-2-arachidonoyl-GPE (18:0/20:4)	**0.58**	**0.58**	0.94	**0.54**
		1,2-dioleoyl-GPE (18:1/18:1)	**0.54**	**0.59**	0.89	**0.56**
		1-oleoyl-2-linoleoyl-GPE (18:1/18:2)*	**0.61**	**0.57**	0.81	**0.61**
		1-oleoyl-2-arachidonoyl-GPE (18:1/20:4)*	**0.55**	**0.64**	0.69	**0.54**
		1-oleoyl-2-docosahexaenoyl-GPE (18:1/22:6)*	**0.65**	**0.70**	0.87	**0.71**
	Phosphatidylserine (PS)	1-palmitoyl-2-oleoyl-GPS (16:0/18:1)	**0.51**	**0.41**	0.79	**0.46**
		1-stearoyl-2-oleoyl-GPS (18:0/18:1)	**0.53**	**0.45**	0.85	**0.43**
		1-stearoyl-2-arachidonoyl-GPS (18:0/20:4)	**0.57**	**0.53**	0.96	**0.66**
	Phosphatidylinositol (PI)	1,2-dioleoyl-GPI (18:1/18:1)	**0.37**	0.56	1.85	0.44
		1-stearoyl-2-arachidonoyl-GPI (18:0/20:4)	**0.54**	**0.63**	1.08	0.70
		1-oleoyl-2-arachidonoyl-GPI (18:1/20:4) *	0.60	0.70	1.42	0.56
	Lysophospholipid	1-palmitoyl-GPC (16:0)	0.76	**0.70**	**0.44**	**0.54**
		2-palmitoyl-GPC (16:0)*	**0.57**	**0.65**	**0.75**	**0.60**
		1-palmitoleoyl-GPC (16:1)*	**0.75**	0.86	1.31	1.07
		1-stearoyl-GPC (18:0)	0.82	**0.64**	**0.33**	**0.27**

		1-oleoyl-GPC (18:1)	0.79	0.89	0.96	1.27
		1-linoleoyl-GPC (18:2)	0.93	0.80	0.81	**1.64**
		1-arachidonoyl-GPC (20:4n6)*	0.86	0.84	1.43	**3.44**
		1-palmitoyl-GPE (16:0)	0.71	0.77	1.15	**0.45**
		1-stearoyl-GPE (18:0)	**0.72**	0.74	**0.52**	**0.39**
		1-oleoyl-GPE (18:1)	**0.58**	**0.53**	1.15	**0.61**
		1-arachidonoyl-GPE (20:4n6)*	**0.53**	**0.54**	1.00	**0.52**
		1-palmitoyl-GPS (16:0)*	**0.50**	**0.43**	**0.57**	0.75
		1-stearoyl-GPS (18:0)*	**0.63**	**0.70**	**0.61**	**0.41**
		1-oleoyl-GPS (18:1)	**0.57**	**0.57**	0.80	0.92
		1-palmitoyl-GPI (16:0)	**0.67**	**0.70**	0.74	0.72
		1-stearoyl-GPI (18:0)	0.89	1.47	0.68	0.73
		1-oleoyl-GPI (18:1)*	0.67	0.80	**0.67**	1.25
		1-arachidonoyl-GPI (20:4)*	**0.61**	**0.43**	1.14	**8.54**
	Plasmalogen	1-(1-enyl-palmitoyl)-2-oleoyl-GPE (P-16:0/18:1)*	**0.58**	**0.55**	1.05	**0.52**
		1-(1-enyl-palmitoyl)-2-palmitoyl-GPC (P-16:0/16:0)*	0.74	0.79	**1.60**	0.74
		1-(1-enyl-palmitoyl)-2-palmitoleoyl-GPC (P-16:0/16:1)*	1.48	1.16	**1.73**	0.93
		1-(1-enyl-palmitoyl)-2-arachidonoyl-GPE (P-16:0/20:4)*	**0.64**	**0.63**	0.88	**0.55**
		1-(1-enyl-palmitoyl)-2-oleoyl-GPC (P-16:0/18:1)*	1.05	1.11	**1.78**	1.04
		1-(1-enyl-stearoyl)-2-oleoyl-GPE (P-18:0/18:1)	0.56	0.57	1.13	**0.50**
		1-(1-enyl-palmitoyl)-2-arachidonoyl-GPC (P-16:0/20:4)*	1.22	1.08	**1.55**	1.23
		1-(1-enyl-stearoyl)-2-arachidonoyl-GPE (P-18:0/20:4)*	**0.56**	**0.58**	0.94	**0.53**

	Lysoplasmalogen	1-(1-enyl-palmitoyl)-GPC (P-16:0)*	1.16	1.31	1.00	0.73
		1-(1-enyl-palmitoyl)-GPE (P-16:0)*	1.12	1.04	0.86	**0.53**
		1-(1-enyl-oleoyl)-GPE (P-18:1)*	1.08	**1.36**	0.86	**0.60**
		1-(1-enyl-stearoyl)-GPE (P-18:0)*	1.03	0.96	0.79	**0.48**
		1-(1-enyl-oleoyl)-2-oleoyl-GPE (P-18:1/18:1)*	0.68	0.67	1.11	**0.56**
	Glycerolipid Metabolism	glycerol	0.96	0.75	0.12	0.96
		glycerol 3-phosphate	**2.83**	**1.44**	0.94	**0.72**
		glycerophosphoglycerol	**2.69**	1.36	1.21	**0.48**
	Monoacylglycerol	1-myristoylglycerol (14:0)	0.74	**0.42**	**0.38**	1.17
		1-palmitoylglycerol (16:0)	**0.68**	**0.55**	1.16	**0.59**
		1-oleoylglycerol (18:1)	0.97	1.50	0.54	**2.55**
		2-palmitoylglycerol (16:0)	0.53	**0.44**	1.12	0.65
	Diacylglycerol	palmitoyl-palmitoyl-glycerol (16:0/16:0) [2]*	**0.40**	0.63	1.14	0.63
		palmitoyl-arachidonoyl-glycerol (16:0/20:4) [1]*	**0.33**	1.55	1.22	**0.38**
		palmitoyl-arachidonoyl-glycerol (16:0/20:4) [2]*	**0.34**	0.52	**1.99**	**0.46**
		stearoyl-arachidonoyl-glycerol (18:0/20:4) [1]*	**0.32**	0.52	0.91	**0.43**
		stearoyl-arachidonoyl-glycerol (18:0/20:4) [2]*	**0.30**	0.60	0.82	**0.48**
		oleoyl-arachidonoyl-glycerol (18:1/20:4) [1]*	**0.39**	0.62	0.87	**0.40**
		oleoyl-arachidonoyl-glycerol (18:1/20:4) [2]*	**0.35**	**0.42**	0.81	**0.38**
	Sphingolipid Synthesis	sphinganine	0.95	0.92	**1.41**	1.18
		sphingadienine	0.74	**0.70**	**0.61**	**0.41**
		phytosphingosine	0.94	0.91	**0.72**	**0.66**

	Dihydroceramides	N-palmitoyl-sphinganine (d18:0/16:0)	0.69	1.03	**4.17**	**3.18**
	Ceramides	N-palmitoyl-sphingosine (d18:1/16:0)	0.84	0.76	**1.53**	0.73
		N-stearoyl-sphingosine (d18:1/18:0)*	0.71	0.75	**2.37**	0.90
		N-palmitoyl-sphingadienine (d18:2/16:0)*	0.97	0.87	0.94	**0.66**
		N-palmitoyl-heptadecasphingosine (d17:1/16:0)*	0.83	0.91	**1.45**	0.77
		ceramide (d18:1/14:0, d16:1/16:0)*	0.94	0.79	1.31	0.72
		ceramide (d18:1/17:0, d17:1/18:0)*	0.80	1.07	**1.70**	0.76
		ceramide (d16:1/24:1, d18:1/22:1)*	0.42	1.44	**1.87**	0.86
		ceramide (d18:2/24:1, d18:1/24:2)*	**0.51**	0.59	0.88	**0.36**
	Hexosylceramides (HCER)	glycosyl-N-palmitoyl-sphingosine (d18:1/16:0)	0.69	0.74	0.81	**0.50**
		glycosyl-N-stearoyl-sphingosine (d18:1/18:0)	0.62	1.00	1.26	0.68
		glycosyl ceramide (d16:1/24:1, d18:1/22:1)*	0.56	1.00	1.05	0.40
		glycosyl ceramide (d18:2/24:1, d18:1/24:2)*	0.52	0.49	0.51	**0.29**
	Lactosylceramides (LCER)	lactosyl-N-palmitoyl-sphingosine (d18:1/16:0)	**0.51**	**0.55**	0.78	**0.40**
		lactosyl-N-nervonoyl-sphingosine (d18:1/24:1)*	0.46	0.96	0.64	**0.19**
	Dihydrosphingomyelins	myristoyl dihydrosphingomyelin (d18:0/14:0)*	0.73	0.89	1.16	**2.42**
		palmitoyl dihydrosphingomyelin (d18:0/16:0)*	**0.59**	0.77	1.18	1.47
		sphingomyelin (d18:0/18:0, d19:0/17:0)*	**0.49**	0.95	**1.85**	**2.55**
	Sphingomyelins	palmitoyl sphingomyelin (d18:1/16:0)	**0.70**	**0.71**	0.94	**0.65**
		stearoyl sphingomyelin (d18:1/18:0)	**0.66**	0.73	1.06	**0.62**

		behenoyl sphingomyelin (d18:1/22:0)*	**0.49**	0.63	1.03	**0.52**
		tricosanoyl sphingomyelin (d18:1/23:0)*	0.32	0.54	1.04	0.47
		lignoceroyl sphingomyelin (d18:1/24:0)	**0.40**	0.57	0.89	**0.52**
		sphingomyelin (d18:2/23:1)*	**0.48**	0.60	0.76	0.52
		sphingomyelin (d17:1/14:0, d16:1/15:0)*	**0.75**	0.80	**0.72**	**0.61**
		sphingomyelin (d18:1/14:0, d16:1/16:0)*	**0.72**	0.81	0.79	**0.62**
		sphingomyelin (d18:2/14:0, d18:1/14:1)*	**0.73**	0.82	0.81	**0.61**
		sphingomyelin (d17:1/16:0, d18:1/15:0, d16:1/17:0)*	**0.71**	0.78	0.81	**0.60**
		sphingomyelin (d17:2/16:0, d18:2/15:0)*	0.76	0.85	0.80	**0.67**
		sphingomyelin (d18:2/16:0, d18:1/16:1)*	**0.72**	0.79	**0.74**	**0.58**
		sphingomyelin (d18:1/17:0, d17:1/18:0, d19:1/16:0)	**0.63**	0.76	0.89	**0.62**
		sphingomyelin (d18:1/20:0, d16:1/22:0)*	0.56	0.69	1.28	**0.57**
		sphingomyelin (d18:1/20:1, d18:2/20:0)*	0.93	0.74	1.25	0.70
		sphingomyelin (d18:1/21:0, d17:1/22:0, d16:1/23:0)*	1.00	1.00	0.97	**0.39**
		sphingomyelin (d18:1/22:1, d18:2/22:0, d16:1/24:1)*	**0.59**	0.65	1.04	**0.60**
		sphingomyelin (d18:2/23:0, d18:1/23:1, d17:1/24:1)*	**0.59**	0.65	0.99	**0.55**
		sphingomyelin (d18:1/24:1, d18:2/24:0)*	**0.54**	0.62	1.01	**0.55**

		sphingomyelin (d18:2/24:1, d18:1/24:2)*	**0.58**	**0.62**	0.90	**0.57**
	Sphingosines	sphingosine	0.90	0.80	**0.72**	**0.50**
		hexadecasphingosine (d16:1)*	0.95	0.75	**0.62**	**0.39**
		heptadecasphingosine (d17:1)	**0.69**	**0.65**	0.79	**0.48**
		eicosanoylsphingosine (d20:1)*	0.91	0.86	0.76	1.28
	Mevalonate Metabolism	3-hydroxy-3-methylglutarate	**3.90**	**2.94**	**3.25**	**3.08**
	Sterol	cholesterol	**0.54**	**0.67**	0.86	**0.68**
		7-alpha-hydroxy-3-oxo-4-cholestenoate	0.68	0.70	**0.25**	**0.25**
		4-cholesten-3-one	**18.09**	**14.37**	**47.3**	**27.66**
	Primary Bile Acid Metabolism	glycochenodeoxycholate	0.76	0.63	0.95	1.13
		taurochenodeoxycholate	0.71	0.75	0.84	1.12
	Secondary Bile Acid Metabolism	deoxycholate	**6.69**	1.00	1.43	1.00
Nucleotide	Purine Metabolism, (Hypo)Xanthine/Inosine containing	inosine	**0.27**	**0.51**	**0.41**	**0.39**
		hypoxanthine	**0.22**	**0.54**	**0.40**	**0.46**
		xanthine	1.25	1.08	**2.21**	1.33
		allantoin	**3.59**	**1.38**	1.00	**1.79**
	Purine Metabolism, Adenine containing	adenosine 5'-diphosphate (ADP)	1.01	1.30	0.97	**0.51**
		adenosine 5'-monophosphate (AMP)	**1.72**	**1.36**	**1.53**	1.24
		adenosine 3',5'-cyclic monophosphate	0.92	**1.73**	0.74	**0.40**
		adenosine	**1.51**	0.99	1.32	1.15
		adenine	**1.95**	**1.88**	**4.03**	**4.51**
		N1-methyladenosine	**2.25**	2.19	1.10	1.73
		N6-carbamoylthreonyladenosine	**2.33**	**2.86**	**1.83**	1.10
		2'-deoxyadenosine 5'-diphosphate	**3.63**	**2.61**	**4.66**	**2.43**
		2'-deoxyadenosine	**1.52**	**2.19**	**3.79**	**3.31**
		guanosine 5'-triphosphate	0.99	1.34	1.23	**0.17**

	Purine Metabolism, Guanine containing	guanosine 5'- diphosphate (GDP)	1.03	1.13	1.00	**0.34**
		guanosine 5'- monophosphate (5'-GMP)	**2.62**	**2.23**	**2.09**	**1.54**
		guanosine	0.77	0.95	0.70	**0.61**
		guanine	**0.29**	0.95	**0.49**	0.64
		7-methylguanine	**2.68**	**3.35**	**14.8**	**8.80**
	Pyrimidine Metabolism, Orotate containing	dihydroorotate	**11.48**	**7.07**	**4.99**	**5.22**
		orotate	**6.24**	**5.76**	**11.94**	**3.27**
		orotidine	**3.32**	**3.16**	1.16	1.05
	Pyrimidine Metabolism, Uracil containing	uridine 5'-triphosphate (UTP)	1.10	1.18	0.80	**0.27**
		uridine 5'-diphosphate (UDP)	1.16	1.16	0.81	**0.30**
		uridine 5'-monophosphate (UMP)	**2.63**	**1.51**	1.13	0.80
		uridine	**0.48**	0.95	**0.51**	**0.44**
		uracil	0.65	1.16	**0.51**	**0.33**
		pseudouridine	0.79	1.00	0.99	**1.41**
		3-ureidopropionate	1.03	0.70	**2.78**	**2.16**
		beta-alanine	**1.78**	**2.12**	**1.80**	1.16
	Pyrimidine Metabolism, Cytidine containing	cytidine triphosphate	1.30	1.50	**1.61**	0.68
		cytidine diphosphate	1.38	1.57	1.51	0.74
		cytidine 5'-monophosphate (5'-CMP)	**1.59**	1.49	**1.57**	1.47
		cytidine	**0.69**	0.96	**0.54**	0.72
		cytosine	0.55	0.67	1.11	0.57
		2'-deoxycytidine	**2.75**	**3.19**	**2.63**	**2.42**
	Purine and Pyrimidine Metabolism	methylphosphate	0.60	0.66	0.71	**0.46**
Cofactors and Vitamins	Nicotinate and Nicotinamide Metabolism	nicotinamide	**0.57**	1.00	1.29	1.10
		nicotinamide ribonucleotide (NMN)	**0.69**	0.81	0.84	**0.69**
		nicotinamide riboside	**0.41**	**0.54**	**0.14**	**0.13**

		nicotinamide adenine dinucleotide (NAD+)	1.09	0.98	1.05	**0.66**
		nicotinamide adenine dinucleotide reduced (NADH)	0.96	0.83	**0.38**	**0.23**
		1-methylnicotinamide	**2.28**	**1.96**	**1.94**	1.04
		adenosine 5'-diphosphoribose (ADP-ribose)	0.84	1.12	1.08	1.36
	Riboflavin Metabolism	riboflavin (Vitamin B2)	1.34	0.91	1.00	1.19
		flavin adenine dinucleotide (FAD)	0.77	0.91	0.85	0.79
	Pantothenate and CoA Metabolism	pantothenate	**1.74**	**1.43**	**1.45**	0.92
		coenzyme A	2.20	4.86	1.47	0.77
	Ascorbate and Aldarate Metabolism	gulonate*	**4.65**	**2.60**	0.69	**0.32**
	Tocopherol Metabolism	alpha-tocopherol	0.67	0.67	0.62	**1.93**
	Folate Metabolism	folate	0.98	0.72	0.76	**0.55**
	Thiamine Metabolism	thiamin (Vitamin B1)	1.26	1.13	**1.45**	**0.70**
	Vitamin B6 Metabolism	pyridoxine (Vitamin B6)	1.18	0.95	1.00	0.88
		pyridoxamine	1.35	**0.27**	**0.48**	0.99
		pyridoxal phosphate	0.85	0.91	**0.72**	**0.46**
		pyridoxal	**1.85**	1.58	1.27	0.78
Xenobiotics	Benzoate Metabolism	hippurate	0.96	0.95	**0.54**	1.13
		benzoate	0.94	1.50	0.92	0.84
		p-cresol sulfate	1.19	0.46	**0.37**	0.71
	Food Component/Plant	gluconate	**2.59**	1.34	**5.29**	1.15
		beta-guanidinopropanoate	**4.07**	**2.37**	**2.21**	1.00
		coumaroylquinate (4)	1.00	1.00	1.00	1.00
		ergothioneine	**4.03**	**4.16**	**1.96**	0.95
		N-glycolylneuraminate	1.22	0.99	0.95	0.72
		quinate	0.89	0.67	0.23	1.42

		methyl glucopyranoside (alpha + beta)	0.47	1.65	0.61	1.49
	Drug - Antibiotic	penicillin G	**0.47**	**0.50**	1.14	0.73
	Chemical	sulfate*	0.90	0.90	1.01	0.84
		O-sulfo-L-tyrosine	1.19	1.15	0.94	**0.57**
		phenol red	0.88	0.77	0.60	0.81
		trizma acetate	**6.41**	**0.07**	**0.14**	**0.11**
		thioproline	1.13	1.14	1.05	0.97

Chapter 4 - Viral Growth Factor Mediated Upregulation of Akt Pathway Enhances ACLY Phosphorylation during Vaccinia Virus Infection

Introduction

Metabolism has emerged as a new frontier for studying the interactions between host cells and viruses during viral infections. The host cell possesses the nutritional resources necessary for replication, and viral infections often result in the alteration of the metabolic landscape of the infected cell, with different viruses deploying various strategies to hijack the host cell machineries [1,2]. Although the study of virus-induced metabolic reprogramming has gained considerable interest, the mechanisms underlying the viral repurposing of host cell resources to generate the energy and biomolecules required for viral replication remain largely unexplained. A better understanding of virus-induced metabolic regulation might reveal unique opportunities for the development of novel antiviral strategies and uncover the fundamental mechanisms that regulate cellular metabolism.

Vaccinia virus (VACV), the prototypical poxvirus, induces profound alterations in the metabolism of its host cells [3–6]. VACV induces the oxidative phosphorylation (OXPHOS) and the oxygen consumption rate (OCR) indicating the increased energy metabolism during VACV infection [4]. Even when most host cell translation is suppressed, VACV induces the selective upregulation of OXPHOS-associated mRNA translation [7]. VACV infection enhances the levels of several intermediates of the tricarboxylic acid (TCA) cycle, including citrate [6]. Interestingly, VACV also depends on *de novo* fatty acid (FA) synthesis to generate an energy-favorable environment [4], indicating the need for VACV to modulate FA metabolism. We have

previously reported that VACV infection is associated with an increase in the levels of carnitine-conjugated FAs, which are essential for beta-oxidation, whereas the steady-state levels of long-chain FAs (LCFAs) were reduced [6], suggesting that the VACV infection induced changes in FA metabolism. Here, we examined the molecular mechanisms underlying the VACV-mediated modulation of a key step linking the TCA cycle and FA metabolism.

Citrate, which is the first metabolite produced by the TCA cycle, can be shuttled out of the mitochondria to generate Acetyl-CoA [8,9]. Acetyl-CoA represents a key precursor of FA biosynthesis and serves as an important source of the acetyl groups used for histone acetylation [10]. The conversion rate from citrate to Acetyl-CoA is governed by the enzyme ATP citrate lyase (ACLY) [9]. Therefore, ACLY links carbohydrate metabolism (glycolysis and the TCA cycle), glutamine metabolism (reductive carboxylation), FA synthesis, and histone acetylation, making it a pivotal enzyme in cellular metabolism [11,12]. Unsurprisingly, the expression and activity of ACLY are significantly upregulated in several malignancies such as bladder, breast, lung, liver, stomach, prostate, and colon cancers [11,13–17], and the overexpression of ACLY correlates with poor prognosis in lung adenocarcinoma and blood cancers [14,18]. In addition, the chemical and genetic suppression of ACLY has been shown to inhibit the proliferation and progression of various cancers [19]. Because ACLY acts at a critical juncture of host metabolism (**Fig 4.1A**), ACLY expression levels could also be affected by many viruses. However, the mechanisms through which viral infection might modulate this key host metabolic enzyme are poorly understood.

The phosphorylation of ACLY at serine 455 (S455; in humans and mice) increases enzymatic activity [20]. ACLY expression is regulated by various signals that communicate nutritional status and stimulate growth signaling [19]. VACV activates growth factor signaling in

infected cells via viral growth factor (VGF), the viral homolog of cellular epidermal growth factor (EGF) and transforming growth factor [21–26]. In addition to critical functions in the induction of proliferative effects and viral spread, VGF is important for VACV replication in quiescent cells and mouse models [27,28]. We previously demonstrated that VGF is a key viral protein that enhances citrate levels in infected cells by increasing EGFR and MAPK activation and inducing the non-canonical phosphorylation STAT3 [6]. Interestingly, the activation of the PI3K/Akt pathway by EGFR and insulin signaling represents a primary regulatory mechanism for ACLY phosphorylation and activation [19,20,29]. VACV infection also enhances the phosphorylation of Akt in a VGF-dependent manner [21,30], suggesting a key role for VGF in the regulation of ACLY in VACV-infected cells.

Here, we report that VACV infection stimulates the S455 phosphorylation of ACLY in cultured cells, and the chemical and genetic inhibition of ACLY severely suppresses VACV replication. We demonstrated that ACLY phosphorylation is necessary for the efficient expression of VACV early proteins. Remarkably, we found that VGF-induced growth factor signaling is essential for the VACV-mediated upregulation of ACLY phosphorylation. We further showed that the upregulation of ACLY phosphorylation during VACV infection is dependent on the activation of the cellular Akt pathway. These findings identified a novel function for VGF in the governance of virus-host interactions through the induction of a key enzyme associated with host FA metabolism. Our study also provides a basis for the role played by VGF and its downstream signaling cascades in the modulation of lipid metabolism in VACV-infected cells. Furthermore, our findings expand our understanding of the role played by growth factors in the regulation of cellular metabolism.

Materials and methods

Cells and viruses

Primary HFFs were a kind gift from Dr. Nicholas Wallace at Kansas State University. Primary HFFs and HeLa cells (ATCC CCL-2) were grown in Dulbecco's modified Eagle medium (DMEM; Fisher Scientific), supplemented with 10% fetal bovine serum (FBS; Peak Serum), 2 mM glutamine (VWR), 100 U/ml of penicillin, and 100 μg/ml streptomycin (VWR) in a humidified incubator at 37 °C with 5% CO_2. BS-C-1 cells (ATCC CCL-26) were cultured in Eagle's minimal essential medium (EMEM; Fisher Scientific) using the same supplements and environments described for HFF culture. The WR strain of VACV (ATCC VR-1354) was amplified, purified, and quantified using previously described titration methods [58]. When the cells reached the desired confluency of approximately 90-95%, they were infected with the indicated MOI of the indicated viruses in special DMEM (Fisher Scientific) lacking glucose, L-glutamine, L-asparagine, sodium pyruvate, and phenol red, which was supplemented with 2% dialyzed FBS (Gibco), 100 U/ml of penicillin, and 100 μg/ml streptomycin (VWR). The medium was further supplemented with 1 g/L glucose (Fisher Scientific), glucose plus 2 mM glutamine, or glucose plus 2 mM L-asparagine as required.

Generation of VGF (C11R) deletion and revertant VACV

vΔVGF and vΔVGF_Rev mutant VACV strains were generated using a previously described protocol [6]. Briefly, the VGF-encoded C11R gene was replaced with a green fluorescent protein (GFP) gene through homologous recombination. An overlapping polymerase chain reaction (PCR) was performed to generate a DNA fragment containing the VACV P11 promoter, followed by the GFP coding sequence. Flanking regions including 500-bp homologous sequences upstream and downstream of the C11R gene were included to facilitate

recombination. Recombinant viruses expressing GFP were harvested from HeLa cells (ATCC CCL-2) and were plaque purified in BS-C-1 cells. After several rounds of purification, when 100% of the plaques expressed GFP, the deletion of both C11R copies at both ends of the virus genome was verified by PCR. The VGF revertant VACV (vΔVGF_Rev) virus was generated using a similar approach. A DNA fragment containing one copy of the C11R gene under the natural VACV C11 promoter and followed by a dsRED coding sequence under the P11 promoter was inserted in the central region of the VACV genome, between the loci VACWR146 and VACWR147.

Antibodies and chemicals

Antibodies against phospho-ACLY (S455), total ACLY, phospho-STAT3 (S727), phospho-STAT3 (Y705), and total STAT3, phospho-EGFR (Y1068), total EGFR, phospho-Akt (S473), total Akt, and horseradish peroxidase-conjugated secondary antibodies were purchased from Cell Signaling Technology. The anti-glyceraldehyde-3-phosphate dehydrogenase (anti-GAPDH) antibody was purchased from Santa Cruz Biotechnology.

The ACLY inhibitor SB 204990 was purchased from Cayman Chemicals. Other chemical inhibitors, including etomoxir, MK-2206 2HCl, H89, stattic, afatinib, and PD0325901 were purchased from Selleck chemicals and used at the indicated concentrations. Cytosine-1-β-D-arabinofuranoside (AraC) and cycloheximide were purchased from Sigma-Aldrich.

Cell viability assay

Cell viability assays were performed using a hemocytometer and the trypan blue exclusion assay, as described previously [59]. Briefly, after performing each indicated treatment for the indicated time, cells grown in a 12-well plate were harvested with 300 μL trypsin and mixed with 500 μL DMEM using a micropipette. Equal volumes (20 μL) of the cell suspension

and 4% trypan blue (VWR) were gently mixed, and the numbers of live and dead cells in each condition were counted using a hemocytometer.

Western blotting

Western blot was performed as previously described [60]. Briefly, after the indicated treatment for the indicated time, the cells were lysed in NP-40 cell lysis buffer and reduced with 100 mM dithiothreitol (DTT), followed by denaturation in sodium dodecyl sulfate-polyacrylamide gel electrophoresis (SDS-PAGE) loading buffer. The samples were boiled at 99 °C for 5 min and separated by SDS-PAGE, followed by transfer to a polyvinylidene difluoride (PVDF) membrane. Membrane blocking was performed for 1 h at room temperature in 5% bovine serum albumin (BSA; VWR) in Tris-buffered saline containing Tween-20 (TBST). The indicated primary antibodies were diluted in the BSA blocking buffer and incubated overnight at 4 °C. After three washes with TBST for 10 minutes, the membrane was incubated with horseradish peroxidase-conjugated secondary antibody for 1 h at room temperature. Finally, the membranes were developed with Thermo Scientific SuperSignal West Femto Maximum Sensitivity Substrate and imaged using a c300 Chemiluminescent Western Blot Imaging System (Azure Biosystems). If western blotting analysis using another antibody was required, the antibodies were stripped from the membrane by Restore (Thermo Fisher Scientific, Waltham, MA, United States), and the processes of blocking, primary antibody, secondary antibody, and imaging were repeated.

Quantitative reverse transcription PCR (qRT-PCR)

After the indicated treatment, total RNA was extracted from cells using TRIzol reagent (Ambion). The obtained RNA was then purified using Invitrogen PureLink RNA mini kit (Thermo Fisher Scientific), and the concentration and purity of the extract RNA were determined

using a nanodrop. To reverse transcribe (RT) the RNA into cDNA, 500 ng RNA was used as a template. The RT step was performed using random hexamer primers and SuperScript III first-strand synthesis kit (Invitrogen). The relative levels of the indicated mRNA were detected by performing a quantitative PCR (qPCR) using an All-in-One 2X qPCR mix (GeneCopoeia) and primers specific to the indicated genes. qRT-PCR was performed in a CFX96 Real-Time PCR Detection System (Bio-Rad) machine using the following settings: initial denaturation at 95 °C for 3 min, followed by 39 cycles of denaturation at 95 °C for 10 s, annealing and reading fluorescence at 52 °C for 30 s, and extension at 72 °C for 30 s. 18sRNA served as the internal control for normalization using the $2^{-\Delta\Delta CT}$ method.

RNA interference

Specific siRNAs for the indicated target genes and the negative control siRNAs were purchased from Qiagen. The siRNAs were mixed in Lipofectamine RNAiMAX transfection reagent (Fisher Scientific) and transfected to the HFFs in a 6 well plate at a final concentration of 5 nm in OPTIMEM media as per the manufacturer's instructions. After 48 hours post transfection, the efficiency of knockdown was confirmed using a western blotting assay.

Gaussia luciferase assay

The *Gaussia* luciferase activity assay in the cell culture supernatant was performed as previously described [33]. In short, cells were infected with recombinant VACV encoding *Gaussia* luciferase under the control of the VGF (C11R) viral early promoter (vEGluc). After the indicated time points, the cell culture media was collected, and luciferase activity was measured using Pierce *Gaussia* luciferase flash assay kit (Thermo Scientific) and a luminometer.

Statistical analyses

Unless otherwise stated, the data presented represent the mean of at least three biological replicates. Data analysis was performed in Microsoft Excel (version 16.14) using a two-tailed paired t-test to evaluate any significant differences between two means. The error bars indicate the standard deviation of the experimental replicates. The following convention for symbols was used to indicate statistical significance: ns, $P > 0.05$; *, $P \leq 0.05$; **, $P \leq 0.01$; ***, $P \leq 0.001$; ****, $P \leq 0.0001$.

Results

VACV infection upregulates ACLY phosphorylation

We previously showed that VACV infection increases the levels of citrate [6] and other TCA cycle intermediates in primary human foreskin fibroblasts (HFFs). Citrate is a key biomolecule that not only governs TCA cycle activity but also regulates FA metabolism [12]. Citrate can be transported out of the mitochondria into the cytoplasm, where it is converted into Acetyl-CoA and oxaloacetate (OAA), and Acetyl-CoA serves as a precursor for FA biosynthesis. The conversion of citrate to Acetyl-CoA is catalyzed by the enzyme ACLY [9]. The phosphorylation of ACLY at S455 in humans and mice or S454 in rats increases enzymatic activity [20]. We first tested the effect of VACV infection on ACLY phosphorylation using primary HFFs infected with the WT Western Reserve (WR) VACV strain. Remarkably, we found that VACV infection increased ACLY phosphorylation at S455 (**Fig 4.1B**). To determine the timing of the upregulation of ACLY phosphorylation relative to viral infection, we infected HFFs with WT VACV and examined ACLY phosphorylation at different time post-infection. We found that VACV infection increased ACLY phosphorylation as early as 30 minutes post-

infection, and this increase remained observable 8 hours post-infection (hpi) (**Fig 4.1C**), indicating that the virus was able to modulate ACLY activity starting early during the infection.

Next, we examined the effects of inhibiting ACLY phosphorylation on VACV replication using SB 204990, which is a selective and potent inhibitor of ACLY [31]. Notably, SB 204990 treatment significantly reduced the VACV titers by 18- and 13-fold in cells infected at multiplicity of infection (MOI) values of 2 and 0.1, respectively (**Fig 4.1D**), without affecting HFF viability as measured by a trypan blue assay (**Fig 4.1E**). We then examined the genetic suppression of ACLY levels using small interfering RNAs (siRNAs). ACLY-specific siRNAs effectively reduced the protein expression levels of ACLY (**Fig 4.1F**) without affecting cell viability (**Fig 4.1G**). ACLY silencing severely suppressed VACV replication (**Fig 4.1H**). Taken together, these results demonstrated an important role for ACLY in VACV replication.

Stimulation of ACLY phosphorylation requires the efficient expression of VACV early proteins

VACV gene expression occurs in a cascade, with early, intermediate, and late stages [32], and each step in this cascade produces the proteins and precursors that are required for the next stage. Accordingly, the VACV replication stages can also be classified into three stages, characterized by the stage of gene expression. Next, we aimed to determine which stages of VACV replication require ACLY activity. To study the effects of ACLY inhibition on VACV gene expression, we infected HFFs with a recombinant VACV that encodes *Gaussia* luciferase under the control of a viral early-protein promoter (C11R, vEGluc). Viral gene expression can be assessed by measuring the activity of *Gaussia* luciferase secreted in the cell culture media [33]. ACLY inhibition by SB 204990 suppressed early VACV gene expression (**Fig 4.2A**). The observed upregulation of ACLY phosphorylation at an early timepoint post-infection (**Fig 4.1C**)

and the suppression of VACV early gene expression following ACLY inhibition (**Fig 4.2A**) suggest that an early VACV replication event is involved in the induction of ACLY phosphorylation in infected cells. We further examined whether the inhibition of DNA replication affected ACLY phosphorylation in VACV-infected cells using AraC, a well-established inhibitor of DNA replication that does not disrupt early viral protein synthesis [34]. Treatment with AraC did not affect the increased ACLY phosphorylation observed in VACV-infected cells (**Fig 4.2B**), which suggested that the enhancement of ACLY phosphorylation was able to occur prior to DNA replication. Next, we tested whether the inhibition of protein synthesis affected ACLY phosphorylation following VACV infection by treating the HFFs with cycloheximide (CHX), a well-known inhibitor of translation [35]. Interestingly, the inhibition of protein synthesis significantly reduced the increase in ACLY phosphorylation following VACV infection (**Fig 4.2C**). CHX treatment reduced ACLY phosphorylation levels in uninfected HFFs but the effect was minimal compared to that in infected cells. Taken together, these results indicated that an early viral protein is necessary for the upregulation of ACLY phosphorylation in VACV-infected HFFs.

Growth factor signaling is essential for the VACV-mediated upregulation of ACLY phosphorylation

Next, we sought to identify the VACV early protein responsible for inducing ACLY phosphorylation. Because VGF is the most highly expressed gene among the 118 VACV early genes [36,37], and because we previously identified VGF as a key player in the upregulation of citrate levels in VACV-infected cells [6], we made VGF the primary candidate of our investigation. We used a recombinant VACV from which both copies of the VGF gene were deleted (vΔVGF) from the inverted terminal repeats of the VACV DNA. Furthermore, we

generated another recombinant VACV containing only one copy of the VGF gene under the control of its natural promoter but inserted into a different locus than the original VGF gene in the central region of the viral genome (vΔVGF_Rev). Remarkably, although infection with WT VACV upregulated ACLY phosphorylation, infection with vΔVGF abolished this upregulation (**Fig 4.3A**). Notably, phosphorylation could be rescued by infection with vΔVGF_Rev, indicating that VGF is a crucial viral protein required to induce ACLY activity (**Fig 4.3A**). Further tests remain necessary to determine whether VGF alone is sufficient to activate ACLY phosphorylation or whether co-factors are involved in this process.

VGF is a VACV protein that is secreted early following VACV infection and represents a viral homolog of cellular EGF and transforming growth factor [24,26,38]. VGF is vital for the replication and virulence of VACV in animal models and quiescent cells [27,28]. Furthermore, VGF induces proliferative effects in infected cells and facilitates cellular motility and spread [21,23] through the activation of the EGFR signaling cascade [21,25]. Because VGF deletion renders VACV unable to increase ACLY phosphorylation, we surmised that VGF-mediated EGFR signaling is involved in the upregulation of ACLY phosphorylation. To explore this possibility, we first tested the effects of an irreversible EGFR inhibitor, afatinib [39], on ACLY levels at a concentration that was previously shown to not affect HFF viability [6]. Remarkably, afatinib treatment reduced the observed increase in ACLY phosphorylation in VACV-infected cells, with minimal effects observed on uninfected controls (**Fig 4.3B**). Combined with the previous findings from our lab and others, showing significant reductions in VACV titers following the inhibition of the EGFR pathway [6,40], our current results indicated that VGF-induced EGFR signaling and ACLY phosphorylation play major roles in VACV replication.

MAPK is a downstream effector molecule of EGFR [41,42]. To test whether the MAPK pathway is involved in the induction of ACLY phosphorylation, we used PD0325901, a selective inhibitor of the MAPK/ERK pathway [43]. We found that PD0325901 treatment had minimal effects on ACLY phosphorylation in VACV-infected samples (**Fig 4.3B**). We have also previously demonstrated that VGF induces the non-canonical phosphorylation of STAT3 at S727 [6]. To determine whether STAT3 inhibition affected ACLY phosphorylation, we treated cells with stattic, a well-known STAT3 inhibitor [44]. The effects of stattic treatment on ACLY phosphorylation were insignificant (**Fig 4.3B**). These results suggested that ACLY activation during VACV infection occurs independently of the MAPK and STAT3 signaling pathways.

VACV infection upregulates ACLY phosphorylation in an Akt signaling-dependent manner

Growth factors activate the PI3K-Akt cascade to elicit a variety of cellular functions [45]. Akt is the predominant activator of ACLY phosphorylation [14,20]. Interestingly, VACV infection is known to activate Akt phosphorylation, which can be observed at an early post-infection time point [30] and appears to be VGF-dependent [21] (**Fig 4.4A**). We, therefore, examined whether Akt is necessary for the induction of ACLY phosphorylation in VACV-infected cells. We measured the levels of ACLY phosphorylation in uninfected and VACV-infected HFFs treated with MK-2206, a highly selective Akt inhibitor [46]. MK-2206 treatment reduced ACLY phosphorylation in both uninfected and VACV-infected conditions (**Fig 4.4B**). The reduction in the uninfected control was less pronounced than that observed in VACV-infected HFFs (**Fig 4.4B**). After Akt, protein kinase A (PKA) is another well-studied activator of ACLY [47]. We used H89, a selective inhibitor of PKA [48], to test the effects of PKA inhibition on ACLY levels following VACV infection. PKA inhibition, however, was not as efficient as

Akt inhibition for reducing ACLY phosphorylation in either uninfected or VACV-infected conditions (**Fig 4.4B**), which suggested that PKA plays a less important role than Akt in ACLY phosphorylation. The chemical inhibition of Akt using MK-2206 also significantly reduced VACV titers by 11- and 21-fold at an MOI of 2 and 0.1, respectively (**Fig 4.4C**), without affecting HFF viability (**Fig 4.4D**). These findings agree with previous report showing reduction of VACV titers upon Akt inhibition [30] and highlight the importance of Akt-induced ACLY phosphorylation for VACV replication. We further tested the effects of EGFR, MAPK, and STAT3 inhibition on Akt levels during VACV infection. Unsurprisingly, the inhibition of EGFR, but not MAPK or STAT3, suppressed Akt phosphorylation in VACV-infected cells but not in uninfected controls (**Fig 4.4E**). Taken together, these results indicated that the VGF-induced EGFR pathway serves as an upstream activator of Akt phosphorylation during VACV infection, which results in enhanced ACLY phosphorylation. ACLY phosphorylation during VACV infection occurs independently of EGFR-induced MAPK, which is a mechanism that is also evident in several cancers [14].

Discussion

We report that VACV infection increases the S455 phosphorylation of ACLY and provide evidence to support the dependence of this activation on VGF, the VACV homolog of cellular EGF. EGFR-induced Akt phosphorylation is critical to the enhancement of ACLY phosphorylation in VACV-infected cells. These findings provide a platform for examining the role played by VGF in the modulation of aspects of the host cell metabolism that involve the functions of ACLY.

ACLY sits at the crossroads of the TCA cycle, FA metabolism, and glutamine metabolism. Interestingly, VACV induces changes in all three aforementioned aspects of cell metabolism, suggesting that ACLY serves as a key player in the mediation of VACV-host interactions. We have previously shown that VACV infection increases the levels of TCA cycle intermediates [6]. VACV has also been shown to upregulate glutamine metabolism, such that the absence of glutamine from the growth media severely attenuates VACV replication [3,4], and VACV depends on FA metabolism for efficient replication [4]. Paradoxically, despite the increased phosphorylation of the catalyst (ACLY), VACV infection appears to induce the production of higher levels of the reactant (citrate) and lower levels of the product (Acetyl-CoA). We did not observe a significant increase in the protein levels of the mitochondrial citrate transporter or any obvious increases in levels of phosphorylated ACC1, which catalyzes the irreversible carboxylation of Acetyl-CoA required for FA synthesis (not shown). Furthermore, a general decrease in the steady-state levels of LCFA was observed following VACV infection [6]. LCFAs are acylated and then carnitylated by carnitine palmitoyltransferase (CPT1), and the modified LCFAs are then transported into the mitochondrial matrix, where they undergo beta-oxidation to fuel the TCA cycle [49]. Interestingly, the levels of carnitylated FAs increase following VACV infection, suggesting the VACV-induced upregulation of FA beta-oxidation [6]. Furthermore, the mRNA levels of CPT1B, which mediates the carnitylation of fatty acyl CoAs targeted for transport into the mitochondria for beta-oxidation, increased during VACV infection in a VGF-dependent manner (not shown). VACV infection upregulates the beta-oxidation of FAs in a VGF-dependent manner (not shown). Our observations indicated that the observed increase in ACLY phosphorylation led to increased FA metabolism, geared toward generating beta-oxidation intermediates that are eventually recycled to the TCA cycle to generate

energy. These findings support a previous report that ACLY positively regulated the carnitine system [50].

Our results raised an intriguing question: why does VACV go through such lengths to upregulate the levels of TCA cycle intermediates? By upregulating ACLY phosphorylation and redirecting the host metabolism toward the carnitylation of FAs, VACV could achieve two separate goals. First, because VACV is an enveloped virus, it requires lipid molecules to synthesize its membrane [51]. The decrease in LCFA levels may reflect the enhanced consumption of lipids during virion morphogenesis. Second, lipid metabolism is essential for the generation of an energy-rich state to support the increased demands associated with viral replication [4]. Although VACV generally inhibits the overall protein synthesis of the host cell, OXPHOS-related genes that are essential for energy generation are selectively upregulated [7]. Our results that VACV induced increases in carnitylated FAs, CPT1B mRNA, and the beta-oxidation of FAs provide physiological relevance to the selective upregulation of CPT1B mRNA observed during VACV infection [7].

VGF is crucial for the induction of ACLY phosphorylation in VACV-infected cells. VACV activates the PI3K-Akt pathway early during infection [30], and Akt phosphorylation increases upon VACV infection in a VGF-dependent manner [21]. Here, we showed that VACV induced ACLY phosphorylation via the VGF-induced EGFR-Akt signaling pathway, starting early during infection, and ACLY inhibition suppressed VACV early gene expression, demonstrating a crucial role for the interaction between VGF and ACLY in VACV replication. Our preliminary experiments indicate that VGF is sufficient to induce ACLY phosphorylation in the absence of VACV infection (not shown). Additional mechanistic studies remain necessary to characterize the motifs involved in the molecular interactions between VGF and ACLY and the

impacts of this interaction on the beta-oxidation of FAs. Taken together, these results combined with the report that VGF upregulates non-canonical STAT3 phosphorylation to induce citrate levels, our current study highlights the importance of VGF as a “master” regulator of cellular metabolic alterations during VACV infection.

ACLY is not the sole source of Acetyl-CoA and is not exclusively localized to the cytoplasm [52]. During nutrient-restricted conditions, such as starvation, the enzyme ACCS2 can convert acetate into Acetyl-CoA [53,54]. During human cytomegalovirus (HCMV) infection, the loss of the ability to utilize citrate for Acetyl-CoA synthesis through ACLY has little effect on either lipid synthesis or viral growth because ACCS2 compensates for the loss of ACLY [55]. Because acetate supplementation did not enhance VACV replication (not shown) and ACLY inhibition severely suppressed viral replication, the function of ACCS2 appears unlikely to be of similar importance as ACLY during VACV infection. Although ACLY is a predominantly cytosolic enzyme, several studies have reported its localization to the nucleus [52,56]. The Acetyl-CoA generated in the nucleus by nuclear ACLY is vital for homologous recombination [56] and histone acetylation [52]. Further studies remain necessary to determine the intracellular distribution of ACLY during VACV infection and the effects, if any, of altered localization patterns on the modulation of transcription.

In conclusion, this study demonstrated that the VGF-EGFR-Akt-induced ACLY phosphorylation is crucial for VACV replication. Because poxviruses are widely used to develop oncolytic agents [57], and the ACLY-induced metabolism is often dysregulated in cancer cells [12,19], our findings could lead to improvements in poxvirus-based oncolytic virotherapy and the development of better antipoxvirus agents.

References

1. Sanchez EL, Lagunoff M. Viral activation of cellular metabolism. Virology. 2015;479–480: 609–618. doi:10.1016/j.virol.2015.02.038

2. Thaker SK, Ch'ng J, Christofk HR. Viral hijacking of cellular metabolism. BMC Biol. 2019;17: 59. doi:10.1186/s12915-019-0678-9

3. Fontaine KA, Camarda R, Lagunoff M. Vaccinia Virus Requires Glutamine but Not Glucose for Efficient Replication. J Virol. 2014;88: 4366–4374. doi:10.1128/JVI.03134-13

4. Greseth MD, Traktman P. De novo Fatty Acid Biosynthesis Contributes Significantly to Establishment of a Bioenergetically Favorable Environment for Vaccinia Virus Infection. PLOS Pathog. 2014;10: e1004021. doi:10.1371/journal.ppat.1004021

5. Mazzon M, Peters NE, Loenarz C, Krysztofinska EM, Ember SWJ, Ferguson BJ, et al. A mechanism for induction of a hypoxic response by vaccinia virus. Proc Natl Acad Sci. 2013;110: 12444–12449. doi:10.1073/pnas.1302140110

6. Pant A, Dsouza L, Cao S, Peng C, Yang Z. Viral growth factor- and STAT3 signaling-dependent elevation of the TCA cycle intermediate levels during vaccinia virus infection. PLOS Pathog. 2021;17: e1009303. doi:10.1371/journal.ppat.1009303

7. Dai A, Cao S, Dhungel P, Luan Y, Liu Y, Xie Z, et al. Ribosome Profiling Reveals Translational Upregulation of Cellular Oxidative Phosphorylation mRNAs during Vaccinia Virus-Induced Host Shutoff. J Virol. 2017;91. doi:10.1128/JVI.01858-16

8. Kaplan RS, Mayor JA, Wood DO. The mitochondrial tricarboxylate transport protein. cDNA cloning, primary structure, and comparison with other mitochondrial transport proteins. J Biol Chem. 1993;268: 13682–13690. doi:10.1016/S0021-9258(19)38701-0

9. Srere PA. The Citrate Cleavage Enzyme: I. DISTRIBUTION AND PURIFICATION. J Biol Chem. 1959;234: 2544–2547. doi:10.1016/S0021-9258(18)69735-2

10. Pietrocola F, Galluzzi L, Bravo-San Pedro JM, Madeo F, Kroemer G. Acetyl Coenzyme A: A Central Metabolite and Second Messenger. Cell Metab. 2015;21: 805–821. doi:10.1016/j.cmet.2015.05.014

11. Icard P, Wu Z, Fournel L, Coquerel A, Lincet H, Alifano M. ATP citrate lyase: A central metabolic enzyme in cancer. Cancer Lett. 2020;471: 125–134. doi:10.1016/j.canlet.2019.12.010

12. Zaidi N, Swinnen JV, Smans K. ATP-Citrate Lyase: A Key Player in Cancer Metabolism. Cancer Res. 2012;72: 3709–3714. doi:10.1158/0008-5472.CAN-11-4112

13. Halliday KR, Fenoglio-Preiser C, Sillerud LO. Differentiation of human tumors from nonmalignant tissue by natural-abundance 13C NMR spectroscopy. Magn Reson Med. 1988;7: 384–411. doi:10.1002/mrm.1910070403

14. Migita T, Narita T, Nomura K, Miyagi E, Inazuka F, Matsuura M, et al. ATP Citrate Lyase: Activation and Therapeutic Implications in Non–Small Cell Lung Cancer. Cancer Res. 2008;68: 8547–8554. doi:10.1158/0008-5472.CAN-08-1235

15. Turyn J, Schlichtholz B, Dettlaff-Pokora A, Presler M, Goyke E, Matuszewski M, et al. Increased Activity of Glycerol 3-phosphate Dehydrogenase and Other Lipogenic Enzymes in Human Bladder Cancer. Horm Metab Res. 2003;35: 565–569. doi:10.1055/s-2003-43500

16. Varis A, Wolf M, Monni O, Vakkari M-L, Kokkola A, Moskaluk C, et al. Targets of Gene Amplification and Overexpression at 17q in Gastric Cancer. Cancer Res. 2002;62: 2625–2629.

17. Yancy HF, Mason JA, Peters S, Thompson CE, Littleton GK, Jett M, et al. Metastatic progression and gene expression between breast cancer cell lines from African American and Caucasian women. J Carcinog. 2007;6: 8. doi:10.1186/1477-3163-6-8

18. Wang J, Ye W, Yan X, Guo Q, Ma Q, Lin F, et al. Low expression of ACLY associates with favorable prognosis in acute myeloid leukemia. J Transl Med. 2019;17: 149. doi:10.1186/s12967-019-1884-5

19. Hatzivassiliou G, Zhao F, Bauer DE, Andreadis C, Shaw AN, Dhanak D, et al. ATP citrate lyase inhibition can suppress tumor cell growth. Cancer Cell. 2005;8: 311–321. doi:10.1016/j.ccr.2005.09.008

20. Berwick DC, Hers I, Heesom KJ, Moule SK, Tavare JM. The identification of ATP-citrate lyase as a protein kinase B (Akt) substrate in primary adipocytes. J Biol Chem. 2002;277: 33895–33900. doi:10.1074/jbc.M204681200

21. Beerli C, Yakimovich A, Kilcher S, V. Reynoso G, Fläschner G, Müller D, et al. Vaccinia virus hijacks EGFR signalling to enhance virus spread through rapid and directed infected cell motility. Nat Microbiol. 2018;4. doi:10.1038/s41564-018-0288-2

22. Brown JP, Twardzik DR, Marquardt H, Todaro GJ. Vaccinia virus encodes a polypeptide homologous to epidermal growth factor and transforming growth factor. Nature. 1985;313: 491–492. doi:10.1038/313491a0

23. Buller RM, Chakrabarti S, Moss B, Fredrickson T. Cell proliferative response to vaccinia virus is mediated by VGF. Virology. 1988;164: 182–192. doi:10.1016/0042-6822(88)90635-6

24. Chang W, Lim JG, Hellström I, Gentry LE. Characterization of vaccinia virus growth factor biosynthetic pathway with an antipeptide antiserum. J Virol. 1988;62: 1080–1083.

25. Postigo A, Martin MC, Dodding MP, Way M. Vaccinia-induced epidermal growth factor receptor-MEK signalling and the anti-apoptotic protein F1L synergize to suppress cell death during infection. Cell Microbiol. 2009;11: 1208–1218. doi:10.1111/j.1462-5822.2009.01327.x

26. Twardzik DR, Brown JP, Ranchalis JE, Todaro GJ, Moss B. Vaccinia virus-infected cells release a novel polypeptide functionally related to transforming and epidermal growth factors. Proc Natl Acad Sci. 1985;82: 5300–5304. doi:10.1073/pnas.82.16.5300

27. Buller RM, Chakrabarti S, Cooper JA, Twardzik DR, Moss B. Deletion of the vaccinia virus growth factor gene reduces virus virulence. J Virol. 1988;62: 866–874.

28. Lai AC, Pogo BG. Attenuated deletion mutants of vaccinia virus lacking the vaccinia growth factor are defective in replication in vivo. Microb Pathog. 1989;6: 219–226. doi:10.1016/0882-4010(89)90071-5

29. Buzzai M, Bauer DE, Jones RG, DeBerardinis RJ, Hatzivassiliou G, Elstrom RL, et al. The glucose dependence of Akt-transformed cells can be reversed by pharmacologic activation of fatty acid β -oxidation. Oncogene. 2005;24: 4165–4173. doi:10.1038/sj.onc.1208622

30. Soares JAP, Leite FGG, Andrade LG, Torres AA, Sousa LPD, Barcelos LS, et al. Activation of the PI3K/Akt Pathway Early during Vaccinia and Cowpox Virus Infections Is Required for both Host Survival and Viral Replication. J Virol. 2009;83: 6883–6899. doi:10.1128/JVI.00245-09

31. Cotter CA, Earl PL, Wyatt LS, Moss B. Preparation of Cell Cultures and Vaccinia Virus Stocks. Curr Protoc Microbiol. 2015;39: 14A.3.1-14A.318. doi:10.1002/9780471729259.mc14a03s39

32. Strober W. Trypan Blue Exclusion Test of Cell Viability. Curr Protoc Immunol. 2015;111: A3.B.1-A3.B.3. doi:10.1002/0471142735.ima03bs111

33. Cao S, Realegeno S, Pant A, Satheshkumar PS, Yang Z. Suppression of Poxvirus Replication by Resveratrol. Front Microbiol. 2017;8. doi:10.3389/fmicb.2017.02196

34. Pant A, Cao S, Yang Z. Asparagine Is a Critical Limiting Metabolite for Vaccinia Virus Protein Synthesis during Glutamine Deprivation. J Virol. 2019;93. doi:10.1128/JVI.01834-18

35. Pearce NJ, Yates JW, Berkhout TA, Jackson B, Tew D, Boyd H, et al. The role of ATP citrate-lyase in the metabolic regulation of plasma lipids. Hypolipidaemic effects of SB-204990, a lactone prodrug of the potent ATP citrate-lyase inhibitor SB-201076. Biochem J. 1998;334 (Pt 1): 113–119. doi:10.1042/bj3340113

36. Moss B. Poxviridae: the viruses and their replication. 5th ed. In: Knipe DM, Howley PM, editors. Fields virology. 5th ed. Philadelphia, PA: Lippincott Williams & Wilkins; 2013. pp. 2129–2159.

37. Renis HE, Johnson HG. Inhibition of plaque formation of vaccinia virus by cytosine arabinoside hydrochloride. Bacteriol Proc. 1962; 140.

38. Young CW, Robinson PF, Sacktor B. Inhibition of the synthesis of protein in intact animals by acetoxycycloheximide and a metabolic derangement concomitant with this blockade. Biochem Pharmacol. 1963;12: 855–865. doi:10.1016/0006-2952(63)90116-3

39. Yang Z, Bruno DP, Martens CA, Porcella SF, Moss B. Simultaneous high-resolution analysis of vaccinia virus and host cell transcriptomes by deep RNA sequencing. Proc Natl Acad Sci. 2010;107: 11513–11518. doi:10.1073/pnas.1006594107

40. Yang Z, Cao S, Martens CA, Porcella SF, Xie Z, Ma M, et al. Deciphering Poxvirus Gene Expression by RNA Sequencing and Ribosome Profiling. J Virol. 2015;89: 6874–6886. doi:10.1128/JVI.00528-15

41. Blomquist MC, Hunt LT, Barker WC. Vaccinia virus 19-kilodalton protein: relationship to several mammalian proteins, including two growth factors. Proc Natl Acad Sci. 1984;81: 7363–7367. doi:10.1073/pnas.81.23.7363

42. Li D, Ambrogio L, Shimamura T, Kubo S, Takahashi M, Chirieac L, et al. BIBW2992, an irreversible EGFR/HER2 inhibitor highly effective in preclinical lung cancer models. Oncogene. 2008;27: 4702–4711. doi:10.1038/onc.2008.109

43. Langhammer S, Koban R, Yue C, Ellerbrok H. Inhibition of poxvirus spreading by the anti-tumor drug Gefitinib (Iressa^{TM}). Antiviral Res. 2011;89: 64–70. doi:10.1016/j.antiviral.2010.11.006

44. Cargnello M, Roux PP. Activation and Function of the MAPKs and Their Substrates, the MAPK-Activated Protein Kinases. Microbiol Mol Biol Rev. 2011;75: 50–83. doi:10.1128/MMBR.00031-10

45. Hoshi M, Nishida E, Inagaki M, Gotoh Y, Sakai H. Activation of a serine/threonine kinase that phosphorylates microtubule-associated protein 1B in vitro by growth factors and phorbol esters in quiescent rat fibroblastic cells. Eur J Biochem. 1990;193: 513–519. doi:https://doi.org/10.1111/j.1432-1033.1990.tb19366.x

46. Barrett SD, Bridges AJ, Dudley DT, Saltiel AR, Fergus JH, Flamme CM, et al. The discovery of the benzhydroxamate MEK inhibitors CI-1040 and PD 0325901. Bioorg Med Chem Lett. 2008;18: 6501–6504. doi:10.1016/j.bmcl.2008.10.054

47. Schust J, Sperl B, Hollis A, Mayer TU, Berg T. Stattic: A Small-Molecule Inhibitor of STAT3 Activation and Dimerization. Chem Biol. 2006;13: 1235–1242. doi:10.1016/j.chembiol.2006.09.018

48. Ward PS, Thompson CB. Signaling in Control of Cell Growth and Metabolism. Cold Spring Harb Perspect Biol. 2012;4. doi:10.1101/cshperspect.a006783

49. Yan L. Abstract #DDT01-1: MK-2206: A potent oral allosteric AKT inhibitor. Cancer Res. 2009;69: DDT01-1-DDT01-1.

50. Pierce MW, Palmer JL, Keutmann HT, Hall TA, Avruch J. The insulin-directed phosphorylation site on ATP-citrate lyase is identical with the site phosphorylated by the cAMP-dependent protein kinase in vitro. J Biol Chem. 1982;257: 10681–10686.

51. Chijiwa T, Mishima A, Hagiwara M, Sano M, Hayashi K, Inoue T, et al. Inhibition of forskolin-induced neurite outgrowth and protein phosphorylation by a newly synthesized selective inhibitor of cyclic AMP-dependent protein kinase, N-[2-(p-bromocinnamylamino)ethyl]-5-isoquinolinesulfonamide (H-89), of PC12D pheochromocytoma cells. J Biol Chem. 1990;265: 5267–5272.

52. Houten SM, Wanders RJA. A general introduction to the biochemistry of mitochondrial fatty acid β-oxidation. J Inherit Metab Dis. 2010;33: 469–477. doi:10.1007/s10545-010-9061-2

53. Migita T, Okabe S, Ikeda K, Igarashi S, Sugawara S, Tomida A, et al. Inhibition of ATP citrate lyase induces triglyceride accumulation with altered fatty acid composition in cancer cells. Int J Cancer. 2014;135: 37–47. doi:10.1002/ijc.28652

54. Sodeik B, Doms RW, Ericsson M, Hiller G, Machamer CE, van't Hof W, et al. Assembly of vaccinia virus: role of the intermediate compartment between the endoplasmic reticulum and the Golgi stacks. J Cell Biol. 1993;121: 521–541.

55. Wellen KE, Hatzivassiliou G, Sachdeva UM, Bui TV, Cross JR, Thompson CB. ATP-Citrate Lyase Links Cellular Metabolism to Histone Acetylation. Science. 2009;324: 1076–1080. doi:10.1126/science.1164097

56. Comerford SA, Huang Z, Du X, Wang Y, Cai L, Witkiewicz AK, et al. Acetate Dependence of Tumors. Cell. 2014;159: 1591–1602. doi:10.1016/j.cell.2014.11.020

57. Mashimo T, Pichumani K, Vemireddy V, Hatanpaa KJ, Singh DK, Sirasanagandla S, et al. Acetate Is a Bioenergetic Substrate for Human Glioblastoma and Brain Metastases. Cell. 2014;159: 1603–1614. doi:10.1016/j.cell.2014.11.025

58. Vysochan A, Sengupta A, Weljie AM, Alwine JC, Yu Y. ACSS2-mediated acetyl-CoA synthesis from acetate is necessary for human cytomegalovirus infection. Proc Natl Acad Sci. 2017;114: E1528–E1535. doi:10.1073/pnas.1614268114

59. Sivanand S, Rhoades S, Jiang Q, Lee JV, Benci J, Zhang J, et al. Nuclear Acetyl-CoA Production by ACLY Promotes Homologous Recombination. Mol Cell. 2017;67: 252-265.e6. doi:10.1016/j.molcel.2017.06.008

60. Chan WM, McFadden G. Oncolytic Poxviruses. Annu Rev Virol. 2014;1: 191–214. doi:10.1146/annurev-virology-031413-085442

Figures- Chapter 4

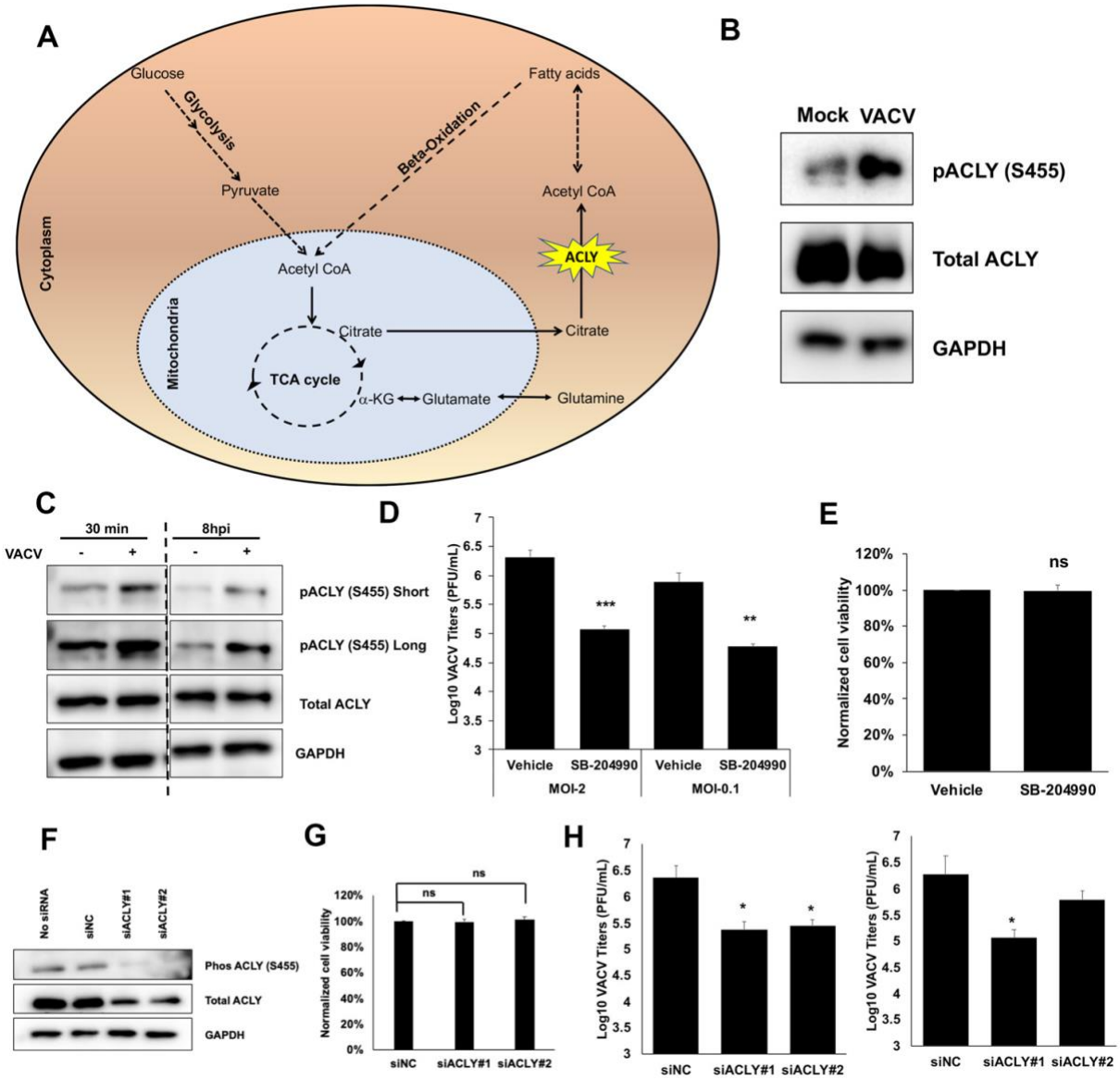

Figure 4.1. VACV upregulates ACLY phosphorylation.

(A) ATP citrate lyase (ACLY) is a key player in cell metabolism. The enzyme ACLY converts citrate, generated by the TCA cycle from glucose or glutamine, into acetyl coenzyme A and oxaloacetate. Acetyl coenzyme A can be further utilized for lipid synthesis, sterol synthesis, and histone acetylation **(B)** Vaccinia virus (VACV) infection induces the activation of ACLY phosphorylation at serine 455. Human foreskin fibroblasts (HFFs) were infected with wild-type (WT) VACV at a multiplicity of infection (MOI) of 5. Western blotting analysis was performed

to measure the levels of ACLY at 4 h post-infection (hpi). **(C)** The upregulation of ACLY S455 phosphorylation can be observed early during VACV infection. HFFs infected with WT VACV at an MOI of 5. The samples were collected at 10 minutes, and 1, 2, 4, and 8 hpi, followed by western blotting analysis. **(D)** The inhibition of ACLY suppresses VACV replication. HFFs were infected with WT VACV in the presence or absence of 100 µM SB-204990. Virus titers were measured by a plaque assay at 24 hpi (MOI = 2) and 48 hpi (MOI = 0.1). **(E)** The inhibition of the ACLY does not alter HFF viability. HFFs were grown in the presence or absence of 100 µM SB-204990 for 48 h. Cell viability was determined by trypan blue exclusion assay using a hemocytometer. **(F)** siRNA-mediated knockdown of ACLY. HFFs were transfected with a negative control siRNA or two specific siRNAs targeting ACLY for 48 h. Western blot was performed to measure the levels of ACLY protein expression. **(G)** ACLY knockdown does not affect HFF viability. HFFs were transfected with the indicated siRNAs for 48 h, and cell viability was determined by trypan blue exclusion assay. **(H)** siRNA-mediated knockdown of STAT3 decreases VACV infection. HFFs were transfected with the indicated siRNAs for 48 h and infected with WT VACV at an MOI of 2 or 0.1. Viral titers were measured at 24 hpi (MOI = 2) and 48 hpi (MOI = 0.1). Unless otherwise stated, all infections were performed in media containing both glucose and glutamine. Error bars represent the standard deviation of at least three biological replicates. ns, $P > 0.05$; *, $P \leq 0.05$; **, $P \leq 0.01$; ***, $P \leq 0.001$.

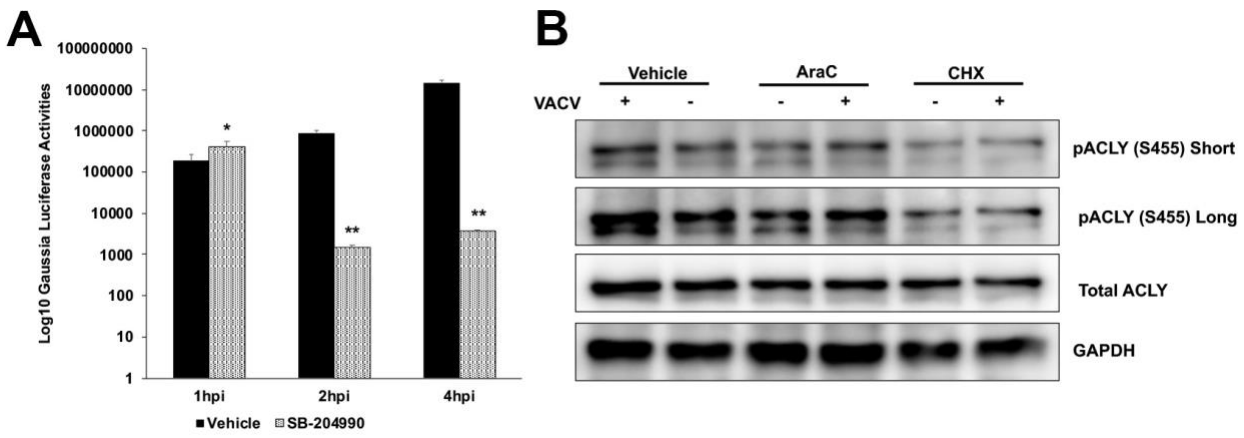

Figure 4.2. ACLY phosphorylation is required for the efficient expression of VACV early proteins.

(A) ATP citrate lyase (ACLY) inhibition reduces vaccinia virus (VACV) early gene expression. Human foreskin fibroblasts (HFFs) were infected at a multiplicity of infection (MOI) of 2 with recombinant VACV expressing *Gaussia* luciferase under the control of the virus growth factor (VGF) early gene promoter in the presence or absence of 100 µM SB-204990. Early gene expression was measured using a *Gaussia* luciferase activity assay kit at 1, 2, and 4 h post-infection (hpi). **(B)** The inhibition of translation but not of DNA synthesis does inhibit increased ACLY phosphorylation upon VACV infection. HFFs were infected with wild-type (WT) VACV at an MOI of 5 in the presence or absence of 40 µg/mL AraC or 100 µg/mL cycloheximide. ACLY levels were measured at 4 hpi by a Western blotting. Unless otherwise stated, all the infections were performed in media containing both glucose and glutamine. Error bars represent the standard deviation of at least three biological replicates. *, $P \leq 0.05$; **, $P \leq 0.01$.

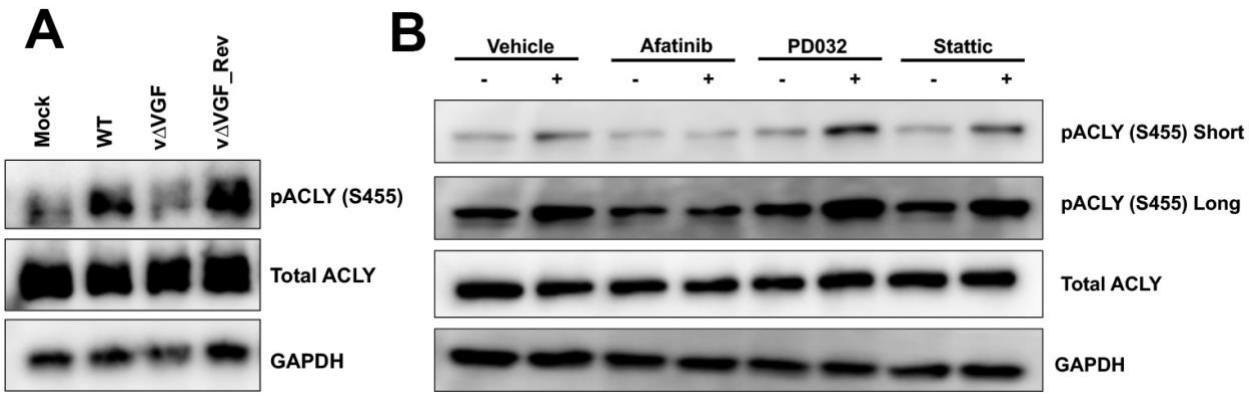

Figure 4.3. VACV infection induces ACLY S455 phosphorylation in a VGF-dependent manner.

(A) Vaccinia virus (VACV) virus growth factor (VGF) is crucial for the activation of ATP citrate lyase (ACLY) phosphorylation (S455). Human foreskin fibroblasts (HFFs) were infected with the indicated viruses at an MOI of 5. Western blotting analysis was performed to measure the levels of ACLY at 4 h post-infection (hpi). **(B)** VGF-induced epidermal growth factor receptor (EGFR) signaling is required to activate ACLY phosphorylation in VACV-infected cells. HFFs infected with WT VACV at an MOI of 5 in the presence or absence of 3 µM afatinib, 20 µM PD0325901, or 3 µM stattic. ACLY levels were detected by western blotting at 4 hpi. Unless otherwise stated, all the infections were performed in media containing both glucose and glutamine.

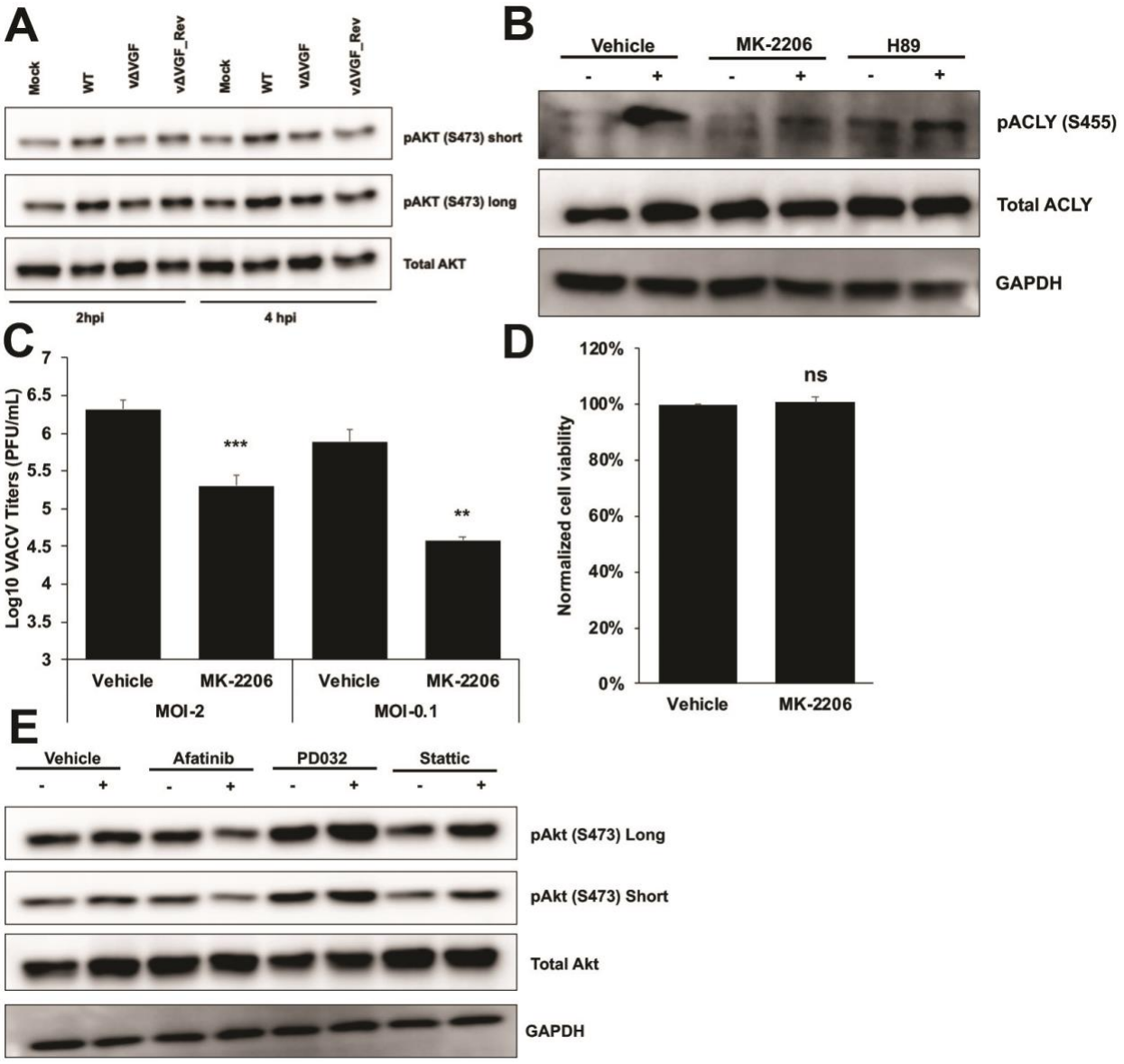

Figure 4.4. VACV infection upregulates ACLY phosphorylation in an Akt-dependent manner.

(A) Vaccinia virus (VACV) infection induces protein kinase B (Akt) phosphorylation in a virus growth factor (VGF)-dependent manner. Human foreskin fibroblasts (HFFs) were infected with the indicated viruses at a multiplicity of infection (MOI) of 5 for indicated time points. Western blotting analysis was performed to measure the levels of ATP citrate lyase (ACLY). **(B)** Akt inhibition suppresses ACLY phosphorylation under VACV-infected conditions. HFFs infected with MOI 5 of wild-type (WT) VACV for 4 h in the presence or absence of 5 μM MK 2206 (Akt inhibitor) or 5 μM H89 (PKA inhibitor). ACLY levels were measured by western blot. **(C)** The

inhibition of the Akt suppresses VACV replication. HFFs were infected with WT VACV in the presence or absence of 5 μM MK 2206. Virus titers were measured by a plaque assay at 24 hpi (MOI = 2) and 48 hpi (MOI = 0.1). **(D)** The inhibition of Akt does not affect HFF viability. HFFs were grown in the presence or absence of 5 μM MK 2206 for 48 h. Cell viability was determined by trypan blue exclusion assay. **(E)** The inhibition of epidermal growth factor receptor (EGFR) signaling suppresses Akt phosphorylation upon VACV infection. HFFs infected with WT VACV at an MOI of 5 in the presence or absence of 3 μM afatinib, 20 μM PD0325901, or 3 μM stattic. Akt levels were detected by western blotting assay at 4 hpi. Unless otherwise stated, all the infections were performed in media containing both glucose and glutamine. ns, $P > 0.05$; **, $P \leq 0.01$; ***, $P \leq 0.001$.

Chapter 5 - Asparagine: an Achilles Heel of Virus Replication?

Anil Pant, Zhilong Yang*

Division of Biology, Kansas State University, Manhattan, Kansas, 66506

*Correspondence: zyang@ksu.edu

Published as: **Pant, A**., & Yang, Z. (2020). Asparagine: An Achilles Heel of Virus Replication? *ACS Infectious Diseases*, *6*(9), 2301-2303.

Abstract

Asparagine biosynthesis and breakdown are tightly regulated in mammalian cells. Recent studies indicate that asparagine supply could be a limiting factor for the replication of some viruses such as vaccinia virus and human cytomegalovirus. In this Viewpoint, we highlight the importance of asparagine metabolism during virus replication and rationalize that asparagine metabolism could be a viable target for broad-spectrum antiviral development. To achieve this goal, more studies into asparagine metabolism during viral infections are demanded. These efforts would benefit beyond viral diseases, as asparagine supply is also a limiting factor in various stages of cancer development.

Key words: Asparagine, Metabolism, Vaccinia virus, Human cytomegalovirus, antiviral

Background

Viruses are obligate intracellular parasites that rely on their host cells for macromolecules and other resources needed for replication. It has been known since the 1950s that viruses depend on specific host metabolic pathways for efficient replication. Therefore, it was not surprising when cellular metabolism recently emerged as a major interface in studying virus-host interactions. While a virus takes advantage of its host cell metabolism, it may have different metabolic requirements as compared to the host cell. Viruses often hijack and alter cellular metabolism to fulfill their needs for replication. However, a cellular metabolic pathway can also be a barrier to viral replication if the metabolic pathway does not meet virus demands.

Amino acids are vital biomolecules for both cellular and viral protein synthesis. They also act as anaplerotic substrates to feed the tri-carboxylic acid (TCA) cycle and gluconeogenesis, as precursors for nucleotide metabolism, and as precursors for non-essential amino acids and specialized metabolites such as polyamines. Given their critical roles in various processes, many viruses target the amino acid metabolic pathways to meet their needs for replication. Recent findings from our own and others indicate that the highly regulated and limited supply of asparagine in mammals could be a barrier for the replication of certain viruses, making it an attractive target for antiviral development.

Asparagine metabolism is highly regulated in mammalian cells

Asparagine metabolism is tailored in mammalian cells such that the supply of this amino acid is limited, and its breakdown restricted (**Figure 5.1**). After the transamination of oxaloacetate (OAA) to generate aspartate, glutamine acts as the sole source of the amino group in a reaction catalyzed by asparagine synthetase (ASNS) to produce asparagine and glutamate. Therefore, unlike most other amino acids with multiple biosynthetic pathways, the only way for

the *de novo* cellular biosynthesis of asparagine is via ASNS, a process completely dependent on the availability of glutamine. Furthermore, asparagine is synthesized at the very end of the TCA cycle (from OAA), which limits its *de novo* supply. Asparaginase is the enzyme that hydrolyzes asparagine to aspartate. While mammalian cells can synthesize asparagine, asparaginase activity, though found in lower organisms, is lost in mammalian cells [1]. This results in an inability to catabolize asparagine, making mammalian cells maintain the limited level of asparagine. Moreover, ASNS is suppressed by its substrate, glutamine [2], suggesting that it is a regulatory mechanism to prevent excess asparagine biosynthesis. These mechanisms combine to tightly regulate asparagine metabolism.

It is intriguing to ponder why asparagine metabolism regulation is so unique compared to other amino acids in mammals. Recent advances in cancer research may provide clues to an answer. Excess amounts of asparagine seem to promote cancer development, as high ASNS expression indicates a poor prognosis for many tumor types [3]. On the other hand, genetic or chemical interference of asparagine biosynthesis is detrimental to cancer cells [3–5]. These findings suggest that cells need a low, yet uninterrupted supply of asparagine. To ensure this balance is maintained, mammalian cells developed the strategies mentioned earlier to regulate the supply and breakdown of asparagine. Because of these outstanding features, asparagine production can be used as a measure to indicate the availability of TCA cycle intermediates and reduced nitrogen that is required for the biosynthesis of other non-essential amino acids [3].

Asparagine supply is a limiting factor in vaccinia virus (VACV) and human cytomegalovirus (HCMV) infections

Several recent publications have demonstrated that asparagine supply is a limiting factor for viral replication under certain circumstances. Our finding showed that this is the case for viral

protein synthesis during VACV infection in the absence of glutamine[6]. VACV has a large double-stranded DNA genome that encodes for more than 200 viral proteins. VACV infection causes an acute increase in the demand for nascent protein synthesis. This is especially true during the late stage of virus infection when large numbers of viral particles are being produced. Notably, VACV-encoded proteins also contain almost 100% more asparagine content than human proteins. When glutamine, the precursor of asparagine, is absent during VACV infection, there is an accumulation and imbalance in the levels of most amino acids. Under such conditions, asparagine is the least abundant amino acid. Interestingly, the addition of exogenous asparagine reduces the buildup of amino acids observed under glutamine-depleted conditions. This indicates that asparagine availability is a critical limiting factor in maintaining amino acid balance for efficient protein synthesis in VACV-infected cells. In line with this finding, the addition of asparagine fully rescues VACV replication from glutamine depletion, specifically by rescuing the viral protein synthesis.

Another study by Lee et al. showed that asparagine metabolism is also crucial for the acute replication of HCMV[7]. A screen of almost 7,000 small interfering RNAs (siRNA) targeting host genes identified ASNS as a critical host factor for HCMV replication. When *ASNS* was knocked down, HCMV replication was severely limited. Moreover, inhibition of asparagine biosynthesis suppresses viral immediate-early gene expression during HCMV infection. The data suggest asparagine biosynthesis is critical for HCMV replication. Furthermore, HCMV replication is dependent on the availability of asparagine because the addition of exogenous asparagine can fully rescue the HCMV replication from ASNS inhibition.

Because many viral infections cause a rapid and robust increase in nascent protein synthesis to facilitate the production of virus particles, it is possible that asparagine supply can be

a limiting factor for the replication of other viruses, even for those that do not have high asparagine content in their proteomes. Interestingly, in both VACV and HCMV infections, no upregulation of ASNS was reported. However, a review paper indicates that adenovirus infection causes selective upregulation of *ASNS* in infected cells and the knockdown of *ASNS* severely impairs its replication[8]. This suggests that some viruses may have evolved ways of modulating asparagine biosynthesis.

In fact, in physiological conditions where protein synthesis is in high demand, asparagine supply could also be a limiting factor. Asparagine metabolism is gaining attention in cancer research as tumors require increased biomolecule synthesis to sustain their rapid growth. For example, asparagine availability determines the invasiveness and metastatic potential of breast cancer [5]. Asparagine is also important for the proliferation of multiple cancer cells, especially in the absence of glutamine [1,3]. Kaposi's sarcoma-associated herpesvirus (KSHV) transformed cancer cells utilize asparagine for the biosynthesis of purine and pyrimidines, which are the essential building blocks of nucleic acids[9]. It is not clear whether asparagine level directly impacts KSHV replication. In addition to cancers, asparagine is also crucial for blood vessel formation [10]. In agreement with these observations, a growing body of evidence indicates that asparagine is essential in coordinating general translation, regulating cellular signaling for amino acid homeostasis, and governing the metabolic availability during biological processes. When cells are starved of several different amino acids, they enhance asparagine biosynthesis to regulate gene expression [2,11]. Conversely, asparagine governs the coordination of protein and nucleotide synthesis by acting as an amino acid exchange factor to promote cancer cell proliferation [4].

Is asparagine metabolism a viable target for antiviral development?

Given that asparagine supply governs the efficient replication of some viruses, asparagine metabolism could be targeted to develop effective antiviral approaches. In fact, genetic or chemical interference of asparagine metabolism results in severe suppression of the replication of VACV in cultured cells[6]. Many poxviruses cause significant morbidity and mortality in humans and economically important animals. With further testing in animal models, this approach may result in the treatment of diseases caused by other poxviruses. The inhibition of early phenotype and inhibition of virus replication that occurs shortly after viral entry implies asparagine synthetase inhibitors could alleviate the HCMV-related complications seen in immunocompromised and transplant recipient patients[7]. The benefits of targeting asparagine metabolism likely extend to other diseases, including cancers. In fact, for decades, L-asparaginase-mediated depletion of asparagine has been successfully used to treat various cancers such as acute lymphoblastic leukemia, acute myeloid leukemia, and non-Hodgkin's lymphoma[12].

Multiple approaches could be used to develop drugs targeting asparagine metabolism. Inhibiting ASNS would limit asparagine biosynthesis, while increasing asparaginase activity/expression would deplete the pool of asparagine. Combinatorial treatment of ASNS inhibition and asparagine depletion may offer a more effective treatment. Since asparagine and glutamine metabolism go hand-in-hand, the development of novel inhibitors that target both metabolic pathways would be more efficient in treating some diseases. Additionally, a dietary or therapeutic intervention of asparagine levels could also be a possible approach to slow the development of some cancers that are reliant on asparagine [5]. These developments will require

collaborative efforts among virologists, medicinal chemists, structure biologists, pharmacologists, and clinicians.

In conclusion, we argue that the study of asparagine metabolism in viral infection and other pathological conditions is more relevant than ever. Going forward, more insights into this perspective will facilitate understanding the viral replication mechanism, and provide new intervention strategies of viral diseases, as well as cancers.

Notes

The authors declare no competing financial interest.

Acknowledgments

We thank Dr. Nicholas Wallace, Mark Gray, Lara Dsouza, and Lake Winter for critical reading and comments.

Z.Y. is supported by grants from the National Institutes of Health (R01AI143709 from NIAID, P20GM103418 Bridging Award from NIGMS). The content is solely the responsibility of the authors and does not necessarily represent the official views of the National Institutes of Health.

References

1. Pavlova NN, Hui S, Ghergurovich JM, Fan J, Intlekofer AM, White RM, et al. As Extracellular Glutamine Levels Decline, Asparagine Becomes an Essential Amino Acid. Cell Metab. 2018;27: 428-438.e5. doi:10.1016/j.cmet.2017.12.006

2. Hutson RG, Kilberg MS. Cloning of rat asparagine synthetase and specificity of the amino acid-dependent control of its mRNA content. Biochem J. 1994;304 (Pt 3): 745–750. doi:10.1042/bj3040745

3. Zhang J, Fan J, Venneti S, Cross JR, Takagi T, Bhinder B, et al. Asparagine Plays a Critical Role in Regulating Cellular Adaptation to Glutamine Depletion. Mol Cell. 2014;56: 205–218. doi:10.1016/j.molcel.2014.08.018

4. Krall AS, Xu S, Graeber TG, Braas D, Christofk HR. Asparagine promotes cancer cell proliferation through use as an amino acid exchange factor. Nat Commun. 2016;7: 1–13. doi:10.1038/ncomms11457

5. Knott SRV, Wagenblast E, Khan S, Kim SY, Soto M, Wagner M, et al. Asparagine bioavailability governs metastasis in a model of breast cancer. Nature. 2018;554: 378–381. doi:10.1038/nature25465

6. Pant A, Cao S, Yang Z. Asparagine Is a Critical Limiting Metabolite for Vaccinia Virus Protein Synthesis during Glutamine Deprivation. J Virol. 2019;93. doi:10.1128/JVI.01834-18

7. Lee C-H, Griffiths S, Digard P, Pham N, Auer M, Haas J, et al. Asparagine Deprivation Causes a Reversible Inhibition of Human Cytomegalovirus Acute Virus Replication. mBio. 2019;10. doi:10.1128/mBio.01651-19

8. Thaker SK, Ch'ng J, Christofk HR. Viral hijacking of cellular metabolism. BMC Biol. 2019;17: 59. doi:10.1186/s12915-019-0678-9

9. Zhu Y, Li T, Silva SR da, Lee J-J, Lu C, Eoh H, et al. A Critical Role of Glutamine and Asparagine γ-Nitrogen in Nucleotide Biosynthesis in Cancer Cells Hijacked by an Oncogenic Virus. mBio. 2017;8. doi:10.1128/mBio.01179-17

10. Huang H, Vandekeere S, Kalucka J, Bierhansl L, Zecchin A, Brüning U, et al. Role of glutamine and interlinked asparagine metabolism in vessel formation. EMBO J. 2017;36: 2334–2352. doi:10.15252/embj.201695518

11. Gong SS, Guerrini L, Basilico C. Regulation of asparagine synthetase gene expression by amino acid starvation. Mol Cell Biol. 1991;11: 6059–6066. doi:10.1128/mcb.11.12.6059

12. Broome JD. Evidence that the L -Asparaginase Activity of Guinea Pig Serum is responsible for its Antilymphoma Effects. Nature. 1961;191: 1114–1115. doi:10.1038/1911114a0

Figure- Chapter 5

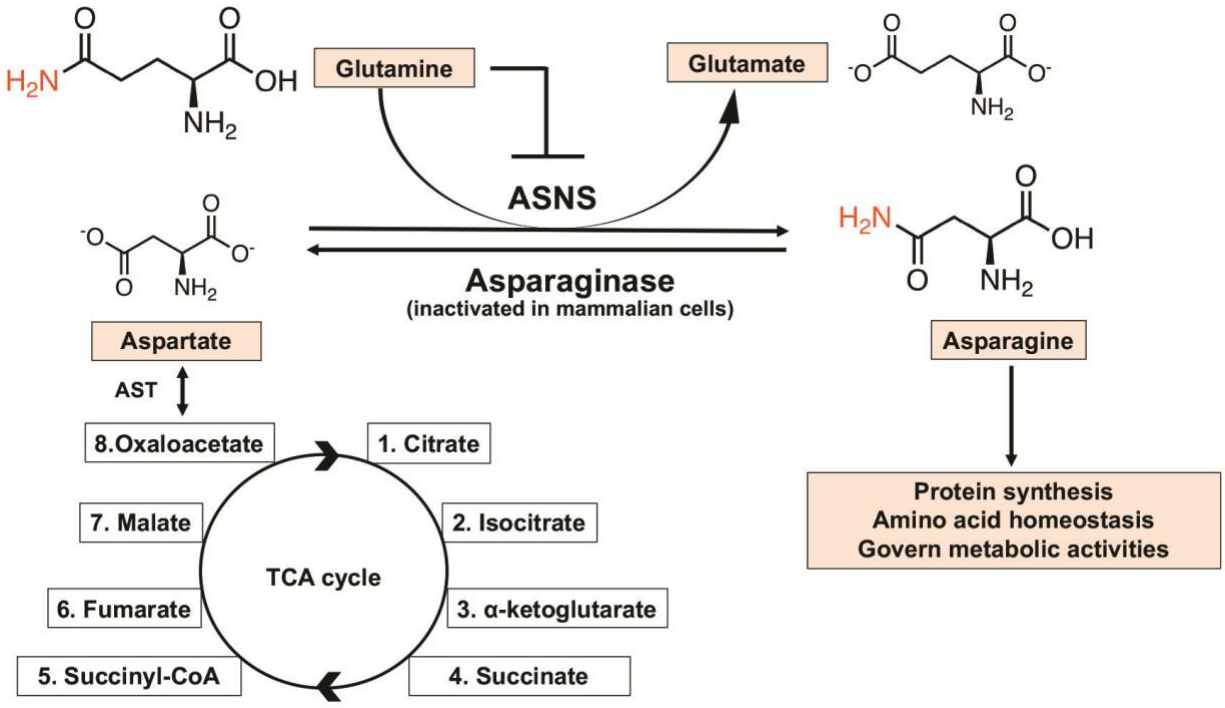

Figure 5.1. De novo biosynthesis and breakdown of asparagine in mammalian cells.
The final product of the TCA cycle, oxaloacetate, gets converted into aspartate by the enzyme aspartate transaminase (AST). The enzyme asparagine synthetase (ASNS) catalyzes the transfer of amino group (highlighted in red) from glutamine to aspartate to form asparagine and glutamate as a by-product. ASNS is inhibited by its substrate, glutamine (indicated by the blunt arrow). The hydrolysis of asparagine to aspartate is mediated by asparaginase. However, this activity is absent in mammalian cells.

Chapter 6 - Conclusions and Future Directions

To date, the vaccine using VACV remains the only vaccine to have eradicated a human disease: smallpox. Smallpox is considered one of the deadliest diseases in human history, responsible for the deaths of approximately 300 million people in the 20th century alone [1]. Despite the eradication of smallpox, poxviruses continue to have significant impacts on public health. Many members of the *Poxviridae* family, such as monkeypox, cowpox, and molluscum contagiosum virus, can cause significant morbidity and mortality in both humans and animals. Moreover, the resurgence of smallpox remains a possible biothreat due to the existence of unregistered stocks or potential *de novo* synthesis. However, poxviruses have also been widely developed as vaccine vectors and oncolytic agents. Understanding poxvirus replication strategies and the interactions of poxviruses with host cells is essential to the development of novel strategies for poxvirus infection management and to facilitate the development of poxvirus-based tools as vaccine vectors and oncolytic treatments. This chapter aims to highlight how the findings reported in this dissertation could further the fields of virology and cancer biology and contribute to therapeutic development. We also aim to propose future directions based on the findings reported in this dissertation.

Asparagine metabolism as a novel therapeutic target

Asparagine is an amino acid that plays a key role in controlling the metabolic functions of cells. Until recently it was thought that unlike the other 19 common amino acids, asparagine is merely a subunit of polypeptide; a non-essential amino acid. Because asparagine plays an essential role in the coordination of the cellular signaling involved in amino acid homeostasis, the coordination of general translation, and the regulation of metabolic availability during various pathologies, including cancer, asparagine metabolism could represent an attractive target

for the development of novel therapeutics. The study of asparagine metabolism has become even more relevant given that the crucial role of asparagine in the replication of several viruses, as highlighted in Chapters 2 and 5.

Our findings that asparagine is a critical limiting amino acid for VACV protein synthesis could lead to the development of novel antipoxvirus agents that target asparagine metabolism [2,3]. The genetic and chemical inhibition of asparagine synthetase (ASNS) drastically reduced VACV replication in cell culture, laying the foundation for further studies examining the effects of suppressing asparagine biosynthesis on poxvirus replication in an animal model. We further showed that treatment with L-asparaginase (ASNase; the enzyme that degrades asparagine) suppressed VACV replication. The verification of this finding *in vivo* could lead to the development of treatment strategies aimed against diseases caused by pathogenic poxviruses. The approach of modulating asparagine metabolism, if successful, could have implications on the development of therapeutic strategies against other viruses that depend on asparagine for efficient replication (see Chapter 5).

Our study could also lead to the development of novel anti-cancer agents using VACV as a vector to target asparagine metabolism. The successful use of bacterial ASNase for the treatment of acute lymphoblastic leukemia (ALL), acute myeloid leukemia (AML), and non-Hodgkin's lymphoma are pioneering examples of anti-cancer treatment strategies that target the metabolic vulnerabilities of cancer cells [4,5]. One noteworthy feature of asparagine metabolism is that the enzyme asparaginase is typically inactive in mammalian cells (for reasons not yet known), making the use of asparagine to feed the TCA cycle through conversion to aspartate unlikely [6]. Further, the expression of an L-asparaginase homolog from a lower organism (such as yeast or zebrafish) compromises the growth of tumors that depend on the availability of

asparagine [6]. More recently, asparagine bioavailability was demonstrated to serve as a key determinant of the metastatic potential in a mouse model of breast cancer [7]. Decreasing asparagine availability was also shown to decrease the invasive potential and metastasis of breast cancer [7]. This metabolic susceptibility in breast cancer can be targeted by arming VACV, which is already widely used as an oncolytic agent, with the asparaginase enzyme from zebrafish (zASPG) to generate a recombinant virus that is safe and therapeutically efficacious. zASPG mRNA can be extracted, reverse transcribed, and inserted into the VACV genome through homologous recombination using specific primers. After the successful generation and amplification of the recombinant zASPG-encoding VACV, its efficacy for the suppression of breast cancer progression can be tested in a mouse model. A similar approach could be used against several other human cancers because high ASNS expression has been found to serve as a poor prognostic marker in tumors [8].

Taken together, combined with further optimization and testing in animal models, our findings regarding the role of asparagine metabolism during VACV replication has the potential to be applied in the development of novel antiviral strategies and cancer therapeutics.

Outlook to the VACV-induced reprogramming of host metabolism

By using cutting-edge metabolic profiling, combined with classical genetic, chemical, and biochemical approaches, we showed that VACV infection induces profound alterations in the metabolism of host cells. We found that VACV infection elevates the levels of intermediates produced by the central metabolic hub: the TCA cycle. We also identified VACV VGF as a key viral protein involved in the alteration of host metabolism. Remarkably, VGF induces non-canonical STAT3 phosphorylation through the EGFR and MAPK axis. We further identified the EGFR, MAPK, and STAT3 pathways as the major cellular pathways that are induced by VACV

to increase host citrate levels for efficient replication. These findings, although noteworthy in themselves, posed several exciting questions that, when answered, could significantly advance current knowledge regarding virus-induced metabolic reprogramming. Further, the VGF-mediated selective activation of the non-canonical STAT3 pathway provides a unique tool for exploring the functions of the canonical and non-canonical STAT3 pathways. Additionally, the findings from our study could result in the development of unique molecular tools to facilitate our understanding of metabolic regulation mediated by growth factor signaling. In the following section, we will discuss how we can follow up our findings to further our understanding of the role played by VACV VGF in the modulation of host metabolism.

A major question that remains unanswered is which molecular mechanisms underlie the VGF-induced non-canonical STAT3 signaling that results in the elevation of TCA cycle intermediates. Although we found that treatment with VGF peptides alone was not sufficient to enhance citrate levels in uninfected HFFs [9], this finding remains inconclusive because whether the peptide is fully biologically active remains unclear. Further tests that more closely mimic the natural route of VGF expression and processing, in the absence of VACV infection, remain necessary to answer this question. Fully biologically active VGF alone may not be sufficient to induce metabolic changes in VACV-infected cells. Previous studies have identified VACV C16 protein as a key player in the modulation of glutamine metabolism [10,11]. VACV mutants featuring the deletion of C16, either alone or in combination with the deletion of VGF, could be a great starting point to further explore the contributions of this protein to the altered metabolism mediated by VACV.

Another “black box” in our current understanding is the exact functions and mechanisms of canonical (Y705) and non-canonical (S727) STAT3 phosphorylation and their roles in the

elevation of citrate levels during VACV infection. Although VACV infection does not induce canonical STAT3 phosphorylation, canonical STAT3 phosphorylation appears to be important for increasing citrate levels [9]. Because no inhibitors have been identified that can specifically inhibit the canonical or non-canonical STAT3 pathways, attributing functional roles to these axes during virus-induced metabolic changes has been challenging. The use of mouse embryonic fibroblasts (MEFs) expressing various phospho-resistant STAT3 mutations could provide valuable information regarding the contributions of these two functional arms of the STAT3 signaling pathway. The alterations in the subcellular localization of STAT3, if any, that occur under uninfected, WT and VGF-deleted VACV-infected, or VGF-treated conditions also remain to be determined.

Another piece of information that is missing is the contribution of glucose to the TCA cycle in support of VACV replication. Although glutamine is preferred over glucose for the efficient replication of VACV [12,13], we have found that the glucose can also sustain virus replication at an appreciable level [3]. Furthermore, our metabolic profiling revealed similar or decreased levels of glycolytic intermediates in VACV-infected cells compared to uninfected controls. These findings could indicate one of the following three possibilities: (a) glucose transport or uptake is impaired during VACV infection, (b) VACV induces the Warburg effect in infected cells to induce aerobic glycolysis, or (c) glycolytic intermediates are heavily consumed to feed the TCA cycle. The first option is unlikely because glucose levels are comparable between infected and uninfected controls. The second option, although theoretically possible, is also unlikely for the following reasons. First, the levels of lactate (which serves as a readout for Warburg effect) were similar between VACV infected and uninfected cells [9]. Second, VACV induces hypoxic responses under normoxic conditions but did not decrease the level of TCA

cycle intermediates in infected cells, which would be expected during the Warburg effect [11]. These observations indicate the likelihood that the third option is most likely occurring, which suggests an increase in glycolytic metabolism during VACV infection. Further experiments are warranted to test this possibility.

Another piece of the puzzle that remains to be solved is the determination of whether glucose or glutamine is driving the increases in the citrate levels that induce FA biosynthesis and oxidation. In addition to glucose, glutamine and the beta-oxidation of FAs are major contributors to TCA cycle intermediates. Although VACV is well-established to induce glutaminolysis [11,12], we have also demonstrated that VACV can induce the TCA cycle in a glutamine-independent manner [9]. However, VACV appears to depend on FA metabolism to generate an energy-favorable environment [13], and VACV infection increases the levels of fatty acyl-carnitines [9], which are indispensable contributors to beta-oxidation. In addition, VACV infection increases the phosphorylation of ACLY, a protein that has been shown to positively regulate FA oxidation [14]. All of these findings indicate an increase in FA oxidation during VACV infection, which is supported by our preliminary results showing increased CPT1B mRNA levels and FA oxidation during VACV infection. An increase in ACLY phosphorylation combined with decreased levels of Acetyl-CoA and long chain FAs during VACV infection appears to be almost paradoxical. These findings could be due to the rapid utilization of FAs to synthesize virus particles or to feed beta-oxidation. To fully understand the effects of VACV infection on FA metabolism, *de novo* FA biosynthesis should also be measured, in addition to measuring FA oxidation. More work remains necessary to identify the cell signaling pathways and viral factors that contribute to these changes.

As discussed briefly in the chapter 4, ACLY can be localized not only in the cell cytoplasm but also in the nucleus. Cytoplasmic ACLY generates Acetyl-CoA for FA biosynthesis, whereas its nuclear counterpart is known to regulate gene transcription by modulating histone acetylation [15]. Because a significant decrease can be observed in the levels of Acetyl-CoA in virus-infected cells, and Acetyl-CoA is the sole donor of acetyl groups used for histone acetylation, VACV likely induces changes to histone acetylation upon infection. Further tests remain necessary to determine the subcellular distribution of ACLY and the effects of VACV infection on histone acetylation.

For all of the experiments discussed above, these effects remain to be verified in an animal model, which is likely to present a more complex response to viral infection. The effects of VACV (WT, VGF-deleted, or the revertant mutant) infection and VGF peptide treatment on metabolic reprogramming *in vivo* should be explored. Whether VACV infection induces STAT3 phosphorylation, ACLY phosphorylation, and TCA cycle enrichment in a mouse model should also be examined. Differences in the metabolism and signaling pathways following infection in different tissues with different basal metabolic statuses would also be interesting to examine.

In the long-term, the findings from these studies will advance our understanding of virus-host interactions at the metabolic interface to a whole new level.

References

1. Henderson DA. The eradication of smallpox – An overview of the past, present, and future. Vaccine. 2011;29: D7–D9. doi:10.1016/j.vaccine.2011.06.080

2. Pant A, Yang Z. Asparagine: An Achilles Heel of Virus Replication? ACS Infect Dis. 2020 [cited 18 Aug 2020]. doi:10.1021/acsinfecdis.0c00504

3. Pant A, Cao S, Yang Z. Asparagine Is a Critical Limiting Metabolite for Vaccinia Virus Protein Synthesis during Glutamine Deprivation. J Virol. 2019;93. doi:10.1128/JVI.01834-18

4. Egler RA, Ahuja SP, Matloub Y. L-asparaginase in the treatment of patients with acute lymphoblastic leukemia. J Pharmacol Pharmacother. 2016;7: 62–71. doi:10.4103/0976-500X.184769

5. Broome JD. Evidence that the L -Asparaginase Activity of Guinea Pig Serum is responsible for its Antilymphoma Effects. Nature. 1961;191: 1114–1115. doi:10.1038/1911114a0

6. Pavlova NN, Hui S, Ghergurovich JM, Fan J, Intlekofer AM, White RM, et al. As Extracellular Glutamine Levels Decline, Asparagine Becomes an Essential Amino Acid. Cell Metab. 2018;27: 428-438.e5. doi:10.1016/j.cmet.2017.12.006

7. Knott SRV, Wagenblast E, Khan S, Kim SY, Soto M, Wagner M, et al. Asparagine bioavailability governs metastasis in a model of breast cancer. Nature. 2018;554: 378–381. doi:10.1038/nature25465

8. Zhang J, Fan J, Venneti S, Cross JR, Takagi T, Bhinder B, et al. Asparagine Plays a Critical Role in Regulating Cellular Adaptation to Glutamine Depletion. Mol Cell. 2014;56: 205–218. doi:10.1016/j.molcel.2014.08.018

9. Pant A, Dsouza L, Cao S, Peng C, Yang Z. Viral growth factor- and STAT3 signaling-dependent elevation of the TCA cycle intermediate levels during vaccinia virus infection. PLOS Pathog. 2021;17: e1009303. doi:10.1371/journal.ppat.1009303

10. Mazzon M, Peters NE, Loenarz C, Krysztofinska EM, Ember SWJ, Ferguson BJ, et al. A mechanism for induction of a hypoxic response by vaccinia virus. Proc Natl Acad Sci. 2013;110: 12444–12449. doi:10.1073/pnas.1302140110

11. Mazzon M, Castro C, Roberts LD, Griffin JL, Smith GL. A role for vaccinia virus protein C16 in reprogramming cellular energy metabolism. J Gen Virol. 2015;96: 395–407. doi:10.1099/vir.0.069591-0

12. Fontaine KA, Camarda R, Lagunoff M. Vaccinia Virus Requires Glutamine but Not Glucose for Efficient Replication. J Virol. 2014;88: 4366–4374. doi:10.1128/JVI.03134-13

13. Greseth MD, Traktman P. De novo Fatty Acid Biosynthesis Contributes Significantly to Establishment of a Bioenergetically Favorable Environment for Vaccinia Virus Infection. PLOS Pathog. 2014;10: e1004021. doi:10.1371/journal.ppat.1004021

14. Migita T, Okabe S, Ikeda K, Igarashi S, Sugawara S, Tomida A, et al. Inhibition of ATP citrate lyase induces triglyceride accumulation with altered fatty acid composition in cancer cells. Int J Cancer. 2014;135: 37–47. doi:10.1002/ijc.28652

15. Sivanand S, Rhoades S, Jiang Q, Lee JV, Benci J, Zhang J, et al. Nuclear Acetyl-CoA Production by ACLY Promotes Homologous Recombination. Mol Cell. 2017;67: 252-265.e6. doi:10.1016/j.molcel.2017.06.008